จุฬาลงกรณ์มหาวิทยาลัย
CHULALONGKORN UNIVERSITY

รายงานวิจัยฉบับสมบูรณ์

โครงการ การสร้างคลังข้อมูลวัสดุเชิงประกอบระดับนาโนเมตรพอลิไดแอเซทิลีน/สารประกอบซิงก์ที่สามารถควบคุมพฤติกรรมการเปลี่ยนสีและมีสมบัติฟลูออเรสเซนส์ที่ดีสำหรับเทคโนโลยีการตรวจวัด

โดย รองศาสตราจารย์ ดร.นิศานาถ ไตรผล

มิถุนายน พ.ศ. 2562

สัญญาเลขที่ RSA5980020

รายงานวิจัยฉบับสมบูรณ์

โครงการ การสร้างคลังข้อมูลวัสดุเชิงประกอบระดับนาโนเมตรพอลิไดแอเซทิลีน/สารประกอบซิงก์ที่สามารถควบคุมพฤติกรรมการเปลี่ยนสีและมีสมบัติฟลูออเรสเซนส์ที่ดีสำหรับเทคโนโลยีการตรวจวัด

รองศาสตราจารย์ ดร.นิศานาถ ไตรผล
จุฬาลงกรณ์มหาวิทยาลัย

สนับสนุนโดยสำนักงานกองทุนสนับสนุนการวิจัย
และจุฬาลงกรณ์มหาวิทยาลัย

สารบัญ

กิตติกรรมประกาศ

งานวิจัยนี้ได้รับการสนับสนุนทุนวิจัยจากสำนักงานกองทุนสนับสนุนการวิจัย และจุฬาลงกรณ์มหาวิทยาลัย ผู้วิจัยขอขอบคุณภาควิชาวัสดุศาสตร์ คณะวิทยาศาสตร์ จุฬาลงกรณ์มหาวิทยาลัย ที่ให้การสนับสนุนสถานที่ เครื่องมือ และอุปกรณ์ในการทำงานวิจัย ซึ่งมีส่วนสำคัญในการทำให้งานวิจัยนี้สำเร็จลุล่วงไปได้ด้วยดี

บทคัดย่อ

รหัสโครงการ: RSA5980020

ชื่อโครงการ: การสร้างคลังข้อมูลวัสดุเชิงประกอบระดับนาโนเมตรพอลิไดแอเซทิลีน/สารประกอบซิงก์ที่สามารถควบคุมพฤติกรรมการเปลี่ยนสีและมีสมบัติฟลูออเรสเซนส์ที่ดีสำหรับเทคโนโลยีการตรวจวัด

ชื่อนักวิจัย: รองศาสตราจารย์ ดร.นิศานาถ ไตรผล จุฬาลงกรณ์มหาวิทยาลัย

E-mail Address: Nisanart.t@chula.ac.th

ระยะเวลาโครงการ: 3 ปี ตั้งแต่วันที่ 16 มิถุนายน พ.ศ.2559 ถึงวันที่ 15 มิถุนายน พ.ศ.2562

งานวิจัยนี้ได้ทำการศึกษาการตอบสนองโดยการเปลี่ยนสีแบบผันกลับได้ที่สภาวะอุณหภูมิต่ำของวัสดุเชิงประกอบระดับนาโนเมตรพอลิไดแอเซทิลีน/ซิงก์ (II) ไอออน/ซิงก์ออกไซด์ โดยได้ทำการเตรียมวัสดุเชิงประกอบจากมอนอเมอร์ 7 ชนิดที่มีความยาวสายโซ่อัลคิลที่แตกต่างกัน เมื่อความยาวของสายโซ่อัลคิลส่วนหางลดลงจาก 12 เป็น 6 หน่วยเมทิลีน จะทำให้อุณหภูมิที่เกิดการเปลี่ยนสีของวัสดุเชิงประกอบลดลงจาก 90 เป็น 30 องศาเซลเซียส สำหรับการเปลี่ยนแปลงความยาวสายโซ่อัลคิลที่ตำแหน่งถัดจากส่วนหัวของพอลิไดแอเซทิลีน จะทำให้อุณหภูมิการเปลี่ยนสีเปลี่ยนแปลงอย่างไม่เป็นระบบ ซึ่งจากการตรวจสอบด้วยเทคนิคต่าง ๆ พบว่า การเปลี่ยนแปลงมุมภายในโครงสร้างสองชั้นของ

พอลิไดแอเซทิลีน การเปลี่ยนแปลงของอันตรกิริยา และการจัดเรียงตัวของสายโซ่หลักขึ้นอยู่กับความยาวสายโซ่อัลคิลภายในโมเลกุล นอกจากนี้ยังได้ทำการศึกษาถึงผลของระยะเวลาในการฉายแสงเพื่อให้เกิดพอลิเมอไรเซชันระหว่างกระบวนการเตรียมสาร ทำให้ควบคุมอุณหภูมิการเปลี่ยนสีของวัสดุเชิงประกอบได้อย่างละเอียดมากขึ้นจากการปรับเปลี่ยนความยาวของสายโซ่หลัก โดยสามารถเตรียมวัสดุเปลี่ยนสีแบบผันกลับได้ต่ออุณหภูมิที่มีค่าอุณหภูมิการเปลี่ยนสีในช่วง 10-90 องศาเซลเซียส รวมถึงศึกษาการควบคุมการจัดเรียงตัวของพอลิเมอร์บนอนุภาคซิงก์ออกไซด์ โดยทำการปรับค่าความเป็นกรดเบสในกระบวนการเตรียมสาร ซึ่งเป็นการควบคุมประจุที่พื้นผิวของอนุภาคซิงก์ออกไซด์และการแตกตัวของหมู่คาร์บอกซิลิกที่ส่วนหัวของพอลิไดแอเซทิลีน ทำให้ได้ปริมาณของวัสดุเชิงประกอบที่เพิ่มมากขึ้นเมื่อทำการเตรียมในสภาวะเบส และสามารถทำการควบคุมสมบัติการเปลี่ยนสีต่ออุณหภูมิและสารเคมีได้ด้วย ซึ่งเป็นการขยายขอบเขตการใช้งานด้านการตรวจวัดของวัสดุชนิดนี้

เมื่อทำการปรับเปลี่ยนชนิดของมอนอเมอร์ให้ส่วนหัวมีหมู่เบนโซอิกเพิ่มเข้ามา คือ 3-(pentacosa-10,12-diynamido) benzoic acid (PCDA-mBzA) และทำการเตรียมวัสดุเชิงประกอบระดับนาโนเมตร poly(PCDA-mBzA)/ซิงก์ (II) ไอออน/ซิงก์ออกไซด์ โดยใช้ปริมาณซิงก์ออกไซด์ตั้งแต่ 5-20 เปอร์เซ็นโดยน้ำหนักมอนอเมอร์ พบว่าวัสดุเชิงประกอบมีอุณหภูมิการเปลี่ยนสีลดลงเป็น 80 70 และ 60 องศาเซลเซียสเปรียบเทียบกับ poly(PCDA-mBzA) ที่เกิดการเปลี่ยนสีที่ 90 องศาเซลเซียส โดยยังคงแสดงสมบัติการเปลี่ยนสีต่ออุณหภูมิแบบผันกลับได้ นอกจากนี้การเติมซิงก์ออกไซด์ยังเพิ่มความไวในการตอบสนองต่อสารเคมีประเภทสารช่วยกระจายตัวชนิดประจุบวกและตัวทำละลายอินทรีย์ วัสดุเชิง

ประกอบที่เตรียมได้นี้สามารถนำไปใช้งานได้หลากหลาย เช่น วัสดุตรวจวัดโดยการเปลี่ยนสี ป้ายฉลาด หมึกพิมพ์/สี ที่เปลี่ยนสีได้เมื่ออุณหภูมิเปลี่ยนแปลงไป เป็นต้น

คำหลัก: พอลิไดแอเซทิลีน, การเปลี่ยนสีด้วยความร้อนแบบผันกลับได้, วัสดุเชิงประกอบระดับนาโนเมตร, ความยาวสายโซ่อัลคิล, เซนเซอร์ตรวจวัดสารเคมี

Abstract

Project Code: RSA5980020

Project Title: Creating a library of polydiacetylene/zinc compound nanocomposites with controllable color-transition behaviors and improved fluorescent property for sensing technologies

Investigator: Associate Prof. Dr.Nisanart Traiphol

E-mail Address: Nisanart.t@chula.ac.th

Project Period: 3 Years From 16 June 2016 to 15 June 2019

A series of reversible thermochromic polydiacetylene/zinc(II) ion/zinc oxide (PDA/Zn^{2+}/ZnO) nanocomposites has been prepared using 7 types of diacetylene monomer. The shortening of PDA alkyl tail from 12 to 6 methylene units systematically decreases color-transition temperature (T_{CT}) from 90 to 30 ^{o}C. The shortening of alkyl segment adjacent to PDA headgroup causes unpredictable changes of T_{CT}. Examination by various techniques reveal that variation of molecular tilting angle within the bilayer structure of PDA, change of local interactions and backbone conformation within the nanocomposites depend on the length of alkyl segment. In addition, effects of polymerization time during material preparation are studied. Fine-tuning of the T_{CT} of PDA/Zn^{2+}/ZnO nanocomposites is achieved by altering backbone chain length. Reversible thermochromic materials with T_{CT} ranging from 10 ^{o}C to 90 ^{o}C can be produced. Self-assembling of PDA on ZnO nanoparticles is also

investigated. By adjusting pH during material preparation, ZnO surface charge and dissociation of carboxylic at PDA headgroup can be altered. An increase of the nanocomposite amount after photopolymerization is observed when preparing in basic conditions. Thermochromism and chemical responses of the nanocomposites can also be controlled. This can extend working ranges of the material in sensing applications.

Next, 3-(pentacosa-10,12-diynamido) benzoic acid (PCDA-mBzA) monomer is used to prepare poly(PCDA-mBzA)/Zn2+/ZnO nanocomposites using 5, 10 and 20 wt.% of ZnO nanoparticles. It is found that T_{CT} of the nanocomposites decreases to about 80, 70 and 60 °C, respectively, comparing to 90 °C of poly(PCDA-mBzA). The reversible thermochromism still remains. Moreover, adding ZnO increase sensitivity to chemicals i.e., cationic surfactant and organic solvent. These nanocomposite materials can be utilized in various applications such as colorimetric sensors, smart labels, thermochromic inks/paints that change color in the hot, cold or ambient conditions.

Keywords: Polydiacetylene, Reversible Thermochromism, Nanocomposites,

Alkyl chain length, Chemical sensor

คำนำ

ผลการวิจัยในโครงการวิจัยนี้ได้ถูกจัดเตรียมเป็น manuscript สำหรับการตีพิมพ์ลงวารสารทั้งหมดแล้ว และได้รับการตีพิมพ์ และตอบรับให้ตีพิมพ์แล้วบางส่วน โดยแต่ละ manuscript มีองค์ประกอบทางวิชาการครบถ้วน มีการนำเสนอผลการทดลอง และวิเคราะห์ผลการทดลองอย่างละเอียด ดังนั้นผู้วิจัยได้นำเนื้อหาของแต่ละ manuscript มารวมไว้ในรายงานวิจัยฉบับนี้ เพื่อคงรูปแบบการนำเสนอผลงานวิจัยให้เป็นไปตามแบบแผน ซึ่งในแต่ละส่วนจะมีเนื้อหาที่จบในตัวเองพร้อมทั้งเอกสารอ้างอิง ในส่วนของผลการทดลองทางด้านสมบัติฟลูออเรสเซนส์นั้น ผลการทดลองที่ได้ยังไม่มีข้อสรุปที่ชัดเจน ผู้วิจัยจึงยังไม่ได้รวมไว้ในรายงานฉบับนี้ อย่างไรก็ตาม ผู้วิจัยได้ศึกษาเพิ่มเติมในส่วนของผลของค่าความเป็นกรดเบสในกระบวนการเตรียมสารต่อการจัดเรียงตัวของพอลิเมอร์บนอนุภาคซิงก์ออกไซด์ ซึ่งได้ผลการทดลองที่ดี มีความน่าสนใจ และผลงานวิจัยได้รับการตีพิมพ์ในวารสารวิชาการระดับนานาชาติที่มีค่า impact factor เป็นที่เรียบร้อยแล้ว

รองศาสตราจารย์ ดร.นิศานาถ ไตรผล

ผู้จัดทำ

บทที่ 1

Low-Temperature Reversible Thermochromic Polydiacetylene/Zinc(II)/Zinc Oxide Nanocomposites for Colorimetric Sensing

Abstract

A series of reversible thermochromic polydiacetylene/zinc(II) ion/zinc oxide (PDA/Zn^{2+}/ZnO) nanocomposites has been prepared using 7 types of diacetylene monomer. The shortening of PDA alkyl tail from 12 to 6 methylene units systematically decreases color-transition temperature (T_{CT}) from 90 to 30 ^{o}C. Increasing of photopolymerization time during the preparation process further reduces the T_{CT} down to 10 ^{o}C. The shortening of alkyl segment adjacent to PDA headgroup causes unpredictable changes of T_{CT}. X-ray diffraction reveals variation of molecular tilting angle within the bilayer structure of PDA depending on the length of alkyl segment. Infrared and Raman spectroscopies also detect the change of local interactions and backbone conformation within the nanocomposites. Our study provides a guideline for preparing reversible thermochromic materials with T_{CT} ranging from 10 ^{o}C to 90 ^{o}C. These nanocomposite materials

can be utilized in various applications such as colorimetric sensors, smart labels, thermochromic inks/paints that change color in the hot, cold or ambient conditions.

Keywords: Polydiacetylene; Nanocomposites; Reversible Thermochromism, Alkyl chain length, Packing structure

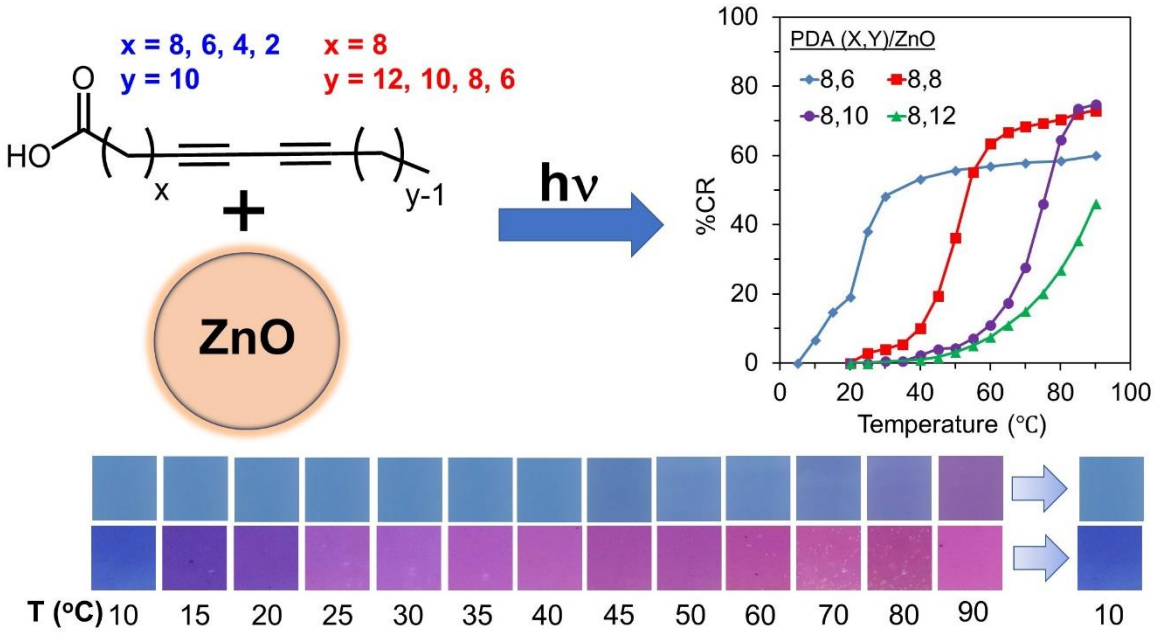

Highlights

- Series of reversible thermochromic polydiacetylene/zinc(II) ion/zinc oxide nanocomposites were prepared.
- Low-temperature reversible thermochromism is achieved by molecular engineering.
- Color-transition temperature can be tuned between 10 and 90 °C.

- Molecular packing structure varies with polydiacetylene alkyl chain length.
- Alkyl chain length affects local interaction and backbone conformation of polydiacetylene.

Introduction

Nowadays, colorimetric sensors have become popular tools to detect various classes of stimuli. Their unique advantages include simple detection, high sensitivity, and ease of sample preparation. Polydiacetylene (PDA) is a type of conjugated polymers that has been widely utilized for sensing applications [1,2]. This class of polymer is normally prepared via topotactic photopolymerization, providing a metastable state with blue color. It has been known that environmental perturbation of PDA assemblies by heat [3-12], acid/base [6,11,13-17], surfactants [5,18-20], gases [10,13,21], near-infrared light [3], mechanical stress [22], and biomolecules [2,23-26] results in color transition. Conformational changes of conjugated backbone and alkyl side chains have been suggested as main reasons for the color transition of PDA assemblies [6,8,27-30].

Over the past few decades, development of reversible thermochromic PDA-based materials has received tremendous attention [1,3-10,12,27,28,31-42]. This mainly stems from their potential utilization in various technologies such as electro-thermochromic displays [43], counterfeiting materials [44], smart textiles [45], and ink-jet printable thermal sensors [1]. Generally,

reversible thermochromism can be obtained by increasing intra- and intermolecular interactions within the PDA assemblies. This can be achieved by two major approaches. The first one involves structural modification of PDA head group and alkyl side chain [3-5,7,10,12,32-39]. For example, while PDA prepared from 10,12-pentacosadiynoic acid (PCDA) exhibits irreversible color transition [5,11], studies by Kim et.al demonstrated that modification of the poly(PCDA) headgroup with aromatic moieties resulted in reversible thermochromism at 90 ^{o}C [39]. Different headgroups were explored by other research works [3,4,32,36,38]. Wacharasindhu et.al connected the poly(PCDA) headgroup using various chemical linkers [33-35]. This class of bisdiynamide PDAs also exhibited reversible thermochromism at 90 ^{o}C [12]. An attempt to tune down the reversible color-transition temperature (T_{CT}) was performed by reducing alkyl chain length. The lowest T_{CT} of 45 ^{o}C was achieved. The second approach utilizes foreign materials to enhance interactions within the PDA assemblies. Several research groups reported that addition of various cations promoted strong ionic interactions with carboxylate headgroup of poly(PCDA) [27,28,31,40,46,47]. The resulting poly(PCDA)/M^{n+} nanocomposites exhibited reversible thermochromism with T_{CT} of 90 ^{o}C. The noticeable advantage of this approach over the structural modification is the simpler preparation process.

Recent studies by our group demonstrated that a simple method of mixing poly(PCDA) with ZnO nanoparticle provides reversible thermochromism [6,8,41,42,48,49]. The Zn^{2+} ions released from ZnO nanoparticles intercalated with the carboxylate headgroup of poly(PCDA) via strong electronic interaction [48]. The poly(PCDA)/Zn^{2+}/ZnO nanocomposite exhibited reversible thermochromism at 90 ^{o}C. In an attempt to tune down $T_{CT,}$ 5,7-hexadecadiynoic acid (HDDA) was used in our previous study [42]. The shortening of alkyl segments reduced T_{CT} to 55 ^{o}C. We also introduced a new strategy for fine tuning the T_{CT} by increasing photopolymerization time, which induced partial relaxation of PDA segments [8,49]. As a result, the poly(PCDA)/Zn^{2+}/ZnO nanocomposites with T_{CT} ranging from 45 to 90 ^{o}C were obtained.

Low-temperature thermochromic PDAs have been reported by several groups[50-52]. Studies by Kim et.al showed that the modification of headgroup using isocyanate or ester moieties reduced the strength of interactions within PDA assemblies, resulting in a drastic drop of T_{CT}. The resultant PDAs exhibited irreversible blue-to-red color transition, ranging from 5 to 30 ^{o}C. Comprehensive work by Rougeau et.al also demonstrated that a systematic variation of headgroup structure and alkyl side chain length provided series of PDAs with wide range of T_{CT}. The irreversible T_{CT} as low as -50 ^{o}C was reported. These low-temperature thermochromic PDAs can be utilized as intelligent labels that determine thermal history of products during the

transportation or storage period. However, the PDA-based material that exhibits reversible thermochromism at low temperature region is quite rare. In fact, the reversible thermochromic PDA-based materials reported to date have a color-transition temperature above 40 ^{o}C.

In this study, we take a step toward demonstrating that the reversible thermochromic nanocomposite with T_{CT} below ambient condition can be achieved. We can obtain a reversible T_{CT} as low as 10 ^{o}C, which has never been reported in any other PDA-based material. The reversible T_{CT} can be tuned between 10 to 90 ^{o}C. The nanocomposites with wide range of reversible T_{CT} have a potential for being utilized as colorimetric sensors, thermochromic inks/paints and smart labels that determine a real-time temperature of foods, beverages and other products. Various types of diacetylene (DA) monomer were used to prepare PDA(x,y)/Zn^{2+}/ZnO nanocomposites, where x and y represent methylene units adjacent to the carboxylic headgroup and at the alkyl tail, respectively (Fig. 1). The photopolymerization time was also varied to control the conformation of PDA backbone. The influences of PDA alkyl chain length on molecular packing, interfacial interactions, and backbone conformation are explored by various techniques.

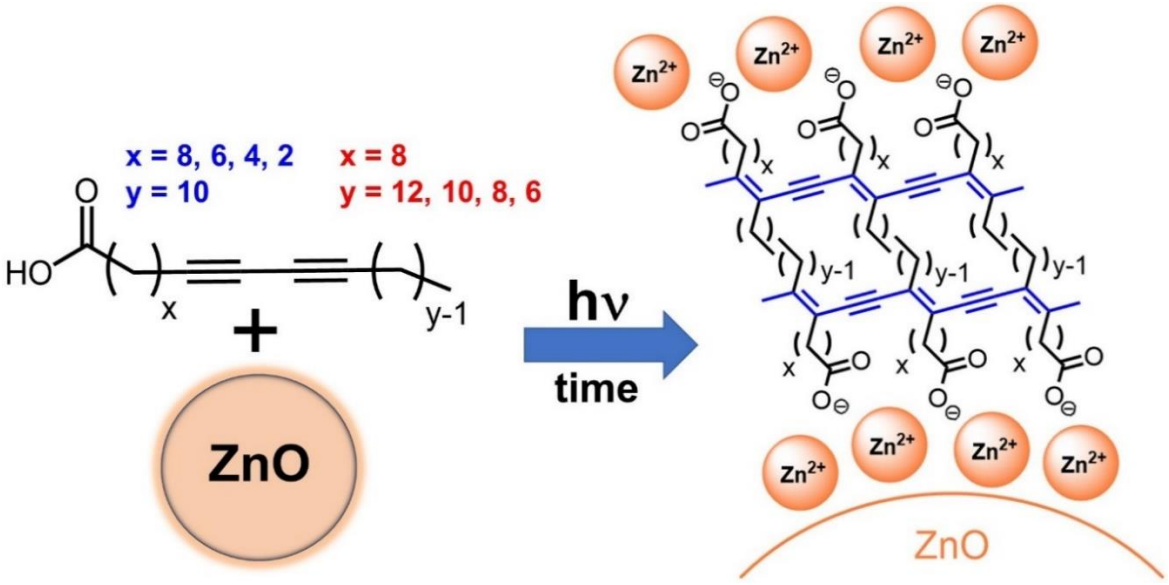

Fig. 1 Schematic representation of the preparation of the PDA/Zn^{2+}/ZnO nanocomposites. The length of alkyl side chain and photopolymerization time are systematically varied.

Experimental

DA monomers, 4, 6-heptadecadiynoic acid (DA(2,10)), 6,8-nonadecadiynoic acid (DA(4,10)), and 8,10-henicosadiynoic acid (DA(6,10)) were commercially available at Wako Chemical (Japan) whereas 10,12-tricosadiynoic acid (DA(8,10)) and 10,12-pentacosadiynoic acid (DA(8,12)) were purchased from Aldrich. The 10,12-nonadecadiynoic acid (DA(8,6)) and 10,12-henicosadiynoic acid (DA(8,8)) were synthesized as reported in a literature [34]. ZnO nanoparticles with particle size ranging from 20 to160 nm were purchased from Nano Materials Technology (Thailand) [8]. The PDA(x,y)/Zn^{2+}/ZnO nanocomposites were prepared as described in our previous

reports [41,42]. The concentration of PDAs was 1 mM while the ZnO/PDA ratio was kept at 10 wt%. The blue phase of all nanocomposites was obtained by UV light irradiation (λ = 254 nm, 10 watts) for 1 min.

Molecular packing structure of the nanocomposites was studied using X-ray diffractometer (XRD) (Bruker AXS Model D8 Discover, λ(Cu-K_α) = 1.54 Å). Dried samples were prepared by drop casting onto glass slides. Morphologies and particle size distribution of the nanocomposites were investigated by scanning electron microscopy (SEM, JOEL, JSM-6400) and dynamic light scattering (DLS, Brookhaven, ZetaPaLs). The infrared (IR) and Raman spectra were measured using Nicolet 6700 FT-IR spectrometer and FT-Raman spectrometer (PerkinElmer Spectrum GX) with a 1064 nm laser (Nd:YAG) as an excitation source. Thermochromic properties were investigated using UV-Vis spectrophotometer equipped with a temperature-control unit (Analytik Jena Specord S100).

Results and discussion

Morphologies and Molecular packing

Morphologies of PDA(x,y)/Zn^{2+}/ZnO nanocomposites are shown in Fig. 2. The SEM image of PDA(8,12)/Zn^{2+}/ZnO nanocomposite reveals round-shape particles with diameter of ~200 nm.

A systematic increase of particle size is observed when the alkyl tail of PDA is shortened. The diameter of the PDA(8,6)/Zn^{2+}/ZnO nanocomposite is ~1 μm. The morphology of the particle also changes to a sheet-like structure. The shortening of the alkyl segment adjacent to the carboxylate head group of PDA shows a similar trend. Micron-size particles are detected in the systems of PDA(4,10)/Zn^{2+}/ZnO and PDA(2,10)/Zn^{2+}/ZnO nanocomposites. The investigation of particle sizes in aqueous suspension by DLS also shows the increase in particle size with shortening of the length of PDA alky segment (Fig. 3). As shown in our previous studies, this class of nanocomposite forms a core-shell structure (Fig. 2h), in which, the ZnO nanoparticle acts as an anchoring substrate for the PDA carboxylate head group [41,48]. Since this study uses the same batch of ZnO nanoparticle, the increase of particle size indicates the growth of PDA/Zn^{2+} outer layer. Therefore, the shortening of PDA alkyl segment promotes the molecular assembly of PDA/Zn^{2+} layer within the nanocomposite. Theoretical study of surfactant systems has shown that the shortening of alkyl side chain strongly affects the packing parameter and aggregation number of the assemblies[53]. We believe that the change of packing parameter influences the growth mechanism of Zn^{2+}-intercalated bilayer structure within the nanocomposite. However, our nanocomposite system is quite complex due to the presence of strong coulombic interaction between carboxylate headgroup and Zn^{2+}/ZnO. More detailed study is required to understand

the origins of this result. In comparison with our previous study on the system of pure PDAs [11], the particle size of the nanocomposites is much larger. This observation also indicates that the presence of ZnO nanoparticle as an anchoring substrate facilitates the molecular organization within this system.

Molecular packing structure of the PDA(x,y)/Zn^{2+}/ZnO nanocomposites can be explored by XRD. It has been known that the PDAs form a bilayer lamellar structure where the interlamellar d-spacing can be determined from the length of the alkyl side chain [5,11,28-31,41]. In our previous study on this series of pure PDAs, a systematic decrease of d-spacing value with shortening of the alkyl side chain was observed [11]. For the bilayer structure of pure PDA(8,12), d-spacing value of 4.5 nm was reported. The XRD pattern of PDA(8,12)/Zn^{2+}/ZnO nanocomposite in Fig. 4 corresponds to the bilayer structure. The average d-spacing value calculated from the diffraction peaks is 5.5 nm. The increase of d-spacing value indicates the intercalation of Zn^{2+} ions, released from ZnO nanoparticles, with PDA layers [48]. The XRD patterns of other nanocomposites also show larger d-spacing values compared to those of their pure PDA counterparts. The XRD patterns of DA(x,y)/Zn^{2+}/ZnO assemblies were also recorded (Fig. S1, supporting information) to explore the change of molecular packing during topotactic photopolymerization process. Table 1 summarizes the average d-spacing values of all nanocomposites. Our XRD measurements show

a slight decrease of d-spacing values when DA(x,y)/Zn^{2+}/ZnO assemblies are photopolymerized to form PDA(x,y)/Zn^{2+}/ZnO nanocomposites. The result is consistent with the previous studies, which reported the shrinkage of unit cell during the photopolymerization process [29,30]. However, a discrepancy was observed for the systems of DA(8,6)/Zn^{2+}/ZnO and DA(2,10)/Zn^{2+}/ZnO nanocomposite, where the d-spacing values did not decrease during the photopolymerization. Similar results were also reported in our previous study of pure DA(8,6) and DA(2,10) monomers [11]. We believe that the shortening of the PDA alkyl segment could cause the increase of molecular confinement within the bilayer structure, affecting the mechanism of structural transition. More detailed study is required in order to reveal the origins of this behavior.

The d-spacing values of the bilayer structure were then used to estimate the molecular tilting angle (θ) with respect to lamellar plane as shown in Fig. 4c. Here, we assume all-trans conformation of alkyl segment, head-to-head and tail-to-tail arrangement of the DA monomers. Since the DA molecules arrange into highly organized lamellar structure, the assumption of all-trans conformation of alkyl segment is reasonable. We also measure FT-IR spectra of all samples to investigate the conformation of alkyl segment (Fig. S2, supporting information). The $\nu_s(CH_2)$ and $\nu_{as}(CH_2)$ of all samples are detected at 2848 cm^{-1} and 2919 cm^{-1}, respectively, indicating the presence of all-trans conformation[15,47]. The formation of gauche conformation would shift the

vibrational bands to higher wavenumber. The L values are estimated from the extended length (L_0) of DA monomers and ionic diameter of Zn^{2+} ion (0.18 nm). The L_0 value of all DA monomers in Table 1 were reported in the previous studies [11,40]. The estimated θ value for the system of pure DA(8,12) monomer is 48° [11]. The shortening of alkyl segment of DA(x,y) causes a slight variation of the θ value ranging from 47° to 48°. Interestingly, the θ value significantly increases to 55° in the bilayer structure of pure DA(2,10) monomer where the alkyl segment adjacent to head group is relatively short. In the system of DA(8,12)/Zn^{2+}/ZnO nanocomposite, a drastic increase of θ value to 59° is detected. This result indicates that the coulombic interaction between Zn^{2+} ion and carboxylate headgroup of DA(8,12) strongly influences the molecular arrangement within the bilayer structure. The shortening of DA alkyl tail also results in a systematic decrease of θ value. The bilayer structure of DA(8,6)/Zn^{2+}/ZnO nanocomposite exhibits θ value of 54°. A similar trend is observed when the alkyl segment adjacent to carboxylate headgroup is shortened (Table 1). The θ value of DA(2,10)/Zn^{2+}/ZnO nanocomposite is 53°. It is worthwhile to note that DA(2,10)/Zn^{2+}/ZnO nanocomposite exhibits a smaller θ value compared to that of the pure DA(2,10) monomer. This observation is opposite to the other DA(x,y) systems investigated in this study. Our results further emphasize the important role of the length of the alkyl chain adjacent to PDA head group on the molecular packing structure within the assemblies. A previous study

of 2D monolayer structure also observed a significant change of packing structure when the length of the alkyl chain adjacent to the head group became relatively short[54].

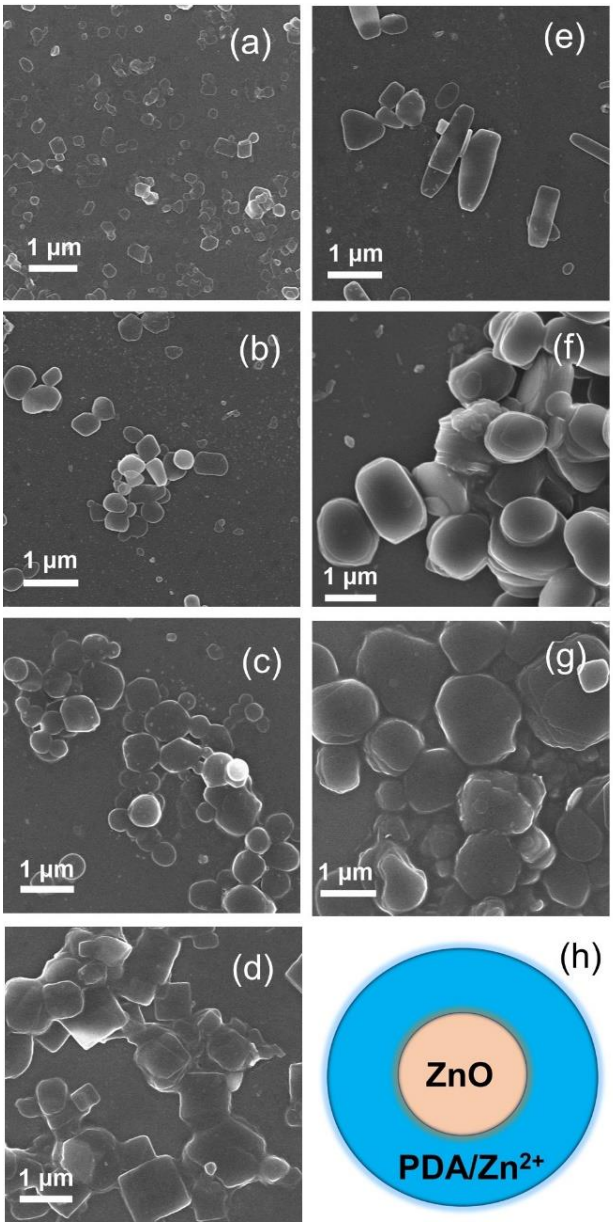

Fig. 2 SEM images of PDA(x,y)/Zn^{2+}/ZnO nanocomposites where (x,y) are (a) (8,12), (b) (8,10), (c) (8,8), (d) (8,6), (e) (6,10), (f) (4,10), and (g) (2,10). (h) Schematic core-shell structure of the nanocomposites.

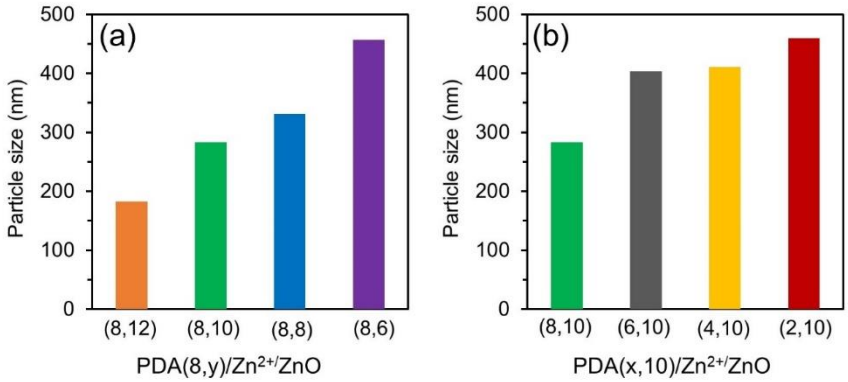

Fig.3 Median diameter of (a) PDA(8,y)/Zn^{2+}/ZnO and (b) PDA(x,10)/ Zn^{2+}/ZnO nanocomposites obtained using DLS

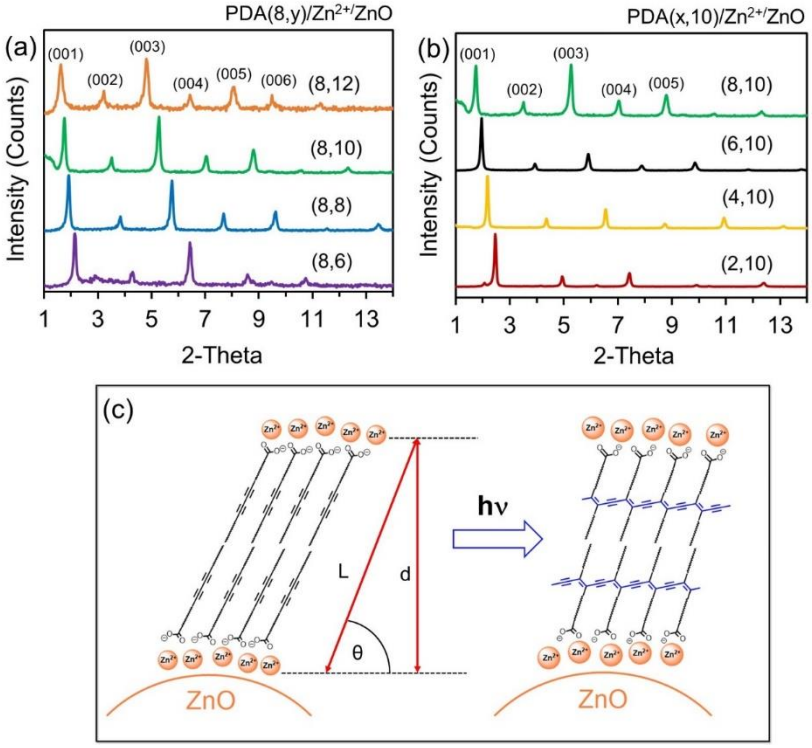

Fig. 4 XRD patterns of (a) PDA(8,y)/Zn^{2+}/ZnO and (b) PDA(x,10)/ Zn^{2+}/ZnO nanocomposites. (c) An estimation of tilting angle (θ) in the bilayer structure of DAs. The L values are estimated from the extended length (L_0) of DA monomers and ionic diameter of Zn^{2+} ion. The d values of the crystalline phase are calculated from the XRD data.

Table 1. The bilayer d-spacing values of DA(x,y)/Zn^{2+}/ZnO and resultant PDA(x,y)/Zn^{2+}/ZnO nanocomposites. Tilting angle (θ) values in the bilayer structure are estimated by using L= $2L_0$ + Zn^{2+} diameter, where L_0 is a molecular length of extended DAs.

DA(x,y)/Zn^{2+}/ZnO	Molecular length (L_0, nm)	Bilayer d-spacing (d, nm)	Tilting angle (θ, °)	PDA(x,y)/Zn^{2+}/ZnO	Bilayer d-spacing (d, nm)
DA(8,12)	3.18	5.6	59	PDA(8,12)	5.5
DA(8,10)	2.93	5.1	58	PDA(8,10)	5.0
DA(8,8)	2.68	4.7	58	PDA(8,8)	4.6
DA(8,6)	2.43	4.1	54	PDA(8,6)	4.1
DA(6,10)	2.68	4.5	54	PDA(6,10)	4.5
DA(4,10)	2.43	4.1	54	PDA(4,10)	4.0
DA(2,10)	2.18	3.6	53	PDA(2,10)	3.6

Tunable reversible thermochromism

In this section, the reversible thermochromic behavior of PDA(x,y)/Zn^{2+}/ZnO nanocomposites is adjusted by varying the alkyl chain and UV light irradiation time. The shortening of alkyl chain length reduces dispersion interactions within the system while the increase in UV light irradiation time affects the conformation of the conjugated backbone [8,11]. Absorption spectra of the initial blue phase of all nanocomposites are shown in Fig. 5. The spectra of PDA(8,12)/Zn^{2+}/ZnO, PDA(8,10)/Zn^{2+}/ZnO, and PDA(8,8)/Zn^{2+}/ZnO nanocomposites exhibit the same λ_{max} value at 640 nm. The λ_{max} shifts to 670 nm in the nanocomposite system of PDA(8,6)/Zn^{2+}/ZnO (Fig. 5a). The red-shift of λ_{max} value indicates the increase of conjugation length within PDA backbone when the alkyl tail becomes relatively short. We believe that the shortening of alkyl tail results in the increase of backbone rigidity and planarity, which, in turn, promotes the delocalization of π electrons within the PDA(8,6)/Zn^{2+}/ZnO nanocomposite. The shortening of alkyl segment adjacent to the carboxylate headgroup shows a similar trend. The spectra of PDA(6,10)/Zn^{2+}/ZnO and PDA(4,10)/Zn^{2+}/ZnO nanocomposites exhibit the shift of λ_{max} value to 660 nm (Fig. 5b). However, the nanocomposite prepared from PDA(2,10) has a shorter conjugation length with λ_{max} value of 645 nm.

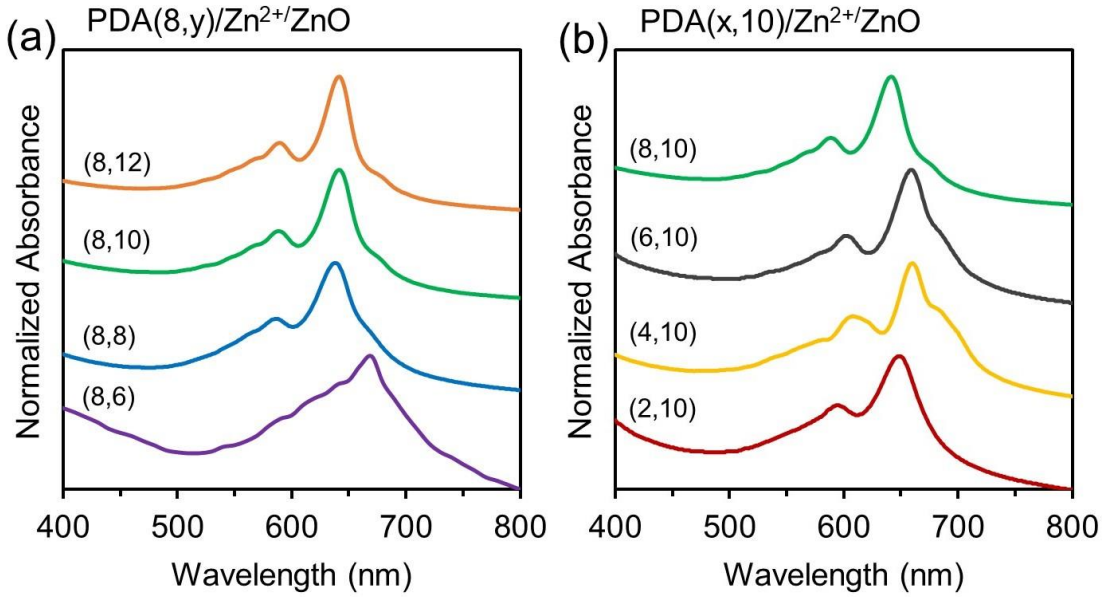

Fig. 5 Absorption spectra of the initial blue phase of (a) PDA(8,y)/Zn^{2+}/ZnO and (b) PDA(x,10)/Zn^{2+}/ZnO nanocomposites. All spectra were measured at 20 °C except for PDA(8,6)/Zn^{2+}/ZnO, which was measured at 10 °C due to its color change at room temperature.

All PDA(x,y)/Zn^{2+}/ZnO nanocomposites prepared in this study exhibit reversible thermochromism. The effect of alkyl tail length on color-transition temperature (T_{CT}) is illustrated in Fig. 6. Temperature-dependent absorption spectra of PDA(8,6)/Zn^{2+}/ZnO nanocomposite are shown in Fig. 6a. An isosbestic point is clearly observed indicating the transition of two district electronic species. A drastic drop of λ_{max} value from 670 nm to 620 nm is detected at ~20 °C. However, the color of aqueous suspension remains blue at this temperature. A gradual transition

to purple is detected at ~30 °C (Fig. 6c). The increase of alkyl tail length in the nanocomposite system of PDA(8,8)/Zn^{2+}/ZnO results in the increase of T_{CT} to 50 °C where λ_{max} descends to 590 nm (Fig. 6b). Color photographs taken upon a heating/cooling cycle of PDA(8,y)/Zn^{2+}/ZnO nanocomposites are shown in Fig. 6c. From naked-eye observation, the blue-to-purple color transition of PDA(8,6)/Zn^{2+}/ZnO, PDA(8,8)/Zn^{2+}/ZnO, PDA(8,10)/Zn^{2+}/ZnO, and PDA(8,12)/Zn^{2+}/ZnO nanocomposites occurs at 30, 50, 70, and 90 °C, respectively. Therefore, the increase of two methylene units within alkyl tail causes the increase of T_{CT} by ~20 °C. A complete color reversibility is observed upon cooling to room temperature. The color reversibility persists up to 10 times of heating/cooling cycles between 25 °C and 90 °C (Fig. S4, supporting information). Study by differential scanning calorimetry (DSC) in our previous report showed that the reversible color transition related to the melting of alkyl side chain[8]. Plots of colorimetric response (%CR) and λ_{max} versus temperature are shown in Fig. 6d and e. The result demonstrates the systematic increase of the T_{CT} with the longer alkyl tail length, which is parallel to the pure PDA systems [11]. However, the pure PDAs of this series exhibit irreversible thermochromism with T_{CT} ranging from ~40 to ~60 °C. It is worthwhile to note that the PDA(8,6)/Zn^{2+}/ZnO nanocomposite exhibits color transition near ambient temperature. The T_{CT} of

30 °C is lower than those of other reversible thermochromic PDA-based materials previously reported in literature.

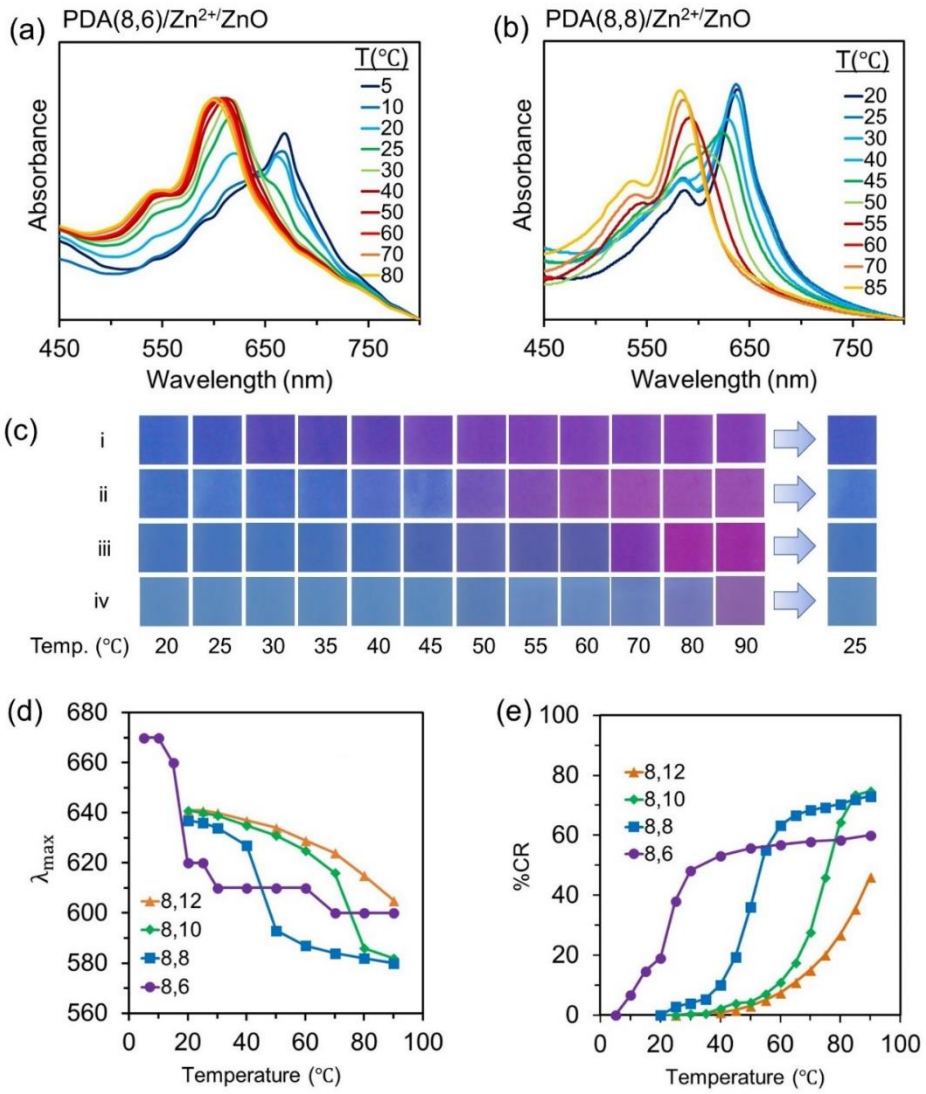

Fig. 6 Absorption spectra of (a) PDA(8,6)/Zn^{2+}/ZnO and (b) PDA(8,8)/Zn^{2+}/ZnO nanocomposites measured upon increasing temperature. (c) Color photographs of PDA(8,y)/ Zn^{2+}/ZnO nanocomposites taken upon heating/cooling ((i) y=6, (ii) y=8, (iii) y=10 and (iv) y=12). Plots of (d) λ_{max} and (e) %CR as a function of temperature.

The variation of methylene unit adjacent to PDA headgroup leads to rather different results. Absorption spectra of PDA(2,10)/Zn^{2+}/ZnO and PDA(6,10)/Zn^{2+}/ZnO nanocomposites measured upon increasing temperature are shown in Fig. 7(a,b). The PDA(2,10)/Zn^{2+}/ZnO nanocomposite exhibits a sharp transition at ~55°C where the λ_{max} drops from 640 nm to 580 nm. The color photographs in Fig. 7c show a clear blue-to-purple color transition in this system. The increase of two methylene units in PDA(4,10)/Zn^{2+}/ZnO nanocomposite causes a significant increase of T_{CT} to 80 ^{o}C. However, color transition gradually occurs in this system, in which, λ_{max} gradually decreases to ~600 nm at 90 ^{o}C (Fig. 7d). The two additional methylene units in the PDA(6,10)/Zn^{2+}/ZnO nanocomposite, however, scarcely increase the T_{CT} or alter the color-transition behavior (Fig. 7d and e). Further increase of two methylene units results in the PDA(8,10)/Zn^{2+}/ZnO nanocomposite with the longest methylene segment in this series, which shows a sharp blue-to-purple color transition at ~70 ^{o}C. Our results indicate that the change of the length of the methylene segment adjacent to PDA headgroup provides an unpredictable trend of T_{CT}. The investigation of pure PDAs of this series showed rather interesting thermochromic behaviors [11]. The shortening of alkyl segment in pure PDA(2,10) caused drastic increase of T_{CT}, which is related to the increase in local interactions between the headgroups. Studies by other research groups also detected the change of local interactions and molecular packing when the

alkyl segment adjacent to the headgroup became relatively short [54,55]. The nature of local interactions of PDA(x,y)/ Zn^{2+}/ZnO nanocomposites is explored in the following section utilizing FT-IR spectroscopy. It is worthwhile to note that these nanocomposites exhibit dual colorimetric response to both acid and base[16,17,56]. However, the color transition is not reversible due to the corrosion of ZnO core at low and high pH region. The colorimetric response of PDA(2,10)/Zn^{2+}/ZnO nanocomposite to acid and base is shown as an example (Fig. S5, supporting information). Our previous study also shows that the PDA(8,12)/Zn^{2+}/ZnO nanocomposite can be dispersed in various organic solvents without changing the color[57]. We investigate the colorimetric response of PDA(2,10)/Zn^{2+}/ZnO nanocomposite to organic solvents in this study. This nanocomposite exhibits a colorimetric response to THF and propanol (Fig. S6, supporting information). When the solvents are removed, the color does not reverse back to the original state. However, the colorimetric response to organic solvents allows their utilization as chemical sensors. This topic is currently being under investigation in our group.

Our previous studies demonstrated that the increase of UV photopolymerization time caused a systematic decrease of T_{CT} of the PDA(8,12)/Zn^{2+}/ZnO nanocomposite [8,49]. Here, we explore the nanocomposite systems of PDA(8,6)/Zn^{2+}/ZnO and PDA(2,10)/Zn^{2+}/ZnO with the shortest alkyl segment at the tail and headgroup position, respectively. Fig. 8 illustrates

thermochromic behavior of the nanocomposites prepared using photopolymerization time of 1, 2, and 4 min. It is clear that the increase of photopolymerization time exhibits rather strong effect on the T_{CT} of PDA(8,6)/Zn^{2+}/ZnO nanocomposite. The color transition takes place at 30, 15, and 10 ^{o}C when the photopolymerization times are 1, 2, and 4 min., respectively. The plot of λ_{max} value versus temperature in Fig. 8c shows an abrupt change at the transition region. These nanocomposites still exhibit complete reversible thermochromism upon cooling to 5 ^{o}C. The decrease of T_{CT} is attributed to partial relaxation of conjugated PDA backbone upon increasing photopolymerization time. Detailed discussion of this topic is available in our previous report [8]. It is important to point out that this nanocomposite is the first example of reversible thermochromic PDA-based material with T_{CT} lower than the ambient temperature. This property allows cold-activated color transition, which can extend their utilization in various technologies.

The investigation of the PDA(2,10)/Zn^{2+}/ZnO nanocomposite, however, shows different results. The increase of photopolymerization time from 1 to 4 min. hardly affects the T_{CT} as shown in Fig. 8b. Even after further increase of the photopolymerization time to 60 min., the T_{CT} remains roughly at ~55 ^{o}C. Our observation suggests that it is more difficult to induce the relaxation of the PDA(2,10) conjugated backbone via the photopolymerization process. This is attributed to the relatively short alkyl segment adjacent to the PDA headgroup, which could cause the variation of

local interactions and confinement of the backbone. Further study is required in order to understand the origin of this behavior.

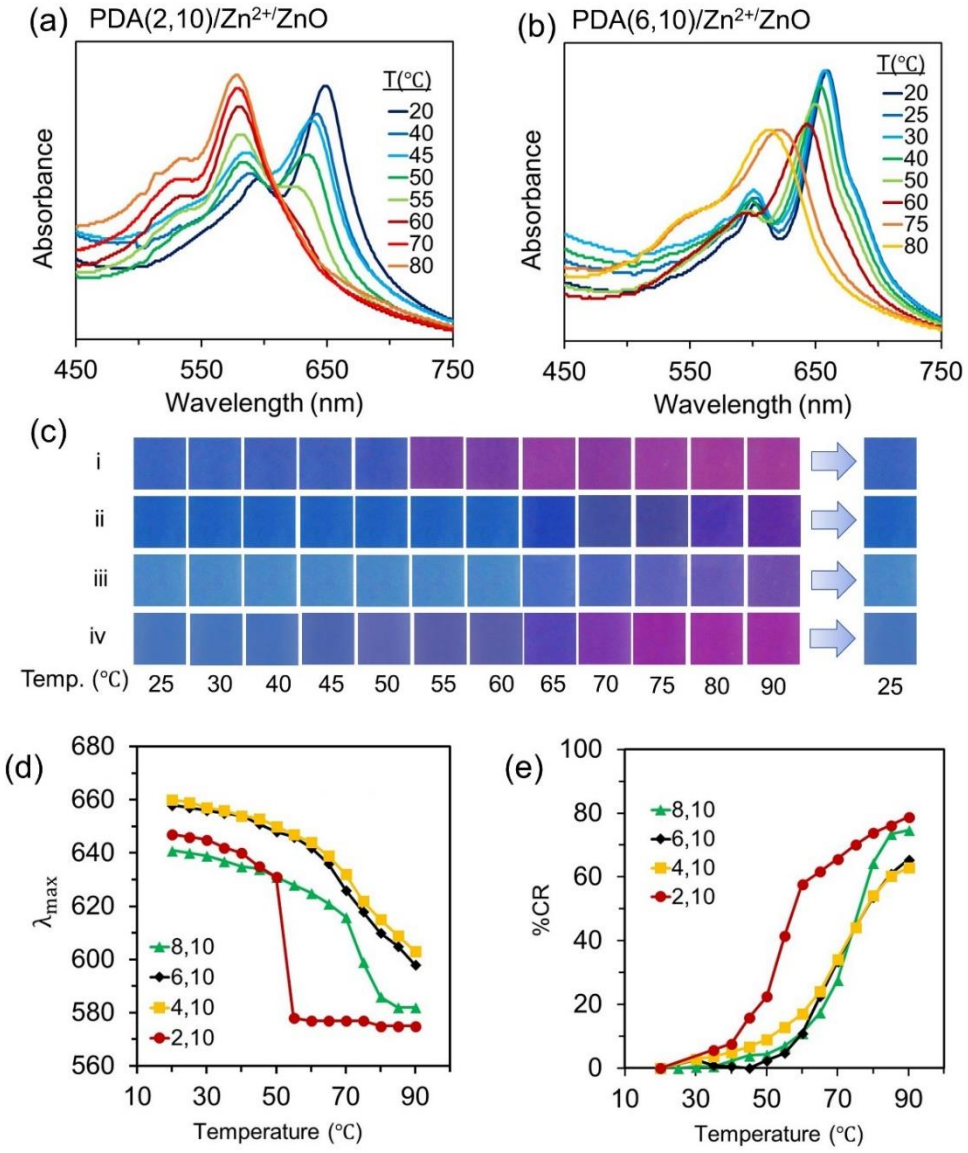

Fig. 7 Absorption spectra of (a) PDA(2,10)/Zn^{2+}/ZnO and (b) PDA(6,10)/Zn^{2+}/ZnO nanocomposites measured upon increasing temperature. (c) Color photographs of PDA(x,10)/ Zn^{2+}/ZnO nanocomposites taken upon heating/cooling ((i) x=2, (ii) x=4, (iii) x=6 and (iv) x=8). Plots of (d) λ_{max} and (e) %CR as a function of temperature.

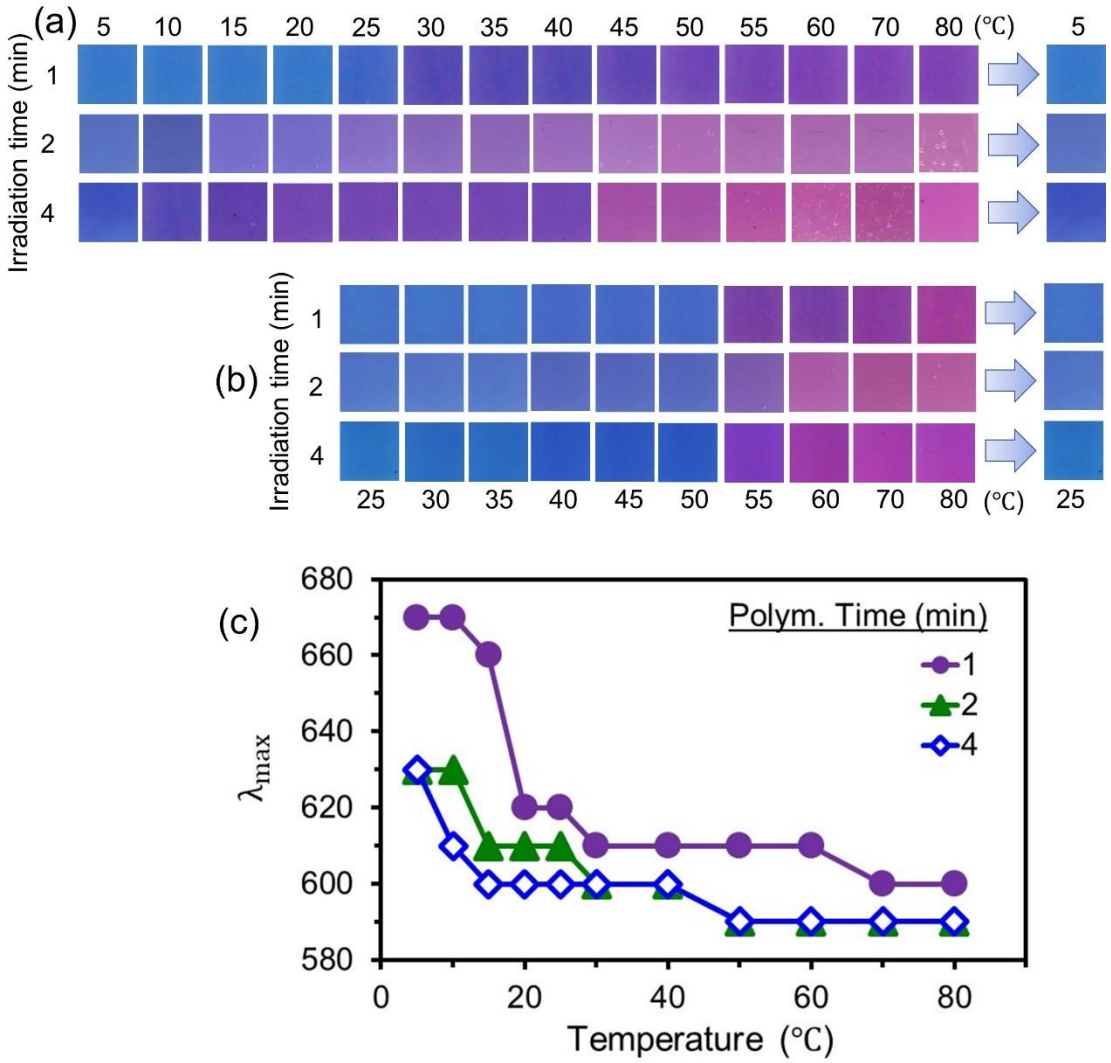

Fig. 8 Color photographs of (a) PDA(8,6)/Zn^{2+}/ZnO and (b) PDA(2,10)/Zn^{2+}/ZnO nanocomposites taken upon heating/cooling. The nanocomposites were prepared using UV light irradiation time of 1, 2, and 4 min. (c) Plot of λ_{max} as a function of temperature of the PDA(8,6)/$Zn^{2+/}$ZnO nanocomposites.

Low-temperature thermochromic PDAs have been reported by several previous studies[50-52]. However, the color transition of those PDAs at low temperature is the irreversible one. Our nanocomposites exhibit reversible thermochromism at low temperature, which is never been reported. We also emphasize on the effect of alkyl chain length at different position. The shortening of alkyl tail results in systematic decrease of the T_{CT}. On the other hand, the shortening of alkyl segment adjacent to the headgroup provides unpredictable change of T_{CT}. The photopolymerization time is also a key factor for T_{CT} in this study. The nanocomposites with wide range of reversible T_{CT} have a potential for being utilized as colorimetric sensors, thermochromic inks/paints and smart labels that determine a real-time temperature of foods, beverages and other products.

Interfacial interaction and backbone conformation

In this section, the FT-IR and FT-Raman spectroscopies are employed to explore the nature of local interactions and backbone conformation within the nanocomposites. The IR spectra of all PDA(x,y)/Zn^{2+}/ZnO nanocomposites are shown in Fig. 9. In the system of PDA(8,y)/Zn^{2+}/ZnO nanocomposites, all spectra exhibit the same pattern. Peaks in the region of 2800 to 3000 cm^{-1} correspond to vibrational frequencies of alkyl segments [5,6,15,47]. Our previous

studies showed that the IR spectra of pure PDAs constituted a broad peak near 1690 cm^{-1}, corresponding to hydrogen-bonded carbonyl stretching of –COOH headgroup[6,8,11]. This peak disappears from the IR spectra of nanocomposites. We detect a new peak at 1539 cm^{-1}, assigned to the ν_{as}COO stretching vibration of the carboxylate anion, which interacts strongly with the Zn^{2+} ion (Fig. 9a). The increase of overall interactions within this system results in the reversible thermochromism. Detailed analysis of the roles of ZnO nanoparticles and Zn^{2+} ion is available in our previous reports[6,48]. We observe that the shortening of PDA(8,y) alkyl tail hardly affects the position of peak at 1539 cm^{-1}. Therefore, nature of local interactions between the carboxylate headgroup and the Zn^{2+} ion remains the same in this series. This observation suggests that the systematic decrease of color-transition temperature of the PDA(8,y)/Zn^{2+}/ZnO nanocomposites shown in Fig. 6 mainly arises from the reduction of dispersion interactions due to the shortening of alkyl side chain.

The variation of alkyl segment adjacent to the carboxylate headgroup of PDA (x,10)/Zn^{2+}/ZnO nanocomposites shows rather interesting results (Fig. 9b). In the nanocomposite system of PDA(6,10)/Zn^{2+}/ZnO, we observe the splitting of ν_{as}COO stretching vibration into 1543 cm^{-1} and 1531 cm^{-1}. Previous studies reported that the ν_{as}COO peak of PDA shifted to different positions depending on the nature of local interactions with various cations [27,47].

Therefore, the detection of two vibrational peaks in this study indicates that the carboxylate headgroup of the PDA interacts with the Zn^{2+} ion in two different forms. A similar splitting pattern of ν_{as}COO stretching vibration is also observed in the nanocomposite system of PDA(4,10)/Zn^{2+}/ZnO. Our results shows that the shortening of alkyl segment adjacent to the PDA headgroup strongly influences the strength of local interactions between the carboxylate group and the Zn^{2+} ion. This behavior affects the color transition of the nanocomposites in an unpredictable manner as discussed in Fig. 7. These two nanocomposites exhibit a gradual color transition with relatively high color-transition temperature. In the nanocomposite system of PDA(2,10)/Zn^{2+}/ZnO containing the shortest alkyl segment, a single peak of ν_{as}COO stretching vibration is detected. However, it is shifted from 1539 cm^{-1} to 1547 cm^{-1}. This nanocomposite exhibits a sharp color transition with the lowest T_{CT} in this series.

The variation of alkyl chain length strongly affects the conformation of the PDA conjugated backbone within the nanocomposites. Raman spectra of all samples are shown in Fig. 10. It is known that a blue phase of pure PDA(8,12) exhibits distinct C≡C and C=C stretching frequencies at 2080 cm^{-1} and 1451 cm^{-1}, respectively [8,27,58]. Thermal treatment of the metastable blue phase normally causes relaxation of PDA conjugated backbone into new local environment, resulting in color transition into red phase. The C≡C and C=C stretching frequencies shift to 2116 cm^{-1} and

1511 cm^{-1}, respectively for red phase. Raman spectrum of PDA(8,12)/Zn^{2+}/ZnO nanocomposite shows two peaks at 2076 cm^{-1} and 1448 cm^{-1}, corresponding to the backbone conformation in the blue phase. The shortening of the alkyl tail of PDA(8,10)/Zn^{2+}/ZnO and PDA(8,8)/Zn^{2+}/ZnO nanocomposites does not alter the position of the Raman peaks. In the nanocomposite system of PDA(8,6)/Zn^{2+}/ZnO, however, the peaks shift to 2105 cm^{-1} and 1474 cm^{-1} indicating the relaxation of the PDA conjugated backbone. Since the positions of these peaks are different from those of the red phase, this type of relaxation is not due to the blue-to-red color transition. In fact, the absorption spectrum of PDA(8,6)/Zn^{2+}/ZnO nanocomposite measured at room temperature exhibits λ_{max} at 610 nm, and its color appears purple (Fig. 6). We suggest that the shortening of alkyl tail causes the reduction of dispersion interaction within the nanocomposite, allowing partial relaxation of conjugated backbone. This type of backbone relaxation is similar to previous studies exploring the effects of temperature and photopolymerization time [8,27].

The shortening of alkyl segment adjacent to the PDA headgroup also leads to partial relaxation of the conjugated backbone within the nanocomposite. The Raman spectrum of PDA(2,10)/Zn^{2+}/ZnO nanocomposite shows splitting peaks in both vibrational regions. The peaks of C≡C and C=C stretching modes are observed at 2103/2079 and 1477/1446 cm^{-1}, respectively (Fig. 10b). The growth of new peaks at 2103 and 1477 cm^{-1} indicates the relaxation of some PDA

backbones into the purple phase. Absorption spectra in Fig. 7a also show the growth of peak at 585 nm. However, large fraction of the PDA remains in the blue phase. Therefore, the sample appears blue at ambient conditions. Fig. 10c illustrates the stacking of PDA conjugated backbone within its bilayer structure. We suggest that the structural relaxation relates to the decrease of stacking distance between the conjugated backbone of PDA. Our hypothesis is parallel to previous studies by X-ray scattering techniques reporting the shrinkage of unit cell during the color transition process of PDA [29,30].

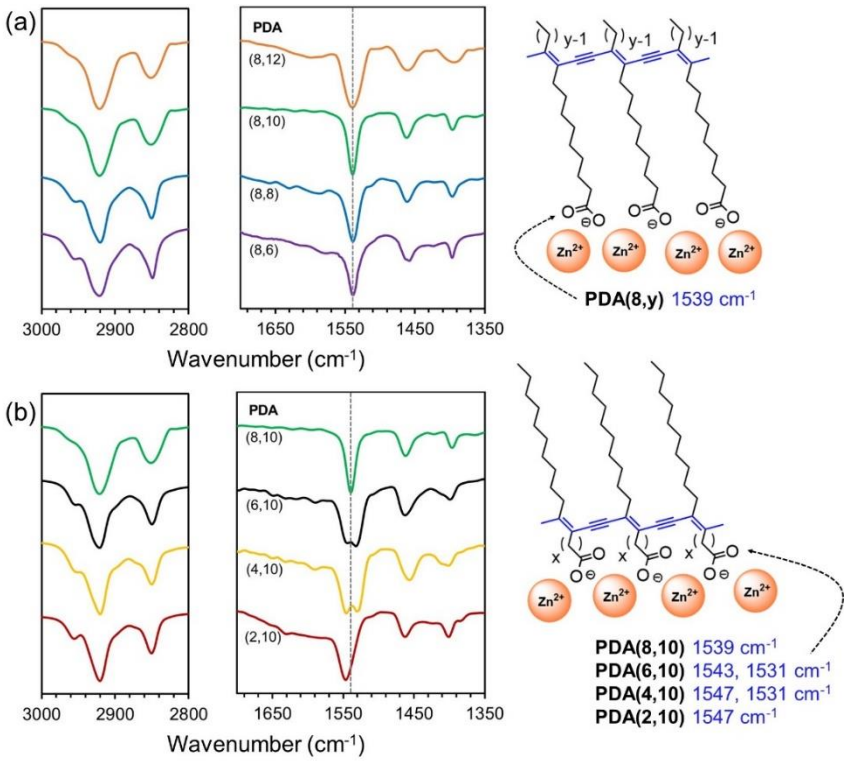

Fig. 9 FT-IR spectra measured at room temperature and schematic representation of the interaction between Zn^{2+} ions and COO^- at PDAs head group of (a) PDA(8,y)/Zn^{2+}/ZnO and (b) PDA(x,10)/Zn^{2+}/ZnO nanocomposites.

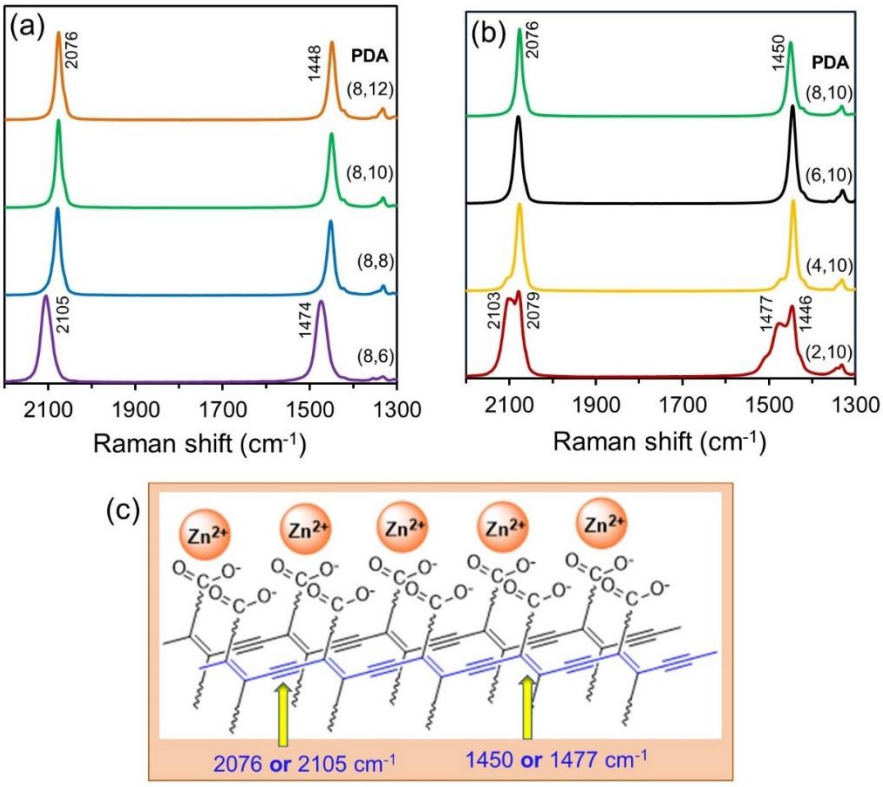

Fig. 10 FT-Raman spectra of (a)PDA(8,y)/Zn^{2+}/ZnO and (b)PDA(x,10)/Zn^{2+}/ZnO nanocomposites measured at room temperature. (c) Vibrational wavenumbers of the triple bond and double bond within the conjugated backbone of PDA.

Conclusion

Our study introduces a new approach for preparing reversible thermochromic PDA-based materials with color-transition temperature ranging from 10 to 90 ^{o}C. The reversible thermochromism below ambient condition is achieved via the combined molecular engineering at side chain moieties and PDA conjugated backbone. The shortening of side chain length at the

tail position of the PDA provides a predictable reduction of the color-transition temperature, attributed to the decrease of dispersion interactions within the nanocomposite. On the other hand, it is rather difficult to predict the thermochromic behavior when the alkyl segment adjacent to the PDA headgroup is varied. This is mainly due to the variation in nature of local interactions between PDA headgroup and Zn^{2+} ion within the nanocomposite. The XRD and Raman spectroscopy also detect systematic changes of molecular tilting angle and backbone conformation within the bilayer structure when the side chain length is varied. Our major finding in this study provides a guideline for fabricating reversible thermochromic PDA-based materials with a wide range of color-transition temperature. This can extend their utilization in various applications such as colorimetric sensors, thermochromic inks/paints and smart labels.

References

(1) Qian, X.; Stadler, B. Recent Developments in Polydiacetylene-Based Sensors. *Chem. Mater.* **2019**, *31*, 1196-1222.

(2) Wen, J. T.; Roper, J. M.; Tsutsui, H. Polydiacetylene Supramolecules: Synthesis, Characterization, and Emerging Applications. *Ind. Eng. Chem. Res.* **2018**, *57*, 9037-9053.

(3) Hu, B.; Sun, S.; Wu, B.; Wu, P. Colloidally Stable Monolayer Nanosheets with Colorimetric Responses. *Small* **2019**, *15*, 1804975.

(4) Mergu, N.; Kim, H.; Heo, G.; Son, Y.-A. Development of Naphthalimide-Functionalized Thermochromic Conjugated Polydiacetylenes and their Reversible Green-to-Red Chromatic Transition in the Solid State. *Dyes Pigm.* **2019**, *164*, 355-362.

(5) Khanantong, C.; Charoenthai, N.; Kielar, F.; Traiphol, N.; Traiphol, R. Influences of Bulky Aromatic Head Group on Morphology, Structure and Color-Transition Behaviors of Polydiacetylene Assemblies upon Exposure to Thermal and Chemical Stimuli. *Colloids Surf. A* **2019**, *561*, 226-235.

(6) Seetha, S.; Saymung, R.; Traiphol, R.; Traiphol, N. Controlling Self-Assembling and Color-Transition of Polydiacetylene/Zinc(II) ion/Zinc Oxide Nanocomposites by Varying pH: Effects of Surface Charge and Head Group Dissociation. *J. Ind. Eng. Chem.* **2019**, *72*, 423-431.

(7) Kim, M. J.; Angupillai, S.; Min, K.; Ramalingam, M.; Son, Y.-A. Tuning of the Topochemical Polymerization of Diacetylenes Based on an Odd/Even Effect of the Peripheral Alkyl Chain: Thermochromic Reversibility in a Thin Film and a Single-Component Ink for a Fountain Pen. *ACS Appl. Mater. Interfaces* **2018**, *10*, 24767-24775.

(8) Potai, R.; Faisadcha, K; Traiphol, R.; Traiphol, N. Controllable Thermochromic and Phase Transition Behaviors of Polydiacetylene/Zinc(II) Ion/Zinc Oxide Nanocomposites via Photopolymerization: An Insight into the Molecular Level. *Colloids Surf. A* **2018**, *555*, 27-36.

(9) Oaki, Y.; Ishijima, Y.; Imai. H. Emergence of Temperature-Dependent and Reversible Colorchanging Properties by the Stabilization of Layered Polydiacetylene through Intercalation. *Polymer J.* **2018**, *50*, 319-326.

(10) Jeong, W.; Khazi, M.I.; Lee, D. G.; Kim. J.-M. Intrinsically Porous Dual-Responsive Polydiacetylenes Based on Tetrahedral Diacetylenes. *Macromolecules* **2018**, *51*, 10312-10322.

(11) Khanantong, C.; Charoenthai, N.; Phuangkaew, T.; Kielar, F.; Traiphol, N.; Traiphol, R. Phase Transition, Structure and Color-Transition Behaviors of Monocarboxylic Diacetylene and Polydiacetylene Assemblies: The Opposite Effects of Alkyl Chain Length. *Colloids Surf. A* **2018**, *553*, 337-348.

(12) Khanantong, C.; Charoenthai, N.; Wacharasindhu, S.; Sukwattanasinitt, M.; Traiphol, N.; Traiphol, R. Influences of Solvent Media on Chain Organization and Thermochromic Behaviors of Polydiacetylene Assemblies Prepared from Monomer with Symmetric Alkyl Tails. *J. Ind. Eng. Chem.* **2018**, *58*, 258-265.

(13) Nguyen, L. H.; Naficy, S.; McConchie, R.; Dehghani, F.; Chandrawati, R. Polydiacetylene-Based Sensors to Detect Food Spoilage at Low Temperatures. *J. Mater. Chem. C* **2019**, *7*, 1919-1926.

(14) Song, S.; Cho, H.-B.; Lee, H. W.; Kim, H. T. Onsite Paper-Type Colorimetric Detector with Enhanced Sensitivity for Alkali Ion via Polydiacetylene-Nanoporous Rice Husk Silica Composites. *Mater. Sci. Eng. C* **2019**, *99*, 900-904.

(15) Kew, S. J.; Hall, E. A. H. pH Response of Carboxy-Terminated Colorimetric Polydiacetylene Vesicles. *Anal. Chem.* **2006**, *78*, 2231-2238.

(16) Chanakul, A.; Traiphol, R.; Traiphol, N. Utilization of Polydiacetylene/Zinc Oxide Nanocomposites to Detect and Differentiate Organic Bases in Various Media. *J. Ind. Eng. Chem.* **2017**, *45*, 215-222.

(17) Chanakul, A.; Traiphol, R.; Traiphol, N. Colorimetric Sensing of Various Organic Acids by Using Polydiacetylene/Zinc Oxide Nanocomposites: Effects of Polydiacetylene and Acid Structures. *Colloids Surf. A* **2016**, *489*, 9-18.

(18) Chen, X.; Kang, S.; Kim, M. J.; Kim, J.; Kim, Y. S.; Kim, H.; Chi, B.; Kim, S. J.; Lee, J. Y.; Yoon, J. Thin-Film Formation of Imidazolium-Based Conjugated Polydiacetylenes and Their Application for Sensing Anionic Surfactants. *Angew. Chem. Int. Ed.* **2010**, *49*, 1422-1425.

(19) Lee, S.; Lee, K. M.; Lee, M.; Yoon, J. Polydiacetylenes Bearing Boronic Acid Groups as Colorimetric and Fluorescence Sensors for Cationic Surfactants. *ACS Appl. Mater. Interfaces* **2013**, *5*, 4521-4526.

(20) Shin, Y.J.; Shin, M. J.; Shin, J. S. Permeation-Induced Chromatic Change of a Polydiacetylene Vesicle with Nonionic Surfactant. *Colloids Surf. A* **2017**, *520*, 459-466.

(21) Rao, V. K.; Teradal, N. L.; Jelinek, R. Polydiacetylene Capacitive Artificial Nose. *ACS Appl. Mater. Interfaces* **2019**, *11*, 4470-4479.

(22) Terada, H.; Imai, H.; Oaki, Y. Visualization and Quantitative Detection of Friction Force by Self-Organized Organic Layered Composites. *Adv. Mater.* **2018**, *30*, 1801121.

(23) Wang, M.; Yu, Y.; Liu, F.; Ren, L.; Zhang, Q.; Zou, G. Single Polydiacetylene Microtube Waveguide Platform for Discriminating MicroRNA-215 Expression Levels in Clinical Gastric Cancerous, Paracancerous and Normal Tissues. *Talanta* **2018**, *188*, 27-34.

(24) Kamphan, A; Gong, C.; Maiti, K.; Sur, S.; Traiphol, R.; Arya, D. P. Utilization of Chromic Polydiacetylene Assemblies as a Platform to Probe Specific Binding between Drug and RNA. *RSC Adv.* **2017**, *7*, 41435-41443.

(25) He, C.; Wang, M.; Sun, X.; Zhu, Y.; Zhou, X.; Xiao, S.; Zhang, Q.; Liu, F.; Yu, Y.; Liang, H.; Zou, G. Integrating PDA Microtube Waveguide System with Heterogeneous CHA Amplification Strategy towards Superior Sensitive Detection of miRNA. *Biosens Bioelectron.* **2019**, *129*, 50-57.

(26) Jung, Y. K.; Park, H. G. Colorimetric Polydiacetylene (PDA) Liposome-Based Assay for Rapid and Simple Detection of GST-fusion Protein. *Sensors Actuat. B-Chem.* **2019**, *278*, 190-195.

(27) Yu, L.; Hsu, S. L. A Spectroscopic Analysis of the Role of Side Chains in Controlling Thermochromic Transitions in Polydiacetylenes. *Macromolecules* **2011**, *45*, 420-429.

(28) Pang, J.; Yang, L.; McCaughey, B. F.; Peng, H.; Ashbaugh, H. S.; Brinker, C. J.; Lu, Y. Thermochromatism and Structural Evolution of Metastable Polydiacetylenic Crystals. *J. Phys. Chem. B* **2006**, *110*, 7221-7225.

(29) Lifshitz, Y.; Golan, Y.; Konovalov, O.; Berman, A. Structural Transitions in Polydiacetylene Langmuir Films. *Langmuir* **2009**, *25*, 4469-4477.

(30) Fujimori, A.; Ishitsuka, M.; Nakahara, H.; Ito, E.; Hara, M.; Kanai, K.; Ouchi, Y.; Seki, K. Formation of the Newly Greenish Organized Molecular Film of Long-Chain Diynoic Acid Derivatives by Photopolymerization and Its Structural Study Using Near-Edge X-ray Absorption Fine Structure (NEXAFS) Spectroscopy. *J. Phys. Chem. B* **2004**, *108*, 13153-13162.

(31) Takeuchi, M.; Gnanasekaran, K.; Friedrich, H.; Imai, H.; Sommerdijk, N. A. J. M.; Oaki, Y. Tunable Stimuli-Responsive Color-Change Properties of Layered Organic Composites. *Adv. Funct. Mater.* **2018**, *28*, 1804906.

(32) Mapazi, O.; Matabola, K. P.; Moutloali, R. M.; Ngila, C. J. High Temperature Thermochromic Polydiacetylene Supported on Polyacrylonitrile Nanofibers. *Polymer* **2018**, *149*, 106-116.

(33) Wacharasindhu, S.; Montha, S.; Boonyiseng, J.; Potisatityuenyion, A.; Phollookin, C.; Tumcharern, G.; Sukwattanasinitt, M.; Tuning of Thermochromic Properties of Polydiacetylene toward Universal Temperature Sensing Materials through Amido Hydrogen Bonding. *Macromolecules* **2010**, *43*, 716-724.

(34) Phollookin, C.; Wacharasindhu, S.; Ajavakom, A.; Tumcharern, G.; Ampornpun, S.; Eaidkong, T.; Sukwattanasinitt, M.; Tuning Down of Color Transition Temperature of Thermochromically Reversible Bisdiynamide Polydiacetylenes. *Macromolecules* **2010**, *43*, 7540-7548.

(35) Ampornpun, S.; Montha, S.; Tumcharern, G.; Vchirawongkwin, V.; Sukwattanasinitt, M.; Wacharasindhu, S.; Odd−Even and Hydrophobicity Effects of Diacetylene Alkyl Chains on Thermochromic Reversibility of Symmetrical and Unsymmetrical Diyndiamide Polydiacetylenes. *Macromolecules* **2012**, *45*, 9038-9045.

(36) Lee, S.; Lee, J.; Lee, M.; Cho, Y. K.; Baek, J.; Kim, J.; Park, S.; Kim, M. H.; Chang, R.; Yoon, J. Construction and Molecular Understanding of an Unprecedented, Reversibly Thermochromic Bis-Polydiacetylene. *Adv. Funct. Mater.* **2014**, *24*, 3699-3705.

(37) Ahn, D. J.; Lee, S.; Kim, J. M. Rational Design of Conjugated Polymer Supramolecules with Tunable Colorimetric Responses. *Adv. Funct. Mater.* **2009**, *19*, 1483-1496.

(38) Ye, Q.; You, X.; Zou, G.; Yu, X.; Zhang, Q. Morphology, Structure and Chromatic Properties of Azobenzene-Substituted Polydiacetylene Supramolelular Assemblies. *J. Mater. Chem.* **2008**, *18*, 2775-2780.

(39) Kim, J.-M.; Lee, J.-S.; Choi, H.; Sohn, D.; Ahn, D. J. Rational Design and in-Situ FTIR Analyses of Colorimetrically Reversibe Polydiacetylene Supramolecules. *Macromolecules* **2005**, *38*, 9366-9376.

(40) Takeuchi, M.; Imai, H.; Oaki, Y. Effects of the Intercalation Rate on the Layered Crystal Structures and Stimuli-Responsive Color-Change Properties of Polydiacetylene. *J. Mater. Chem. C* **2017**, *5*, 8250-8255.

(41) Traiphol, N.; Rungruangviriya, N.; Potai, R.; Traiphol, R. Stable Polydiacetylene/ZnO Nanocomposites with Two-Steps Reversible and Irreversible Thermochromism: The Influence of Strong Surface Anchoring. *J. Colloid Interface Sci.* **2011**, *356*, 481-489.

(42) Chanakul, A.; Traiphol, N.; Traiphol, R. Controlling the Reversible Thermochromism of Polydiacetylene/Zinc Oxide Nanocomposites by Varying Alkyl Chain Length. *J. Colloid Interface Sci.* **2013**, *389*, 106-114.

(43) Shin, H.; Yoon, B.; Park, I. S.; Kim, J.-M. An Electrothermochromic Paper Display Based on Colorimetrically Reversible Polydiacetylenes. *Nanotechnology* **2014**, *25*, 094011.

(44) Yoon, B.; Lee, J.; Park, I. S.; Jeon, S.; Lee, J.; Kim, J.-M. Recent Functional Material Based Approaches to Prevent and Detect Counterfeiting. *J. Mater. Chem. C* **2013**, *1*, 2388-2403.

(45) Varghese Hansen, R.; Zhong, L.; Khor, K. A.; Zheng, L.; Yang, J. Tuneable Electrochromism in Weavable Carbon Nanotube/Polydiacetylene Yarns. *Carbon* **2016**, *106*, 110-117.

(46) Takeuchi, M.; Imai, H.; Oaki, Y. Real-Time Imaging of 2D and 3D Temperature Distribution: Coating of Metal-Ion-Intercalated Organic Layered Composites with Tunable Stimuli-Responsive Properties. *ACS Appl. Mater. Interfaces* **2017**, *9*, 16546-16552.

(47) Huang, X.; Jiang, S.; Liu, M. Metal Ion Modulated Organization and Function of the Langmuir-Blodgett Films of Amphiphilic Diacetylene: Photopolymerization, Thermochromism, and Supramolecular Chirality. *J. Phys. Chem. B* **2005**, *109*, 114-119.

(48) Traiphol, N.; Chanakul, A.; Kamphan, A.; Traiphol, R.; Role of Zn^{2+} Ion on the Formation of Reversible Thermochromic Polydiacetylene/Zinc Oxide Nanocomposites. *Thin Solid Films* **2017**, *622*, 122-129.

(49) Traiphol, N.; Faisadcha, K.; Potai, R.; Traiphol, R. Fine Tuning the Color-Transition Temperature of Thermoreversible Polydiacetylene/Zinc Oxide Nanocomposites: The Effect of Photopolymerization Time. *J. Colloid Interface Sci.* **2015**, *439*,105-111.

(50) Park, I.S.; Park, H.J.; . Kim, J.-M A Soluble, Low-Temperature Thermochromic and Chemically Reactive Polydiacetylene. *ACS Appl. Mater. Interfaces* **2013**, *5*, 8805-8812.

(51) Park, I.S.; Park, H.J.; Jeong, W.; Nam, J.; Kang, Y.; Shin, K.; Chung, H.; Kim, J.-M. Low Temperature Thermochromic Polydiacetylenes: Design, Colorimetric Properties, and Nanofiber Formation. *Macromolecules* **2016**, *49*, 1270-1278.

(52) Rougeau, L.; Picq, D.; Rastello, M.; Frantz, Y. New Irreversible Thermochromic Polydiacetylenes. *Tetrahedron* **2008**, *64*, 9430-9436.

(53) Nagarajan, R. Molecular Packing Parameter and Surfactant Self-Assembly: The Neglected Role of the Surfactant Tail. *Langmuir* **2002**, *18*, 31-38.

(54) Guo, C.; Xue, J. D.; Cheng, L. X.; Liu, R. C.; Kang, S. Z.; Zeng, Q. D.; Li, M. Two Dimensional Self-Assembly of Diacetylenic Acid Derivatives and their Light-Induced Polymerization on HOPG Surfaces. *Phys. Chem. Chem. Phys.* **2017**, *19*, 16213-16218.

(55) Villarreal, T. A.; Russell, S. R.; Bang, J. J.; Patterson, J. K.; Claridge, S. A. Modulating Wettability of Layered Materials by Controlling Ligand Polar Headgroup Dynamics. *J. Am. Chem. Soc.* **2017**, *139*, 11973-11979.

(56) Chanakul, A.; Traiphol, N.; Faisadcha, K.; Traiphol, R. Dual Colorimetric Response of Polydiacetylene/ZnO Nanocomposites to Low and High pH. *J. Colloid Interface Sci.* **2014**, *418*, 43-51.

(57) Toommee, S.; Traiphol, R.; Traiphol, N. High Color Stability and Reversible Thermochromism of Polydiacetylene/Zinc Oxide Nanocomposite in Various Organic Solvents and Polymer Matrices. *Colloids and Surfaces A* **2015**, *468*, 252-261.

(58) Kamphan, A.; Traiphol, N.; Traiphol, R. Versatile Route to Prepare Reversible Thermochromic Polydiacetylene Nanocomposite Using Low Molecular Weight Poly(vinylpyrrolidone). *Colloid Surf. A* **2016**, *497*, 370-377.

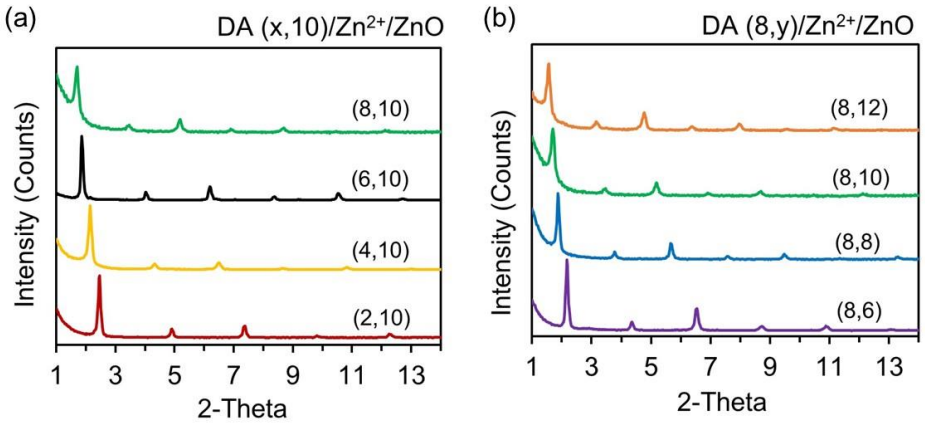

Fig. S1 XRD patterns of (a) DA(x,10)/Zn^{2+}/ZnO and (b) DA(8,y)/Zn^{2+}/ZnO nanocomposites.

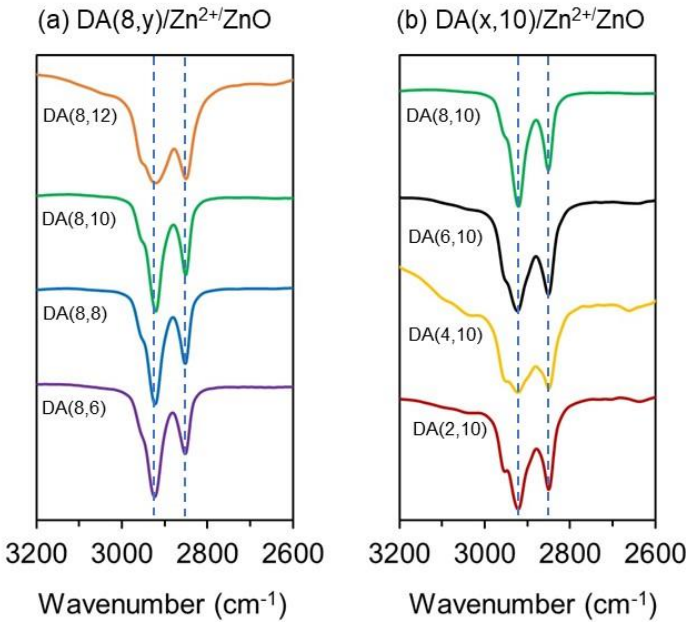

Fig. S2 FT-IR spectra of (a) DA(8,y)/Zn^{2+}/ZnO and (b) DA(x,10)/Zn^{2+}/ZnO nanocomposites. The vibrational bands of $\nu_s(CH_2)$ and $\nu_{as}(CH_2)$ of all samples are detected at 2848 cm^{-1} and 2919 cm^{-1}, respectively, indicating the presence of all-trans conformation[15,47].

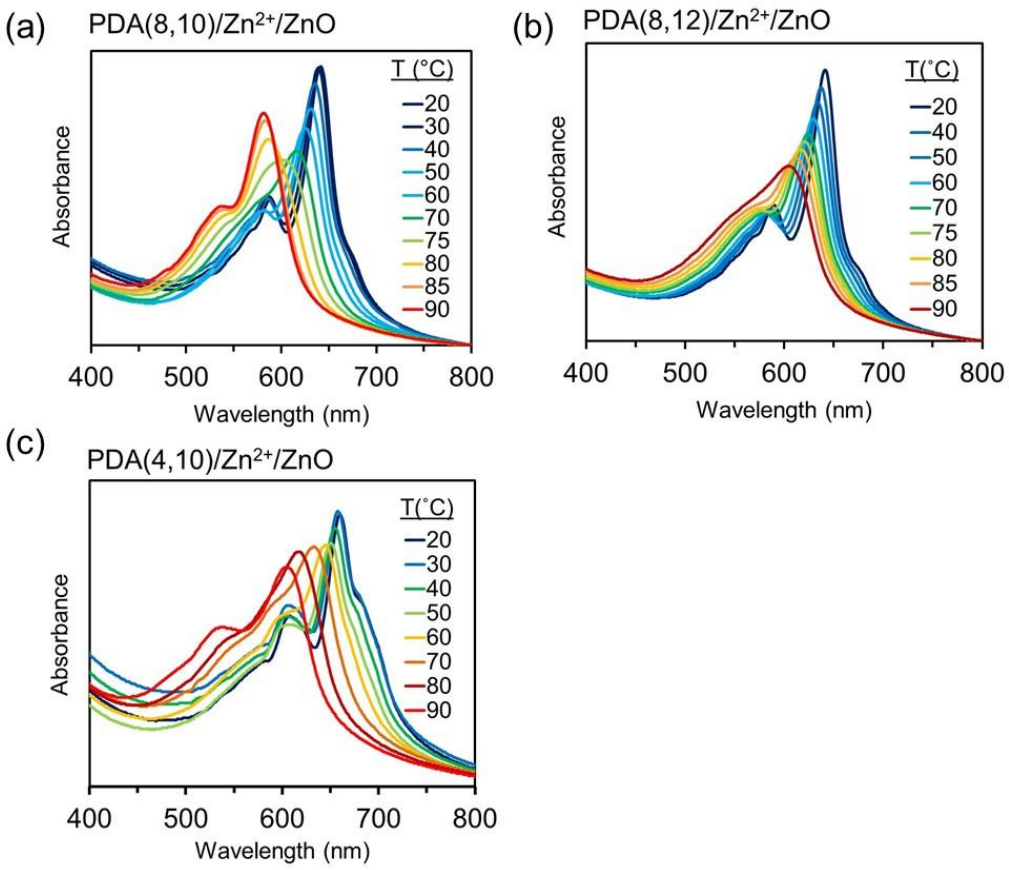

Fig. S3 Absorption spectra upon heating of (a) PDA(8,10), (b) PDA(8,12) and (c) PDA(4,10) /Zn^{2+}/ZnO nanocomposites.

Colorimetric response (CR) calculation

To quantify the extent of colorimetric response (CR) to temperature change, the CR values were calculated according to the equation

$$CR(\%) = \frac{(Pb_0 - Pb)}{Pb_0} \times 100$$

Where the Pb and Pb_0 refer to a fraction of blue phase within considering and beginning temperature respectively.

For the nanocomposites, the blue-to-purple color transition was normally observed instead the blue-to-red because of its strong electrostatic interaction between carboxylate group and Zn^{2+} ions.

Thus $Pb = A_{blue\ phase}/(A_{blue\ phase}+A_{purple\ phase})$

Where A = Absorbance values which were detected from absorption spectra.

According to the differences of color transition pattern of the nanocomposites depending on the alkyl side chain length of DA monomer, the absorbance values which were utilized to calculate the CR value are recorded from wave length (λ) following this table.

PDA(x,y)/Zn^{2+}/ZnO	λ blue phase (nm)	λ purple phase (nm)
8,6	660	600
8,8	637	580
8,10	641	582
8,12	641	605
2,10	647	575

4,10	660	603
6,10	658	598

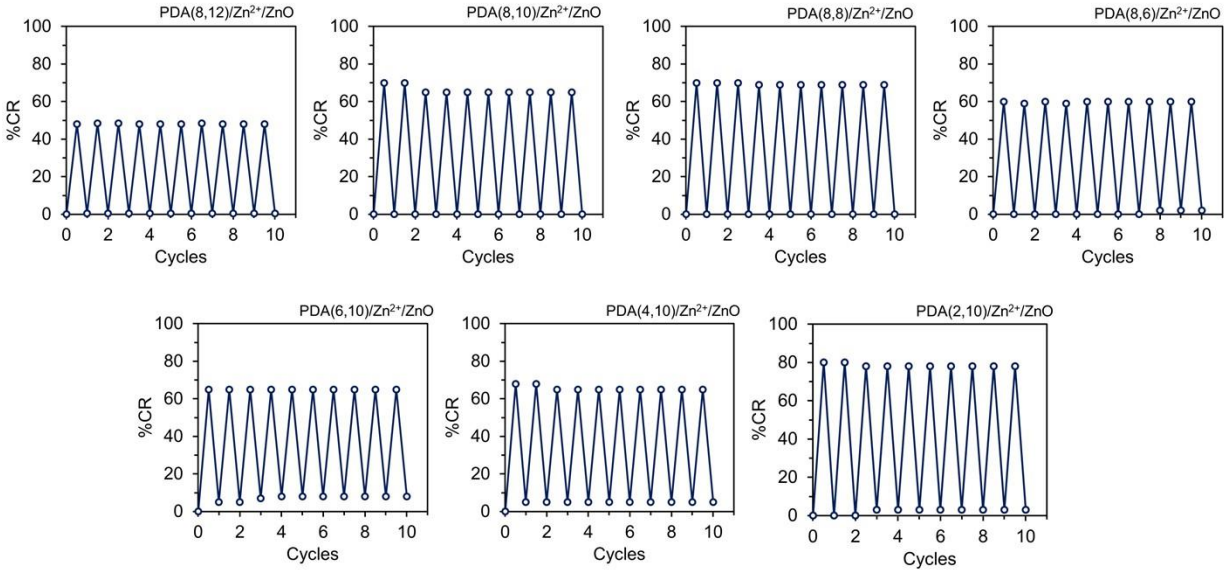

Fig. S4 Change of %CR during 10 heating/cooling cycles between 25°C and 90 °C of PDA(x,y)/Zn^{2+}/ZnO nanocomposites.

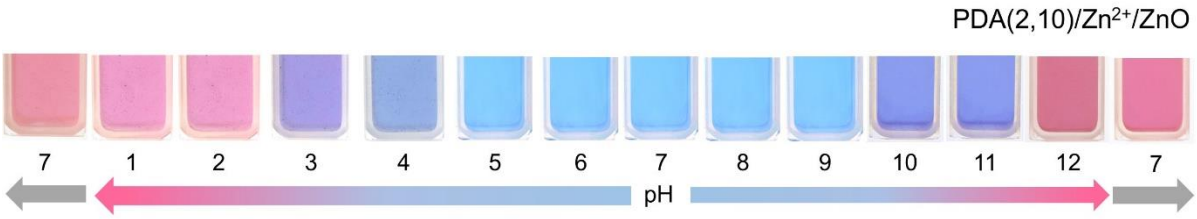

Fig. S5 Color transition of PDA(2,10)/Zn^{2+}/ZnO nanocomposite upon increasing or decreasing pH. The color transition is irreversible upon changing pH back to original pH 7.

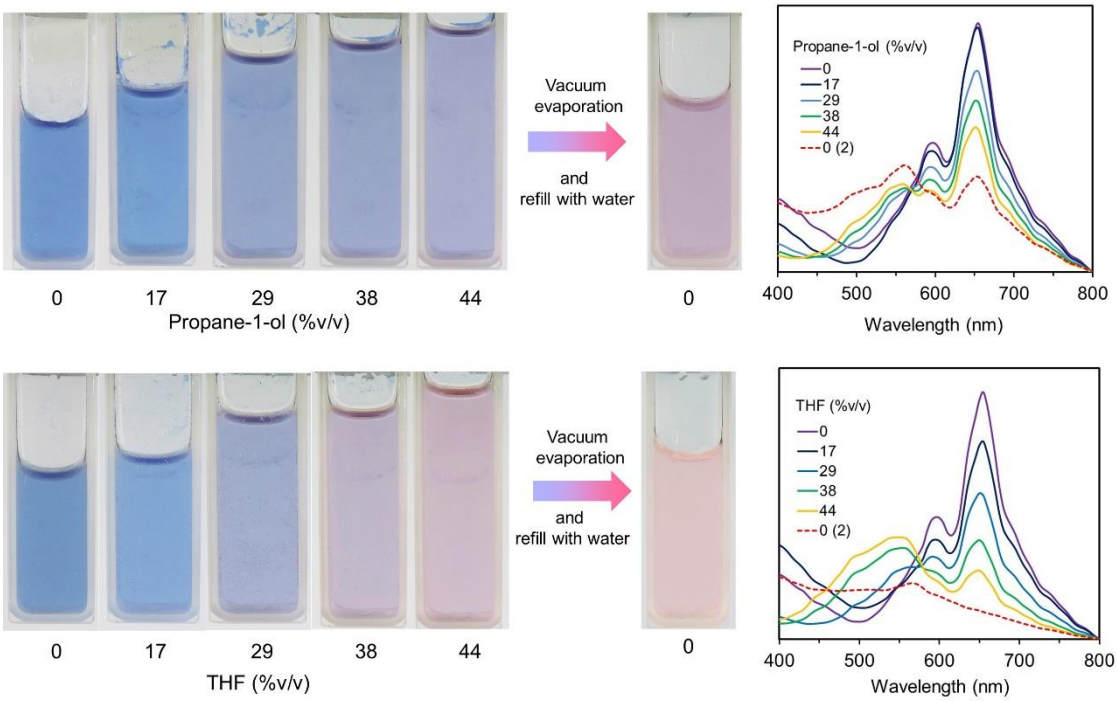

Fig. S6 Color transition of PDA(2,10)/Zn^{2+}/ZnO nanocomposite upon addition of (top) propanol or (bottom) THF. When the solvents are removed by vacuum evaporation, the color does not reverse back to the original color. The corresponding absorption spectra are shown on the left.

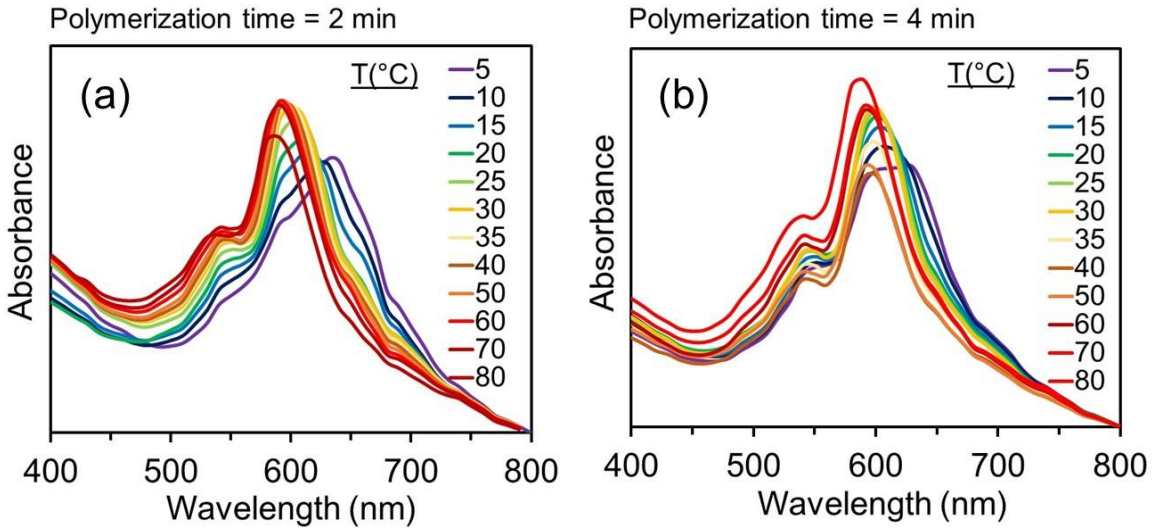

Fig. S7 Absorption spectra upon heating of PDA(8,6)/Zn^{2+}/ZnO nanocomposite polymerized at (a) 2 and (b) 4 min.

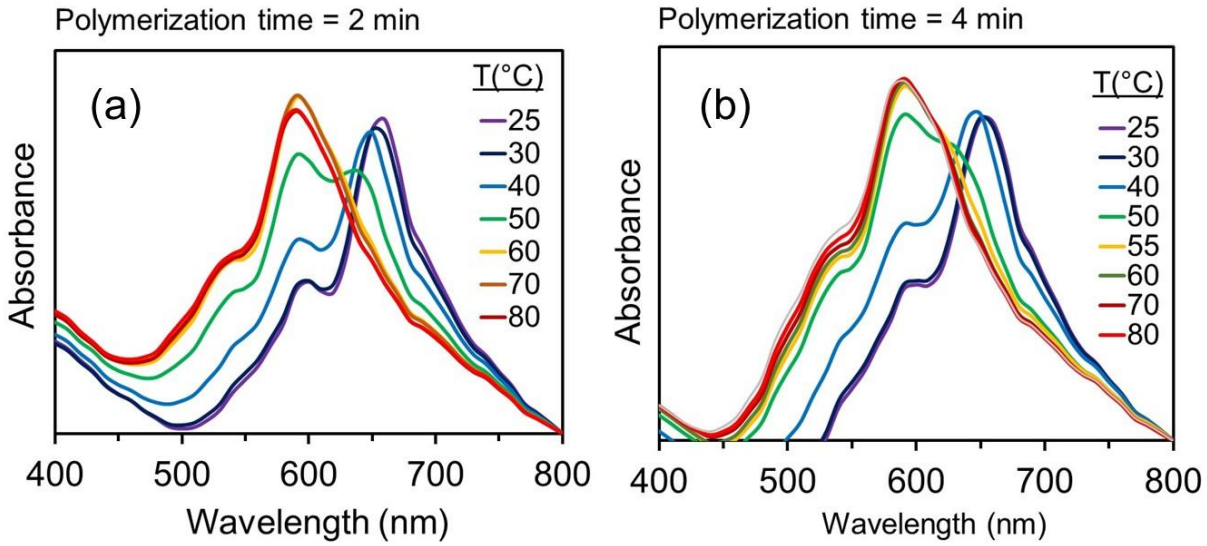

Fig. S8 Absorption spectra upon heating of PDA(2,10)/Zn^{2+}/ZnO nanocomposite polymerized at (a) 2 and (b) 4 min.

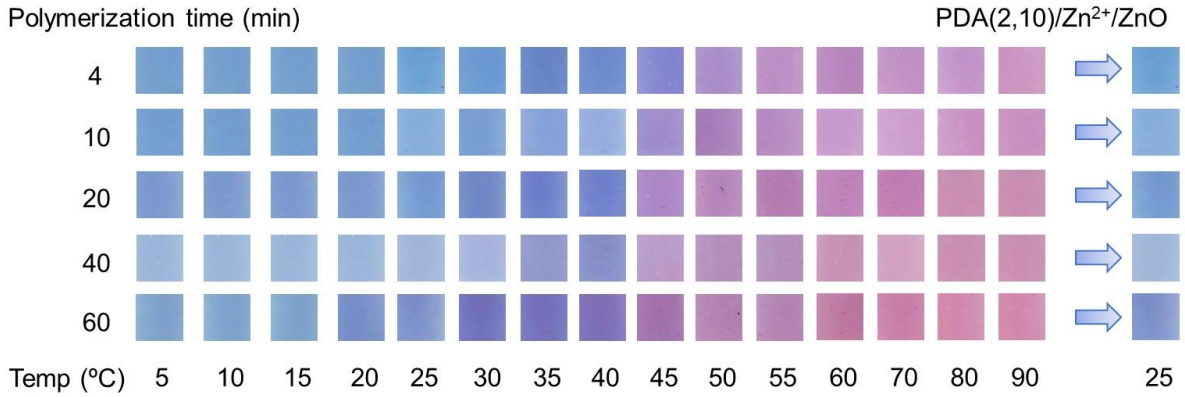

Fig. S9 Color photographs taken upon heating and cooling the aqueous suspensions of varied polymerization time of PDA(2,10)/Zn^{2+}/ZnO nanocomposite.

บทที่ 2

Controllable thermochromic and phase transition behaviors of polydiacetylene/zinc(II) ion/zinc oxide nanocomposites via photopolymerization: An insight into the molecular level

Abstract

Reversible thermochromic polydiacetylene/zinc(II) ion/zinc oxide (PDA/Zn^{2+}/ZnO) nanocomposites with a wide range of color-transition temperature have been prepared by varying photopolymerization time. This contribution presents our continuation study investigating into the molecular origins of this behavior. Infrared spectroscopy is utilized to investigate interfacial interactions of the systems while the conformation of PDA conjugated backbone is probed by Raman spectroscopy. X-ray diffraction explores molecular packing within the nanocomposites. We have found that the increase of photopolymerization time induces the relaxation of PDA backbone into a newly observed state indicated by systematic growth of new vibrational modes of C≡C and C═C bonds. This relaxation process results in the decrease of reversible blue-to-purple color-transition temperature. In contrast, the increase of backbone length with

photopolymerization time causes an opposite trend of the irreversible purple-to-red color transition observed at relatively high temperature region. Differential scanning calorimetry detects two distinct phase transitions corresponding to the melting of alkyl side chains and rigid backbone. These melting temperatures vary with photopolymerization time consistent with the variation of color-transition temperature.

Keywords: Polydiacetylene; Nanocomposite; Thermochromism; Chain length; Phase transition

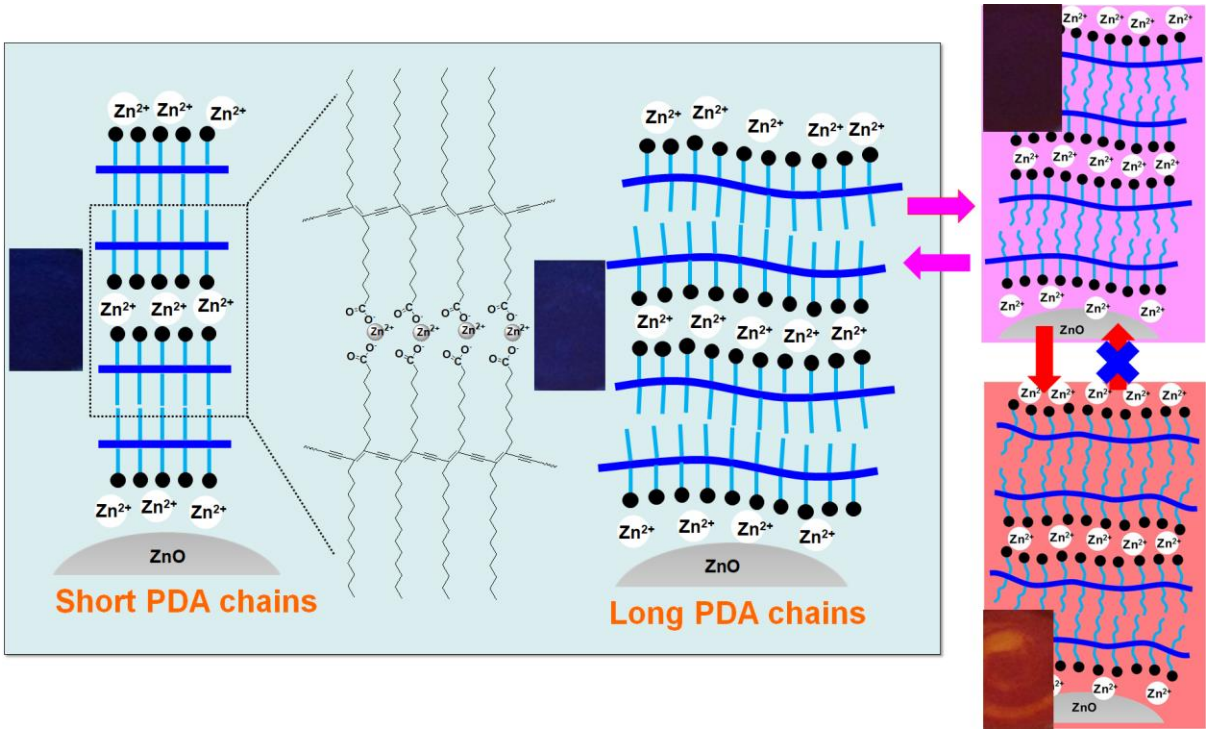

Highlights

- Polydiacetylene/ZnO nanocomposites are prepared by varying polymerization time.
- Distinct chromatic/melting transitions of side chains and rigid backbone are observed.
- Increasing polymerization time causes opposite change of the two transition temperatures.
- Side chains melt at lower temperature while melting point of the long backbone increases.
- Raman spectroscopy detects the relaxation of rigid backbone into a newly observed state.

Introduction

Polydiacetylenes (PDAs) are known to exhibit a color transition when exposed to various external stimuli such as heat, chemicals, biomolecules, UV light and electricity [1-17]. The color transition, normally from blue to red, occurs rapidly and is easily perceived by naked eyes, rendering PDA-based materials potential candidates for various applications such as 2D and 3D temperature sensors [2], sensors for volatile organic compounds [3,4], sensors for biomolecules [7,10] and a sensor for hydrogen peroxide [15]. The as-prepared PDAs usually present blue phase and are not fluorescent [18]. The blue-to-red color transition of PDAs generally involves segmental rearrangement within PDA assemblies causing the decrease of conjugation length [19-21]. The red-phase PDAs become fluorescent with quantum yield of about 0.02.

Microscopic mechanism of the color transition of PDA has been investigated by utilizing various techniques. Early works on urethane-substituted PDAs illustrated that the color transition was dominated by the change of backbone conformation [22,23]. When the systems were perturbed, the inter- and intrachain interactions were weaken. This allowed segmental rearrangement within the PDA assemblies, affecting the conjugation length of systems. Later works on the PDAs constituting carboxylic head group observed the change of molecular packing during the color-transition process [19-21,24]. Atkinson et al. reported that the color transition of PDA prepared from 10,12-pentacosadiynoic acid (PCDA) was related to the change from the orthorhombic to triclinic structure [24]. Lifshitz et al. observed the decrease of spacing between PDA backbones and the rearrangement of side chains during the color transition [20]. Fujimori et al. also detected the shrinkage of unit cell [21]. Our group utilized nuclear magnetic resonance spectroscopy to follow the molecular dynamics of each segment within PDA chain during the color transition [16]. These previous studies indicate that the segmental rearrangement plays an important role on the mechanism of color transition.

The color-transition properties of PDAs prepared from commercially available monomers such as PCDA are generally irreversible, limiting their utilization in various applications [14,16,25,26]. Many research groups have demonstrated that reversible color transition can be

achieved by enhancing the interactions within the PDA assemblies via structural modification [17,27-33] or incorporating foreign materials [1,2,5,14,19,26,34-47]. For example, the PDA functionalized with hydrazide head group exhibits reversible color transition under acid-base treatments [28]. The azobenzene-substituted PDA exhibits reversible thermochromism due to the enhanced intermolecular π-π interaction [29]. The nanocomposites of PDA/polymers [5,14,26], PDA/cations [1,2,9,34-37] and PDA/metal oxides [38-47] can provide reversible thermochromism as well.

Our group has achieved reversible thermochromism of PDAs by incorporating zinc oxide (ZnO) nanoparticles [38-45]. Our latest study revealed the presence of Zn^{2+} ions, releasing from ZnO nanoparticles during the preparation process [44]. These Zn^{2+} ions intercalated between PDA layers and interacted with the carboxylate head groups while the ZnO nanoparticles provided anchoring sites. The PDA/Zn^{2+}/ZnO nanocomposites possesses rather strong inter- and intramolecular interactions, making the system thermochromic reversible [38,39] and highly stable in various organic solvents [42]. The presence of ZnO nanoparticles also allows the colorimetric response to both acids and bases, which extends the utilization as a chemical sensor [40,43,45]. Recently, we have found a simple route for controlling the color-transition temperature of PDA/Zn^{2+}/ZnO nanocomposites. The increase of photopolymerization time caused systematic

variation of the color-transition temperature [41]. In this contribution, we present our continuation work, investigating into the molecular level of the color-transition behaviors of PDA/Zn^{2+}/ZnO nanocomposites obtained by varying photopolymerization time.

Materials and methods

The diacetylene (DA) monomers used in this study, 5,7-hexadecadiynoic acid (HDDA), 10,12-tricosadiyoic acid (TCDA) and 10,12-pentacosadiynoic acid (PCDA) were commercially available at Fluka. The ZnO nanoparticles were purchased from Nano Materials Technology (Thailand). The diameter of ZnO nanoparticles revealed by transmission electron microscopy (TEM, Tecnai 12, D291) is ranged from 20 to 160 nm (Fig.1a) with the averaged diameter of 65 nm. The PDA/Zn^{2+}/ZnO nanocomposites were prepared using a method described in our previous study [41]. Briefly, the DA monomer and ZnO nanoparticles were co-dispersed in water assisted by an ultrasonication. The concentration of DA monomer was 0.5 mM while the ZnO/DA ratio was 10 wt%. The DA/ZnO aqueous suspension was incubated at ~4 ^{o}C for ~24 h, followed by UV light irradiation (λ~254 nm, 10 W). The photopolymerization time was increased from 5 to 120 min, yielding a blue suspension of PDA/Zn^{2+}/ZnO nanocomposite. The suspension was filtered through 1.2 μm pore size cellulose acetate membrane. Thin films were prepared by drop-

casting the nanocomposite suspension onto glass slides and drying in a vacuum oven overnight. Particle size of the nanocomposites investigated by scanning electron microscopy (SEM, JOEL, JSM-6400) is ranged from 50 to 350 nm (Fig. 1b and c). The increase of photopolymerization time hardly affected morphology and size of the nanocomposites.

Absorption spectra of the poly(PCDA)/Zn^{2+}/ZnO nanocomposite films were recorded using Analytica Specord S100 UV/Vis spectrometer. The samples were annealed in a vacuum oven at different temperatures for 5 min. Thermocouple was attached to the samples using thermal conducting glue to measure their temperature. The FT-IR spectra of poly(PCDA)/Zn^{2+}/ZnO nanocomposite were obtained using a Perkin Elmer Spectrum GX spectrometer. Raman spectra of the dried samples were measured using FT-Raman spectrometer (PerkinElmer Spectrum GX) with a 1064 nm laser (Nd:YAG) as an excitation source. Thin film samples of poly(PCDA)/Zn^{2+}/ZnO nanocomposite were investigated using X-ray diffractometer (Bruker AXS Model D8 Discover λ(Cu-Kα) = 1.54 Å) for structural analysis. Thermal properties of PDA/Zn^{2+}/ZnO nanocomposites were explored by the differential scanning calorimetry (DSC, Mettler Toledo DSC1) and thermogravimetric analyses (TGA, Mettler Toledo TGA/DSC1) under nitrogen atmosphere. The DSC measurements were conducted at the heating/cooling rate of 5

°C/min. The TGA measurements were carried out in the temperature range of 25 to 800 °C using the heating rate of 10 °C/min.

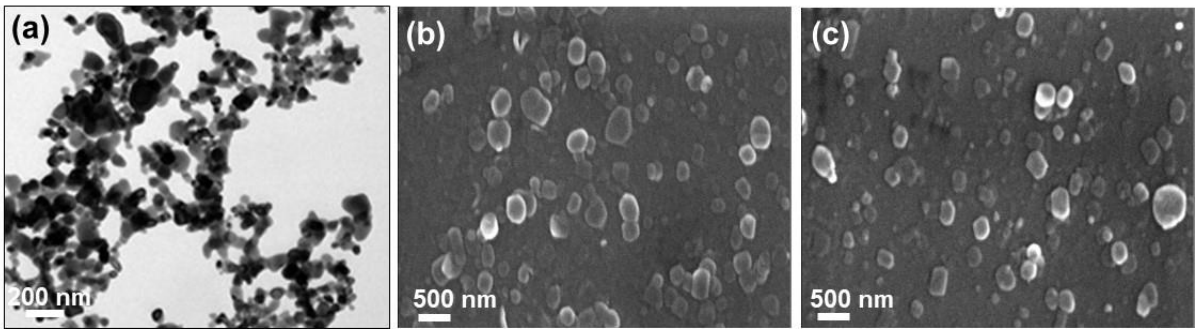

Fig. 1 (a) TEM image of ZnO nanoparticles. SEM images of (b) poly(PCDA)/Zn^{2+}/ZnO5m and poly(PCDA)/Zn^{2+}/ZnO60m prepared by using photopolymerization time of 5 and 60 min, respectively.

Results and discussion

Thermochromism of PDA/Zn^{2+}/ZnO nanocomposite films

In our previous studies, we explored thermochromic properties of poly(PCDA)/Zn^{2+}/ZnO nanocomposite dispersed in aqueous suspension and polymeric matrices [41,42]. The poly(PCDA)/Zn^{2+}/ZnO nanocomposite exhibited a two-step color transition upon increasing temperature, involving reversible blue-to-purple and then irreversible purple-to-red. The color-transition temperature of these two processes can be tuned by varying photopolymerization time

[41]. In this contribution, we take a step forward to investigate molecular origins of this thermochromic behavior.

Fig. 2 illustrates the absorption spectra of poly(PCDA)/Zn^{2+}/ZnO films measured upon increasing photopolymerization time from 5 to 120 min. At photopolymerization time of 5 min, the absorption spectrum constitutes of a peak at 640 nm and a vibronic shoulder at 590 nm, corresponding to the presence of blue phase. The increase of photopolymerization time results in the growth of a broad shoulder at relatively high wavelength region. At 90 min, two peaks at about 670 and 690 nm are detected. The observation of these new red-shift peaks reflects the formation of new electronic species with relatively long conjugation length. We believe that the increase of photopolymerization time affects the backbone length of poly(PCDA) and hence its electronic properties. The further increase of photopolymerization time to 120 min causes the growth of a peak at 610 nm. Detailed analysis of the absorption spectra is available in our previous study [41]. It is worthwhile to note that our samples remain blue during this photopolymerization process. The absorption spectra do not show the growth of a peak at 540 nm, which is a signature of the red phase.

Fig. 3 presents the color-transition behaviors of poly(PCDA)/Zn^{2+}/ZnO films prepared by photopolymerizing for 5 and 30 min. The variation of absorption spectra indicates the color

transition at different temperature regions. At room temperature, the samples are in blue phase with an absorption peak at 640 nm. Upon increasing temperature, the nanocomposite films change color at different temperatures, depending on the photopolymerization time. For poly(PCDA)/Zn^{2+}/ZnO5m polymerized for 5 min, the reversible blue-to-purple color transition is detected at about 90 ^{o}C where the λ_{max} of absorption spectrum shifts to 585 nm (Fig. 3c). Increasing temperature to 110 ^{o}C causes the shift of λ_{max} to about 535 nm corresponding to the purple-to-red color transition.

The increase of photopolymerization time to 30 min significantly affects the thermochromic properties of the nanocomposite film. The blue-to-purple color-transition temperature of poly(PCDA)/Zn^{2+}/ZnO30m drops to about 70 ^{o}C where the λ_{max} of absorption spectrum shifts to 590 nm. In contrast, the purple-to-red color transition temperature is detected at about 150 ^{o}C, which is higher than that of the poly(PCDA)/Zn^{2+}/ZnO5m (Fig. 3c). Therefore, the increase of photopolymerization time causes the decrease of blue-to-purple color-transition temperature while the purple-to-red one shows an opposite trend. The two-step color transition is similar to the thermochromic properties of poly(PCDA)-Na and poly(PCDA)-Zn complexes [19,36,48]. However, the variation of color-transition temperature upon increasing the photopolymerization time has never been reported in these systems.

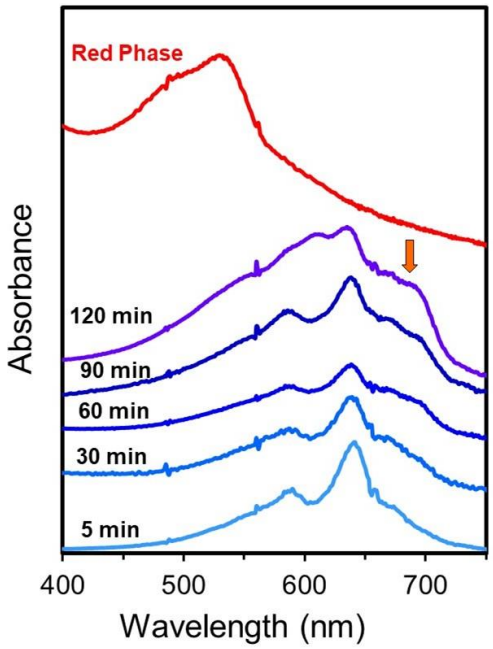

Fig. 2 Absorption spectra of poly(PCDA)/Zn^{2+}/ZnO nanocomposite films measured at room temperature. The samples were prepared by varying photopolymerization time from 5 to 120 min. The arrow indicates the growth of absorption peak at about 690 nm. An absorption spectrum of the red phase is included for comparison.

Interfacial interaction, backbone conformation and molecular packing

In general, the color-transition temperature of pure PDAs can be controlled by varying side chain structure, which in turn affects the strength of interactions within the assemblies. For example, the decrease of alkyl side chain length of PDAs results in systematic decrease of color-transition temperature [26,39]. What are the molecular origins that cause the variation of color-

transition temperature in the system of poly(PCDA)/Zn^{2+}/ZnO nanocomposite? To answer this question, we use infrared spectroscopy to characterize the conformational change of alkyl side chains and the interfacial interactions between poly(PCDA) head groups and ZnO nanoparticle. Raman spectroscopy is utilized to investigate conformational change of poly(PCDA) conjugated backbone upon increasing photopolymerization time.

Fig. 4a illustrates FT-IR spectra of the poly(PCDA)/Zn^{2+}/ZnO30m measured at room temperature after being annealed at different temperatures. The vibrational bands at 2849 and 2918 cm^{-1} of blue-phase nanocomposite are assigned to the $\nu_s(CH_2)$ and $\nu_{as}(CH_2)$ stretching vibrations of alkyl side chains, respectively. These bands indicate all-trans conformation of the alkyl side chains [48,49-51]. The band at 1460 cm^{-1} is assigned to the methylene scissoring, $\delta(CH_2)$. The strong ionic interaction between head group of poly(PCDA) and Zn^{2+}/ZnO nanoparticles is indicated by the peaks at 1540 and 1398 cm^{-1} corresponding to $\nu_{as}(COO^-)$ and $\nu_s(COO^-)$ stretching vibrations of carboxylate anion, respectively (Fig. 4c) [44,48]. We note that a small peak at 1725 cm^{-1} indicates the presence of some carboxylic head groups.

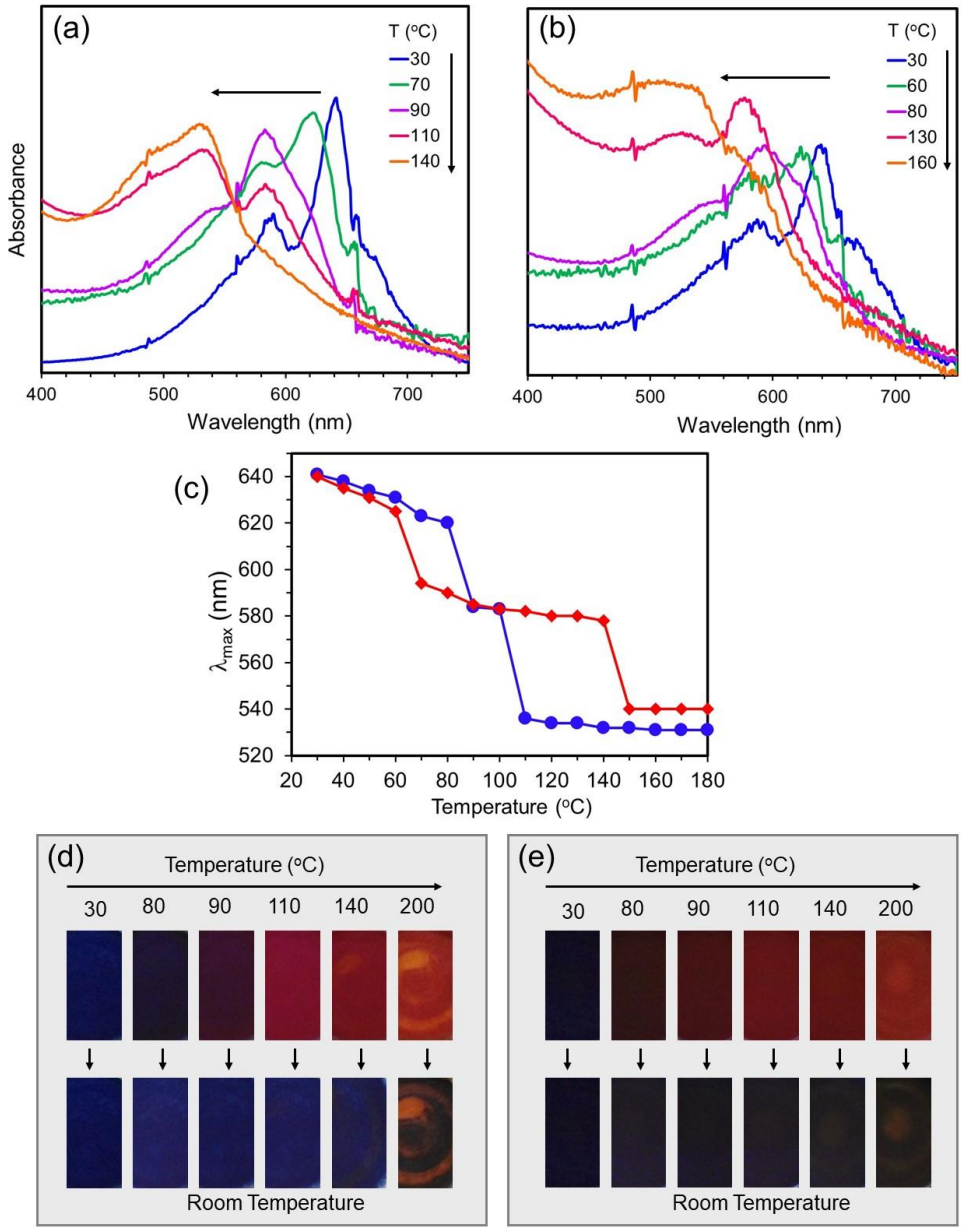

Fig. 3 Absorption spectra and photographs of poly(PCDA)/Zn^{2+}/ZnO nanocomposite films obtained at different temperatures, (a,d) poly(PCDA)/Zn^{2+}/ZnO5m and (b,e) poly(PCDA)/Zn^{2+}/ZnO30m. (c) Plots of λ_{max} versus temperature of (●, blue) poly(PCDA)/Zn^{2+}/ZnO5m and (♦, red) poly(PCDA)/Zn^{2+}/ZnO30m.

The annealing of nanocomposite at 100 ^{o}C for 5 min induces the blue-to-purple color transition, which is a reversible process. The FT-IR pattern measured upon cooling to room temperature remains unchanged indicating that the molecular arrangement of alkyl side chains and head group can be restored to the original state. The increase of annealing temperature to 200 ^{o}C causes the purple-to-red color transition. The color transition is partially irreversible at this state. We observe a line broadening of the peak at 1540 cm^{-1}. The increase of annealing time at 200 ^{o}C to 30 min causes a complete irreversible transition to the red phase. A growth of broad shoulder at about 1600 cm^{-1} is clearly detected. This observation indicates that the local environment of carbonyl group at the interfacial region has changed. This is attributed to the rearrangement of carboxylate head group, causing the variation of its vibrational spring constant. It is worthwhile to note that the vibrational bands at 2849 and 2918 cm^{-1} remain at the same position corresponding to all-trans conformation of alkyl side chains in the red phase. The increase of photopolymerization time from 5 to 120 min hardly affects the FT-IR pattern as shown in Fig. 4b. This observation indicates that the molecular arrangement of alkyl side chains and carboxylate head group does not change with the increasing of photopolymerization time.

Interestingly, we detect a systematic variation of molecular arrangement of PDA conjugated backbone. The Raman spectrum of pure poly(PCDA) in blue phase are known to

exhibit two major peaks at 2080 and 1451 cm^{-1} which can be assigned to the C≡C and C═C stretching modes of the PDA conjugated backbone, respectively [14,36,46]. These peaks shift to 2116 and 1511 cm^{-1} in the red phase attributed to the relaxation of poly(PCDA) backbone into new local environment. This is consistent with previous studies that observe the shrinkage of unit cell during the blue-to-red color transition of poly(PCDA) [20,21]. The Raman spectra of poly(PCDA)/Zn^{2+}/ZnO nanocomposite are shown in Fig. 5a. The poly(PCDA)/Zn^{2+}/ZnO5m polymerized for 5 min exhibits C≡C and C═C stretching modes at 2076 and 1450 cm^{-1}, respectively. When the photopolymerization time is increased to 30 min, the C≡C and C═C stretching bands split into two peaks. New bands are detected at 2094 and 1474 cm^{-1}. These new bands shift to 2097 and 1483 cm^{-1}, respectively, upon increasing the photopolymerization time to 120 min (Table 1s in supporting information). The intensity ratios at 1475/1450 cm^{-1} and 2097/2075 cm^{-1} systematically increase with the photopolymerization time (Fig.1s in supporting information). Our observation indicates that the rearrangement of poly(PCDA) conjugated backbone into new local environment takes place upon increasing the photopolymerization time (Fig. 5b).

The presence of two distinct peaks for the C≡C and C═C bonds indicates the co-existence of two species. The change of intensity ratio corresponds to the variation of mole

fraction of these species. Since the nanocomposites in this study exhibit rather broad size distribution as shown in Fig. 1b, we believe that the poly(PCDA) conjugated backbone relaxes to new local environment at different states of photopolymerization depending on the size of assemblies. It is important to note that the Raman signal of C≡C bond in the PCDA monomer locates at 2101 cm^{-1} [52]. However, previous studies have shown that the intensity of this peak is extremely weak [52,53]. Therefore, the presence of some residual PCDA monomer in this system has a minor effect on the pattern of Raman spectra in this study.

Previous studies of poly(PCDA)/ZnO nanocomposite [46] and poly(PCDA)-Na [36] observed the shift of C≡C and C═C stretching bands to higher wavenumbers upon increasing the temperature to 100 ^{o}C. The blue shift indicates a relaxation of poly(PCDA) conjugated backbone, resulting in the formation of purple phase. In this study, however, all samples still exhibit a blue color at room temperature. The measurements of UV/Vis absorption spectra detect the growth of a broad peak at 690 nm, reflecting the formation of new electronic species with relatively long conjugation length (Fig. 2). We suggest that the increase of poly(PCDA) backbone length upon increasing photopolymerization time reduces the chain rigidity, which in turn allows partial relaxation into new local environment (Fig.5b). Previous studies have shown that the increase of photopolymerization time of pure PDAs causes the shrinkage of unit cell and the

rearrangement of alkyl side chains [20,21]. Similar structural transition possibly takes place in our system. We believe that the relaxation of poly(PCDA) backbone is a major factor that leads to the systematic variation of color-transition temperature.

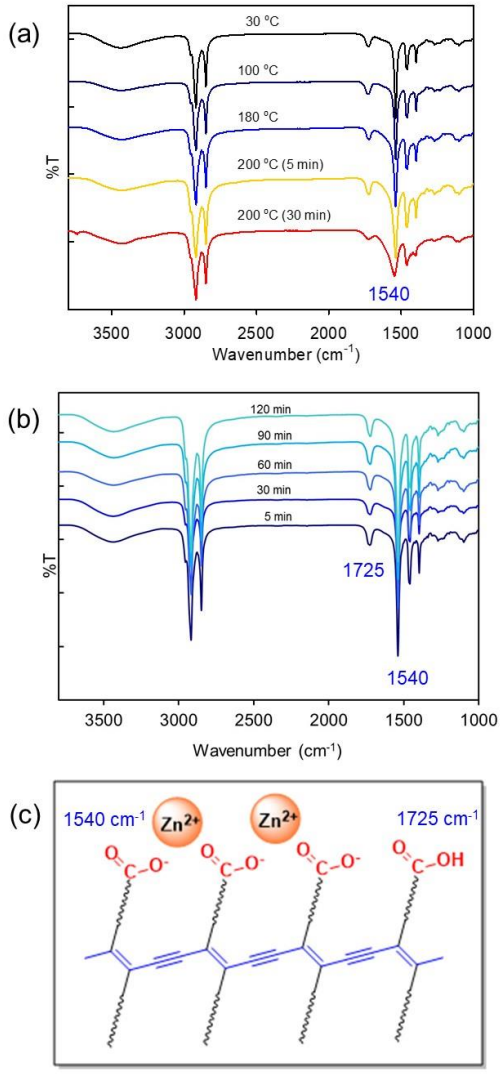

Fig. 4 (a) FT-IR spectra measured at room temperature of poly(PCDA)/Zn^{2+}/ZnO30m nanocomposite after being annealed at different temperatures. (b) FT-IR spectra measured at room temperature of poly(PCDA)/Zn^{2+}/ZnO nanocomposite prepared by varying photopolymerization time. (c) Interaction between carboxylate head group and Zn^{2+} ion.

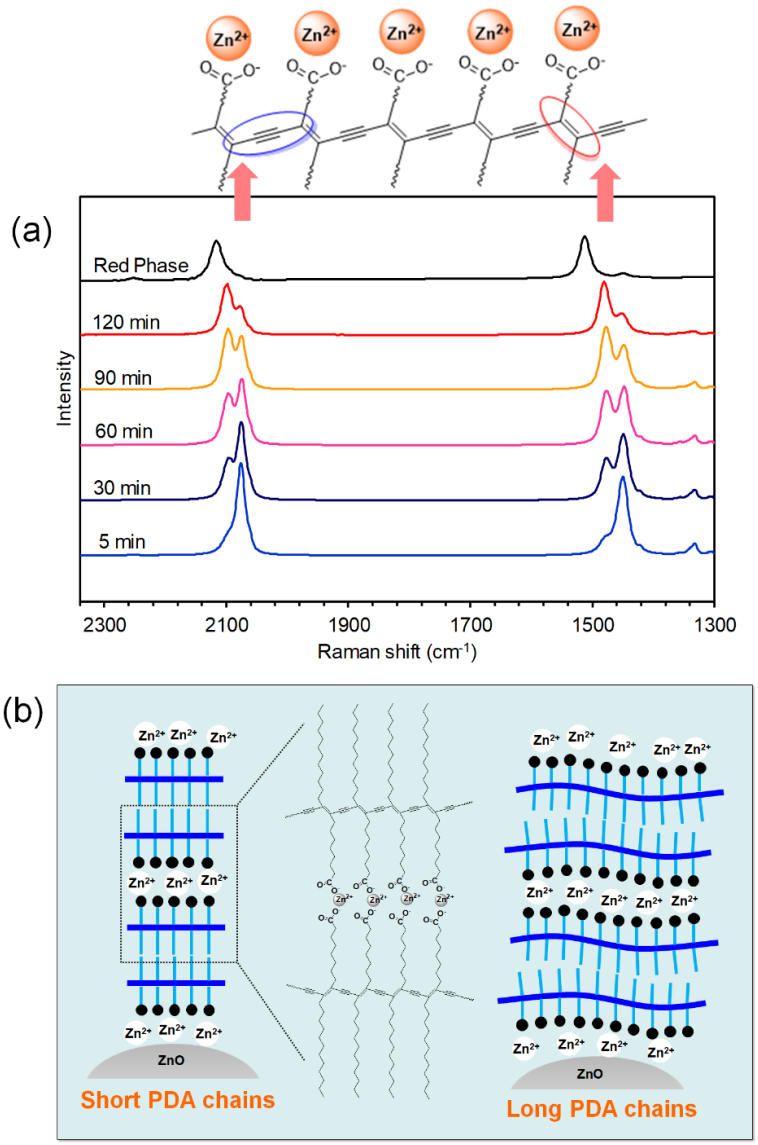

Fig. 5 (a) Raman spectra of poly(PCDA)/Zn^{2+}/ZnO nanocomposite obtained from different photopolymerization times. Spectrum of red-phase poly(PCDA) is included for comparison. (b) Proposed model for the molecular arrangement of short and long PDA chains within the nanocomposites.

It is worthwhile to note that previous studies of pure PDA films normally observe the blue-to-red color transition upon increasing photopolymerization time [52-55]. In our system, however, strong ionic interactions between the carboxylate head group and Zn^{2+}/ZnO resist the blue-to-red color transition. The nanocomposites remain in the blue phase when the photopolymerization time is increased to 120 min as indicated by the UV/Vis absorption and Raman spectra in Fig. 2 and 5, respectively. Our result is parallel to the previous study of PDA/Zn^{2+} system [54].

We also utilize X-ray diffraction (XRD) to explore the molecular packing of poly(PCDA)/Zn^{2+}/ZnO nanocomposite. Fig. 6a illustrates XRD patterns of the nanocomposite prepared with different photopolymerization times. The pattern is consistent with those of the poly(PCDA)-Zn and poly(PCDA)-Na complexes observed in previous studies, corresponding to lamellar structure [1,2,19]. The value of interlamellar d-spacing calculated from these diffraction peaks is about 5.4 nm (Fig. 6b). Since the d-spacing of pure poly(PCDA) is about 4.5 nm, the increase of d-spacing value in this system indicates the intercalation of Zn^{2+} ions into the bilayer structure [1,2]. Detailed investigation of the poly(PCDA)/Zn^{2+}/ZnO nanocomposite structure is given in our previous report [44]. Although Raman spectroscopy detects the relaxation of poly(PCDA) conjugated backbone upon increasing photopolymerization time, the lamellar structure of nanocomposite is hardly affected. Fig. 6a shows that the nanocomposite prepared

by increasing photopolymerization time from 5 to 120 min provide XRD peaks at approximately the same position. This observation indicates that the relaxation of poly(PCDA) backbone probably occurs in the length scale that cannot be detected by our XRD measurements. Our result is parallel with the previous study of poly(PCDA)-Na system, in which, the relaxation of backbone causing the blue-to-purple color transition, hardly affects the d-spacing of lamellar structure [19].

Thermal analysis of PDA/Zn^{2+}/ZnO nanocomposites

In this section, we utilize DSC to investigate the nature of phase transition relating to the color transition of PDA/Zn^{2+}/ZnO nanocomposites. The phase-transition temperatures obtained from two heating/cooling cycles of various pure PDAs and PDA/Zn^{2+}/ZnO nanocomposites are summarized in Table 1. For a comparison purpose, we first evaluate the results obtained from the systems of pure poly(PCDA), poly(TCDA) and poly(HDDA). The 1st heating cycle of pure poly(PCDA) detects a single endothermic peak at 60 ^{o}C. Since this melting transition is close to that of the PCDA monomer, it is assigned to the melting of alkyl side chains [51]. The phase transition of poly(PCDA) is closely related to its color-transition temperature. The cooling cycle reveals an exothermic peak at 43 ^{o}C, indicating the recrystallization of alkyl side chains. However, the poly(PCDA) remains in red phase. The X-ray scattering results from previous studies have

shown that the blue and red phases are actually in different crystalline states at room temperature [19-21]. Our earlier study via XRD also observed lamellar structure for both blue and red phases with slightly different values of interlamellar d-spacing [44]. The 2nd heating cycle of red phase shows a melting peak at 58 ^{o}C, which is quite close to that of the blue phase. The investigation of pure poly(TCDA) and poly(HDDA) provides consistent results. We note that the melting transition of poly(TCDA) and poly(HDDA) shifts to the lower temperature due to the shortening of alkyl side chains. Our results indicate that the melting and crystallization of pure PDAs mainly involve the alkyl side chains.

The system of PDA/Zn^{2+}/ZnO nanocomposites exhibits rather different phase transition behaviors. Fig. 7 illustrates the DSC thermogram of poly(PCDA)/Zn^{2+}/ZnO nanocomposite prepared with various photopolymerization times. Interestingly, the incorporation of ZnO nanoparticles into poly(PCDA) assembly results in two distinct melting points. The 1st heating cycle of poly(PCDA)/Zn^{2+}/ZnO5m reveals two melting peaks at 80 and 162 ^{o}C (Table 1). These phase transitions are consistent with the two-step color transition discussed in the first section. The 1st melting is related to the reversible blue-to-purple color transition. It is assigned to the melting of alkyl side chains. Higher melting temperature of the alkyl side chains for the nanocomposite compared to that of the pure poly(PCDA) is attributed to the presence of strong

interfacial interactions. Additionally, the enhanced interactions provide reversible phase transition as revealed by DSC (Fig. 2s in supporting information).

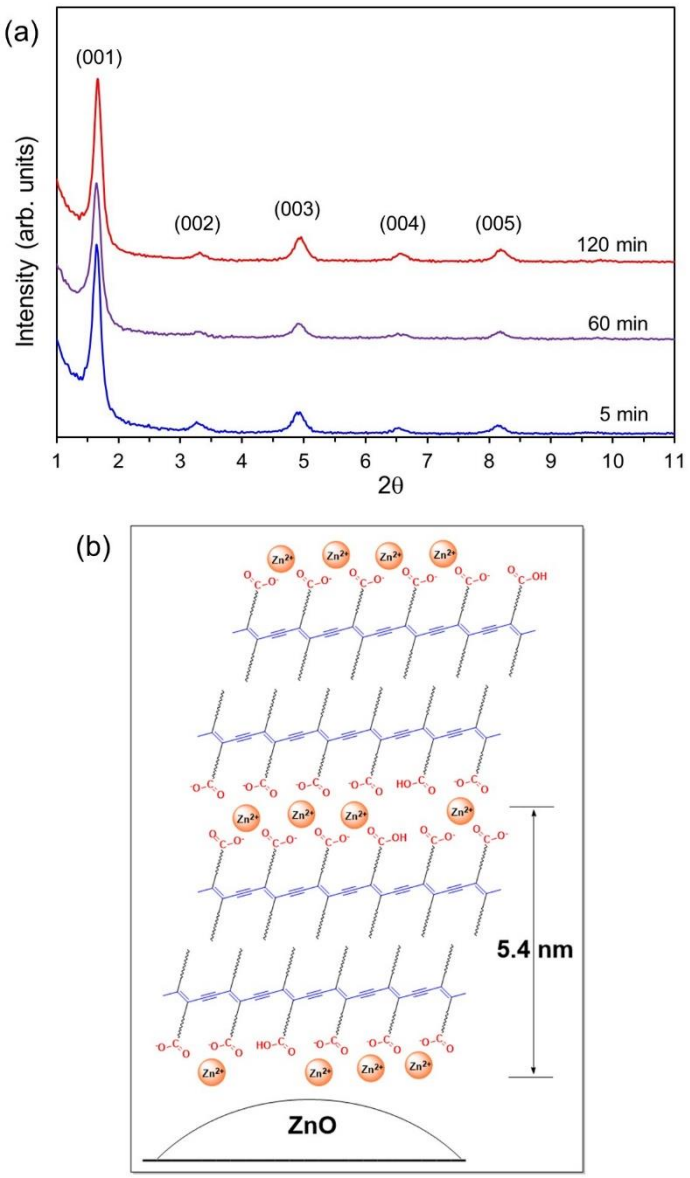

Fig. 6 (a) XRD patterns of poly(PCDA)/Zn^{2+}/ZnO nanocomposite obtained from different photopolymerization times. (b) Model for the molecular arrangement within the nanocomposites.

Table 1 Transition temperature of pure PDAs and PDA/Zn^{2+}/ZnO nanocomposites obtained from different photopolymerization times

Samples	Peak transition temperature (^{o}C)			
	1st heating	1st cooling	2nd heating	2nd cooling
Poly(HDDA)	45	25	42	-
Poly(TCDA)	52	37	50	35
Poly(PCDA)	60	43	58	44
Poly(PCDA)/Zn^{2+}/ZnO1m	86, 151	89	103	89
Poly(PCDA)/Zn^{2+}/ZnO5m	80, 162	84	100	83
Poly(PCDA)/Zn^{2+}/ZnO30m	62, 169	78	97	77
Poly(PCDA)/Zn^{2+}/ZnO60m	62, 177	76	96	75
Poly(PCDA)/Zn^{2+}/ZnO120m	54, 187	70	92	70
Poly(TCDA)/Zn^{2+}/ZnO30m	57, 113	99	110	97
Poly(HDDA)/Zn^{2+}/ZnO30m	39, 151	44	45	45

The further increase of temperature results in the 2nd melting transition that does not exist in the system of pure poly(PCDA). The investigation of poly(TCDA)/Zn^{2+}/ZnO and poly(HDDA)/Zn^{2+}/ZnO nanocomposites reveals consistent results as shown in Table 1. Our observation suggests that the presence of ZnO nanoparticles significantly promotes the organization of poly(PCDA) chains. A previous study on the system of poly(PCDA)-Na also detected two distinct phase transitions by DSC [19]. Their temperature-dependent XRD measurements indicated that the poly(PCDA)-Na maintained a lamellar structure above the 1st melting temperature. The lateral ordering of alkyl side chains, however, was reduced. The poly(PCDA)-Na became completely amorphous during the 2nd phase transition. According to this study, the 2nd phase transition of poly(PCDA)/Zn^{2+}/ZnO nanocomposite is attributed to the melting of rigid conjugated backbone. This melting process is related to the irreversible purple-to-red color transition. Our result is parallel to the previous study of comb-like polymers where two phase transitions are related to the melting of alkyl side chains and rigid backbone [56]. It is worthwhile to point out that DSC does not detect the melting of backbone in the system of pure poly(PCDA). This observation indicates that the ordering of poly(PCDA) backbone is drastically increased within the nanocomposites due to the presence of strong interfacial interactions.

The 2nd melting point, on the other hand, shows the opposite trend. It increases to 169 and 187 °C. The increase of photopolymerization time is expected to cause the increase of backbone length, which in turn induces partial relaxation as revealed by Raman spectroscopy (Fig. 5). We propose that the magnitude of segmental relaxation is a major factor dictating the melting point of alkyl side chains. The higher magnitude of segmental relaxation leads to the lower melting point, which relates to the decrease in reversible blue-to-purple color-transition temperature of the nanocomposite. The 2nd melting point is related to the length of poly(PCDA) backbone. When the backbone of poly(PCDA) becomes longer upon increasing photopolymerization time, it requires higher temperature to melt its crystalline structure. This behavior has been observed in the system of comb-like polymers constituting rigid backbone and flexible side chains [56].

The melting points of alkyl side chains and rigid backbone of poly(PCDA)/Zn^{2+}/ZnO nanocomposite are strongly influenced by the photopolymerization time. The 1st melting point shifts to 62 and 54 °C when the photopolymerizatime is increased to 30 and 120 min, respectively. The 1st cooling cycle of poly(PCDA)/Zn^{2+}/ZnO5m presents a single recrystallization peak at 84 °C, which is slightly higher than the melting temperature of alkyl side chains (Fig. 7b). We do not detect any recrystallization process at high temperature region. This observation indicates that

the original packing structure of poly(PCDA) backbone is not restored upon cooling to room temperature. This is consistent with the color of poly(PCDA)/Zn^{2+}/ZnO nanocomposite, which remains in the red phase. The alkyl side chains, on the other hand, recrystallize into the organized structure. Our XRD results in the previous study showed that the red phase of poly(PCDA)/Zn^{2+}/ZnO nanocomposite exhibited lamellar structure with interlamellar d-spacing greater than that of the original blue phase [44]. The 2nd heating cycle of poly(PCDA)/Zn^{2+}/ZnO5m exhibits a single melting peak at 100 ^{o}C. This transition temperature is much higher than the melting temperature of alkyl side chains observed in the 1st heating cycle. We believe that the poly(PCDA) backbone and alkyl side chains in the nanocomposite organize into densely packed structure in the red phase. Therefore, it requires higher temperature to melt the crystalline structure of the red phase. The 2nd cooling cycle presents recrystallization process similar to that of the 1st cooling cycle. Our hypothesis is parallel to the result of previous study, which detects the shrinkage of unit cell during the blue-to-red color transition of poly(PCDA) [20].

We also investigate the effects of molecular structure on thermal stability of pure PDAs and PDA/Zn^{2+}/ZnO nanocomposites (Fig. 3s in supporting information). The pure PDAs tend to loose significant weight at relatively low temperature range, attributed to the presence of residual monomer. The peak degradation temperature is detected around 438 to 448 ^{o}C. The variation of

alkyl side chain length slightly affects the degradation temperature. In the system of PDA/Zn^{2+}/ZnO nanocomposites, the temperature at 5% weight loss significantly increases. It is clearly observed in the system containing 20 wt% of ZnO nanoparticles. This result suggests that the presence of strong interfacial interaction facilitates the conversion of monomers into PDA chains. Our UV/Vis absorption measurement shows consistent results, demonstrating much higher amount of blue phase PDAs within the nanocomposites compared to the system of pure PDAs. The increase of PDA chain length obtained via the increase of photopolymerization time hardly affects the degradation temperature.

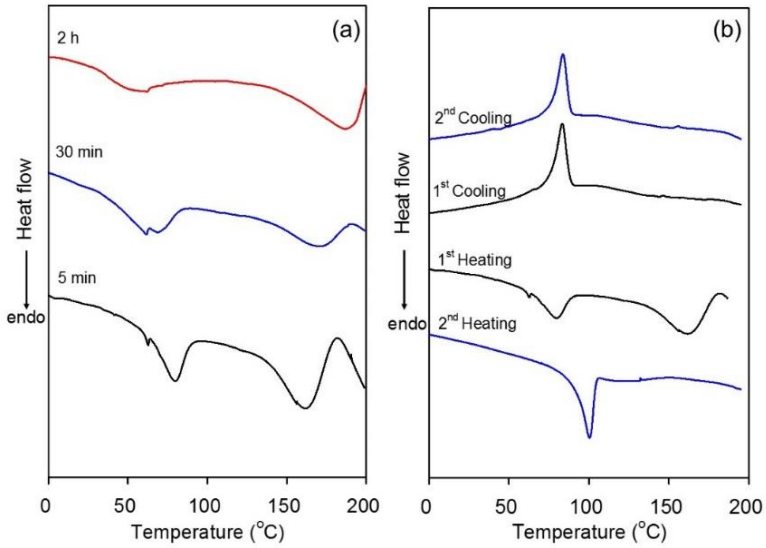

Fig. 7 (a) DSC curves of poly(PCDA)/Zn^{2+}/ZnO nanocomposite recorded from the 1st heating. (bottom) poly(PCDA)/Zn^{2+}/ZnO5m, (middle) poly(PCDA)/Zn^{2+}/ZnO30m and (top) poly(PCDA)/Zn^{2+}/ZnO120m. A small peak detected at about 62 °C is assigned to residual PCDA monomer. (b) DSC curves of poly(PCDA)/Zn^{2+}/ZnO5m obtained from two heating/cooling cycles.

Our major finding of this study is summarized in Fig. 8. The molecular interactions within pure PDA assemblies involve hydrogen bonds between carboxylic head groups, π-π interaction of backbone and dispersion interaction of the alkyl side chains. When thermal energy overcomes the overall interactions, the melting of lamellar structure takes place. This process causes the rearrangement of conjugated backbone, resulting in the irreversible blue-to-red color transition (Fig. 8a). Although the alkyl side chains recrystallize upon cooling to room temperature, the original state of PDA conjugated backbone cannot be restored. The addition of ZnO nanoparticles introduces strong ionic interaction between carboxylate head groups of PDA and Zn^{2+}/ZnO surface, which in turn promotes the molecular ordering of conjugated backbone. This allows the melting of alkyl side chains and conjugated backbone to take place at different temperature ranges. The melting of alkyl side chains induces slight relaxation of conjugated backbone, relating to the reversible blue-to-purple color transition. The further increase of temperature results in the melting of conjugated backbone and hence induces the irreversible purple-to-red color transition. The backbone length of PDA increases with increasing photopolymerization time. In this system, partial relaxation of the molecular segments occurs within the nanocomposites. Therefore, it requires relatively low temperature to melt the alkyl side chains. The melting of conjugated backbone, on the other hand, shifts to higher temperature due to the increase of chain length.

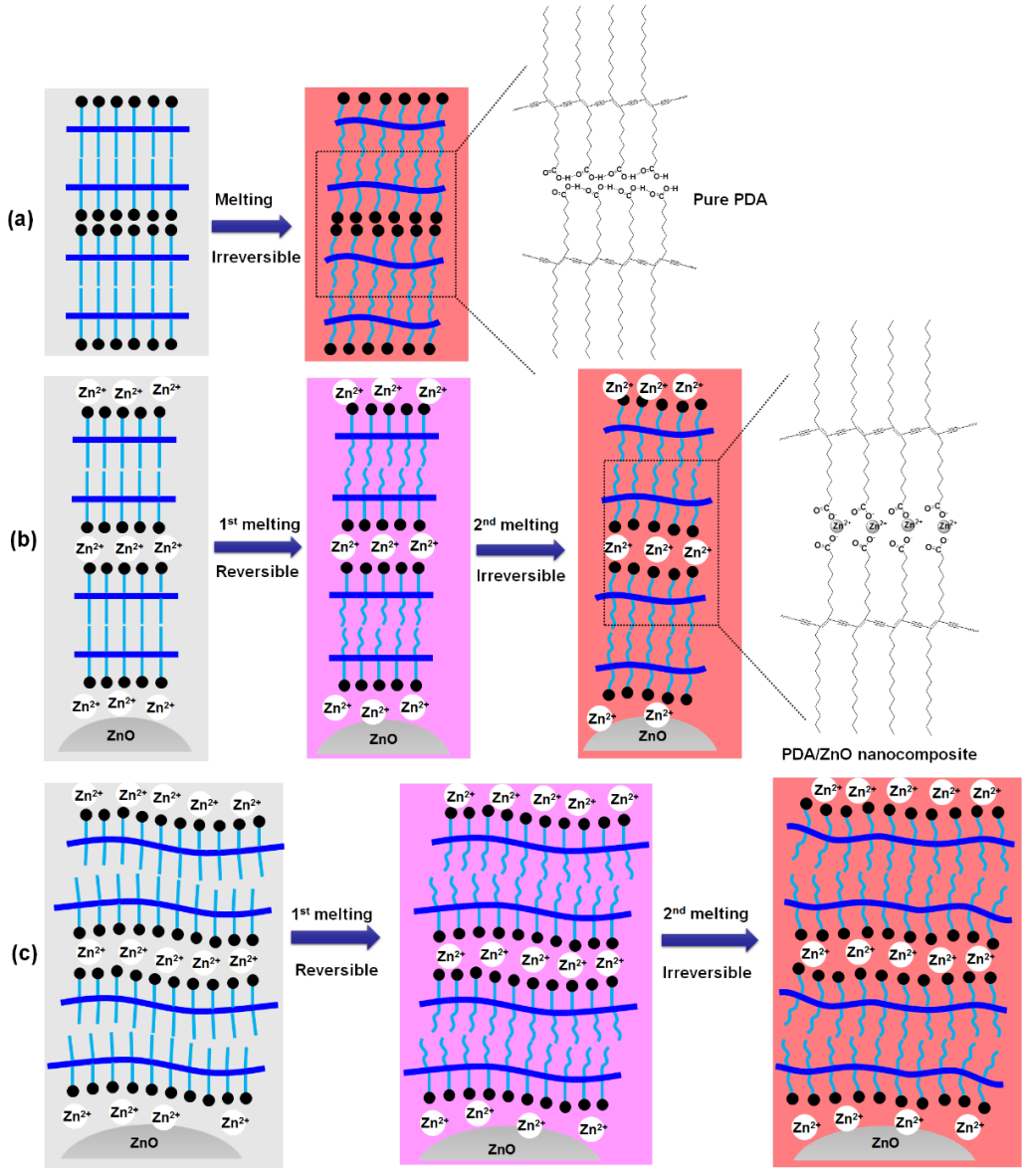

Fig. 8 Proposed models for phase/color transition behaviors upon increasing temperature of (a) pure PDAs (b, c) PDA/Zn^{2+}/ZnO nanocomposites prepared by short and long polymerization times, respectively.

Conclusion

This study demonstrates that the color/phase transition behaviors of PDA/Zn^{2+}/ZnO nanocomposites can be systematically controlled by utilizing molecular engineering approach. The increase of PDA backbone length via photopolymerization process induces partial segmental relaxation within the nanocomposites. Raman spectroscopy detects the formation of new state of PDA conjugated backbone. The magnitude of backbone relaxation, depending on photopolymerization time, dictates the reversible blue-to-purple color transition temperature. The increase of backbone length also affects the irreversible purple-to-red color transition detected at relatively high temperature. The DSC measurements reveal that these color transitions are closely related to the melting transition of alkyl side chains and PDA backbone. Our approach for controlling the color/phase transition behaviors of PDA-based materials is quite unique and never been observed in any other systems. Compared to the structural approach [27-33], our method is much simpler and allows systematic control over their color-transition properties. This approach could be utilized for improving the sensitivity of PDAs upon exposure to other stimuli such as solvents, acid/base and biomolecules. The topic is currently under investigation in our laboratories. Our study can provide a library of materials with controllable color-transition properties, extending their utilization in various applications.

References

[1] M. Takeuchi, H. Imai, Y. Oaki, Effects of the intercalation rate on the layered crystal structures and stimuli-responsive color-change properties of polydiacetylene, J. Mater. Chem. C 5 (2017) 8250-8255.

[2] M. Takeuchi, H. Imai, Y. Oaki, Real-time imaging of 2D and 3D temperature distribution: Coating of metal-ion-intercalated organic layered composites with tunable stimuli-responsive properties, ACS Appl. Mater. Interfaces 9 (2017) 16546-16552.

[3] T. Wang, Y. Guo, P. Wan, X. Sun, H. Zhang, Z. Yua, X. Chen, A flexible transparent colorimetric wrist strap sensor, Nanoscale 9 (2017) 869-874.

[4] S. Dolai, S.K. Bhunia, S.S. Beglaryan, S. Kolusheva, L. Zeiri, R. Jelinek, Colorimetric polydiacetylene–aerogel detector for volatile organic compounds (VOCs), ACS Appl. Mater. Interfaces 9 (2017) 2891-2898.

[5] M. J. Shin, J.-D. Kim, Chromatic reversibility of multilayered polydiacetylene cast film, J. Ind. Eng. Chem. 35 (2016) 211-216.

[6] M. J. Shin, D. H. Byun, J.-D. Kim, Sensitivity limitation of the sensor fabricated with polydiacetylene, J. Ind. Eng. Chem. 23 (2015) 279-284.

[7] J. P. Rezende, G.M.D. Ferreira, G.M.D. Ferreira, L.H.M. Silva, H.S.M. Carmo, M.S. Pinto, A.C.S. Pires, Polydiacetylene/triblock copolymer nanosensor for the detection of native and free bovine serum albumin, Mater. Sci. Eng. C 70 (2017) 535-543.

[8] X. Sun, T. Chen, S. Huang, F. Cai, X. Chen, Z. Yang,L. Li,H. Cao,Y. Lu, H. Peng, UV-induced chromatism of polydiacetylenic assemblies, J. Phys. Chem. B 114 (2010) 2379-2382.

[9] X. You, X. Chen, G. Zou, W. Su, Q. Zhang, P. He, Colorimetric response of azobenzene-terminated polydiacetylene vesicles under thermal and photic stimuli, Chem. Phys. Lett. 482 (2009) 129-133.

[10] A. Kamphan, C. Gong, K. Maiti, S. Sur, R. Traiphol, D.P. Arya, Utilization of chromic polydiacetylene assemblies as a platform to probe specific binding between drug and RNA, RSC Adv. 7 (2017) 41435-41443.

[11] H. Peng, X. Sun, F. Cai, X. Chen, Y. Zhu, G. Liao, D. Chen, Q. Li, Y. Lu, Y. Zhu, Q. Jia, Electrochromatic carbon nanotube/polydiacetylene nanocomposite fibres, Nat. Nanotechnol 4 (2009) 738-741.

[12] R. Varghese Hansen, L. Zhong, K.A. Khor, L. Zheng, J. Yang, Tuneable electrochromism in weavable carbon nanotube/polydiacetylene yarns, Carbon 106 (2016) 110-117.

[13] H. Wang, S. Han, Y. Hu, Z. Qi, C. Hu, Polydiacetylene-based periodic mesoporous organosilicas with colorimetric reversibility under multiple stimuli, Colloid Surf. A-Physicochem. Eng. Asp. 517 (2017) 84-95.

[14] A. Kamphan, N. Traiphol, R. Traiphol, Versatile route to prepare reversible thermochromic polydiacetylene nanocomposite using low molecular weight poly (vinylpyrrolidone), Colloid Surf. A-Physicochem. Eng. Asp. 497 (2016) 370-377.

[15] S. Lu, C. Jia, X. Duan, X. Zhang, F. Luo,Y. Han, H. Huang, Polydiacetylene vesicles for hydrogen peroxide detection, Colloid Surf. A-Physicochem. Eng. Asp. 443 (2014) 488-491.

[16] T. Pattanatornchai, N. Charoenthai, R. Traiphol, Influences of structural mismatch on morphology, phase transition temperature, segmental dynamics and color-transition behaviors of polydiacetylene vesicles, J. Colloid Interface Sci. 432 (2014) 176-181.

[17] C. Khanantong, N. Charoenthai, S. Wacharasindhu, M. Sukwattanasinitt, N. Traiphol, R. Traiphol, Influences of solvent media on chain organization and thermochromic behaviors of polydiacetylene assemblies prepared from monomer with symmetric alkyl tails, J. Ind. Eng. Chem. 58 (2018) 258-265.

[18] J. Olmsted III, M. Strand, Fluorescence of polymerized diacetylene bilayer films, J. Phys. Chem. 87 (1983) 4790-4792.

[19] J. Pang, L. Yang, B.F. McCaughey, H. Peng, H.S. Ashbaugh, C.J. Brinker, Y. Lu, Thermochromatism and structural evolution of metastable polydiacetylenic crystals, J. Phys. Chem. B 110 (2006) 7221-7225.

[20] Y. Lifshitz, Y. Golan, O. Konovalov, A. Berman, Structural transitions in polydiacetylene Langmuir films, Langmuir 25 (2009) 4469-4477.

[21] A. Fujimori, M. Ishitsuka, H. Nakahara, E. Ito, M. Hara, K. Kanai, Y. Ouchi, K. Seki, Formation of the newly greenish organized molecular film of long-chain diynoic acid derivatives by photopolymerization and its structural study using near-edge X-ray absorption fine structure (NEXAFS) spectroscopy, J. Phys. Chem. B 108 (2004) 13153-13162.

[22] R.R. Chance, G.N. Patel, J.D. Witt, Thermal effects on the optical properties of single crystals and solution-cast films of urethane substituted polydiacetylenes, J. Chem. Phys. 71 (1979) 206-211.

[23] R.R. Chance, Chromism in polydiacetylene solutions and crystals, Macromolecules 13 (1980) 396-398.

[24] M. Wenzel, G.H. Atkinson, Chromatic properties of polydiacetylene films, J. Am. Chem. Soc. 111 (1989) 6123-6127.

[25] A. Kamphan, N. Charoenthai, R. Traiphol, Fine tuning the colorimetric response to thermal and chemical stimuli of polydiacetylene vesicles by using various alcohols as additives, Colloid Surf. A-Physicochem. Eng. Asp. 489 (2016) 103-112.

[26] A. Kamphan, C. Khanantong, N. Traiphol, R. Traiphol, Structural-thermochromic relationship of polydiacetylene (PDA)/polyvinylpyrrolidone (PVP) nanocomposites: Effects of PDA side chain length and PVP molecular weight, J. Ind. Eng. Chem. 46 (2017) 130-138.

[27] D.J. Ahn, S. Lee, J.M. Kim, Rational design of conjugated polymer supramolecules with tunable colorimetric responses, Adv. Funct. Mater. 19 (2009) 1483–1496.

[28] U. Jonas, K. Shah, S. Norvez, D.H. Charych, Reversible color switching and unusual solution polymerization of hydrazide-modified diacetylene lipids, J. Am. Chem. Soc. 121 (1999) 4580-4588.

[29] Q. Ye, X. You, G. Zou, X. Yu, Q. Zhang, Morphology, structure and chromatic properties of azobenzene-substituted polydiacetylene supramolelular assemblies, J. Mater. Chem. 18 (2008) 2775-2780.

[30] J.-M. Kim, J.-S. Lee, H. Choi, D. Sohn, D.J. Ahn, Rational design and in-Situ FTIR analyses of colorimetrically reversibe polydiacetylene supramolecules, Macromolecules 38 (2005) 9366-9367.

[31] S. Wacharasindhu, S. Montha, J. Boonyiseng, A. Potisatityuenyion, C. Phollookin, G. Tumcharern, M. Sukwattanasinitt, Tuning of thermochromic properties of polydiacetylene toward universal temperature sensing materials through amido hydrogen bonding, Macromolecules 43 (2010) 716-724.

[32] S. Ampornpun, S. Montha, G. Tumcharern, V. Vchirawongkwin, M. Sukwattanasinitt, S. Wacharasindhu, Odd–even and hydrophobicity effects of diacetylene alkyl chains on thermochromic reversibility of symmetrical and unsymmetrical diyndiamide polydiacetylenes, Macromolecules 45 (2012) 9038-9045.

[33] S. Lee, J. Lee, M. Lee, Y.K. Cho, J. Baek, J. Kim, S. Park, M.H. Kim, R. Chang, J. Yoon, Construction and molecular understanding of an unprecedented, reversibly thermochromic bis-polydiacetylene, Adv. Funct. Mater. 24 (2014) 3699-3705.

[34] J. Lee, M. Pyo, S.-H. Lee, J. Kim, M. Ra, W.-Y. Kim, B.J. Park, C.W. Lee, J.-M. Kim, Hydrochromic conjugated polymers for human sweat pore mapping, Nat. Commun. 5 (2014) Article number: 3736.

[35] S. Balakrishnan, S. Lee, J.-M. Kim, Thermochromic reversibility of conjugated polymers derived from a diacetylenic lipid containing lithium salt, J. Mater. Chem. 20 (2010) 2302–2304.

[36] L. Yu, S.L. Hsu, A spectroscopic analysis of the role of side chains in controlling thermochromic transitions in polydiacetylenes, Macromolecules 45 (2012) 420–429.

[37] K.-Y. Fu, D.-Y. Chen, Nanocomposites of polydiacetylene and rare earth ions with reversible thermochromism, Chin. J. Chem. Phys. 27 (2014) 465–470.

[38] N. Traiphol, N. Rungruangviriya, R. Potai, R. Traiphol, Stable polydiacetylene/ZnO nanocomposites with two-steps reversible and irreversible thermochromism: the influence of strong surface anchoring, J. Colloid Interface Sci. 356 (2011) 481-489.

[39] A. Chanakul, N. Traiphol, R. Traiphol, Controlling the reversible thermochromism of polydiacetylene/zinc oxide nanocomposites by varying alkyl chain length, J. Colloid Interface Sci. 389 (2013) 106-114.

[40] A. Chanakul, N. Traiphol, K. Faisadcha, R. Traiphol, Dual colorimetric response of polydiacetylene/Zinc oxide nanocomposites to low and high pH, J. Colloid Interface Sci. 418 (2014) 43-51.

[41] N. Traiphol, K. Faisadcha, R. Potai, R. Traiphol, Fine tuning the color-transition temperature of thermoreversible polydiacetylene/zinc oxide nanocomposites: the effect of photopolymerization time, J. Colloid Interface Sci. 439 (2015) 105-111.

[42] S. Toommee, R. Traiphol, N. Traiphol, High color stability and reversible thermochromism of polydiacetylene/zinc oxide nanocomposite in various organic solvents and polymer matrices, Colloids Surf. A: Physicochem. Eng. Asp. 468 (2015) 252-261.

[43] A. Chanakul, R. Traiphol, N. Traiphol, Colorimetric sensing of various organic acids by using polydiacetylene/zinc oxide nanocomposites: Effects of polydiacetylene and acid structures, Colloids Surf. A: Physicochem. Eng. Asp. 489 (2016) 9-18.

[44] N. Traiphol, A. Chanakul, A. Kamphan, R. Traiphol, Role of Zn^{2+} ion on the formation of reversible thermochromic polydiacetylene/zinc oxide nanocomposites, Thin Solid Films 622 (2017) 122-129.

[45] A. Chanakul, R. Traiphol, N. Traiphol, Utilization of polydiacetylene/zinc oxide nanocomposites to detect and differentiate organic bases in various media, J. Ind. Eng. Chem. 45 (2017) 215-222.

[46] A. Patlolla, J. Zunino, A.I. Frenkel, Z. Iqbal, Thermochromism in polydiacetylene-metal oxide nanocomposites, J. Mater. Chem. 22 (2012) 7028-7035.

[47] H. Peng, J. Tang, L. Yang, J. Pang, H.S. Ashbaugh, C.J. Brinker, Z. Yang, Y. Lu, Responsive periodic mesoporous polydiacetylene/silica nanocomposites, J. Am. Chem. Soc. 128 (2006) 5304-5305.

[48] X. Huang, S. Jiang, M. Liu, Metal ion modulated organization and function of the Langmuir－Blodgett films of amphiphilic diacetylene: photopolymerization, thermochromism, and supramolecular chirality, J. Phys. Chem. B 109 (2005) 114-119.

[49] H.L. Casal, H.H. Mantsch, D.G. Cameron, Interchain vibrational coupling in phase II (hexagonal) n-alkanes, J. Chem. Phys. 77 (1982) 2825-2830.

[50] S.J. Kew, E.A. Hall, pH response of carboxy-terminated colorimetric polydiacetylene vesicles, Anal. Chem. 78 (2006) 2231-2238.

[51] N. Mino, H. Tamura, K. Ogawa, Analysis of color transitions and changes on Langmuir-Blodgett films of a polydiacetylene derivative, Langmuir 7 (1991) 2336-2341.

[52] Y. Lifshitz, A. Upcher, O. Shusterman, B. Horovitz, A. Berman, Y. Golan, Phase transition kinetics in Langmuir and spin-coated polydiacetylene films, Phys. Chem. Chem. Phys. 12 (2010) 713-722.

[53] E. Shirai, Y. Urai, K. Itoh, Surface-enhanced photopolymerization of a diacetylene derivative in Langmuir-Blodgett films on a silver island film, J. Phys. Chem. B 102 (1998) 3765-3772.

[54] Y. Lifshitz, A. Upcher, A. Kovalev, D. Wainstein, A. Rashkovsky, L. Zeiri, Y. Golan, A. Berman, Zinc modified polydiacetylene Langmuir films, Soft Matter 7 (2011) 9069-9077.

[55] C. Girard-Reydet, R. D. Ortuso, M. Tsemperouli, K. Sugihara, Combined electrical and optical characterization of polydiacetylene, J. Phys. Chem. B 120 (2016) 3511-3515.

[56] S. Chen, H.-B. Luo, H.-L. Xie, H.-L. Zhang, Synthesis of comb polyphenylenes by Suzuki coupling from AB macromonomers, J. Polym. Sci. A: Polym. Chem. 51 (2013) 924-935.

Supporting Information

Table 1 C═C and C≡C Raman peak frequencies of pure poly(PCDA) and poly(PCDA)/Zn^{2+}/ZnO nanocomposite obtained from different polymerization times

Samples	$\boldsymbol{\nu}$ (C═C), cm^{-1}	$\boldsymbol{\nu}$ (C≡C), cm^{-1}
Poly(PCDA) (blue)	1451	2080
poly(PCDA)/Zn^{2+}/ZnO5m	1450	2076
poly(PCDA)/Zn^{2+}/ZnO30m	1450, 1474	2075, 2094
poly(PCDA)/Zn^{2+}/ZnO60m	1450, 1474	2075, 2095
poly(PCDA)/Zn^{2+}/ZnO90m	1450, 1476	2075, 2097
poly(PCDA)/Zn^{2+}/ZnO120m	1451, 1483	2078, 2097
Poly(PCDA) (red)	1511	2116

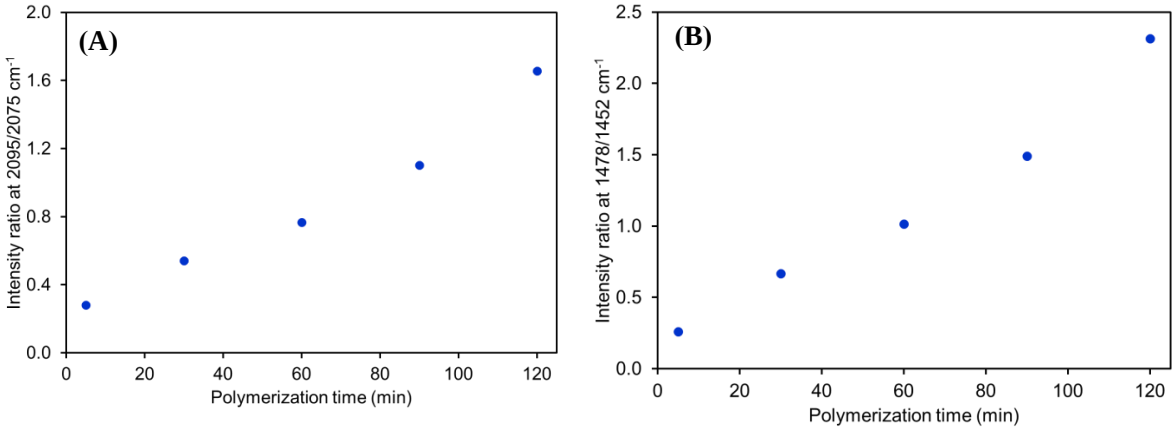

Fig. 1s Raman intensity ratio (A) 2095/2075 cm^{-1} and (b) 1478/1452 cm^{-1}

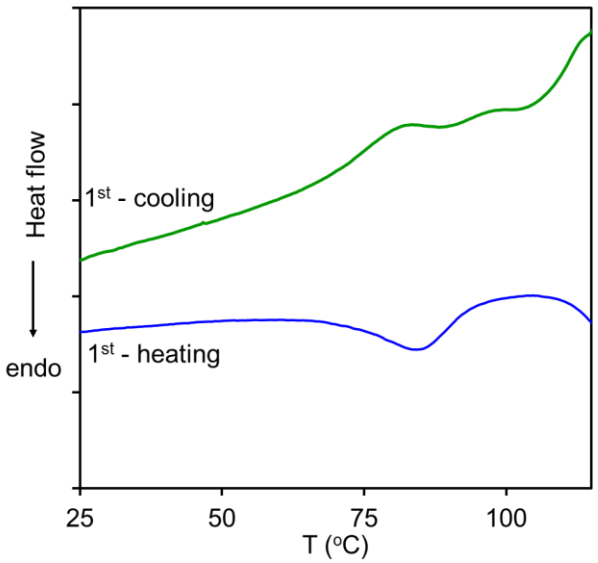

Fig. 2s DSC thermogram of poly(PCDA)/Zn^{2+}/ZnO5m nanocomposite upon heating/cooling cycle from -30 °C to 120 °C.

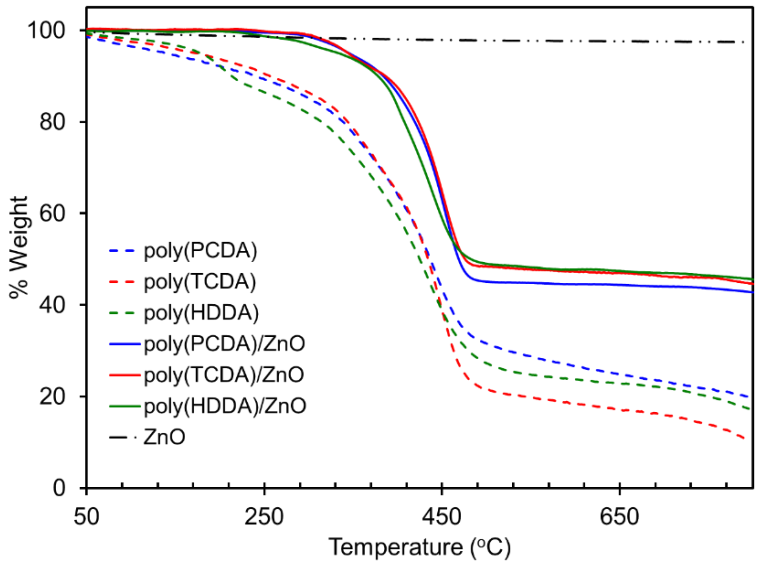

Fig. 3s TGA results of pure PDA, PDA/Zn^{2+}/ZnO nanocomposites and ZnO nanoparticle. The ratio of ZnO is 20 wt%.

บทที่ 3

Controlling self-assembling and color-transition of polydiacetylene/zinc(II) ion/zinc oxide nanocomposites by varying pH: Effects of surface charge and headgroup dissociation

Abstract

Polydiacetylene/zinc(II) ion/zinc oxide (PDA/Zn^{2+}/ZnO) nanocomposite exhibits reversible thermochromism and dual colorimetric response to acid/base. This contribution presents our ongoing development of the PDA/Zn^{2+}/ZnO nanocomposite for sensing applications by controlling ZnO surface charge and dissociation of PDA headgroup via pH adjustment. At pH >10, negative ZnO surface charge and PDA carboxylate headgroup significantly enhance molecular organization during the self-assembling process. An increase of the nanocomposite amount after photopolymerization is observed. Oppositely, pH <6 results in irreversible-thermochromic nanocomposites. Additionally, the nanocomposites prepared at different pH change color at different concentrations of chemical stimuli. Molecular packing, local interactions and PDA conformation are investigated.

Keywords: polydiacetylene; color transition; sensor; self-assembling; surface charge; dissociation

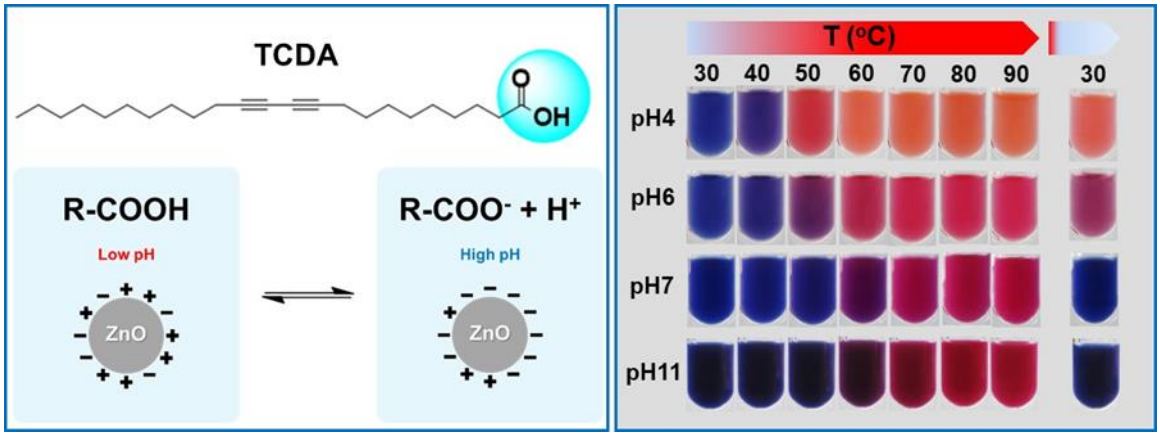

Highlights

- Polydiacetylene/zinc(II) ion/zinc oxide nanocomposites are prepared at various pHs.
- Nanocomposites prepared at pH 7 and 11 provide reversible thermochromism.
- Concentration of nanocomposite significantly increases at pH 11.
- Nanocomposites prepared at pH 6 and 4 provide irreversible thermochromism.
- Colorimetric response of nanocomposites to acid or base can be controlled.

Introduction

Stimuli-responsive polydiacetylenes (PDA) have shown a potential for being utilized in various applications such as thermal, chemical, biological and friction force sensors [1-16], sweat

pore mapping [17], electro-thermochromic displays [18], counterfeiting materials [19], photodetectors [20] and smart textiles [21]. The preparation of PDA-based materials generally involves the self-assembling of diacetylene (DA) monomer into organized structures, following by topotactic polymerization via UV light irradiation [1,11,12]. The process yields a metastable state of PDA exhibiting a deep blue color. Upon subjected to external stimuli such as heat [4,11-13], solvents [5,7,14,15], acids/bases [11, 22-25] and mechanical stress [8], the PDA side chain and/or conjugated backbone relax to a stable state. Segmental rearrangement during the relaxation process affects the conjugation length within the system, which causes the color transition, normally, from blue to red [26-28].

In order to control the color-transition behaviors of PDAs, chemical modification of the DA headgroup and/or side chain has been widely studied [1,3,4,6,7,9,11,13,16,29-35]. The method provides PDA-based materials with controllable color-transition temperature and reversible thermochromism in some cases [3,9,11,13,29-35]. This approach also allows molecular engineering to achieve specific interactions between PDAs and targeted chemical stimuli and biomolecules [1,4,6,16]. However, complicate, multi-step and time-consuming processes along with expensive chemicals and/or catalysts are usually required. Our research group has introduced a simple and cost-effective method to control color-transition behaviors of PDA by

incorporating zinc oxide (ZnO) nanoparticles into the PDA assemblies [12,23-25, 36-40]. The recent work by our group reveals that, in aqueous suspension, Zn^{2+} ions released from ZnO nanoparticles intercalate into the PDA bilayers [12,40]. This process yields strong interfacial interactions between PDA headgroups and ZnO nanoparticles.

The resulting PDA/Zn^{2+}/ZnO nanocomposite exhibits higher color-transition temperature comparing to pure PDA prepared from the same DA monomer [36,37]. The relatively strong overall interactions within this system also provide reversible thermochromism. We further demonstrate that color-transition temperature of the nanocomposite can be tuned by varying alkyl side chain and backbone length of PDA [12,37,38]. In addition, the presence of ZnO nanoparticles allows dual colorimetric response of the nanocomposite to both acid and base [25]. This unprecedented behavior extends their utilization as colorimetric sensors for detecting various organic acids or bases dissolved in different media such as water, toluene and milk [23,24].

In this continuing study, we explore the roles of PDA headgroup dissociation and ZnO surface charge on the formation of nanocomposite and its properties. Upon increasing pH, carboxylic headgroup of the DA monomer, 10,12-tricosadiynoic acid (TCDA), can be converted to negatively charged carboxylate ones (Fig.1) [22]. Surface charge of ZnO nanoparticles is also affected by pH variations (Fig.1s, supporting information). At pH 7, the ZnO surface charge is

positive, then the value decreases and reaches isoelectric point at pH 8. In the higher pH region, the ZnO surface charge becomes negative. We hypothesize that the variations of pH during the preparation process could affect the strength of local interfacial interactions within the nanocomposite, and, hence, its color-transition behaviors. In this work, we prepare the PDA/Zn^{2+}/ZnO nanocomposites at pH ranging from 4 to 13. We have found that color-transition behaviors of the obtained nanocomposites upon exposure to heat, acid or base can be controlled by adjusting the pH during preparation. Origins of this behavior are elucidated by utilizing various techniques including X-ray diffraction, infrared and Raman spectroscopy.

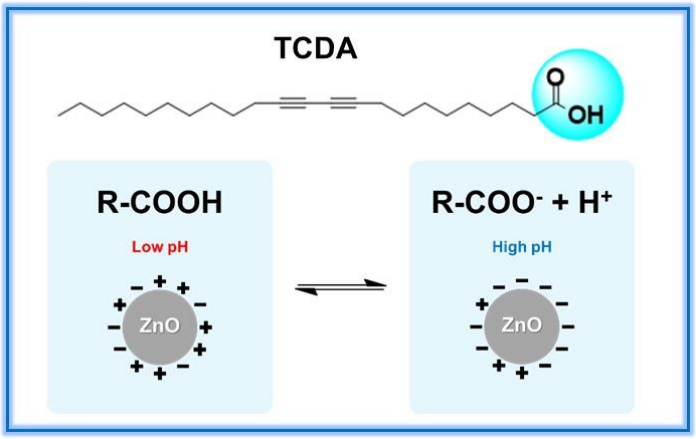

Fig. 1. Chemical structure of 10,12-tricosadiynoic acid (TCDA), its dissociation and surface charge of ZnO nanoparticles at low and high pH regions.

Experimental

The TCDA monomer and ZnO nanoparticles were purchased from Fluka and Nano Materials Technology (Thailand), respectively. The ZnO diameter ranges from about 20 to 200

nm with the averaged value of about 65 nm [12]. Zeta potential of the ZnO nanoparticles in an aqueous suspension was measured at various pH using Brookhaven, ZetaPaLs. The preparation of poly(TCDA)/Zn^{2+}/ZnO nanocomposite was slightly modified from the procedure described in our previous works [36,37]. The concentration of TCDA was 1.0 mM and the ratio of ZnO to TCDA was 10 wt.% in all experiments. The mixtures were co-dispersed in aqueous medium by ultrasonication. HCl and NaOH solutions were used to adjust the pH of suspension during the mixing process. After incubation at 4^{o}C overnight, topotactic polymerization of the organized TCDA was performed by UV light irradiation (λ = 254 nm, 10 watts) for 4 min to obtain blue-phase poly(TCDA)/Zn^{2+}/ZnO nanocomposite. For comparison purpose, the pure poly(TCDA) was prepared employing the same procedure excepting the addition of ZnO nanoparticles.

Particle size distribution of the pure poly(TCDA) and poly(TCDA)/Zn^{2+}/ZnO nanocomposite was obtained using dynamic light scattering technique (Brookhaven, ZetaPaLs). Absorption spectra were measured using a UV-Vis spectrophotometer equipped with a temperature-control unit (Analytik Jena Specord S100). For determination of relative concentration of the nanocomposite, the absorbance (λ = 640 nm) obtained at pH 7 was used to normalize the absorbance obtained from the other conditions. FT-IR spectra were measured using Nicolet 6700 FT-IR spectrometer in a transmittance mode. Raman spectra were obtained using FT-Raman

spectrometer (PerkinElmer Spectrum GX) with a 1064 nm laser (Nd:YAG) as an excitation source. Structure of the nanocomposite was studied using X-ray diffractometer (XRD) (Bruker AXS Model D8 Discover, λ(Cu-K_α) = 1.54 Å). Dried samples for these measurements were obtained by drop casting onto glass slides.

Results and discussion

Effects of pH on self-assembling behaviors

It is known that the aqueous suspension of ZnO nanoparticles at equilibrium state contains $Zn^{2+}_{(aq)}$, $Zn(OH)^{+}_{(aq)}$, $Zn(OH)_{2(aq)}$, $Zn(OH)_3^{-}{}_{(aq)}$, and $Zn(OH)_4^{2-}{}_{(aq)}$ species [41]. Concentration of these species absorbed onto the surface of ZnO nanoparticle gives rise to its surface charge, which strongly depends on pH of the suspension (Fig. 1s, supporting information). ZnO surface charge is highly positive when pH is at 7, then, it converts to negative when pH is above 8. When mixing the pH-adjusted ZnO suspension with the TCDA monomer, the dissociation of carboxylic headgroup (—COOH) of the TCDA also involves. Previous study by Kew et. al showed that the pKa of TCDA monomer ranged from 9.5 to 9.9 [22]. Based on this pKa value, the concentration of carboxylate ion, [—COO^-], in the suspension can be evaluated at specified pH (Fig.2s,

supporting information). The –COOH group begins to dissociate around pH 8, then, [—COO^-] sharply increases with increasing pH from 8 to 11 and reaches 99 % at pH 12.

The variation of pH strongly affects the self-assembling of TCDA monomer onto the ZnO nanoparticles. Fig. 2a illustrates the absorption spectra of poly(TCDA)/Zn^{2+}/ZnO nanocomposites prepared at different pH. A normal preparing condition (pH 7) provides an intense blue color suspension. When adjusting pH to 11, a large fraction of the –COOH headgroup is converted to the $–COO^-$, meanwhile, the surface charge of ZnO nanoparticles becomes highly negative. The suspension with more intense blue color is obtained. It is known that the topotactic photopolymerization of PDA materials requires specific arrangement of the diacetylene moieties within the assemblies [9,42]. Therefore, our observation indicates that increasing pH promotes the molecular ordering of TCDA monomer resulting in the increase of percent conversion to poly(TCDA) with blue color. The absorption spectrum of the suspension prepared at pH 11 is similar to that of pH 7. However, further increase of pH to 13, a suspension with intense red color is obtained with the λ_{max} shifted to 550 nm. The formation of a red-phase material at the high pH condition indicates the change of molecular arrangement within poly(TCDA) assemblies as described in a literature [26]. The dissolution of ZnO nanoparticles occurred at pH 13 as reported in our previous study [25] could be responsible for the formation of red-phase material. To

investigate this hypothesis, samples are prepared at pH 6 and 4, in which the dissolution of ZnO nanoparticles also occurs. However, intense blue color suspensions are obtained at these conditions with small fraction of red phase indicated by a small peak at 550 nm in the absorption spectra. This result suggests that the dissolution of ZnO nanoparticles exhibits a minor effect on this phenomenon.

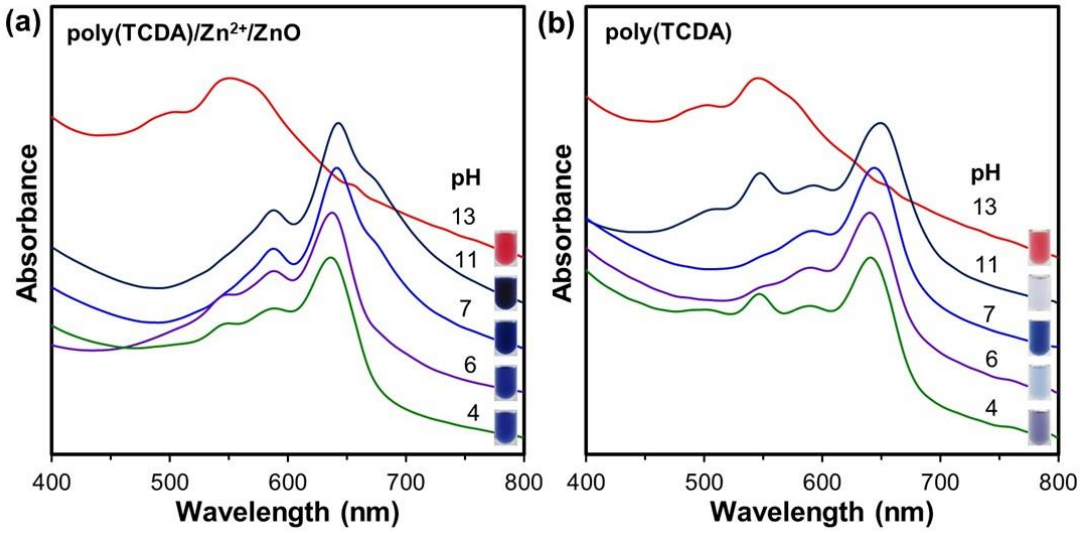

Fig. 2. Normalized absorption spectra of (a) poly(TCDA)/Zn^{2+}/ZnO nanocomposites and (b) pure poly(TCDA) assemblies prepared at various pH. (inset) Color photographs of as-prepared samples in aqueous suspensions.

The preparation of pure poly(TCDA) at the normal condition (pH 7) provides a blue suspension with less intense color compared to that of the nanocomposite. When the preparation process takes place at pH 11, 6 and 4, the blue color of pure poly(TCDA) drastically fades as

shown in Fig. 2b. It indicates that only a small fraction of TCDA monomer is converted to poly(TCDA). Comparing between poly(TCDA) and poly(TCDA)/Zn^{2+}/ZnO, our results illustrates that the presence of ZnO nanoparticles promotes the molecular organization of TCDA monomer. This attributes to strong interactions between –COOH and/or $–COO^-$ headgroups of TCDA monomer and Zn^{2+}/ZnO surface. The increase of pH to 11 results in the increase of $–COO^-$ fraction, which, in turn, increases the strength of local interactions with Zn^{2+}/ZnO surface. Our result also shows that the incorporation of ZnO nanoparticles allows the preparation of PDA-based materials at relatively high and low pH conditions, which could extend their utilization in many applications. It is worthwhile to note that the preparation of pure poly(PCDA) at pH 13 provides an intense red color suspension similar to the system of the nanocomposite. Therefore, the formation of red phase is likely to arise from the complete dissociation of the –COOH headgroup. A previous study by Pang et.al also provided a red phase PDA when adding a large amount of NaOH to the system during the preparation process [26]. The authors observed the intercalation of Na^+ ions with bilayer of PDA, which altered the molecular packing within the assemblies.

We further investigate the relative concentration of the nanocomposite prepared at various pH. Absorbance of the blue phase at 640 nm, proportional to concentration of the nanocomposite,

is determined for each preparing condition. The result is normalized by absorbance value obtained at pH 7. The plot between relative concentration of the nanocomposite and preparing pH is illustrated in Fig. 3. The increase of pH from 7 to 9 hardly affects concentration of the nanocomposite. When the pH is further increased to 10, concentration of the nanocomposite abruptly increases. At pH 11, it increases up to twice the value of the one prepared at pH 7. The increase of nanocomposite concentration at this pH range is parallel to the increase of $–COO^-$ group concentration. This observation signifies the role of $–COO^-$ group on the self-assembling behavior within the nanocomposites. It is worthwhile to note that the decrease of pH to 6 results in a significant decrease of the nanocomposite concentration. This is due to partial dissolution of ZnO nanoparticles in acidic condition [25]. The variation of preparing pH slightly affects the particle size of assemblies (Fig. 3s, supporting information).

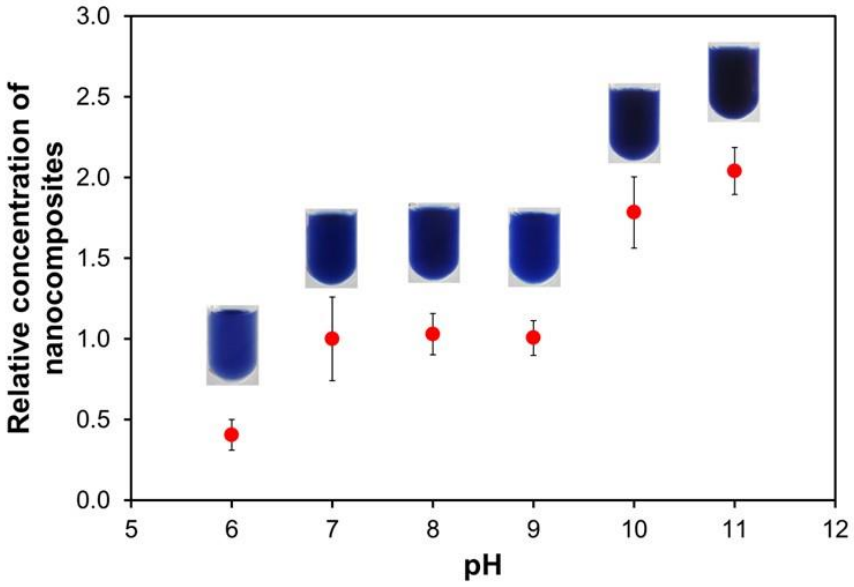

Fig. 3. Relative concentration and color photographs of poly(TCDA)/Zn^{2+}/ZnO nanocomposites prepared at various pHs. Average values and error bars were obtained from 5 batches.

Packing structure, interfacial interaction and molecular conformation

In this section, the molecular organization within assemblies is probed using various techniques. Dried films of all samples were prepared by drop casting on glass slides. Fig. 4a illustrates XRD patterns of the pure poly(TCDA) assembly comparing to the poly(TCDA)/Zn^{2+}/ZnO nanocomposites prepared at various pH. It has been reported in literatures that this class of material exhibits a bilayer lamellar structure [26,28,43,44]. The XRD pattern of pure poly(TCDA) exhibits three peaks corresponding to diffraction planes of the lamellar structure. An interlayer lamellar d-spacing of poly(TCDA) is 4.16 nm (Fig. 4s, supporting information). The XRD pattern

of nanocomposite prepared at pH 7 exhibits five peaks. The detection of additional two diffraction peaks indicates the increase of molecular ordering within the nanocomposite. In addition, the interlayer d-spacing increases to 5.03 nm, indicating the intercalation of Zn^{2+} ions within the bilayer of poly(TCDA) as shown in Fig. 4b. Since the ionic diameter of Zn^{2+} ion is rather small (∼0.18 nm), the intercalation is not a sole contribution to the increase of interlayer d-spacing. Tilting angle of the poly(TCDA) alkyl side chain with respect to the plane of lamellar layer might also increase as described in previous studies [43,44]. We note that the Zn^{2+} ions in our system release from the ZnO nanoparticle during the preparation process [40]. The intercalated structure with comparable interlamellar d-spacing value is also observed for the nanocomposite prepared at pH 11. It is important to point out that the ZnO nanoparticle mostly dissolves at pH 4 [25]. However, the packing structure similar to the other conditions is still attained.

Fig. 5a shows FT-IR spectra of pure poly(TCDA) comparing to those of poly(TCDA)/Zn^{2+}/ZnO nanocomposites prepared at various pH. The spectrum of pure poly(TCDA) exhibits a broad band near 1693 cm^{-1} assigned to hydrogen-bonded carbonyl stretching of the –COOH headgroup [22]. The peaks around 1470-1420 cm^{-1} are due to the methylene scissoring vibration of alkyl side chain. For the nanocomposite prepared at pH 7, new peaks at 1540 and 1398 cm^{-1} are clearly observed corresponding to the asymmetric and symmetric stretching

vibrations, respectively, of the carboxylate anion coordinated with Zn^{2+} cation as illustrated in Fig. 5b [40,46]. The nanocomposite prepared at pH 11 exhibits a similar FT-IR pattern. Additionally, a new peak at 1560 cm^{-1} is detected corresponding to the presence of strong interaction between the carboxylate anion and Na^{+} cation [45]. This observation suggests that the pH modification using NaOH also incorporates Na^{+} ion into the bilayer structure (Fig. 5b). Partial dissolution of ZnO nanoparticles occurs at pH 6, 5 and 4. At these conditions, the growth of broad band at 1618 cm^{-1} is detected. It is known that the vibrational frequency of carboxylate anion varies with the strength of local interaction with cation [46]. Since our system does not contain any other cations, this peak is assigned to a new type of the Zn^{2+}-coordinated carboxylate group (Fig. 5b) with different strength of local interaction from the one detected at 1540 cm^{-1}. We note that the peak of hydrogen bonded –COOH group at 1693 cm^{-1} reappears at pH 4, attributed to the protonation of HCl acid. Our FT-IR results indicate that the variation of preparing pH strongly affects the strength of local interactions within the nanocomposites.

Conformational change of conjugated backbone and alkyl side chain of the poly(TCDA)/Zn^{2+}/ZnO nanocomposites is explored by Raman spectroscopy. It is known that the C≡C and C=C stretching modes of PDA conjugated backbone in a blue phase occur at ~2080 and ~1450 cm^{-1}, respectively [12,45,47-50]. Perturbation of PDA assemblies by thermal treatment

usually induces the relaxation of conjugated backbone and side chain, causing the color transition to red phase. The C≡C and C=C stretching modes in the new local environments shift to ~2116 and ~1511 cm^{-1}, respectively [12,45]. The Raman bands in the region of 1150-1000 cm^{-1} also provide useful information about the conformation of alkyl side chain [51,52]. Previous study by Park et.al showed that the Raman spectrum of crystalline DA monomer exhibited several sharp peaks in this region, corresponding to *all-trans* conformation of the long alkyl side chain [51]. The DA monomer in melted state, on the other hand, showed a rather broad peak, indicating the presence of some *gauche* conformation.

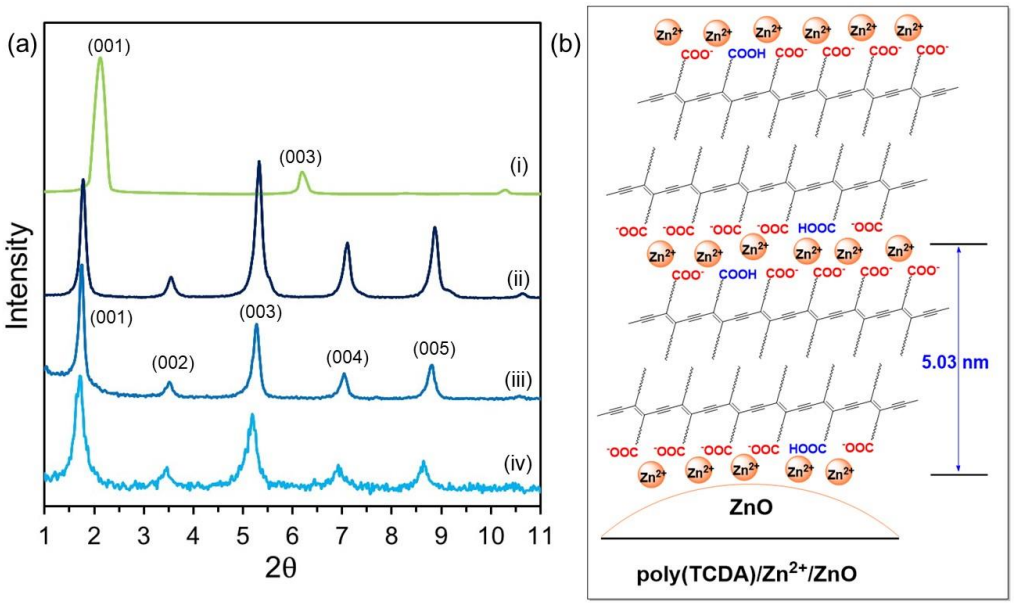

Fig. 4. (a) XRD pattern of (i) pure poly(TCDA) and poly(TCDA)/Zn^{2+}/ZnO nanocomposites prepared at (ii) pH 11, (iii) pH 7 and (iv) pH 4. (b) Molecular packing models of poly(TCDA)/Zn^{2+}/ZnO nanocomposite.

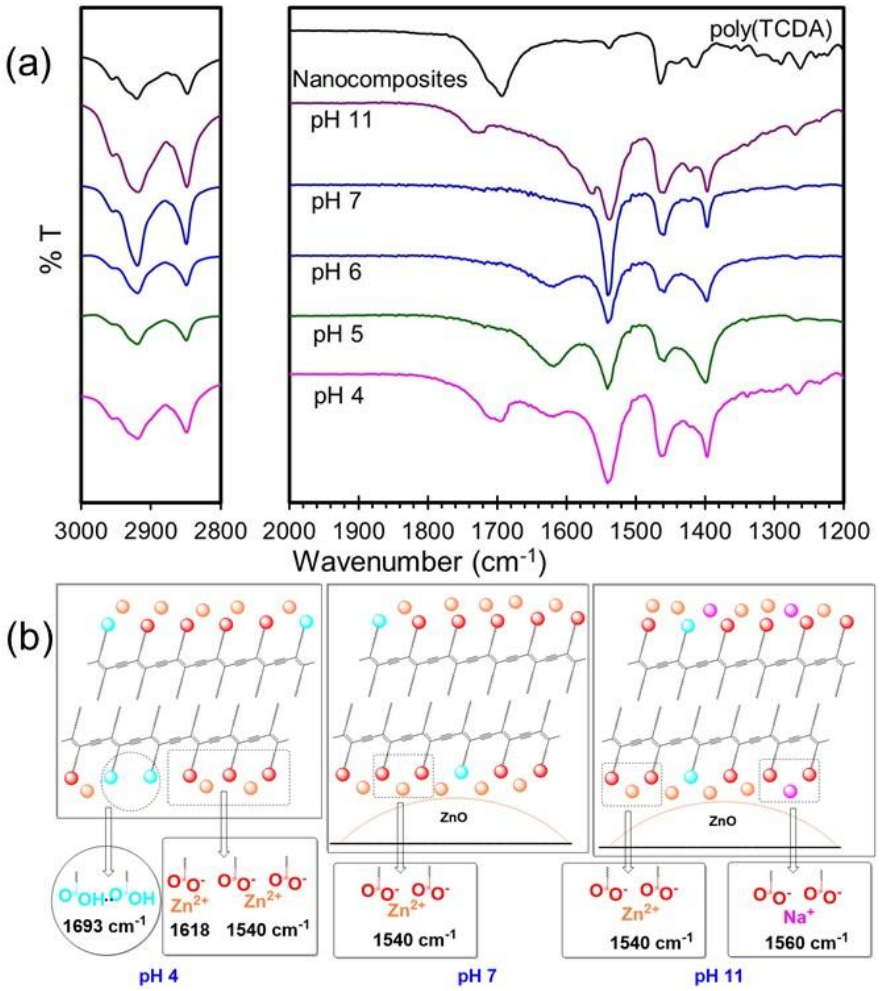

Fig. 5. (a) FT-IR spectra of pure poly(TCDA) and poly(TCDA)/Zn^{2+}/ZnO nanocomposites prepared at pH 11, pH 7, pH 6, pH 5 and pH 4. (b) Models for local molecular interactions within the nanocomposites prepared at pH 4, pH 7 and pH 11.

Raman spectra of the nanocomposites prepared at pH 7 and 11 show strong peaks at 2076 and 1450 cm^{-1} indicating a backbone conformation in blue phase (Fig. 6a). The detection of sharp peaks at 1123, 1101, 1082, 1065 and 1050 cm^{-1} also suggests the presence of *all-trans*

conformation of the alkyl side chain. For the system of nanocomposite prepared at pH 6, a growth of new peaks at 2097 and 1478 cm^{-1} is detected, corresponding to the stretching vibration of the C≡C and C=C bonds, respectively. The result indicates that a large fraction of PDA conjugated backbone relaxes into a new local environment. The new PDA conformation is an intermediate state between the commonly known blue and red phases. This observation is consistent with the results obtained from FT-IR study, in which, two types of Zn^{2+}-coordinated carboxylate group are detected at this preparing condition. We believe that the partial dissolution of ZnO nanoparticles at pH 6 reduces the strength of interfacial interactions within the nanocomposite, allowing partial relaxation of conjugated backbone. The intermediate phase of PDA backbone was also observed in our previous study, in which, the nanocomposites were prepared by increasing photopolymerization time [12]. The presence of this intermediate phase significantly affects their color-transition behaviors.

The preparation of nanocomposites at pH 5 and 4 induces further relaxation of conjugated backbone. An additional peak at 1500 cm^{-1} is detected at preparing condition of pH 5. Decreasing pH to 4 causes a growth of two peaks at 2114 and 1512 cm^{-1}, indicating partial relaxation of some conjugated backbone into the red phase. Previous studies by X-ray scattering detected the shrinkage of unit cell during the blue-to-red color transition, where the stacking distance between

conjugated backbones was reduced (Fig. 6a, bottom) [27,28]. The conformational change of alkyl side chain is also detected. The sharp peaks in the region of 1150-1000 cm^{-1} merge together, becoming a broad peak at 1065 cm^{-1}. The observation of broad peak in this region indicates the presence of some *gauche* conformation within the alkyl side chain as illustrated in Fig. 6(a,b). We suggest that the strength of interfacial interactions is further reduced at preparing condition of pH 4. This allows the relaxation of some conjugated backbone into the red phase and causes the conformational change of alkyl side chain. It is worthwhile to note that the XRD results in Fig. 4 do not detect any change of the interlamellar d-spacing. The change of molecular packing structure is likely to take place at different length scale.

Colorimetric response to temperature, acid and base

The variation of preparing pH significantly affects the strength of inter-/intramolecular interactions and molecular conformation within the nanocomposites, causing a drastic change of their thermochromic behaviors. Fig. 7(a,b) show temperature-dependent absorption spectra of the nanocomposites prepared at pH 11 and pH 4. At room temperature, all nanocomposites in aqueous suspensions are in the blue phase (Fig. 7c). Increasing temperature induces segmental rearrangement of the PDA chains, which, in turn, causes the blue shift of absorption spectra. For the nanocomposite prepared at pH 11, an abrupt change of absorption spectrum is detected at

the transition temperature of 65°C. At this state, the suspension appears purple and the λ_{max} shifts to 597 nm. The plots of colorimetric response (%CR) and λ_{max} values show a sharp increase of %CR and the drop of λ_{max} value at color-transition region (Fig. 5s, supporting information). The nanocomposite prepared at pH 7 also exhibits the blue-to-purple color transition at 65°C. The absorption spectra of these nanocomposites fully reverse back to the original pattern upon cooling to room temperature. Their complete thermochromic reversibility persists for at least 10 heating/cooling cycles (Fig. 6s, supporting information).

The preparation of nanocomposites at pH 6 and 4 provides rather different thermochromic behaviors. The color photographs in Fig. 7c show that color transition takes place at 50°C and 40°C for the nanocomposites prepared at pH 6 and pH 4, respectively. The decrease of color-transition temperature corresponds to the weakening of inter- and intramolecular interactions within the nanocomposites as revealed by the FT-IR and Raman studies in the previous section. The nanocomposite prepared at pH 6 exhibits a partial reversible thermochromism. This result is consistence with the Raman study, in which, two types of backbone conformation are detected at this condition. We believe that the partial dissolution of ZnO nanoparticle plays a major role on the thermochromic reversibility of the nanocomposite. When the preparing pH is decreased to 4, most of the ZnO nanoparticles are dissolved [25]. The nanocomposite prepared at this condition

shows a complete irreversible thermochromism. It is worthwhile to point out that the XRD result in the previous section observes a Zn^{2+}-intercalated structure within the nanocomposite prepared at pH 4. This observation suggests that the presence of ZnO nanoparticle is essential to achieve a complete reversible thermochromism.

Thin films of the nanocomposite prepared at pH 4 exhibit irreversible thermochromism at about 60°C (Fig. 7s, supporting information). On the other hand, films of the nanocomposites prepared at pH 7 and 11 exhibit reversible blue-to-purple color transition at about 90°C. Their thermochromic reversibility persists up to about 160°C. The further increase of temperature to 200°C causes irreversible color transition to the red phase. Raman spectrum of the red phase shows the stretching vibration of the C≡C and C=C bonds at 2115 and 1512 cm^{-1}, respectively, corresponding to the relaxation of poly(TCDA) backbone (Fig. 8s, supporting information). A broad peak at 1065 cm^{-1} is also detected, indicating the presence of some *gauche* conformation of alkyl side chain. However, our previous study via XRD did not observe any significant change of the interlamellar d-spacing of the bilayer structure of nanocomposite in red phase [40].

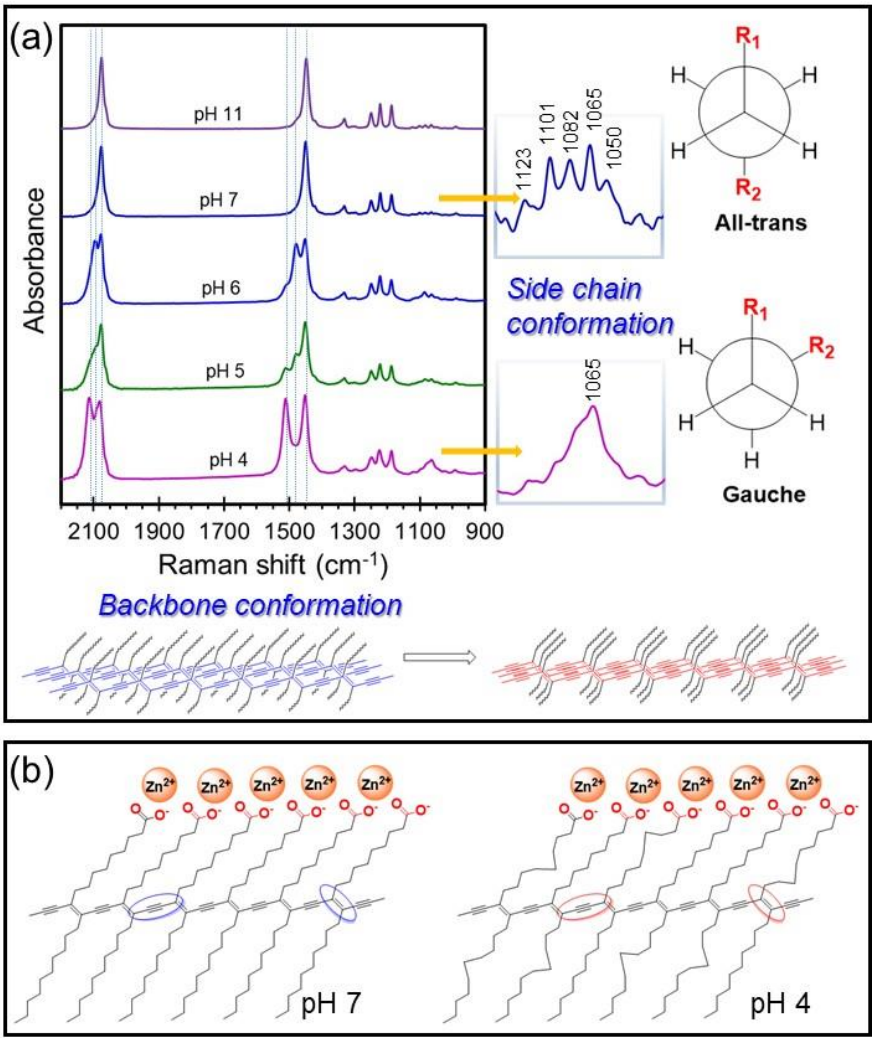

Fig. 6. (a) Raman spectra of poly(TCDA)/Zn^{2+}/ZnO nanocomposites prepared at pH 11, pH 7, pH 6, pH 5 and pH 4. Dotted lines mark peaks at three different positions corresponding to three conformations of backbone. (right) Expanded 1150-1000 cm^{-1} region of Raman spectra shows *all-trans* or *gauche* conformation of alkyl side chain. (bottom) Proposed models of molecular rearrangement causing the shift of vibrational bands of double and triple bonds within the conjugated backbone. (b) Change of side chain conformation at pH 7 and pH 4.

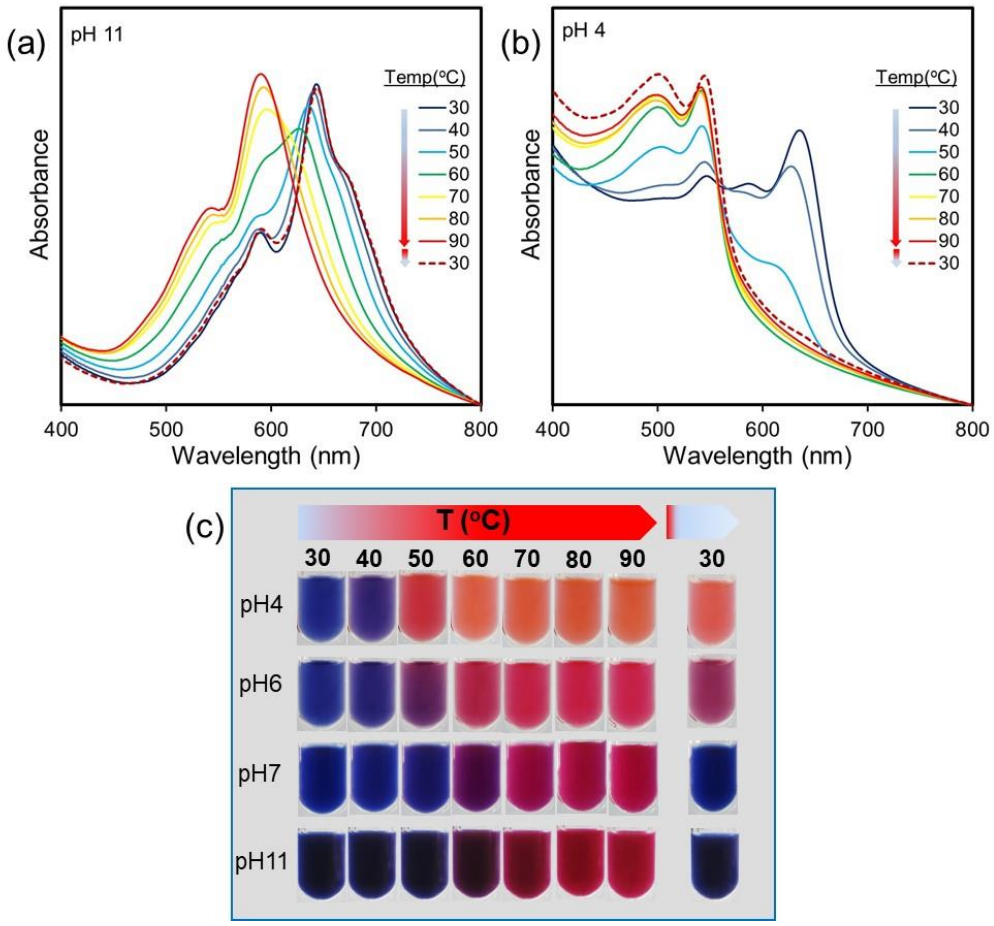

Fig. 7. Temperature-dependent absorption spectra of the poly(TCDA)/Zn^{2+}/ZnO nanocomposites prepared at (a) pH 11 and (b) pH 4. (c) Color photographs of the nanocomposite suspensions prepared at different pH taken upon heating to 90°C, followed by cooling to 30°C.

In the last section, colorimetric response of the nanocomposites to acid and base is investigated. For the nanocomposite prepared at pH 7, the blue-to-red color transition takes place at pH 13 as shown in Fig. 8. The λ_{max} of absorption spectrum shifts to about 545 nm (Fig.9s,

supporting information). Decreasing pH to 1 also induces color transition of the nanocomposite. The mechanism responsible for this dual color-transition behavior was described in our previous studies [23-25]. The dissolution of ZnO nanoparticle in the core region plays a major role for inducing the color-transition. For the nanocomposite prepared at pH 6, the ZnO core is partially dissolved, resulting in the increase of sensitivity. The suspension changes to purple at pH 8. For the acidic region, the color transition is observed at pH 2. The nanocomposite prepared at pH 11 exhibits rather different behavior. The color of nanocomposite suspension remains blue at pH 1 and 13. It indicates that the blue phase of this nanocomposite is rather stable under extremely low and high pH conditions. This finding can extend fabrication and utilization of the nanocomposite as sensing materials in applications with extreme pH conditions. To understand the origins of high color stability of the nanocomposite, we investigate its structure described in the previous section. The FT-IR study reveals that Zn^{2+} and Na^{+} ions incorporate into bilayer structure of the nanocomposite prepared at pH 11. As discussed in our previous report, the color transition of nanocomposite requires the penetration of H^{+} or OH^{-} ions through the PDA shell to react with the ZnO core [25]. Therefore, it could be more difficult to penetrate the PDA shell in the system of nanocomposite prepared at pH 11 due to the presence of additional intercalated Na^{+} ion.

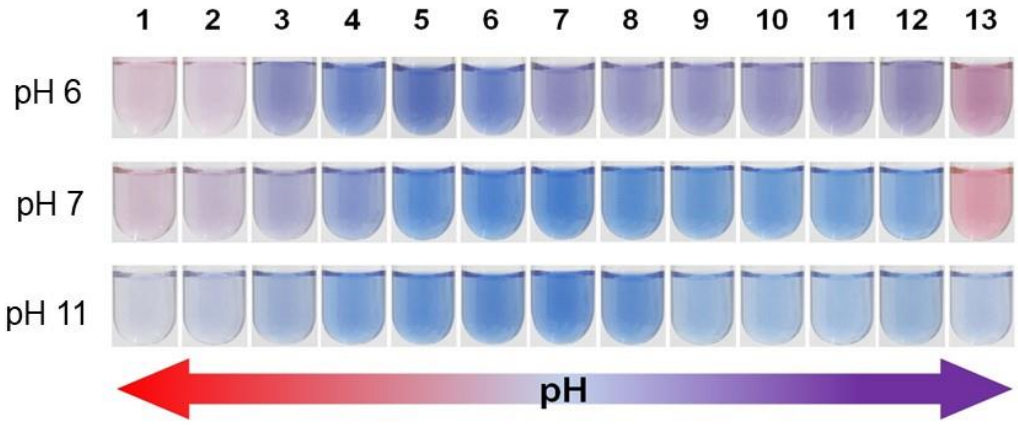

Fig. 8 Color photographs of the nanocomposites taken upon varying pH.

We further investigate the color-transition behavior of nanocomposites using pentylamine as a stimulus. This long chain base provides greater extent of penetration into the PDA shell comparing to the OH^- ion [23]. Both nanocomposites prepared at pH 11 and 7 exhibit blue-to-red color transition as shown in Fig. 9, however, at different concentrations of pentylamine. For the nanocomposite prepared at pH 7, it requires ∼165 mM of pentylamine to induce the color transition (CR of 50%). The concentration increases to ∼230 mM for the nanocomposite prepared at pH 11. We note that the pH of nanocomposite suspension is adjusted to 7 prior to this experiment. The results confirm that color-transition behavior of the nanocomposite can be controlled by manipulating the molecular organization during the self-assembling process.

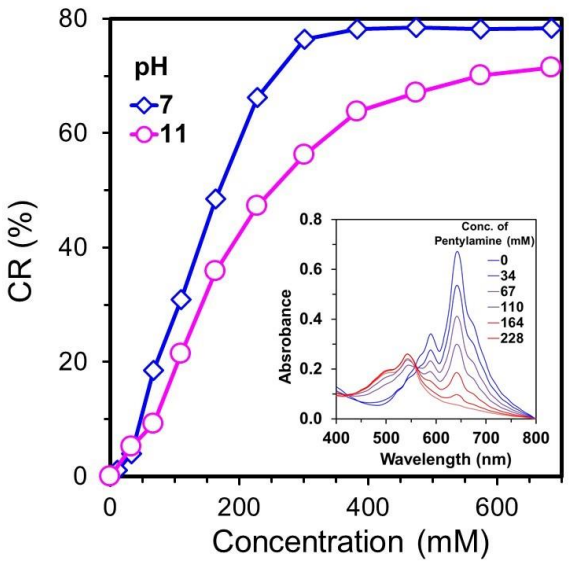

Fig. 9 Colorimetric response (%CR) of poly(TCDA)/Zn^{2+}/ZnO nanocomposite upon increasing concentration of pentylamine. The nanocomposites were prepared at pH 7 and pH 11. (inset) The variation of absorption spectra upon increasing concentration of pentylamine.

Conclusion

This research demonstrates that the molecular assembling and color-transition behavior of the poly(TCDA)/Zn^{2+}/ZnO nanocomposites can be systematically controlled by varying pH of the suspensions during preparation process. The variation of pH affects the surface charge of ZnO nanoparticle and the dissociation of –COOH headgroup. At the normal preparing condition of pH 7, TCDA headgroups are mostly –COOH while the ZnO surface charge is positive. The obtained nanocomposite exhibits reversible thermochromism and dual colorimetric response to

both acid and base. When the preparing pH is increased to 11, the –COOH headgroup is mostly converted to the $–COO^-$ one, meanwhile, the ZnO surface charge becomes highly negative. The molecular ordering of TCDA monomer is promoted at this condition, resulting in the increase of percent conversion during photopolymerization process. The obtained nanocomposite exhibits reversible thermochromism similar to that of the normal condition. Interestingly, blue phase of the nanocomposite obtained at pH 11 is rather stable at extremely high and low pH conditions. The decrease of preparing pH to 4 causes partial dissolution of ZnO nanoparticles, resulting in the decrease of inter-/intramolecular interactions within the nanocomposites. Partial relaxation of conjugated backbone and alkyl side chain of the poly(TCDA) occurs in this system. The nanocomposite exhibits irreversible thermochromism and increasing of sensitivity upon exposure to acid or base. The results in this study provide a new approach to prepare PDA-based materials at a wide range of pH, which is impracticable for the system of pure PDA. The ability to control color-transition behaviors can extend their utilization in various applications.

References

[1] J.T. Wen, J.M. Roper, H. Tsutsui, Ind. Eng. Chem. Res. 57 (2018) 9037-9053.

[2] G.M.D. Ferreira, G.M.D. Ferreira, M.C. Hespanhol, J.P. Rezende, A.C.S. Pires, P.F.R. Ortega, L.H.M. Silva, Food Chem. 241 (2018) 358-363.

[3] O. Mapazi, K.P. Matabola, R.M. Moutloali, C.J. Ngila, Polymer 149 (2018) 106-116.

[4] Y. Zhang, L. Bromberg, Z. Lin, P. Brown, T.V. Voorhis, T.A. Hatton, J. Colloid Interface Sci. 528 (2018) 27-35.

[5] B. Gao, G. Yuan, L. Ren, J. Mater. Sci. 53 (2018) 6698-6706.

[6] M. Wanga, Y. Yub, F. Liu, L. Ren, Q. Zhang, G. Zou, Talanta 188 (2018) 27-34.

[7] D.-H. Park, J.-M. Heo, W. Jeong, Y.H. Yoo, B.J. Park, J.-M. Kim, ACS Appl. Mater. Interfaces 10 (2018) 5014-5021.

[8] H. Terada, H. Imai, Y. Oaki, Adv, Mater. 30 (2018) 1801121.

[9] M.J. Kim, S. Angupillai, K. Min, M. Ramalingam,Y.-A. Son, ACS Appl. Mater. Interfaces 10 (2018) 24767-24775.

[10] M. Kim, Y.J. Shin, S.W. Hwang, M.J. Shin, J.S. Shin, J. Appl. Polym. Sci. 2018, doi:10.1002/APP.46394.

[11] C. Khanantong, N. Charoenthai, T. Phuangkaew, F. Kielar, N. Traiphol, R. Traiphol, Colloids Surf. A 553 (2018) 337-348.

[12] R. Potai, K. Faisadcha, R. Traiphol, N. Traiphol, Colloids Surf. A 555 (2018) 27-36.

[13] C. Khanantong, N. Charoenthai, S. Wacharasindhu, M. Sukwattanasinitt, N. Traiphol, R. Traiphol, J. Ind. Eng. Chem. 58 (2018) 258-265.

[14] M.-C. Tu, J.A. Cheema, U.H. Yildiz, A. Palaniappan, B. Liedberg, J. Mater. Chem. C 5 (2017)1803-1809.

[15] S. Dolai, S.K. Bhunia, S.S. Beglaryan, S. Kolusheva, L. Zeiri, R. Jelinek, ACS Appl. Mater. Interfaces 9 (2017) 2891-2898.

[16] A. Kamphan, C. Gong, K. Maiti, S. Sur, R. Traiphol, D.P. Arya, RSC Adv. 7 (2017) 41435-41443.

[17] D.-H. Park, B. J. Park, J.-M. Kim, Acc. Chem. Res. 49 (2016) 1211-1222.

[18] H. Shin, B. Yoon, I.S. Park, J.-M. Kim, Nanotechnology 25 (2014) 094011.

[19] B. Yoon, J. Lee, I. S. Park, S. Jeon, J. Lee, J.-M. Kim, J. Mater. Chem. C 1 (2013) 2388-2403.

[20] Q.-M. Wang, Z.-Y. Yang, Carbon 138 (2018) 90-97.

[21] R. Varghese Hansen, L. Zhong, K.A. Khor, L. Zheng, J. Yang, Carbon 106 (2016) 110-117.

[22] S.J. Kew, E.A.H. Hall, Anal. Chem. 78 (2006) 2231-2238.

[23] A. Chanakul, R. Traiphol, N. Traiphol, J. Ind. Eng. Chem. 45 (2017) 215-222.

[24] A. Chanakul, R. Traiphol, N. Traiphol, Colloids Surf. A 489 (2016) 9-18.

[25] A. Chanakul, N. Traiphol, K. Faisadcha, R. Traiphol, J. Colloid Interface Sci 418 (2014) 43-51.

[26] J. Pang, L. Yang, B.F. McCaughey, H. Peng, H.S. Ashbaugh, C.J. Brinker, Y. Lu, J. Phys. Chem. B 110 (2006) 7221-7225.

[27] Y. Lifshitz, Y. Golan, O. Konovalov, A. Berman, Langmuir 25 (2009) 4469-4477.

[28] A. Fujimori, M. Ishitsuka, H. Nakahara, E. Ito, M. Hara, K. Kanai, Y. Ouchi, K. Seki, J. Phys. Chem. B 108 (2004) 13153-13162.

[29] N. Charoenthai, T. Pattanatornchai, S. Wacharasindhu, M. Sukwattanasinitt, R. Traiphol, J. Colloid Interface Sci. 360 (2011) 565-573.

[30] T. Pattanatornchai, N. Charoenthai, S. Wacharasindhu, M. Sukwattanasinitt, R. Traiphol, J. Colloid Interface Sci. 391 (2013) 45-53.

[31] T. Pattanatornchai, N. Charoenthai, R. Traiphol, J. Colloid Interface Sci. 432 (2014) 176-181.

[32] S. Wacharasindhu, S. Montha, J. Boonyiseng, A. Potisatityuenyion, C. Phollookin, G. Tumcharern, M. Sukwattanasinitt, Macromolecules 43 (2010) 716-724.

[33] C. Phollookin, S. Wacharasindhu, A. Ajavakom, G. Tumcharern, S. Ampornpun, T. Eaidkong, M. Sukwattanasinitt, Macromolecules 43 (2010) 7540-7548.

[34] S. Ampornpun, S. Montha, G. Tumcharern, V. Vchirawongkwin, M. Sukwatta-nasinitt, S. Wacharasindhu, Macromolecules 45 (2012) 9038-9045.

[35] L. Rougeau, D. Picq, M. Rastello, Y. Frantz, Tetrahedron 64 (2008) 9430-9436.

[36] N. Traiphol, N. Rungruangviriya, R. Potai, R. Traiphol, J. Colloid Interface Sci. 356 (2011) 481-489.

[37] A. Chanakul, N. Traiphol, R. Traiphol, J. Colloid Interface Sci. 389 (2013) 106-114.

[38] N. Traiphol, K. Faisadcha, R. Potai, R. Traiphol, J. Colloid Interface Sci. 439 (2015) 105-111.

[39] S. Toommee, R. Traiphol, N. Traiphol, Colloids Surf. A: Physicochem. Eng. Asp. 468 (2015) 252-261.

[40] N. Traiphol, A. Chanakul, A. Kamphan, R. Traiphol, Thin Solid Films 622 (2017) 122-129.

[41] A. Degen, M. Kosec, J. Eur. Ceram. Soc. 20 (2000) 667-673.

[42] P. Tanphibal, K. Tashiro, S. Chirachanchai, Macromol. Rapid Commun. 37 (2016) 685-690.

[43] M. Takeuchi, H. Imai, Y. Oaki, J. Mater. Chem. C 5 (2017) 8250-8255.

[44] M. Takeuchi, H. Imai, Y. Oaki, ACS Appl. Mater. Interfaces 9 (2017) 16546-16552.

[45] L. Yu, S.L. Hsu, Macromolecules 45 (2012) 420-429.

[46] X. Huang, S. Jiang, M. Liu, J. Phys. Chem. B 109 (2005) 114-119.

[47] A. Kamphan, N. Traiphol, R. Traiphol, Colloid Surf. A 497 (2016) 370-377.

[48] Y. Lifshitz, A. Upcher, O. Shusterman, B. Horovitz, A. Berman, Y. Golan, Phys. Chem. Chem. Phys. 12 (2010) 713-722.

[49] E. Shirai, Y. Urai, K. Itoh, J. Phys. Chem. B 102 (1998) 3765-3772.

[50] Y. Lifshitz, A. Upcher, A. Kovalev, D. Wainstein, A. Rashkovsky, L. Zeiri, Y. Golan, A. Berman, Soft Matter 7 (2011) 9069-9077.

[51] I.S. Park, H.J. Park, W. Jeong, J. Nam, Y. Kang, K. Shin, H. Chung, J.-M. Kim, Macromolecules 49 (2016) 1270-1278.

[52] J.L. Lippert, W. L. Peticolas, Proc. Natl. Acad. Sci. U.S.A. 68 (1971) 1572-1576.

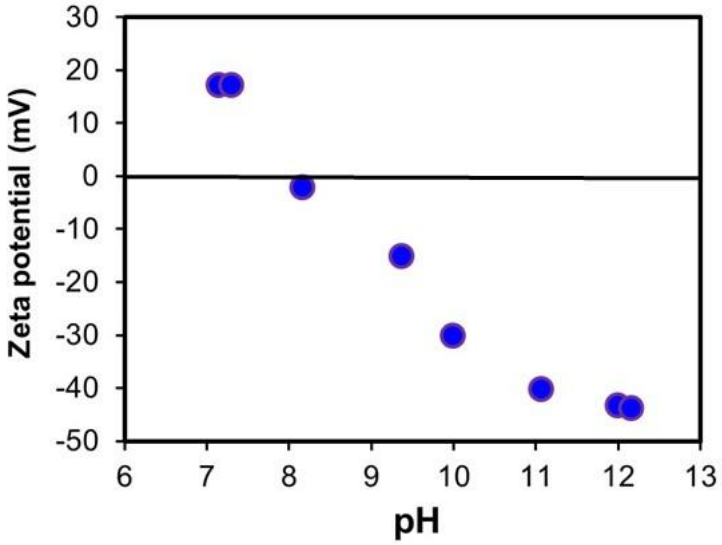

Fig.1s Zeta potential of ZnO nanoparticle at various pH.

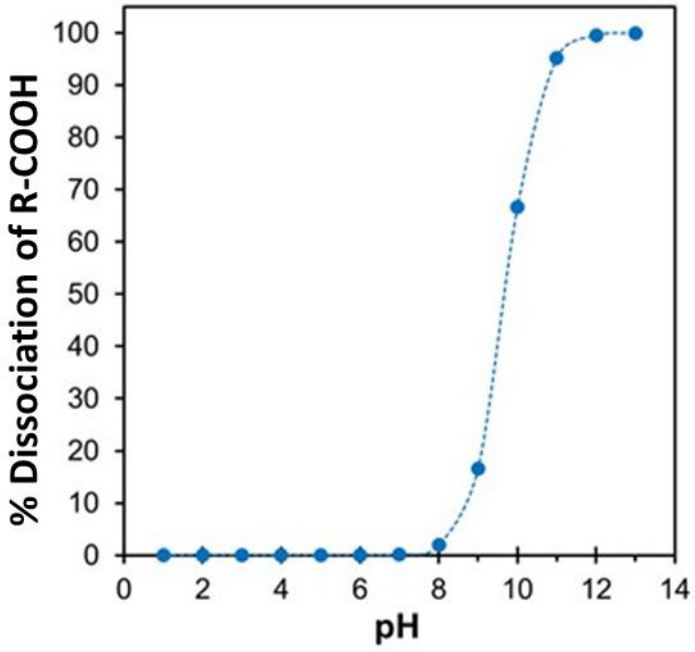

Fig.2s. % Dissociation of –COOH group of TCDA monomer calculated by using pKa of 9.7.

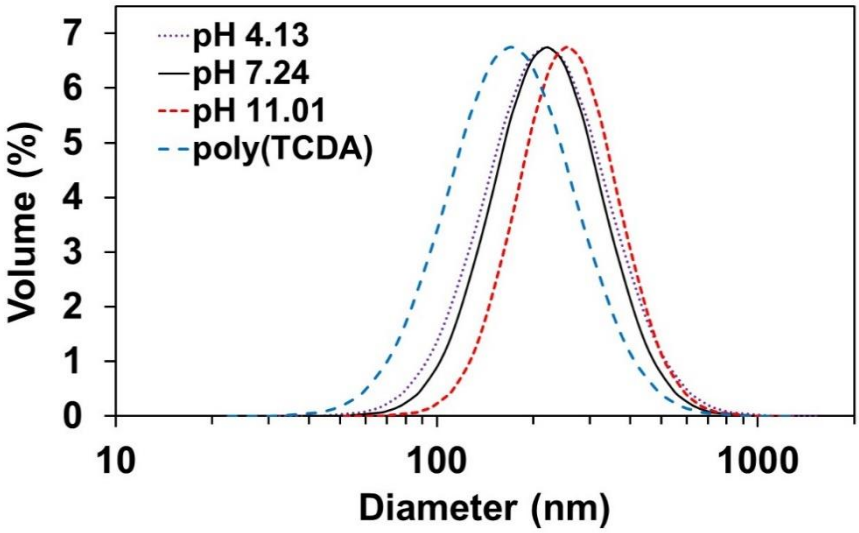

Fig.3s Diameters of pure poly(TCDA) and poly(TCDA)/Zn^{2+}/ZnO nanocomposites prepared at different pHs.

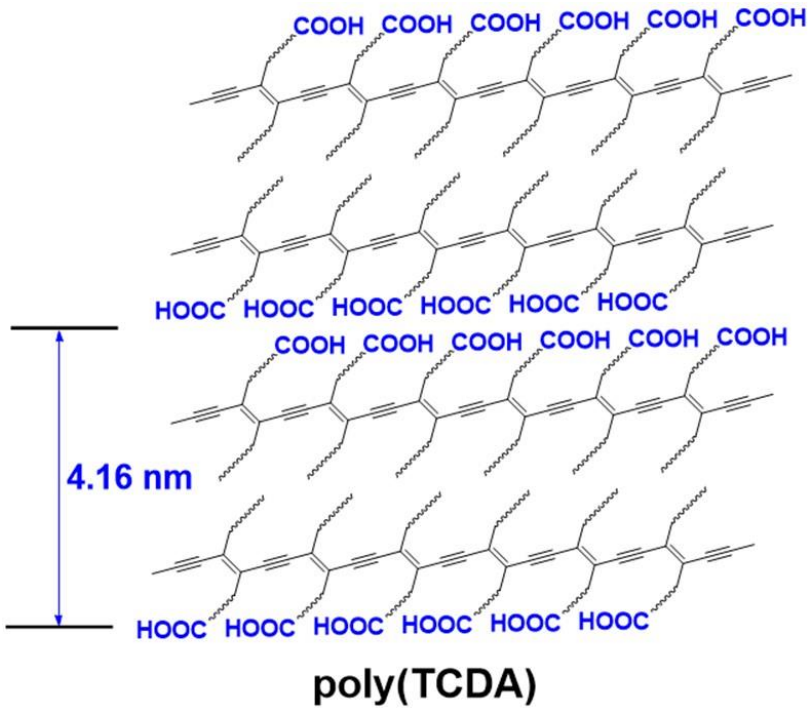

Fig.4s Molecular packing models of pure poly(TCDA).

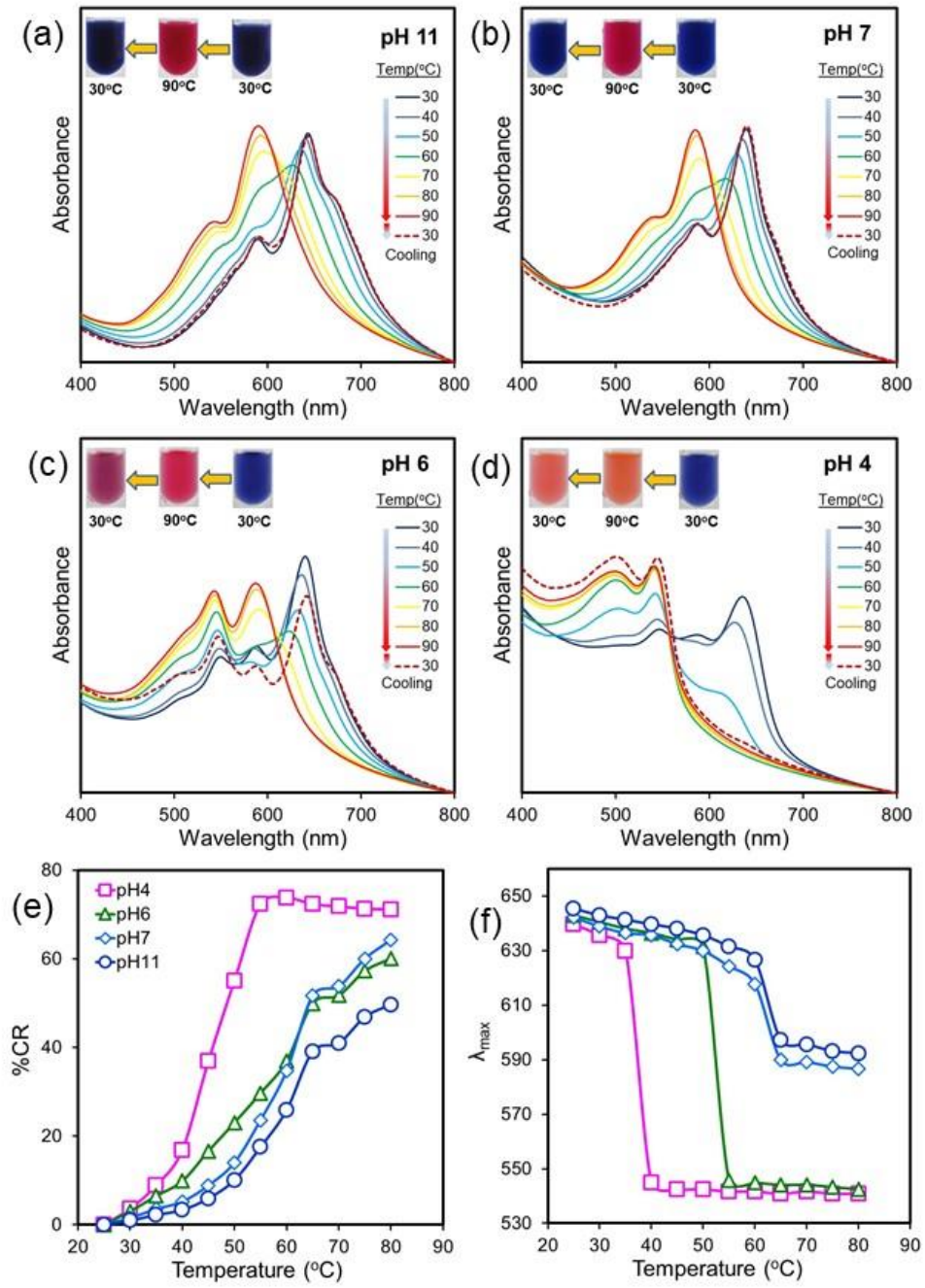

Fig.5s Absorption spectra of the poly(TCDA)/Zn^{2+}/ZnO nanocomposites prepared at (a) pH 11 (b) pH 7 (c) pH 6 and (d) pH 4. The spectra were measured upon increasing temperature from 30 to 90°C and then cooling back to 30°C. Plots of (e) colorimetric response (%CR) and (f) λ_{max} of absorption spectra as a function of temperature.

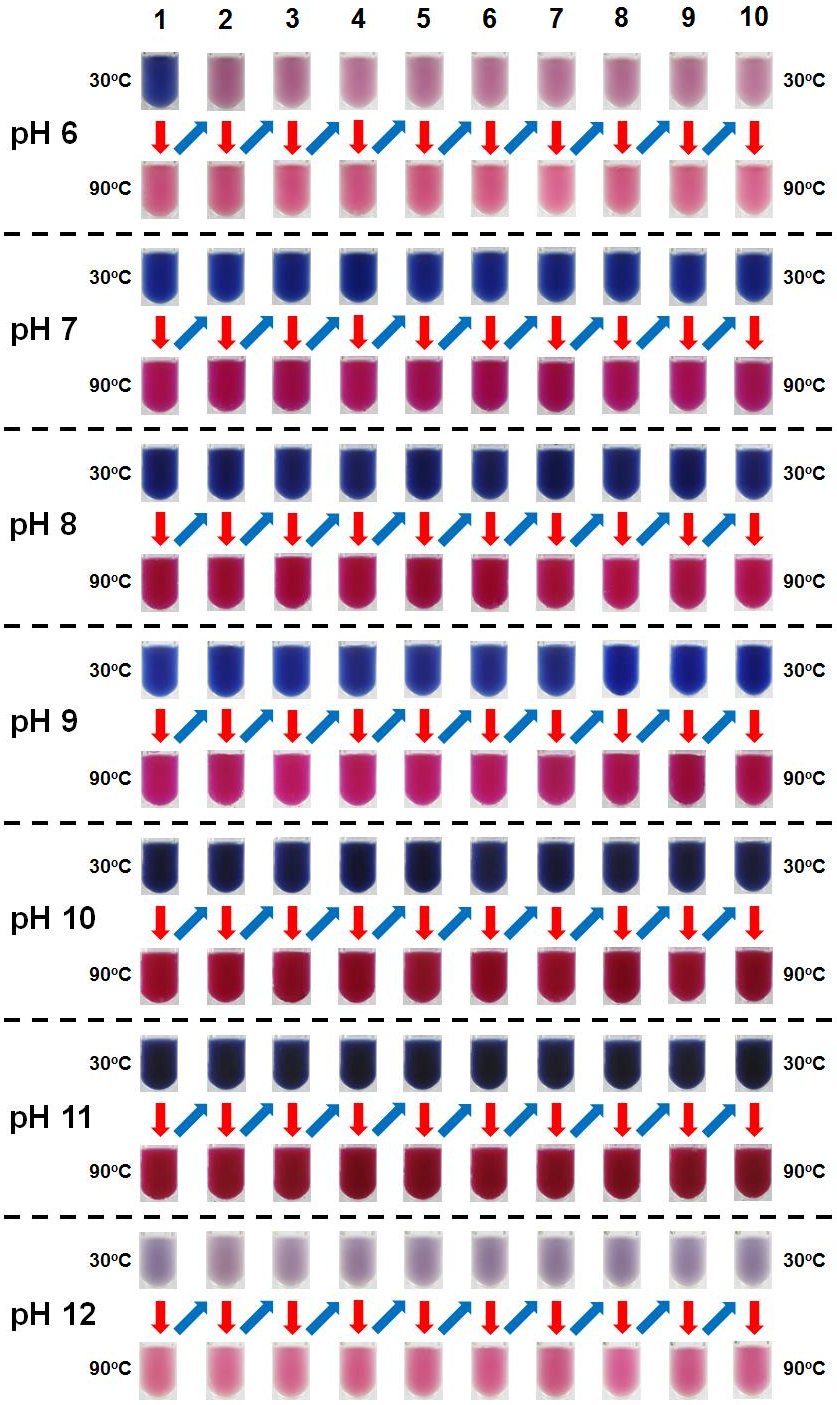

Fig. 6s Color reversibility testing of poly(TCDA)/ZnO nanocomposite prepared from various pHs. The nanocomposite suspensions were heat from 30°C to 90°C and then cooling to 30°C for 10 cycles.

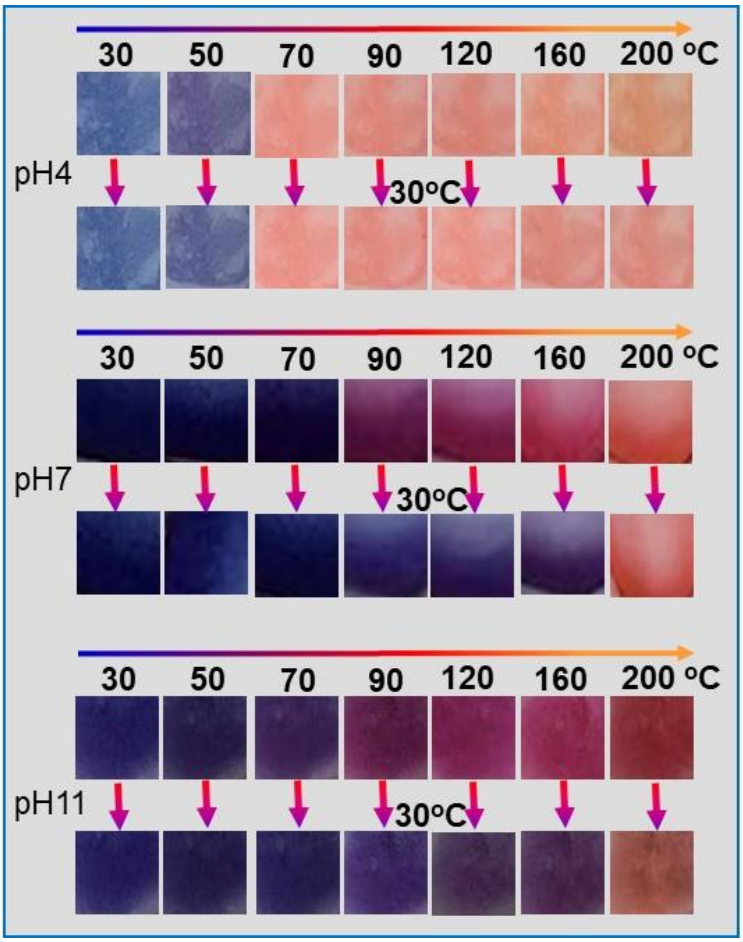

Fig. 7s Color photographs of the nanocomposite films prepared at different pH taken upon heating to 200°C, followed by cooling to 30°C.

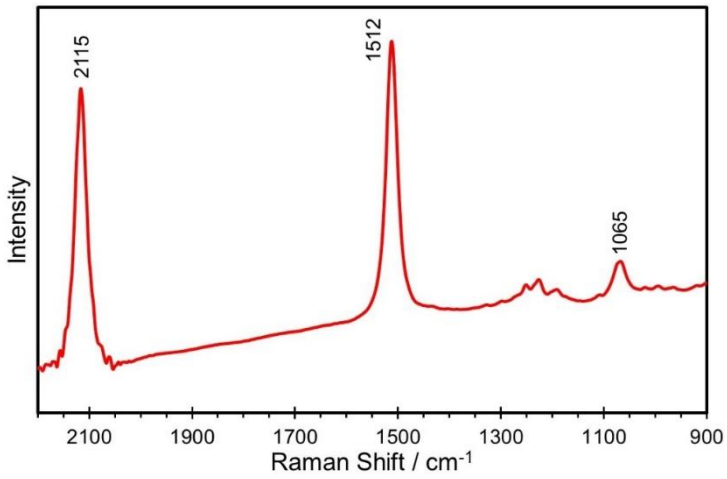

Fig. 8s. Raman spectra of red phase of poly(TCDA)/Zn^{2+}/ZnO nanocomposites prepared at pH 11. The red phase was obtained by annealing at 200^{o}C for 30 min. The peaks at 2115 and 1512 cm^{-1} correspond to backbone conformation in red phase. A broad peak at 1065 cm^{-1} indicates the presence of some *gauche* conformation of alkyl side chain.

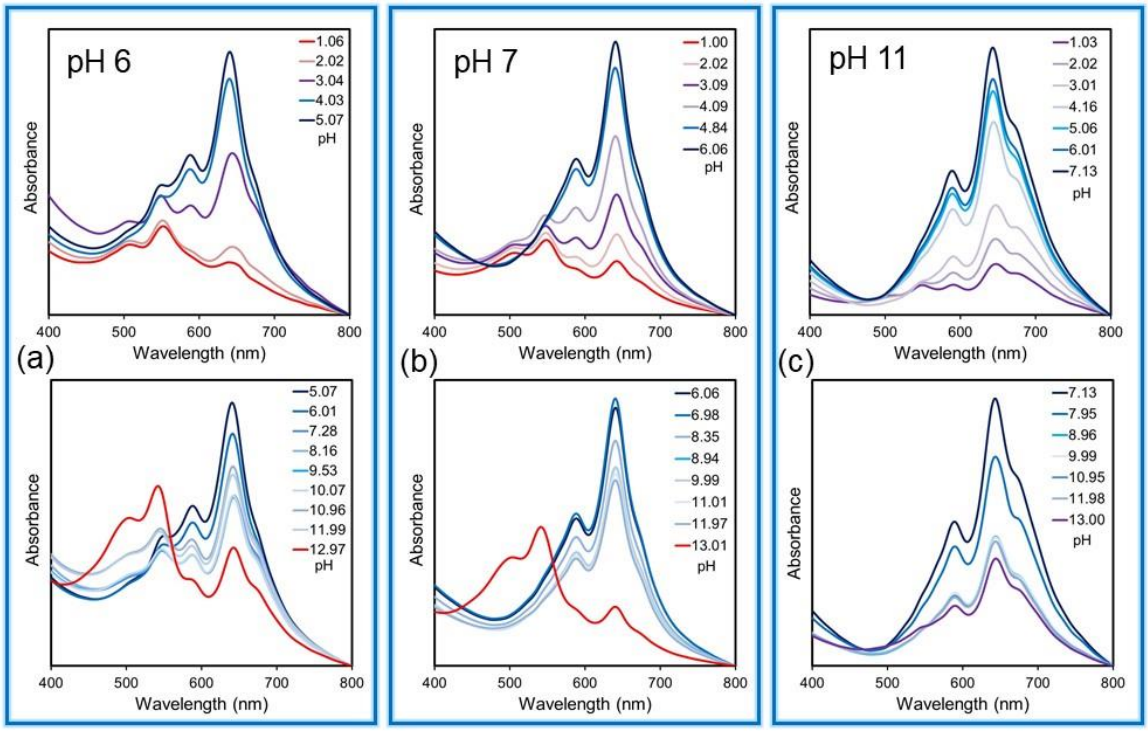

Fig. 9s Absorption spectra of poly(TCDA)/Zn^{2+}/ZnO nanocomposite prepared at (a) pH 6, (b) pH 7, (c) pH 11. The spectra were measured upon (above) decreasing pH and (below) increasing pH.

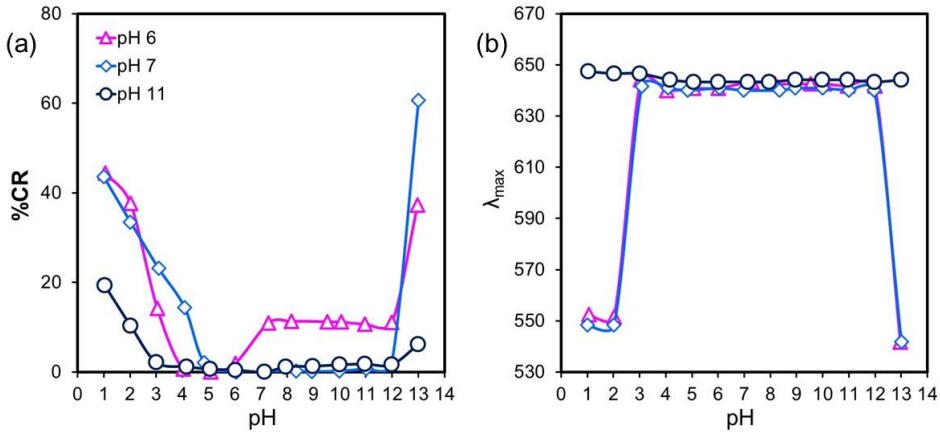

Fig. 10s. Plots of (a) colorimetric response (%CR) and (b) λ_{max} of absorption spectra as a function of pH of the nanocomposites prepared from various pHs.

บทที่ 4

Enhancing the sensitivity of stimuli-responsive polydiacetylene with aromatic headgroup: The opposite effect of ZnO nanoparticle

Abstract

This contribution presents our continuing effort to develop polydiacetylene(PDA)/zinc(II) ion(Zn^{2+})/zinc oxide(ZnO) nanocomposite for colorimetric sensing. In our previous studies, PDAs with monocarboxylic headgroup have been used to fabricate the nanocomposites. The incorporation of Zn^{2+}/ZnO enhances overall interactions, resulting in reversible thermochromism with color-transition temperature (T_{CT}) higher than that of the original PDA. Here, we extend this concept to the system of 3-(pentacosa-10,12-diynamido) benzoic acid (PCDA-mBzA) monomer constituting aromatic headgroup. Pure poly(PCDA-mBzA) assemblies exhibit reversible thermochromism with T_{CT} ~90 ^{o}C. Surprisingly, the fabrication of poly(PCDA-mBzA)/Zn^{2+}/ZnO nanocomposites using 5, 10 and 20 wt.% of ZnO nanoparticles results in the decrease of T_{CT} to about 80, 70 and 60 ^{o}C, respectively. The reversible thermochromism still remains. The observed effect of ZnO nanoparticle is opposite to our previous studies. Structural analysis by utilizing

infrared spectroscopy and x-ray diffraction reveals that the Zn^{2+} ions intercalate with bilayer structure of poly(PCDA-mBzA). The intercalation process perturbs local organization of aromatic headgroup reducing the strength of overall interactions. Paper-based colorimetric sensor with enhanced sensitivity is fabricated to detect cationic surfactant and organic solvent at various concentration range.

Keywords: Polydiacetylene, Reversible thermochromism, Chemical sensor, Packing structure, Intercalation

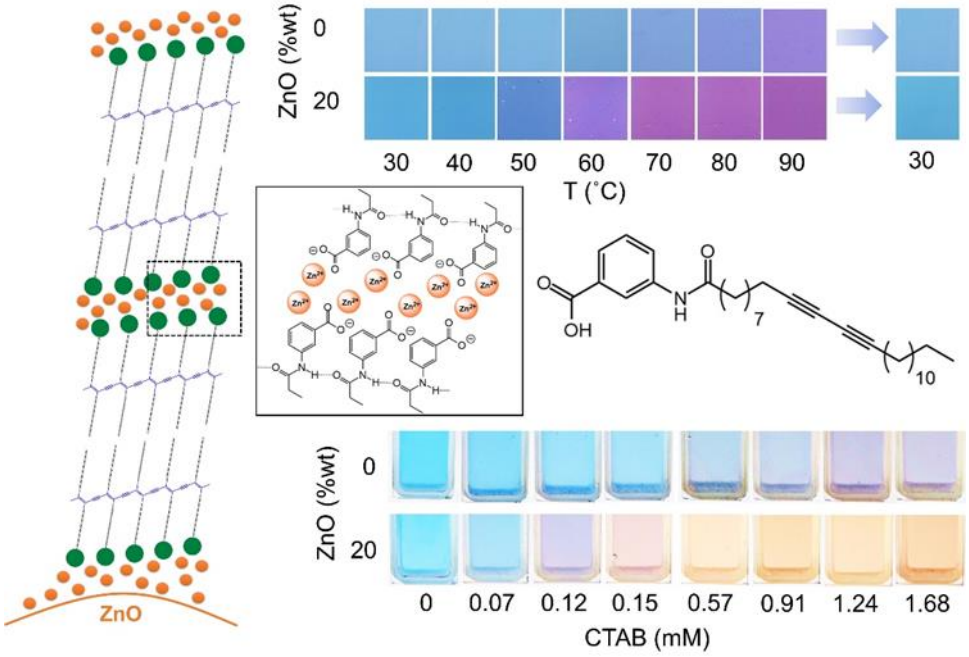

Highlights

- Thermal/chemical sensitivity of polydiacetylene(PDA) is enhanced by ZnO addition.
- Reversible thermochromic temperature of PDA is reduced from 90 ^{o}C to 60 ^{o}C.
- The sensitivity of PDA to cationic surfactant and solvent is also promoted.
- Adding ZnO weakens local interactions between the headgroups of PDA.
- Molecular packing structure within PDA assemblies is altered as well.

Introduction

Over the past few decades, color-responsive materials have played important roles on sensing technologies. Polydiacetylene (PDA), one type of conjugated polymer, has drawn tremendous attention from scientific community due to its unique color-transition properties. This class of polymer exhibits various types of color transition when subjected to heat [1-10], chemicals [11-16], mechanical stress [17, 18] and surfactants [19-23]. Origins of the color transition have been related to segmental rearrangement within PDA assemblies during the external perturbation [6, 9, 24-26]. The unique optical properties of PDA-based materials allow their utilization in various applications including molecular sensors [16, 27, 28] and many kinds of practical devices, thermochromic pen [3, 29], printable thermochromic ink [30-32], photodetector [33] and solar cell

[34]. To realize the full potential of PDA-based materials, however, the fundamental understanding of molecular parameters affecting their properties is rather important.

It has been known that PDAs with monocarboxylic headgroup, which are commercially available, exhibit irreversible thermochromism. To achieve reversible thermochromism, the carboxylic headgroup is usually modified by using various moieties, resulting in the increase of overall inter- and intramolecular interactions within PDA assemblies [6-8, 35-42]. For example, the headgroup of well-known 10,12-pentacosadiynoic acid (PCDA) can be modified by attaching with benzoic group providing 3-(pentacosa-10,12-diynamido) benzoic acid (PCDA-mBzA) as shown in Fig.1 [41,42]. The enhanced hydrogen-bonding and **π-π** stacking interactions among the modified headgroups lead to reversible thermochromism of the poly(PCDA-mBzA) assemblies. The color-transition temperature (T_{CT}) of aqueous suspension and Langmuir-Schaefer film of this functionalized PDA was reported at about 90 °C [20, 41,42]. Our recent study also showed that its color reversibility in thin film persisted up to about 200 ^{o}C. The reversible thermochromic behavior extends the utilization of PDA-based materials in various applications such as smart textiles, ink-jet printable/hand writable thermosensors, counterfeiting materials and electro-thermochromic displays.

Our group has been developing a simple and controllable method to obtain the reversible thermochromism by mixing monocarboxylic PDAs with ZnO nanoparticles [6, 24, 44-46]. The resultant PDA/Zn^{2+}/ZnO nanocomposites exhibit reversible thermochomism in different types of matrices including aqueous suspension, various organic solvents and common polymeric films (polyethylene, polystyrene, poly(methylmethacrylate) and poly(vinylalcohol)). Origin of the reversible thermochromism of this system mainly arises from the enhanced local interactions between carboxylate headgroup and Zn^{2+}/ZnO surface. This approach is quite easy, which is very important for large-scale production, compared to the structural modification one. In addition, reversible T_{CT} of the PDA/Zn^{2+}/ZnO nanocomposites can be finely tuned by varying alkyl side chain length and photopolymerization time during the preparation process. Our recent reports have demonstrated that the reversible T_{CT} ranging from 10 ^{o}C to 90 ^{o}C can be achieved.

In this study, we hypothesized that the incorporation of ZnO nanoparticles into poly(PCDA-mBzA) assemblies could extend its reversible T_{CT} to the higher temperature region. The benzoic acid headgroup is expected to strongly interact with the Zn^{2+}/ZnO surface as shown in Fig. 1 similar to the system of PDA with monocarboxylic headgroup. Surprisingly, we detect an opposite effect of the added ZnO nanoparticles on the reversible T_{CT}. Controlling the ZnO ratio results in systematic variation of the reversible T_{CT} between 90 ^{o}C and 60 ^{o}C. Furthermore, its sensitivity

to chemical stimuli such as cationic surfactant and organic solvent increases significantly. From these interesting results, we prepare solution-based and paper-based colorimetric sensors to detect the chemical stimuli at various concentrations. An insight into the origins of these behaviors is revealed by using infrared spectroscopy and x-ray diffraction. Our major finding in this study can be utilized to finely tune the colorimetric response of PDA-based materials and further extends their applications in colorimetric sensors, thermochromic paints/inks and smart labels.

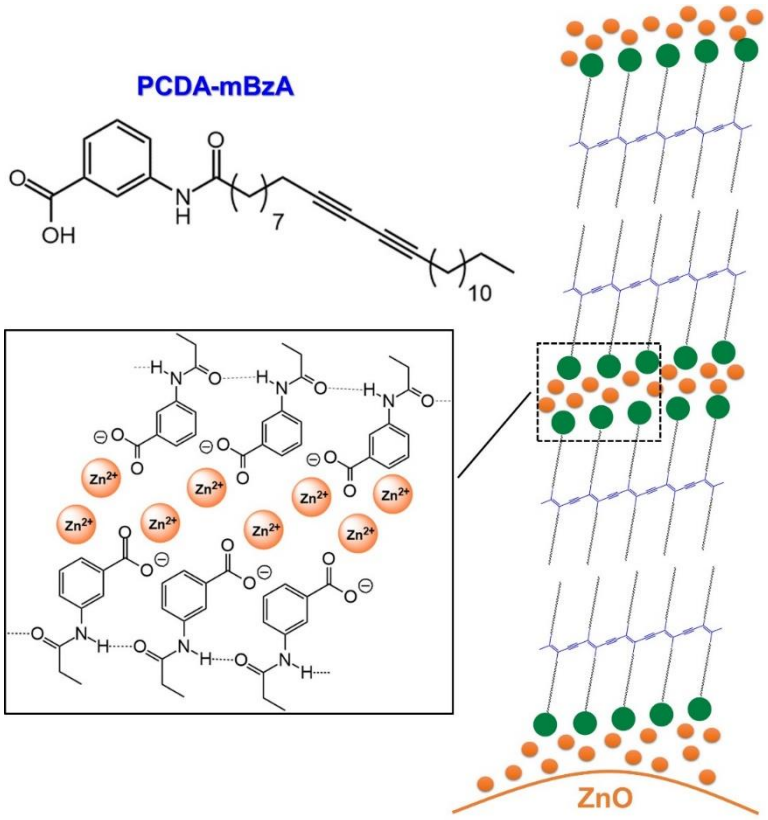

Fig.1 Chemical structure of PCDA-mBzA monomer and graphical model illustrating the molecular interaction of poly(PCDA-mBzA) with Zn^{2+}/ZnO surface and the intercalation of Zn^{2+} ions with the bilayer structure.

Experimental procedures

The 3-(pentacosa-10,12-diynamido) benzoic acid (PCDA-mBzA) monomer was synthesized following the previous works [38, 39]. Preparation of poly(PCDA-mBzA)/Zn^{2+}/ZnO nanocomposite followed the procedure used in our previous reports [xx]. Briefly, 0.5mM solution of PCDA-mBzA in tetrahydrofuran (THF) is filtered and slowly dried in a beaker. An aqueous suspension of ZnO nanoparticles (∼65 nm) was added into the dried PCDA-mBzA film. The ZnO/PCDA-mBzA ratios were varied from 5 wt.% to 60 wt.% while the concentration of PCDA-mBzA was kept at 0.5 mM. The sample was sonicated at 90 ^{o}C for 1 h. After keeping at 4 ^{o}C overnight, the suspension was irradiated by UV light (10 W, λ∼254 nm) for 3 min, providing poly(PCDA-mBzA)/Zn^{2+}/ZnO nanocomposite with blue color.

Absorption spectra of the samples were measured by UV-Vis spectrophotometer (Blue Star, Lab Tech) quipped with variable temperature unit. The colorimetric response (%CR) was calculated following our previous reports [7, 48]. Particle size distribution and morphology of poly(PCDA-mBzA)/Zn^{2+}/ZnO nanocomposite were examined by dynamic light scattering (DLS, Brookhaven, ZetaPaLs) and transmission electron microscopy (TEM, JEM-1400), respectively. Local interactions within nanocomposites were explored by Nicolet 6700 FT-IR spectrophotometer. The molecular packing structure was studied by X-ray diffractometer (XRD,

Bruker AXS Model D8 Discover λ (Cu-K_α) =1.54 Å). Solid-state samples were prepared by drop-casting onto glass slides.

Thermochromic behaviors of nanocomposites were explored in aqueous suspension and thin films coated on glass slides. The colorimetric response to cationic surfactant, cetyl trimethyl ammonium bromide (CTAB), and THF solvent was also investigated. The CTAB and THF were added into the nanocomposite suspension by using micropipette. The nanocomposite films were prepared by drop-casting on 0.2 μm pore-size nylon filter membrane. Solutions of CTAB with various concentrations were dropped on the nanocomposite films. Color photographs were taken after incubating these samples with CTAB for 3 min.

Result and discussion

Tunable Reversible Thermochromism

The poly(PCDA-mBzA) assemblies dispersed in aqueous medium exhibit reversible thermochromism. Its temperature-dependent absorption spectra are illustrated in Fig.2a. At room temperature, the spectrum of blue phase constitutes a peak at about 650 nm. Increasing temperature causes a gradual blue-shift of the spectrum attributed to the enhanced segmental dynamics of PDA due to thermal energy. Growth of a small peak at about 540 nm is detected at

90 ^{o}C, corresponding to the formation of some red phase. The incoporation of 20 wt.% ZnO nanoparticles into the poly(PCDA-mBzA) assemblies strongly affects the color-transition temperature (T_{CT}). At 60 ^{o}C, we detect a significant growth of the peak at 540 nm (Fig.2b). Our observation indicates that the resultant poly(PCDA-mBzA)/Zn^{2+}/ZnO nanocomposite exhibits a lower T_{CT} than that of the original poly(PCDA-mBzA). The plots of λ_{max} and %CR as a function of temperature shown in Fig.2(c,d) clearly indicate the drop of T_{CT} in the nanocomposite system. This result is quite unexpected when compared with our previous studies on the system of poly(PCDA) with monocarboxylic headgroup. We have observed that the incorporation of ZnO nanoparticles enhances local interactions within poly(PCDA) assemblies, resulting in the increase of T_{CT} and also reversible thermochromism.

The effect of ZnO nanoparticles on thermochromic behaviors of poly(PCDA-mBzA) is further investigated by varying the ZnO ratios from 5 to 40 wt.% (Fig. S1, supporting information). Interestingly, we observe a systematic decrease of the T_{CT} to about 80, 70 and 60 ^{o}C when the ZnO ratio is increased to 5, 10 and 20 wt.%, respectively. The further increase of ZnO ratio to 40 wt.% nanocomposite hardly affects the T_{CT} but causes the precipitation of nanocomposite. Color photographs taken upon heating/cooling shown in Fig.2c summarize our major finding. It is important to point out that the reversible thermochromism is still preserved in all systems.

Therefore, the ZnO nanoparticles can be utilized for tuning down the reversible T_{CT} of this class of PDA constituting bulky aromatic headgroup. In fact, it is not trivial to tune its T_{CT} via structural modification approach. Previous study showed that the shortening of its alkyl side chain hardly affected the T_{CT}.

The investigation of thin films prepared by drop-casting on glass slides provides consistent results. Increasing the temperature of pure poly(PCDA-mBzA) film to 80 ^{o}C causes blue-to-purple color transition (Fig.3a). A complete formation of red phase is detected above 100 ^{o}C. The red film fully reverses back to the original blue color upon cooling to room temperature. The reversible thermochromism of poly(PCDA-mBzA) film persists up to about 200 ^{o}C. Further increasing temperature to 250 ^{o}C and 270 ^{o}C causes the irreversible color transition to orange and yellow phases, respectively. Our previous study by XRD revealed that the packing structure of poly(PCDA-mBzA) changed from crystalline lamellar to amorphous at this stage. Thermochromic property of poly(PCDA-mBzA)/Zn^{2+}/ZnO nanocomposite film is illustrated in Fig.3b. The reversible color transition takes place at lower temperature compared to that of the pure poly(PCDA-mBzA) film. The transition to purple color is detected at about 60 ^{o}C. The temperature range for reversible thermochromism also becomes narrower. The nanocomposite film changes to an irreversible orange phase at 150 ^{o}C. Our results indicate that the incorporation of ZnO nanoparticles into

poly(PCDA-mBzA) assemblies weakens the strength of interactions within the system, which in turn causes the decrease of color-transition temperature and also reduces its color stability. Previous study by Lee et.al also observed similar thermochromic behavior when Cd^{2+} ions were incorporated into the poly(PCDA-mBzA) assemblies. The binding of Cd^{2+} ions with headgroup of poly(PCDA-mBzA) weakened the overall interactions, resulting in irreversible thermochromism.

Morphology, size distribution, local interactions and molecular packing

We utilizes various techniques to explore origins of the unexpected thermochromic behaviors of poly(PCDA-mBzA)/Zn^{2+}/ZnO nanocomposite. TEM images reveal that the incorporation of ZnO nanoparticles drastically alters the morphologies of assemblies. Pure poly(PCDA-mBzA) assemblies exhibit a rod-like structure as shown in Fig.4a. The width of these rods are below 50 nm while the length reaches several hundred nanometers. Clusters of round-shape particles are observed in the system of nanocomposite (Fig.4b). This result suggests that the presence of Zn^{2+}/ZnO surface alters the molecular organization within the assemblies and also tends to induce agglomeration. As mentioned earlier, the precipitation occurs when the ZnO ratio is increased above 40 wt.%. The measurement in aqueous suspension by DLS detects the increase of particle size (Fig.4c). Median diameter of pure poly(PCDA-mBzA) assemblies is about

130 nm. It increases to about 200 nm in the system of nanocomposite. We suggest that the Zn^{2+}/ZnO strongly interacts with the headgroup of poly(PCDA-mBzA), providing additional driving forces for the self-assembling process. Our hypothesis is supported by the measurement of zeta potential shown in Fig.4d. The zeta potential value, reflecting its surface charge, is about -30 mV for pure poly(PCDA-mBzA) assemblies. The negative value indicates that the surface of poly(PCDA-mBzA) assemblies is populated by negatively charged carboxylate ($-COO^-$) headgroup. The positive Zn^{2+} ions released from ZnO nanoparticles can bind with the $–COO^-$ headgroup via coulombic interaction. In fact, the systems of nanocomposites show the decrease of zeta potential value to about -25 mV, suggesting the binding between Zn^{2+} ion and $-COO^-$ headgroup. The investigation by FT-IR in the following discussion further support this result.

Local interactions within pure poly(PCDA-mBzA) assemblies and the poly(PCDA-mBzA)/Zn^{2+}/ZnO nanocomposite are explored by utilizing FT-IR spectroscopy (Fig.5). The FT-IR spectrum of pure poly(PCDA-mBzA) assemblies constitutes peaks at 3274, 1690, 1655, 1589 and 1542 cm^{-1} corresponding to the vibrational frequencies of **V**(N-H), **V**(C=O) (carboxylic), **V**(C=O) (amide), **V**(C=C) (phenyl) and **V**(C-N-H) (amide) groups, respectively [20, 38, 39]. The assignment of each peak is illustrated in Fig.5b. According to previous reports, the headgroup of poly(PCDA-mBzA) forms strong interactions via double hydrogen bonding of the carboxylic acid

and amide group. The π- π interaction between the aromatic moieties further enhances the strength of overall interactions within the system. These enhanced interactions are major factors that lead to reversible thermochromism. Our original hypothesis of this study was that the addition of ZnO nanoparticles into poly(PCDA-mBzA) assemblies would increase the strength of total interactions via coulombic interaction between Zn^{2+}/ZnO and carboxylate moiety. Surprisingly, we observe the opposite effect. What is the origin of this behavior?

The FT-IR spectrum of poly(PCDA-mBzA)/Zn^{2+}/ZnO nanocomposite containing 10 wt.% ZnO nanoparticles detects new peak at 3396 cm^{-1} corresponding to vibrational frequency **ν**(N-H) at amide moiety. Intensity of the original peak at 3274 cm^{-1} drastically decreases. The shift to higher frequency indicates the increase of spring constant of this vibrational mode. This is attributed to the breaking of hydrogen bond between the –N-H and –C=O moieties as shown in position 7 of Fig.5b. The increase of ZnO ratio to 20 wt.% shows a consistent result. The peak intensity at 3274 cm^{-1} decreases significantly while the high frequency peak becomes much broader and merges into the baseline. The line broadening indicates that the –N-H group locates in various local environments and hence vibrates at a wide range of frequencies. The signal of **ν**(C=O) (carboxylic) at 1690 cm^{-1} also disappears from the spectra of nanocomposites while new peak at 1537 cm^{-1} emerges (position 6 in Fig.5a). This new peak is a signature of coulombic

interaction between Zn^{2+} ion and $–COO^-$ headgroup of poly(PCDA-mBzA) (position 6 in Fig.5b). The peak at 1589 cm^{-1} corresponding to **ν**(C=C) of phenyl group also shifts to around 1605 cm^{-1} and broadens significantly in the systems of nanocomposites. This observation indicates that the local environments of phenyl group within nanocomposite is altered. The broadening of this band also indicates the decrease of molecular ordering in this region. These IR results suggest that the addition of ZnO nanoparticles into poly(PCDA-mBzA) assemblies still provides the coulombic interaction between $–COO^-$ headgroup and Zn^{2+}/ZnO surface. However, the binding of Zn^{2+} ion also breaks hydrogen bonds at the amide moiety (position 7, Fig.5b) and reduces **π-π** interaction between the phenyl group (position 4, Fig.5b). These concert segmental rearrangements results in the decrease of overall molecular interactions within the system, which, in turn, reduces the T_{CT} systematically. The strength of overall interactions is still strong enough to effort the reversible thermochromism. Our result is consistent with previous study where the incorporation of Cd^{2+} ion into poly(PCDA-mBzA) assemblies drastically reduces the strength of overall interactions and results in irreversible thermochromism.

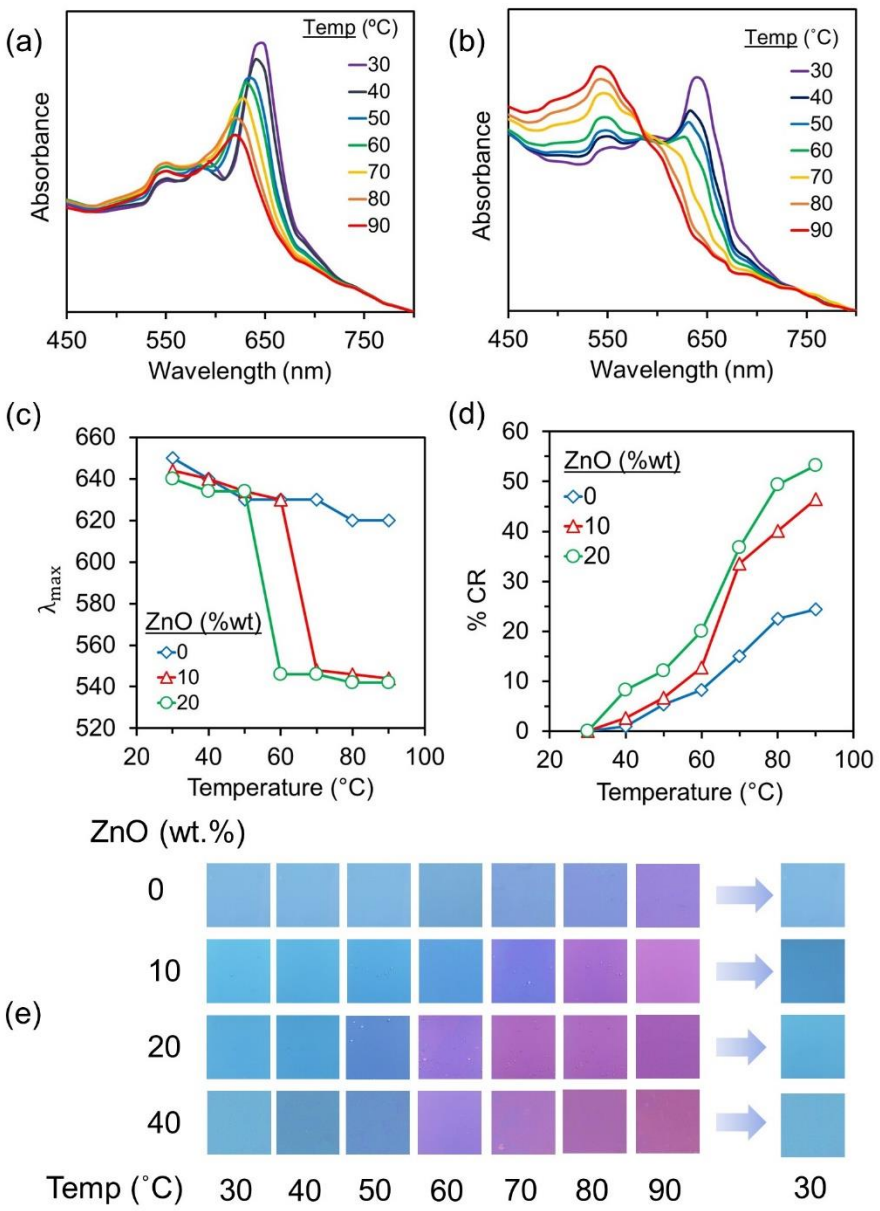

Fig.2 Absorption spectra measured upon increasing temperature of (a) pure poly(PCDA-mBzA) and (b) poly(PCDA-mBzA)/Zn^{2+}/ZnO nanocomposite containing 20 wt.% of ZnO nanoparticle. Plots of (c) λ_{max} and (d) %CR as a function of temperature. (e) Color photographs of pure poly(PCDA-mBzA) and poly(PCDA-mBzA)/Zn^{2+}/ZnO nanocomposite taken upon heating/cooling.

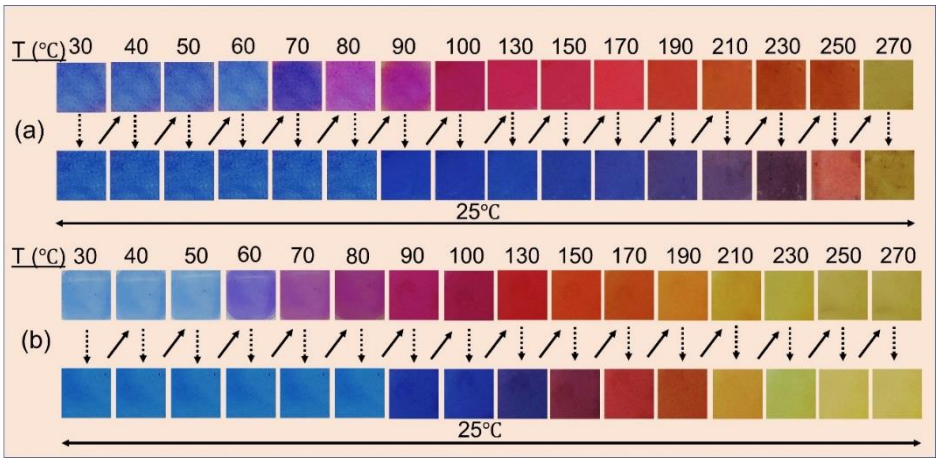

Fig.3 Color photographs of drop-cast films of pure poly(PCDA-mBzA) and poly(PCDA-mBzA)/Zn^{2+}/ZnO nanocomposite containing 20 wt.% of ZnO nanoparticle taken upon heating/cooling cycles.

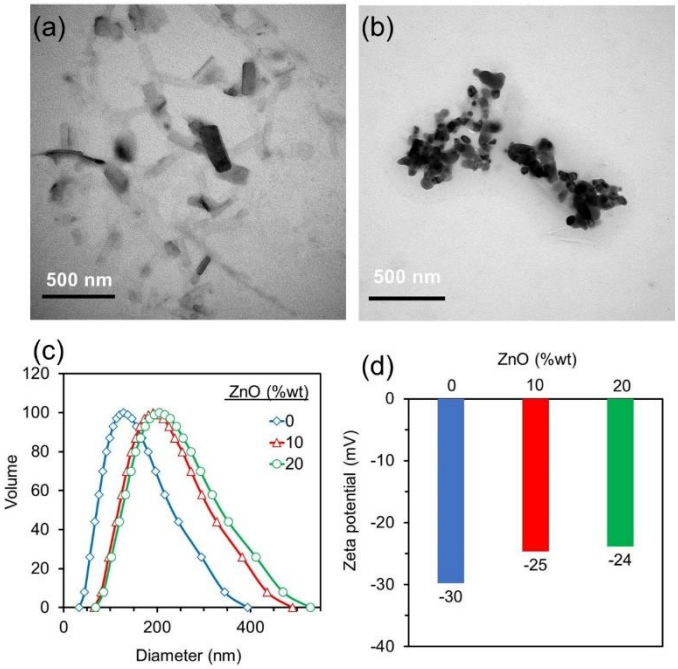

Fig.4 TEM images of (a) pure poly(PCDA-mBzA) assemblies and (b) poly(PCDA-mBzA)/Zn^{2+}/ZnO nanocomposite containing 20 wt.% of ZnO nanoparticle. (c) Size distribution and (d) zeta-potential values in aqueous suspension measured by DLS.

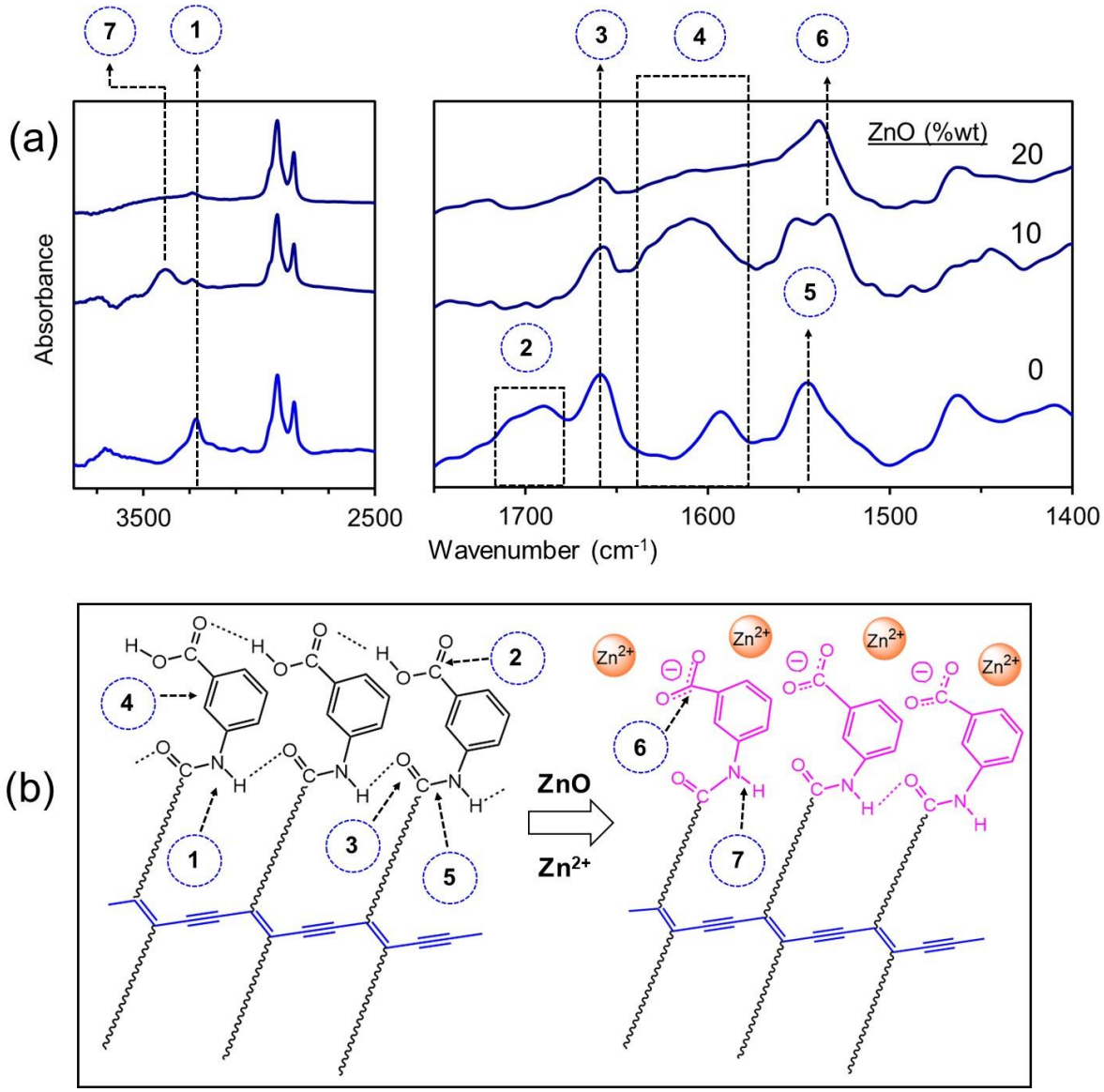

Fig.5 (a) FT-IR spectra of pure poly(PCDA-mBzA) and (b) poly(PCDA-mBzA)/Zn^{2+}/ZnO nanocomposite containing 10 and 20 wt.% of ZnO nanoparticle. (b) Molecular segment of poly(PCDA-mBzA) assigned to each peak in the IR spectra.

Molecular packing structure of pure poly(PCDA-mBzA) and the poly(PCDA-mBzA)/Zn^{2+}/ZnO nanocomposite is probed by XRD. Thin films were prepared by drop-casting onto glass slides and dried under ambient conditions. The nanocomposites were prepared by increasing the ZnO ratios from 5 to 60 wt.%. The XRD patterns shown in Fig. 6a correspond to bilayer lamellar structure similar to that of poly(PCDA). In the system of pure poly(PCDA-mBzA), the 1st diffraction peak (001) is detected at 2θ = 1.66°. The interlamellar d-spacing, calculated using Bragg's law, is equal to 5.31 nm (Fig. 6b). The addition of 5 wt.% ZnO nanoparticles into the poly(PCDA-mBzA) assemblies causes the growth of new peak at 2θ = 1.38° while the intensity of original peak drops significantly. This observation indicates that large fraction of the poly(PCDA-mBzA) transforms to new bilayer lamellar structure with larger interlamellar d-spacing. The further increase of ZnO ratios to 10 and 60 wt.% causes the disappearance of original peak at 1.66° while the new peak at 1.38° dominates the XRD pattern. The d-spacing of new lamellar structure increases to 6.56 nm. The increase of d-spacing value indicates the intercalation of Zn^{2+} ions with the bilayer of poly(PCDA-mBzA) as shown in Fig. 6b. The Zn^{2+}-intercalated bilayer lamellar structure is consistent with the IR result discussed earlier. Our previous studies of the nanocomposites prepared from PDAs with monocarboxylic headgroup also observed similar Zn^{2+}-intercalated packing structure. Since the diameter of Zn^{2+} ion (0.18 nm) is quite small, the

intercalation cannot be a sole factor for the increase of d-spacing from 5.31 nm to 6.56 nm. We suggest that the intercalation of Zn^{2+} ion also causes the increase of molecular tilting angle with respect to the lamellar plan. Detailed discussion of this issue is available in our previous reports.

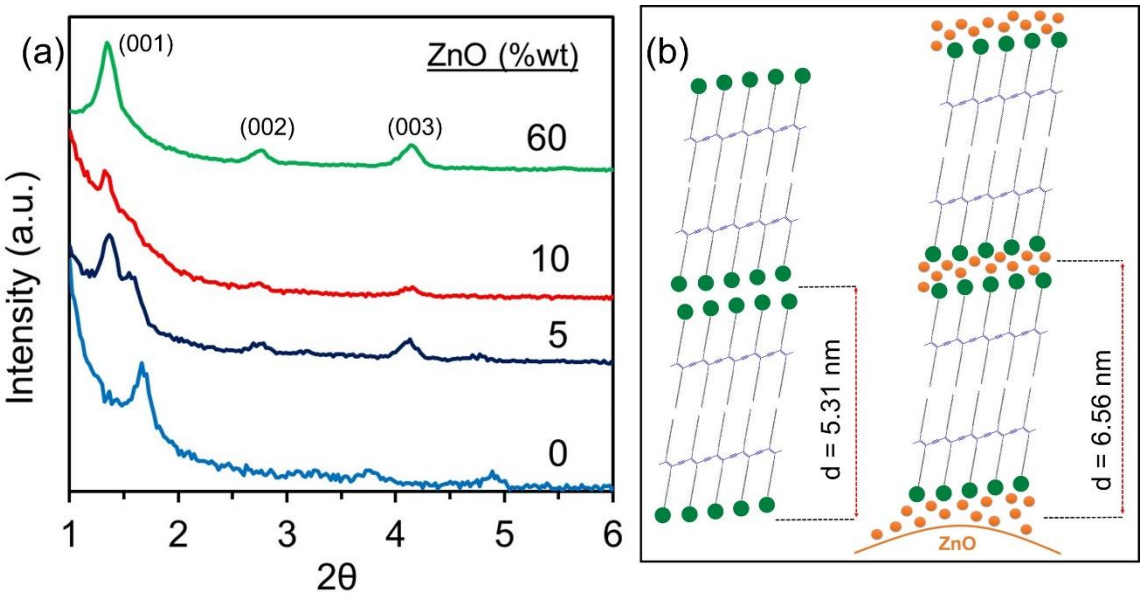

Fig.6 (a) XRD patterns of pure poly(PCDA-mBzA) and poly(PCDA-mBzA)/Zn^{2+}/ZnO nanocomposite containing 5, 10 and 60 wt.% of ZnO nanoparticle. (b) Schematic representation of the bilayer packing structure.

Enhancing the sensitivity to chemical stimuli

Previous studies have demonstrated that the selectivity of PDAs to chemical stimuli can be achieved by structural modification with specific functional groups. However, it is rather difficult

to modify the PDA structure for qualitative analysis purpose. Our recent study showed that the shortening of PDA alkyl tail resulted in systematic increase of sensitivity while the variation of alkyl segment adjacent to the headgroup led to different outcome. The modification of PDA headgroup with benzoic acid or naphthoic acid resulted in unpredictable trend of their sensitivity to cationic surfactant or organic solvent. Alcohols can be used as additives for fine tuning of the sensitivity of PDAs to various chemical stimuli. However, the PDA/alcohol systems cannot be fabricated into thin films due to its relatively low color stability.

In this section, we explore the utilization of ZnO nanoparticles as additives for improving the sensitivity of poly(PCDA-mBzA) assemblies to chemical stimuli. CTAB and THF are used as representatives for cationic surfactant and organic solvent. Absorption spectra of pure poly(PCDA-mBzA) and poly(PCDA-mBzA)/Zn^{2+}/ZnO nanocomposites measured upon addition of CTAB are shown in Fig. 7a and b. The increase of CTAB concentration above 0.2 mM causes a systematic growth of peak at high energy region, corresponding to the transition to new electronic species. The λ_{max} drops to 525 nm at 0.6 mM of CTAB (Fig. 7c). The plot of colorimetric response (%CR) in Fig. 7d shows a sharp increase to 36% in this concentration region. Further increasing CTAB concentration to 1.6 mM causes a gradual increase of CR value to about 42%. The incorporation of ZnO nanoparticles results in a systematic increase of the poly(PCDA-mBzA) sensitivity. For

the nanocomposite systems containing 10 and 20 wt.% ZnO nanoparticles, the drop of λ_{max} is detected at CTAB concentration of 0.17 mM and 0.12 mM, respectively. The increase of sensitivity is clearly observed in the plots of CR value where it reaches about 90% in both systems.

The increase of poly(PCDA-mBzA) sensitivity to cationic surfactant is summarized in Fig. 8. For the system of pure poly(PCDA-mBzA) in aqueous suspension, we observe a clear color transition from blue to purple at 1.2 mM of CTAB (Fig. 8a). The color transition takes place at much lower CTAB concentration in the nanocomposite systems. It drops to 0.17 mM and 0.12 mM in the nanocomposite systems containing ZnO ratios of 10 and 20 wt.%, respectively. The transition is also much more obvious where the blue suspension completely changes to yellow color. It has been proposed that the mechanism of color transition induced by cationic surfactant involves the penetration of its alkyl tail into the bilayer structure causing the rearrangement of PDA backbone [xx]. We suggest that the decrease of intermolecular interactions facilitates the penetration process in the nanocomposite systems. Therefore, it requires a smaller number of CTAB molecules to induce segmental rearrangement and hence color transition of poly(PCDA-mBzA) (Fig. 8b). This result is consistent with the decrease of T_{CT} discussed in the previous section.

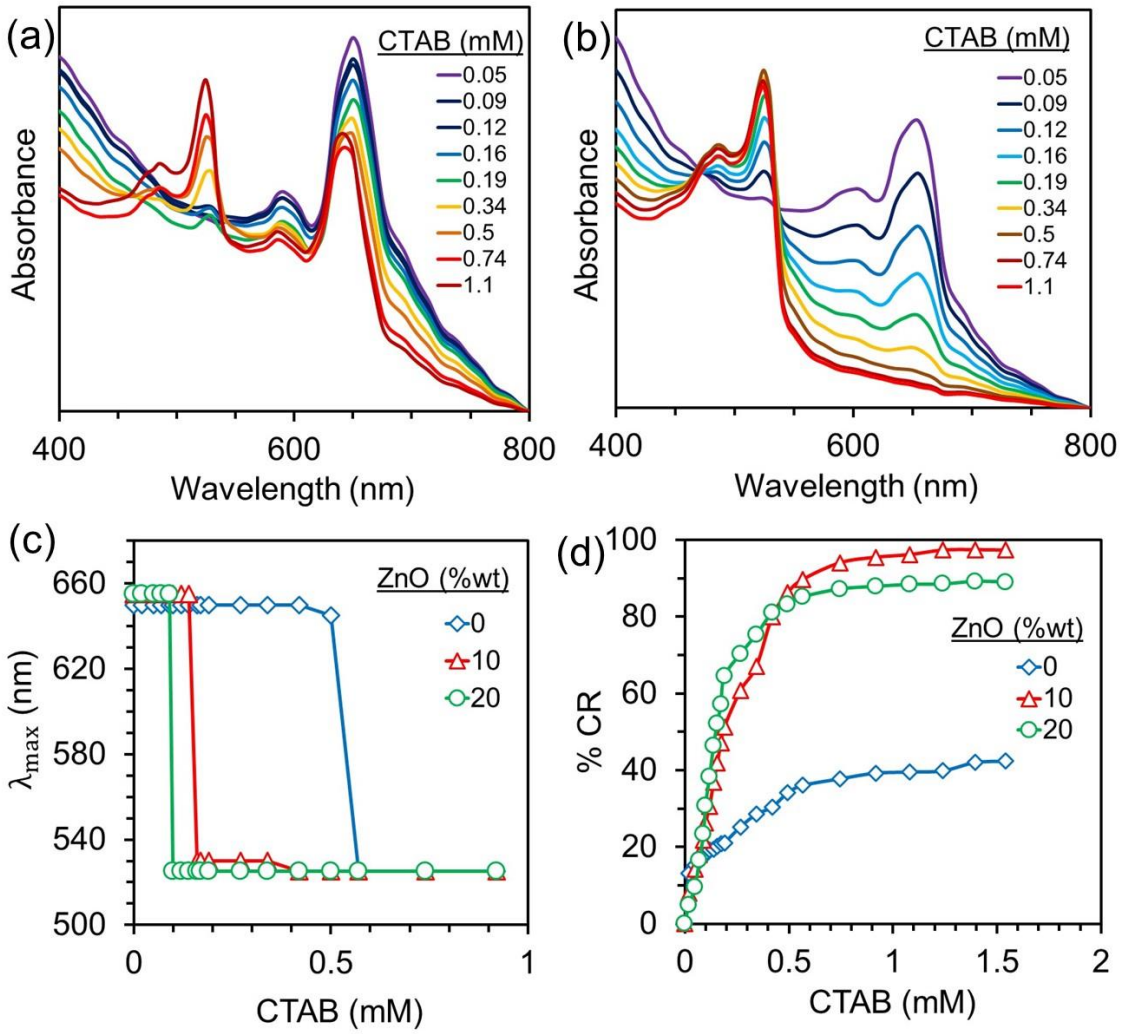

Fig.7 Absorption spectra measured upon increasing CTAB concentration in systems of (a) pure poly(PCDA-mBzA) and (b) poly(PCDA-mBzA)/Zn^{2+}/ZnO nanocomposite containing 20 wt.% of ZnO nanoparticle. Plots of (c) λ_{max} and (d) %CR as a function of CTAB concentration.

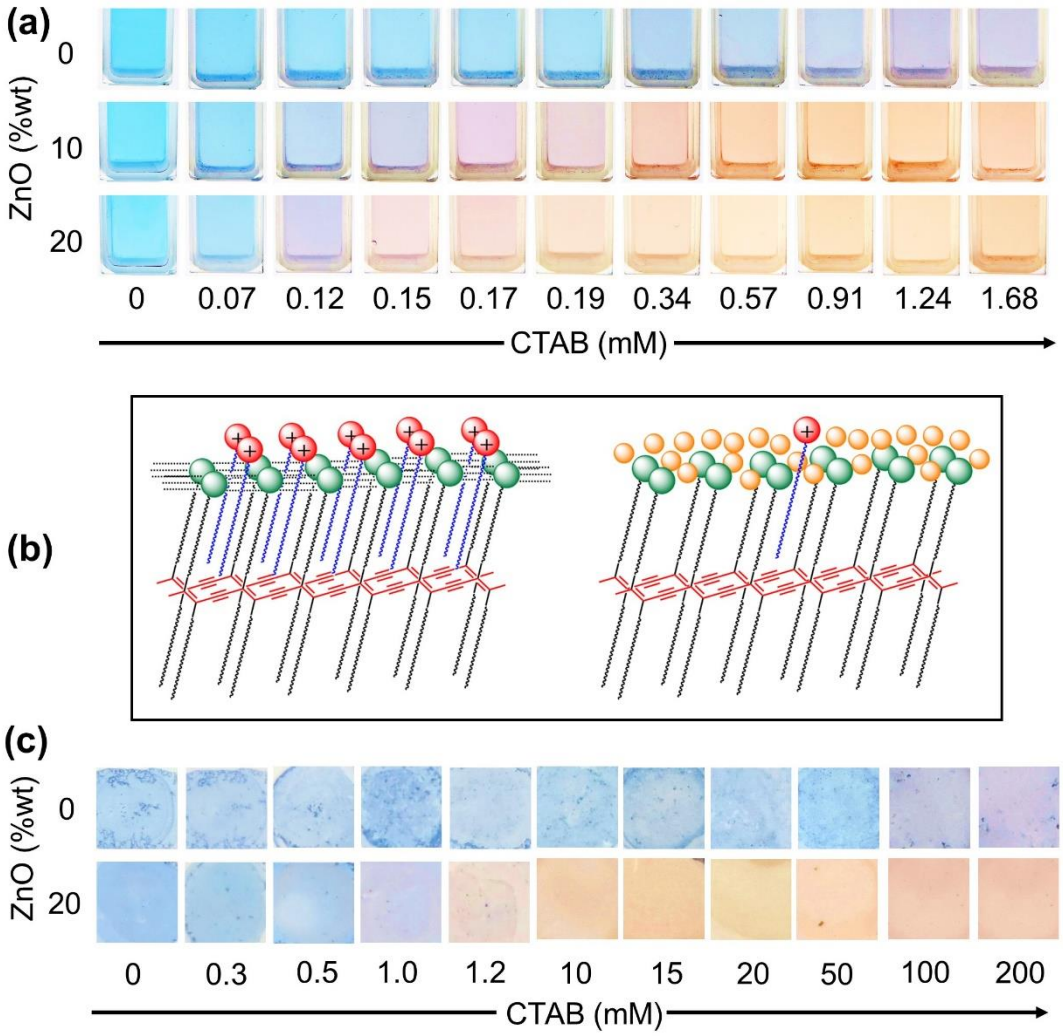

Fig.8 Color photographs of (a) aqueous suspension of pure poly(PCDA-mBzA) and poly(PCDA-mBzA)/Zn^{2+}/ZnO nanocomposite containing 10, 20 wt.% of ZnO nanoparticles taken upon addition of CTAB. (b) Schematic drawing for the insertion of CTAB molecules into alkyl layer of (left) pure poly(PCDA-mBzA) and (right) the nanocomposite. (c) Color photographs of drop-cast films taken after depositing a drop of CTAB solutions with different concentrations.

The increase of sensitivity is preserved when the samples are fabricated into thin films by drop-casting on nylon filter paper. A drop of CTAB aqueous solutions with different concentrations was deposited on the thin films. Color photographs taken after 3 min. of incubation are shown in Fig. 8c. It is very difficult to induce color transition of pure poly(PCDA-mBzA) in solid thin film. The use of 200 mM CTAB solution induces slight change of the thin film to purple color while the color transition of poly(PCDA-mBzA) in aqueous suspension occurs at 1.2 mM. The high color stability of thin film is attributed to the increase of intermolecular interactions in the solid state, hindering the penetration of CTAB molecules. Thin film of the nanocomposite containing 20 wt.% of ZnO nanoparticles exhibits a clear blue-to-yellow color transition at 1.2 mM of CTAB. This concentration is much lower than that of the pure poly(PCDA-mBzA) system. Therefore, the increase of sensitivity still remains in the thin film. The ability to fabricate paper-based PDA sensors that response to different concentrations of cationic surfactant extends their utilization as colorimetric sensors. It allows simple quantitative detection of the cationic surfactant in different forms of products such as fresh foods, meat and cleansing detergents. It is worthwhile to point out that the use of PDA-based materials for quantitative analysis of chemicals is quite rare.

The investigation of colorimetric response to organic solvent provides consistent results. The color of pure poly(PCDA-mBzA) is quite stable. The addition of THF solvent up to 44 %v/v hardly affects the pattern of absorption spectra (Fig. 9a). Our recent study observed the color transition of pure poly(PCDA-mBzA) at about 70 %v/v of THF. For the nanocomposite system, we detect the growth of peak at 540 nm when the THF concentration is increased to 37 % v/v (Fig. 9b). The aqueous suspension changes to slight purple at this condition (Fig. 9c). The color transition becomes more obvious when the THF concentration is further increased to 44 % v/v. Our results indicates that the sensitivity of poly(PCDA-mBzA) to organic solvent can also be improved by adding ZnO nanoparticles. Therefore, this PDA-based material can be utilized for quantitative analysis of organic solvent in various products or samples in industrial processes.

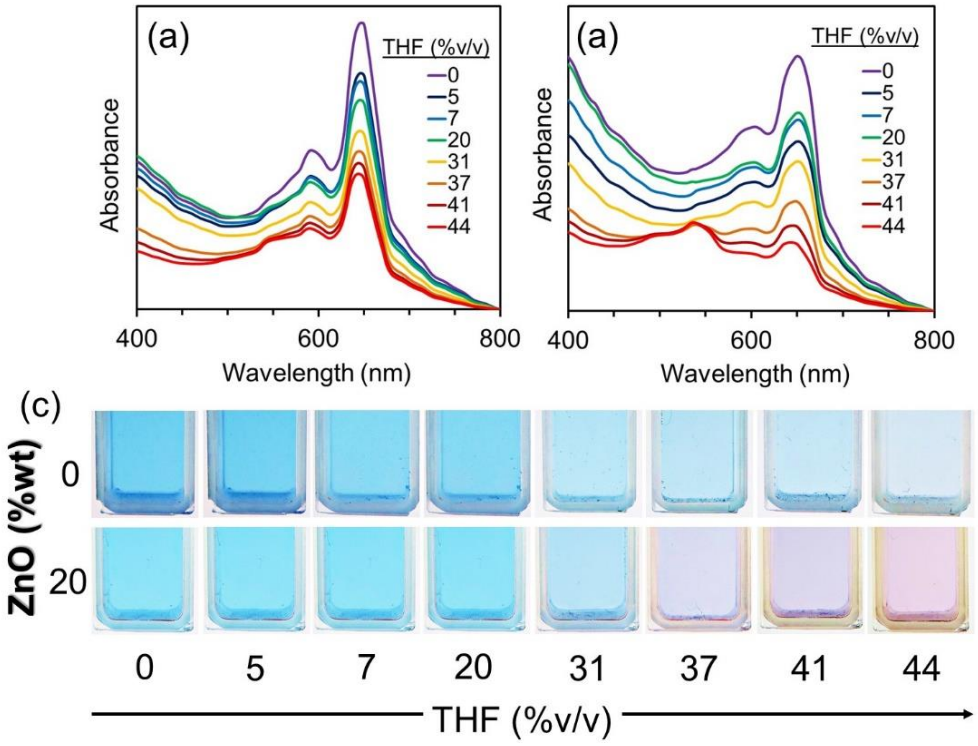

Fig.9 Absorption spectra of aqueous suspension of (a) pure poly(PCDA-mBzA) and (b) poly(PCDA-mBzA)/Zn^{2+}/ZnO nanocomposite containing 20 wt.% of ZnO nanoparticle measured upon addition of THF solvent. (c) Color photographs of the color transition taken upon increasing THF concentration.

Conclusion

This work presents the interesting effect of ZnO nanoparticle on color-transition behaviors of PDA constituting aromatic headgroup. While the incorporation of Zn^{2+}/ZnO into poly(PCDA) assemblies increases the strength of molecular interactions, the opposite result is detected in the

system of poly(PCDA-mBzA). FT-IR and XRD studies reveal that the intercalation of Zn^{2+} ion with bilayer structure of poly(PCDA-mBzA) weakens the hydrogen-bond and π-π interactions between the benzoic headgroup. This physical process can be utilized for tuning down the T_{CT} from about 90 to 60 ^{o}C while the reversible thermochromism is still preserved. The resultant poly(PCDA-mBzA)/Zn^{2+}/ZnO nanocomposites with various T_{CT} can be applied as colorimetric sensor for detecting a real-time local temperature of various systems and reversible thermochromic paint/ink for smart labels of foods, beverages or other products. We also take a step toward demonstrating the ability to enhance the sensitivity of poly(PCDA-mBzA) to chemical stimuli by adding ZnO nanoparticles. The poly(PCDA-mBzA)-based colorimetric sensors exhibit color transition at different concentrations of cationic surfactant or organic solvent, depending on the ZnO ratio within the system. Our major finding can be used as a guideline for fabricating colorimetric sensors that detect specific chemicals at wide range of concentration.

References

[1] O. Mapazi, P.K. Matabola, R.M. Moutloali, C.J. Ngila, Sensors and Actuators B: Chemical, 252 (2017), 671-679.

[2] G.M.D. Ferreira, G.M.D. Ferreira, M.d.C. Hespanhol, J.d.P. Rezende, A.C.d.S. Pires, P.F.R. Ortega, L.H.M. da Silva, Food Chemistry, 241 (2018), 358-363.

[3] S. Chae, J.P. Lee, J.-M. Kim, Advanced Functional Materials, 26 (2016), 1769-1776.

[4] M. Takeuchi, H. Imai, Y. Oaki, ACS Appl Mater Interfaces, 9 (2017), 16546-16552.

[5] M. Takeuchi, K. Gnanasekaran, H. Friedrich, H. Imai, N.A.J.M. Sommerdijk, Y. Oaki, Advanced Functional Materials, 28 (2018), 1804906.

[6] R. Potai, K. Faisadcha, R. Traiphol, N. Traiphol, Colloids and Surfaces A: Physicochemical and Engineering Aspects, 555 (2018), 27-36.

[7] C. Khanantong, N. Charoenthai, T. Phuangkaew, F. Kielar, N. Traiphol, R. Traiphol, Colloids and Surfaces A: Physicochemical and Engineering Aspects, 553 (2018), 337-348.

[8] C. Phollookin, S. Wacharasindhu, A. Ajavakom, G. Tumcharern, S. Ampornpun, T. Eaidkong, M. Sukwattanasinitt, Macromolecules, 43 (2010), 7540-7548.

[9] J. Pang, L. Yang, B.F. McCaughey, H. Peng, H.S. Ashbaugh, C.J. Brinker, Y. Lu, The Journal of Physical Chemistry B, 110 (2006), 7221-7225.

[10] A. Kamphan, C. Khanantong, N. Traiphol, R. Traiphol, Journal of Industrial and Engineering Chemistry, 46 (2017), 130-138.

[11] J. Oh, S. Kang, C.G. Lee, M.S. Han, Analyst, 143 (2018), 4592-4599.

[12] S. Dolai, S.K. Bhunia, S.S. Beglaryan, S. Kolusheva, L. Zeiri, R. Jelinek, ACS Applied Materials & Interfaces, 9 (2017), 2891-2898.

[13] M.J. Shin, D.H. Byun, J.-D. Kim, Journal of Industrial and Engineering Chemistry, 23 (2015), 279-284.

[14] C.P. Oliveira, F. Soares Nde, E.A. Fontes, T.V. Oliveira, A.M. Filho, Food Chem, 135 (2012), 1052-1056.

[15] A. Kamphan, N. Charoenthai, R. Traiphol, Colloids and Surfaces A: Physicochemical and Engineering Aspects, 489 (2016), 103-112.

[16] D.-H. Park, J.-M. Heo, W. Jeong, Y.H. Yoo, B.J. Park, J.-M. Kim, ACS Applied Materials & Interfaces, 10 (2018), 5014-5021.

[17] Y. Ishijima, H. Imai, Y. Oaki, Chem, 3 (2017), 509-521.

[18] H. Wang, S. Han, Y. Hu, Z. Qi, C. Hu, Colloids and Surfaces A: Physicochemical and Engineering Aspects, 517 (2017), 84-95.

[19] Y.J. Shin, M.J. Shin, J.S. Shin, Colloids and Surfaces A: Physicochemical and Engineering Aspects, 520 (2017), 459-466.

[20] C. Khanantong, N. Charoenthai, F. Kielar, N. Traiphol, R. Traiphol, Colloids and Surfaces A: Physicochemical and Engineering Aspects, 561 (2019), 226-235.

[21] A. Nopwinyuwong, T. Kitaoka, W. Boonsupthip, C. Pechyen, P. Suppakul, Applied Surface Science, 314 (2014), 426-432.

[22] Y.-l. Su, J.-r. Li, L. Jiang, Colloids and Surfaces B: Biointerfaces, 39 (2004), 113-118.

[23] K.M. Lee, J.H. Moon, H. Jeon, X. Chen, H.J. Kim, S. Kim, S.-J. Kim, J.Y. Lee, J. Yoon, Journal of Materials Chemistry, 21 (2011), 17160-17166.

[24] N. Traiphol, K. Faisadcha, R. Potai, R. Traiphol, J Colloid Interface Sci, 439 (2015), 105-111.

[25] Y. Lifshitz, Y. Golan, O. Konovalov, A. Berman, Langmuir, 25 (2009), 4469-4477.

[26] A. Fujimori, M. Ishitsuka, H. Nakahara, E. Ito, M. Hara, K. Kanai, Y. Ouchi, K. Seki, The Journal of Physical Chemistry B, 108 (2004), 13153-13162.

[27] T. Eaidkong, R. Mungkarndee, C. Phollookin, G. Tumcharern, M. Sukwattanasinitt, S. Wacharasindhu, Journal of Materials Chemistry, 22 (2012), 5970-5977.

[28] Y. Li, L. Wang, X. Yin, B. Ding, G. Sun, T. Ke, J. Chen, J. Yu, Journal of Materials Chemistry A, 2 (2014), 18304-18312.

[29] M.J. Kim, S. Angupillai, K. Min, M. Ramalingam, Y.-A. Son, ACS Applied Materials & Interfaces, 10 (2018), 24767-24775.

[30] B. Hu, S. Sun, B. Wu, P. Wu, Small, 15 (2019), 1804975.

[31] B. Yoon, H. Shin, E.-M. Kang, D.W. Cho, K. Shin, H. Chung, C.W. Lee, J.-M. Kim, ACS Applied Materials & Interfaces, 5 (2013), 4527-4535.

[32] D.-H. Park, B.J. Park, J.-M. Kim, Macromolecular Research, 24 (2016), 943-950.

[33] Q.-M. Wang, Z.-Y. Yang, Carbon, 138 (2018), 90-97.

[34] S.R. Ha, S. Park, J.T. Oh, D.H. Kim, S. Cho, S.Y. Bae, D.-W. Kang, J.-M. Kim, H. Choi, Nanoscale, 10 (2018), 13187-13193.

[35] O. Mapazi, K.P. Matabola, R.M. Moutloali, C.J. Ngila, Polymer, 149 (2018), 106-116.

[36] C. Khanantong, N. Charoenthai, S. Wacharasindhu, M. Sukwattanasinitt, N. Traiphol, R. Traiphol, Journal of Industrial and Engineering Chemistry, 58 (2018), 258-265.

[37] A. Kamphan, N. Traiphol, R. Traiphol, Colloids and Surfaces A: Physicochemical and Engineering Aspects, 497 (2016), 370-377.

[38] S. Wacharasindhu, S. Montha, J. Boonyiseng, A. Potisatityuenyong, C. Phollookin, G. Tumcharern, M. Sukwattanasinitt, Macromolecules, 43 (2010), 716-724.

[39] D.J. Ahn, S. Lee, J.-M. Kim, Advanced Functional Materials, 19 (2009), 1483-1496.

[40] S. Ampornpun, S. Montha, G. Tumcharern, V. Vchirawongkwin, M. Sukwattanasinitt, S. Wacharasindhu, Macromolecules, 45 (2012), 9038-9045.

[41] J.M. Kim, J.S. Lee, H. Choi, D. Sohn, D.J. Ahn, Macromolecules, 38 (2005), 9366-9376.

[42] D.J. Ahn, E.-H. Chae, G.S. Lee, H.-Y. Shim, T.-E. Chang, K.-D. Ahn, J.-M. Kim, Journal of the American Chemical Society, 125 (2003), 8976-8977.

[43] G.S. Lee, T.Y. Kim, D.J. Ahn, Journal of Industrial and Engineering Chemistry, 67 (2018), 312-315.

[44] N. Traiphol, A. Chanakul, A. Kamphan, R. Traiphol, Thin Solid Films, 622 (2017), 122-129.

[45] A. Chanakul, N. Traiphol, R. Traiphol, J Colloid Interface Sci, 389 (2013), 106-114.

[46] N. Traiphol, N. Rungruangviriya, R. Potai, R. Traiphol, J Colloid Interface Sci, 356 (2011), 481-489.

[47] M. Gou, G. Guo, J. Zhang, K. Men, J. Song, F. Luo, X. Zhao, Z. Qian, Y. Wei, Sensors and Actuators B: Chemical, 150 (2010), 406-411.

[48] J. Lu, J. Zhou, J. Li, Soft Matter, 7 (2011), 6529-6531.

[49] A. Patlolla, J. Zunino, A.I. Frenkel, Z. Iqbal, Journal of Materials Chemistry, 22 (2012), 7028-7035.

[50] J. Lee, M. Pyo, S.-h. Lee, J. Kim, M. Ra, W.-Y. Kim, B.J. Park, C.W. Lee, J.-M. Kim, Nature Communications, 5 (2014), 3736.

[51] S. Balakrishnan, S. Lee, J.-M. Kim, Journal of Materials Chemistry, 20 (2010), 2302-2304.

[52] R. Nagarajan, Langmuir, 18 (2002), 31-38.

[53] M. Takeuchi, H. Imai, Y. Oaki, Journal of Materials Chemistry C, 5 (2017), 8250-8255.

[54] A. Chanakul, R. Traiphol, N. Traiphol, Journal of Industrial and Engineering Chemistry, 45 (2017), 215-222.

[55] B. Yoon, S. Lee, J.-M. Kim, Chemical Society Reviews, 38 (2009), 1958-1968.

[56] X. Chen, S. Kang, M.J. Kim, J. Kim, Y.S. Kim, H. Kim, B. Chi, S.J. Kim, J.Y. Lee, J. Yoon, Angew Chem Int Ed Engl, 49 (2010), 1422-1425.

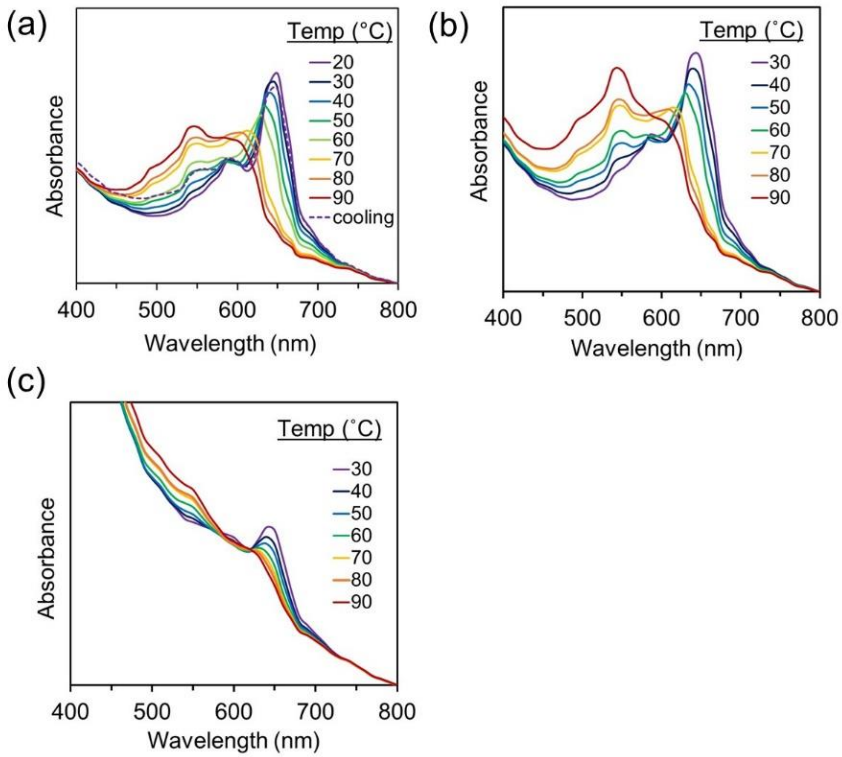

Fig.1s Absorption spectra upon heating of poly(PCDA-mBzA)/Zn^{2+}/ZnO nanocomposites. the ratios of ZnO are (a) 5 wt.%, (b) 10 wt.% and (c) 40 wt.%.

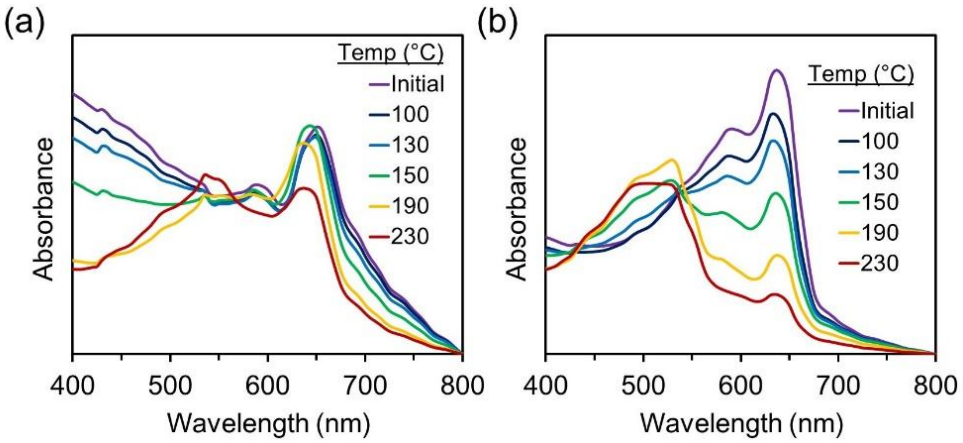

Fig.2s Absorption spectra of (a) pure poly(PCDA-mBzA) thin film and (b) poly(PCDA-mBzA)/Zn^{2+}/ZnO20wt.%. The spectrum measured after heating the thin film at presented temperature.

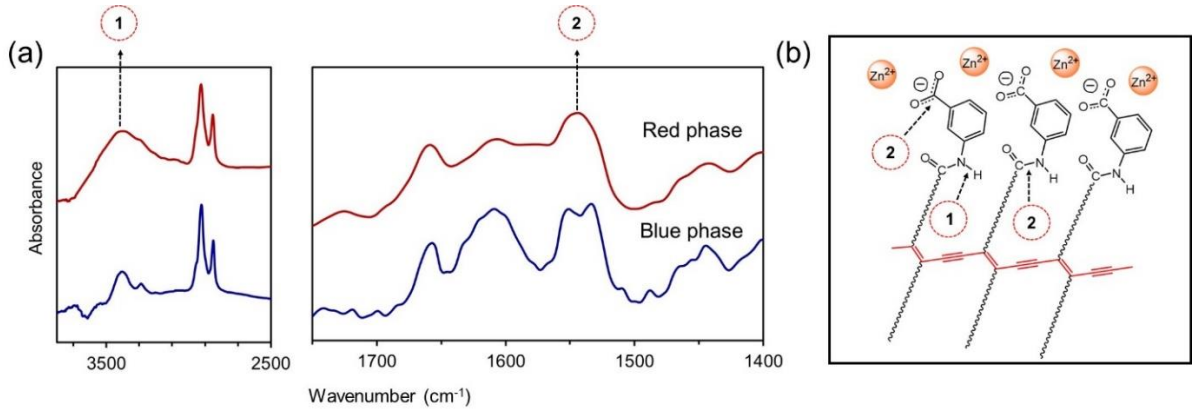

Fig.3s (a) The FT-IR spectra of blue and red phase of poly(PCDA-mBzA)/Zn^{2+}/ZnO20wt.%. (b) The graphical model presented the local interaction of red phase nanocomposite.

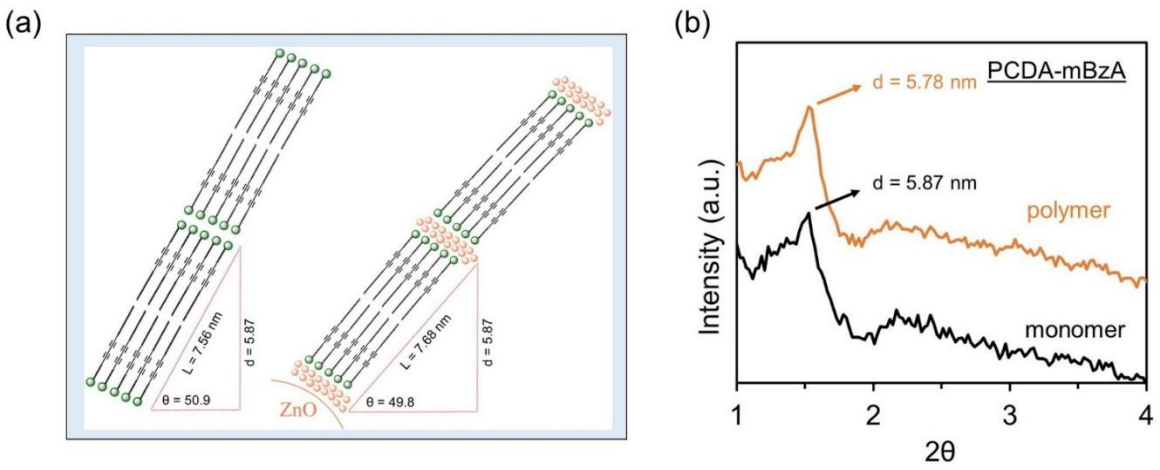

Fig.4s (a) Illustration of tilting angle comparison between pure poly(PCDA-mBzA) and poly(PCDA-mBzA)/Zn^{2+}/ZnO20wt.%. (b) XRD pattern of monomer and polymer of PCDA-mBzA with added ZnO at 20 wt.%.

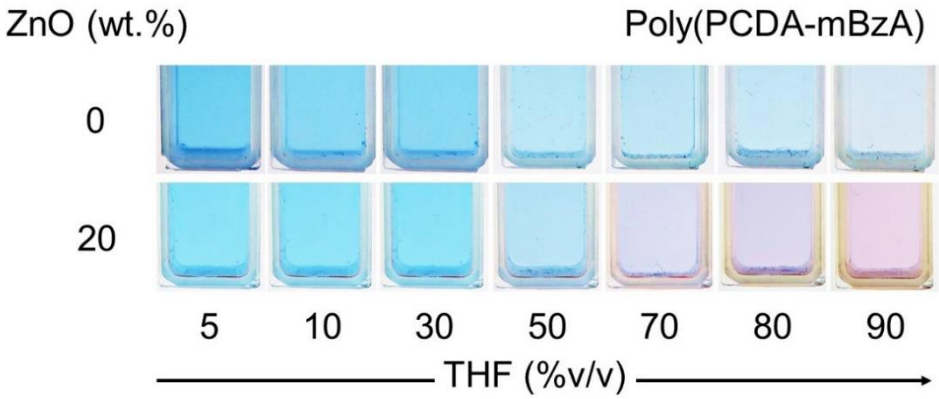

Fig.5s Color photographs taken upon increasing the concentration of THF into poly(PCDA-mBzA) assemblies.

Output จากโครงการวิจัยที่ได้รับทุนจาก สกว.

ผลงานตีพิมพ์ในวารสารวิชาการนานาชาติ

ผลงานที่ได้รับการตีพิมพ์แล้ว

1. Phonchai, N., Khanantong, C., Kielar, F., Traiphol, R., Traiphol, N.* “Low-Temperature Reversible Thermochromic Polydiacetylene/Zinc(II)/Zinc Oxide Nanocomposites for Colorimetric Sensing” *ACS Applied Nano Materials* (2019) https://doi.org/10.1021/acsanm.9b00876

2. Potai, R., Faisadcha, K., Traiphol, R., Traiphol, N.* “Controllable thermochromic and phase transition behaviors of polydiacetylene/zinc(II) ion/zinc oxide nanocomposites via photopolymerization: An insight into the molecular level” *Colloids and Surfaces A: Physicochemical and Engineering Aspects*, 555 (2018), pp. 27–36.

3. Seetha, S., Saymung, R., Traiphol, R., Traiphol, N.* “Controlling self-assembling and color-transition of polydiacetylene/zinc(II) ion/zinc oxide nanocomposites by varying pH: Effects of surface charge and head group dissociation” *Journal of Industrial and Engineering Chemistry,* 72 (2019), pp. 423-431.

ผลงานที่จัดทำเป็น manuscript เตรียมส่งตีพิมพ์

1. Phonchai, N., Khanantong, C., Kielar, F., Traiphol, R., Traiphol, N.* “Enhancing the sensitivity of stimuli-responsive polydiacetylene with aromatic headgroup: The opposite effect of ZnO nanoparticle”

การนำผลงานวิจัยไปใช้ประโยชน์

เชิงวิชาการ (มีการพัฒนาการเรียนการสอน/สร้างนักวิจัยใหม่)

โครงการวิจัยนี้มีส่วนในการผลิตนักวิจัยระดับปริญญาเอกจำนวน 2 คน คือ นายณัฐนนท์ พลชัย และนางสาวชนิตา ขนันทอง และระดับปริญญาโทจำนวน 1 คน คือ นายศุภกร สีทา

อื่น ๆ (เช่น ผลงานตีพิมพ์ในวารสารวิชาการในประเทศ การเสนอผลงานในที่ประชุมวิชาการ หนังสือ การจดสิทธิบัตร)

Plenary, Keynote and Invited Oral Presentations:

1. Colorimetric sensing of temperature and chemicals by PDA-based nanocomposite (Invited speaker), TMU and PetroMat Joint Mini Symposium on Catalysis and Advanced Materials 2017, February 1, 2017, Bangkok, Thailand.

2. Polydiacetylene/Zinc Oxide Nanocomposite As Thermal And Chemical Sensors (Plenary speaker), International Conference on Advances in Science and Engineering (ICASE 2017), January 20-22, 2017, Bangkok, Thailand

3. Thermal and Chemical Sensors Based On Polydiacetylene/Zinc Oxide Nanocomposite (Keynote speaker), The 3rd International Congress on Advanced Materials (AM 2016) November 27-30, 2016, Bangkok, Thailand

4. Polydiacetylene-Based Nanocomposite as Colorimetric Sensors (Keynote speaker), The International Polymer Conference of Thailand (PCT-6), June 30-July 1, 2016, Bangkok, Thailand.

Proceedings:

1. Seetha, S., Traiphol, N., "Effects of Cationic Surfactants on Dispersing Stability and Color Transition of Polydiacetylene/Zinc Oxide Nanocomposite in Toluene," Proceedings of The International Polymer Conference of Thailand (PCT-6) in June 30-July 1, 2016, Bangkok, Thailand.

Presentations:

1. Fine tuning colorimetric response of polydiacetylene/ZnO nanocomposites by varying diacetylene structure, PACCON 2018, February 7-9, 2018, Songkhla, Thailand

2. Developing properties of polydiacetylene/zinc oxide nanocomposite for detection of Sodium Lauryl Sulfate, Science forum 2017, May 29-30, 2017, Bangkok, Thailand
3. Controlling self-assembling and thermochromism of polydiacetylene/zinc oxide nanocomposite by varying pH, 10th international conference on materials science & engineering (BRAMAT 2017), March 8-11, 2017, Brasov, Romania.
4. Polydiacetylene/zinc oxide nanocomposite for detection of Sodium Lauryl Sulfate, International Conference on Advances in Science and Engineering (ICASE 2017), January 20-22, 2017, Bangkok, Thailand
5. Tuning dispersing stability and thermochromic behaviors of polydiacetylene/zinc oxide by using cationic surfactants, International Conference on Advances in Science and Engineering (ICASE 2017), January 20-22, 2017, Bangkok, Thailand
6. Utilization of polydiacetylene/zinc oxide nanocomposites to detect and differentiate organic bases in various media, International Conference on Advances in Science and Engineering (ICASE 2017), January 20-22, 2017, Bangkok, Thailand
7. Effects of diacetylene alkyl chain length on colorimetric response of polydiacetylene/zinc oxide nanocomposites, International Conference on Advances in Science and Engineering (ICASE 2017), January 20-22, 2017, Bangkok, Thailand

8. Role of Zn^{2+} ion on the formation of reversible thermochromic polydiacetylene/zinc oxide nanocomposites, The 4th International Conference on Competitive Materials and Technology Processes (IC-CMTP 4), October 3-7, 2016, Miskolc-Lillafurred, Hungary.
9. Effects of Cationic Surfactants on Dispersing Stability and Color Transition of Polydiacetylene/Zinc Oxide Nanocomposite in Toluene, The International Polymer Conference of Thailand (PCT-6), June 30-July 1, 2016, Bangkok, Thailand.

ภาคผนวก

บทความสำหรับการเผยแพร่

วัสดุเชิงประกอบระดับนาโนเมตรพอลิไดแอเซทิลีน/ซิงก์ (II) ไอออน/ซิงก์ออกไซด์ ถูกเตรียมขึ้นโดยจากมอนอเมอร์ 7 ชนิดที่มีความยาวสายโซ่อัลคิลที่แตกต่างกัน เพื่อทำการศึกษาการตอบสนองโดยการเปลี่ยนสีแบบผันกลับได้ที่สภาวะอุณหภูมิต่ำ เมื่อความยาวของสายโซ่อัลคิลส่วนหางลดลงจาก 12 เป็น 6 หน่วยเมทิลีน จะทำให้อุณหภูมิที่เกิดการเปลี่ยนสีของวัสดุเชิงประกอบลดลงจาก 90 เป็น 30 องศาเซลเซียส อย่างไรก็ตามการเปลี่ยนแปลงความยาวสายโซ่อัลคิลที่ตำแหน่งถัดจากส่วนหัวของพอลิไดแอเซทิลีน จะทำให้อุณหภูมิการเปลี่ยนสีเปลี่ยนแปลงอย่างไม่เป็นระบบ ซึ่งจากการตรวจสอบด้วยเทคนิคต่าง ๆ พบว่า การเปลี่ยนแปลงมุมภายในโครงสร้างสองชั้นของพอลิไดแอเซทิลีน การเปลี่ยนแปลงของอันตรกิริยา และการจัดเรียงตัวของสายโซ่หลักขึ้นอยู่กับความยาวสายโซ่อัลคิลภายในโมเลกุล เมื่อทำการปรับเปลี่ยนระยะเวลาในการฉายแสงเพื่อให้เกิดพอลิเมอไรเซชันระหว่างกระบวนการเตรียมสารร่วมด้วย ทำให้สามารถควบคุมอุณหภูมิการเปลี่ยนสีของวัสดุเชิงประกอบได้อย่างละเอียดมากขึ้นจากการปรับเปลี่ยนความยาวของสายโซ่หลัก และจะได้วัสดุเปลี่ยนสีแบบผันกลับได้ต่ออุณหภูมิที่มีค่าอุณหภูมิการเปลี่ยนสีในช่วง 10-90 องศาเซลเซียส นอกจากนี้การควบคุมการจัดเรียงตัวของพอลิเมอร์บนอนุภาคซิงก์ออกไซด์ โดยทำการปรับค่าความเป็นกรดเบสในกระบวนการเตรียมสาร ซึ่งเป็นการควบคุมประจุที่พื้นผิวของอนุภาคซิงก์ออกไซด์และการแตกตัวของหมู่คาร์บอกซิลิกที่ส่วนหัวของพอลิได

แอเซทิลีน ทำให้ได้ปริมาณของวัสดุเชิงประกอบที่เพิ่มมากขึ้นเมื่อทำการเตรียมในสภาวะเบส และสามารถทำการควบคุมสมบัติการเปลี่ยนสีต่ออุณหภูมิและสารเคมีได้ด้วย

เมื่อทำการเตรียมวัสดุเชิงประกอบโดยใช้มอนอเมอร์ชนิด 3-(pentacosa-10,12-diynamido) benzoic acid (PCDA-mBzA) ซึ่งส่วนหัวมีหมู่เบนโซอิกเพิ่มเข้ามา พบว่าวัสดุเชิงประกอบระดับนาโนเมตร poly(PCDA-mBzA)/ซิงก์ (II) ไอออน/ซิงก์ออกไซด์ ที่เติมซิงก์ออกไซด์ในปริมาณ 5-20 เปอร์เซ็นโดยน้ำหนักมอนอเมอร์ มีอุณหภูมิการเปลี่ยนสีลดลงเป็น 80 70 และ 60 องศาเซลเซียส เมื่อเปรียบเทียบกับ poly(PCDA-mBzA) ที่เกิดการเปลี่ยนสีที่ 90 องศาเซลเซียส นอกจากนี้การเติมซิงก์ออกไซด์ยังเพิ่มความไวในการตอบสนองต่อสารเคมีประเภทสารช่วยกระจายตัวชนิดประจุบวกและตัวทำละลายอินทรีย์ วัสดุเชิงประกอบที่เตรียมได้นี้สามารถนำไปใช้งานได้หลากหลาย เช่น วัสดุตรวจวัดโดยการเปลี่ยนสี ป้ายฉลาด หมึกพิมพ์/สี ที่เปลี่ยนสีได้เมื่ออุณหภูมิเปลี่ยนแปลงไป เป็นต้น

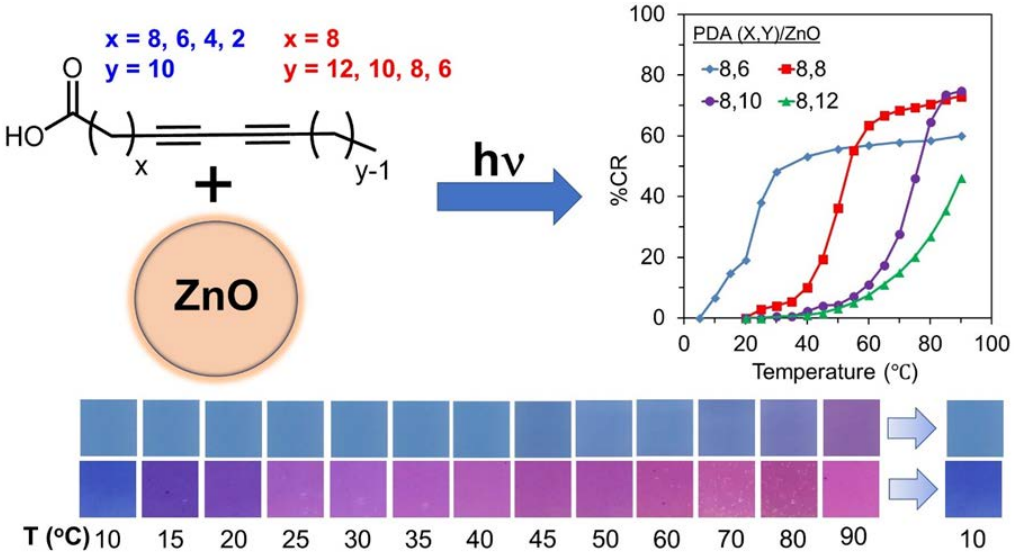

รูปที่ 1 วัสดุเชิงประกอบระดับนาโนเมตรพอลิไดแอเซทิลีน/ซิงก์ (II) ไอออน/ซิงก์ออกไซด์ ที่เตรียมจากมอนอเมอร์ที่มีความยาวสายโซ่อัลคิลที่แตกต่างกันเกิดการเปลี่ยนสีแบบผันกลับได้ต่ออุณหภูมิ และมีค่าอุณหภูมิการเปลี่ยนสีในช่วง 10-90 องศาเซลเซียส

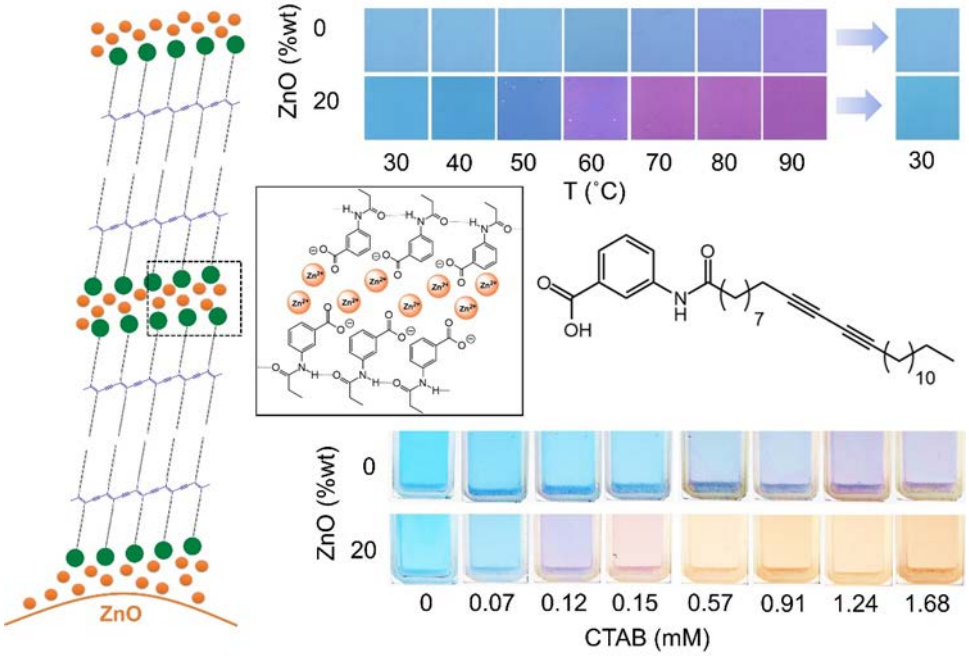

รูปที่ 2 พฤติกรรมการเปลี่ยนสีต่ออุณหภูมิและสารเคมีของวัสดุเชิงประกอบระดับนาโนเมตร poly(PCDA-mBzA)/ซิงก์ (II) ไอออน/ซิงก์ออกไซด์

ผลงานที่ได้รับการตีพิมพ์ในวารสารวิชาการระดับนานาชาติ

Colloids and Surfaces A 555 (2018) 27–36

Contents lists available at ScienceDirect

Colloids and Surfaces A

journal homepage: www.elsevier.com/locate/colsurfa

Controllable thermochromic and phase transition behaviors of polydiacetylene/zinc(II) ion/zinc oxide nanocomposites via photopolymerization: An insight into the molecular level

Ruttayapon Potai[a], Kunruethai Faisadcha[b], Rakchart Traiphol[c,d], Nisanart Traiphol[b,e,*]

[a] Division of Chemistry, Faculty of Science, Nakhon Phanom University, Nakhon Phanom 48000, Thailand
[b] Laboratory of Advanced Chromic Materials, Department of Materials Science, Faculty of Science, Chulalongkorn University, Bangkok 10330, Thailand
[c] Laboratory of Advanced Polymers and Nanomaterials, Center for Materials Science and Innovation, Faculty of Science, Mahidol University at Salaya, Phuttamonthon 4 Road, Nakhon Pathom 73170, Thailand
[d] NANOTEC-MU Excellence Center of Intelligent Materials and Systems, Faculty of Science, Mahidol University, Rama 6 Road, Ratchathewi, Bangkok 10400, Thailand
[e] Center of Excellence on Petrochemical and Materials Technology, Chulalongkorn University, Bangkok 10330, Thailand

GRAPHICAL ABSTRACT

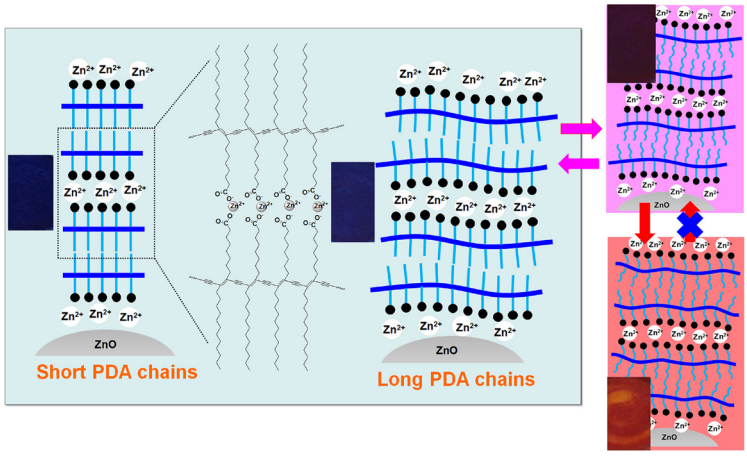

ARTICLE INFO

Keywords:
Polydiacetylene
Nanocomposite
Thermochromism
Chain length
Phase transition

ABSTRACT

Reversible thermochromic polydiacetylene/zinc(II) ion/zinc oxide (PDA/Zn^{2+}/ZnO) nanocomposites with a wide range of color-transition temperature have been prepared by varying photopolymerization time. This contribution presents our continuation study investigating into the molecular origins of this behavior. Infrared spectroscopy is utilized to investigate interfacial interactions of the systems while the conformation of PDA conjugated backbone is probed by Raman spectroscopy. X-ray diffraction explores molecular packing within the nanocomposites. We have found that the increase of photopolymerization time induces the relaxation of PDA backbone into a newly observed state indicated by systematic growth of new vibrational modes of C≡C and C═C bonds. This relaxation process results in the decrease of reversible blue-to-purple color-transition temperature. In contrast, the increase of backbone length with photopolymerization time causes an opposite trend of the irreversible purple-to-red color transition observed at relatively high temperature region. Differential scanning calorimetry detects two distinct phase transitions corresponding to the melting of alkyl side chains and

* Corresponding author at: Laboratory of Advanced Chromic Materials, Department of Materials Science, Faculty of Science, Chulalongkorn University, Bangkok 10330, Thailand.
E-mail address: Nisanart.T@chula.ac.th (N. Traiphol).

https://doi.org/10.1016/j.colsurfa.2018.06.058
Received 7 March 2018; Received in revised form 20 June 2018; Accepted 20 June 2018
Available online 21 June 2018
0927-7757/

rigid backbone. These melting temperatures vary with photopolymerization time consistent with the variation of color-transition temperature.

1. Introduction

Polydiacetylenes (PDAs) are known to exhibit a color transition when exposed to various external stimuli such as heat, chemicals, biomolecules, UV light and electricity [1–17]. The color transition, normally from blue to red, occurs rapidly and is easily perceived by naked eyes, rendering PDA-based materials potential candidates for various applications such as 2D and 3D temperature sensors [2], sensors for volatile organic compounds [3,4], sensors for biomolecules [7,10] and a sensor for hydrogen peroxide [15]. The as-prepared PDAs usually present blue phase and are not fluorescent [18]. The blue-to-red color transition of PDAs generally involves segmental rearrangement within PDA assemblies causing the decrease of conjugation length [19–21]. The red-phase PDAs become fluorescent with quantum yield of about 0.02.

Microscopic mechanism of the color transition of PDA has been investigated by utilizing various techniques. Early works on urethane-substituted PDAs illustrated that the color transition was dominated by the change of backbone conformation [22,23]. When the systems were perturbed, the inter- and intrachain interactions were weaken. This allowed segmental rearrangement within the PDA assemblies, affecting the conjugation length of systems. Later works on the PDAs constituting carboxylic head group observed the change of molecular packing during the color-transition process [19–21,24]. Atkinson et al. reported that the color transition of PDA prepared from 10,12-pentacosadiynoic acid (PCDA) was related to the change from the orthorhombic to triclinic structure [24]. Lifshitz et al. observed the decrease of spacing between PDA backbones and the rearrangement of side chains during the color transition [20]. Fujimori et al. also detected the shrinkage of unit cell [21]. Our group utilized nuclear magnetic resonance spectroscopy to follow the molecular dynamics of each segment within PDA chain during the color transition [16]. These previous studies indicate that the segmental rearrangement plays an important role on the mechanism of color transition.

The color-transition properties of PDAs prepared from commercially available monomers such as PCDA are generally irreversible, limiting their utilization in various applications [14,16,25,26]. Many research groups have demonstrated that reversible color transition can be achieved by enhancing the interactions within the PDA assemblies via structural modification [17,27–33] or incorporating foreign materials [1,2,5,14,19,26,34–47]. For example, the PDA functionalized with hydrazide head group exhibits reversible color transition under acid-base treatments [28]. The azobenzene-substituted PDA exhibits reversible thermochromism due to the enhanced intermolecular π-π interaction [29]. The nanocomposites of PDA/polymers [5,14,26], PDA/cations [1,2,9,34–37] and PDA/metal oxides [38,35–47] can provide reversible thermochromism as well.

Our group has achieved reversible thermochromism of PDAs by incorporating zinc oxide (ZnO) nanoparticles [38–45]. Our latest study revealed the presence of Zn^{2+} ions, releasing from ZnO nanoparticles during the preparation process [44]. These Zn^{2+} ions intercalated between PDA layers and interacted with the carboxylate head groups while the ZnO nanoparticles provided anchoring sites. The PDA/Zn^{2+}/ZnO nanocomposites possesses rather strong inter- and intramolecular interactions, making the system thermochromic reversible [38,39] and highly stable in various organic solvents [42]. The presence of ZnO nanoparticles also allows the colorimetric response to both acids and bases, which extends the utilization as a chemical sensor [40,43,45]. Recently, we have found a simple route for controlling the color-transition temperature of PDA/Zn^{2+}/ZnO nanocomposites. The increase of photopolymerization time caused systematic variation of the color-transition temperature [41]. In this contribution, we present our continuation work, investigating into the molecular level of the color-transition behaviors of PDA/Zn^{2+}/ZnO nanocomposites obtained by varying photopolymerization time.

2. Materials and methods

The diacetylene (DA) monomers used in this study, 5,7-hexadecadiynoic acid (HDDA), 10,12-tricosadiyoic acid (TCDA) and 10,12-pentacosadiynoic acid (PCDA) were commercially available at Fluka. The ZnO nanoparticles were purchased from Nano Materials Technology (Thailand). The diameter of ZnO nanoparticles revealed by transmission electron microscopy (TEM, Tecnai 12, D291) is ranged from 20 to 160 nm (Fig.1a) with the averaged diameter of 65 nm. The PDA/Zn^{2+}/ZnO nanocomposites were prepared using a method described in our previous study [41]. Briefly, the DA monomer and ZnO nanoparticles were co-dispersed in water assisted by an ultrasonication. The concentration of DA monomer was 0.5 mM while the ZnO/DA ratio was 10 wt%. The DA/ZnO aqueous suspension was incubated at ~4 °C for ~24 h, followed by UV light irradiation ($\lambda \sim 254$ nm, 10 W). The photopolymerization time was increased from 5 to 120 min, yielding a blue suspension of PDA/Zn^{2+}/ZnO nanocomposite. The suspension was filtered through 1.2 μm pore size cellulose acetate membrane. Thin films were prepared by drop-casting the nanocomposite suspension onto glass slides and drying in a vacuum oven overnight. Particle size of

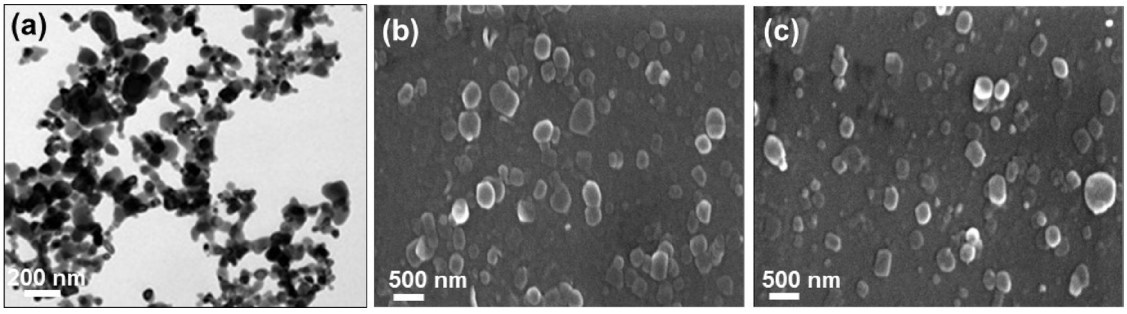

Fig. 1. (a) TEM image of ZnO nanoparticles. SEM images of (b) poly(PCDA)/Zn^{2+}/ZnO5m and poly(PCDA)/Zn^{2+}/ZnO60m prepared by using photopolymerization time of 5 and 60 min, respectively.

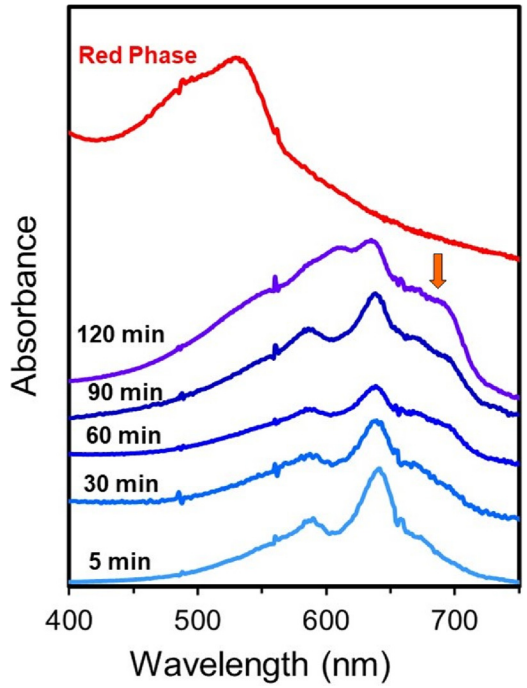

Fig. 2. Absorption spectra of poly(PCDA)/Zn^{2+}/ZnO nanocomposite films measured at room temperature. The samples were prepared by varying photopolymerization time from 5 to 120 min. The arrow indicates the growth of absorption peak at about 690 nm. An absorption spectrum of the red phase is included for comparison. (For interpretation of the references to color in this figure legend, the reader is referred to the web version of this article).

the nanocomposites investigated by scanning electron microscopy (SEM, JOEL, JSM-6400) is ranged from 50 to 350 nm (Fig. 1b and c). The increase of photopolymerization time hardly affected morphology and size of the nanocomposites.

Absorption spectra of the poly(PCDA)/Zn^{2+}/ZnO nanocomposite films were recorded using Analytica Specord S100 UV/Vis spectrometer. The samples were annealed in a vacuum oven at different temperatures for 5 min. Thermocouple was attached to the samples using thermal conducting glue to measure their temperature. The FT-IR spectra of poly(PCDA)/Zn^{2+}/ZnO nanocomposite were obtained using a Perkin Elmer Spectrum GX spectrometer. Raman spectra of the dried samples were measured using FT-Raman spectrometer (PerkinElmer Spectrum GX) with a 1064 nm laser (Nd:YAG) as an excitation source. Thin film samples of poly(PCDA)/Zn^{2+}/ZnO nanocomposite were investigated using X-ray diffractometer (Bruker AXS Model D8 Discover λ(Cu-K_α) = 1.54 Å) for structural analysis. Thermal properties of PDA/Zn^{2+}/ZnO nanocomposites were explored by the differential scanning calorimetry (DSC, Mettler Toledo DSC1) and thermogravimetric analyses (TGA, Mettler Toledo TGA/DSC1) under nitrogen atmosphere. The DSC measurements were conducted at the heating/cooling rate of 5 °C/min. The TGA measurements were carried out in the temperature range of 25–800 °C using the heating rate of 10 °C/min.

3. Results and discussion

3.1. Thermochromism of PDA/Zn^{2+}/ZnO nanocomposite films

In our previous studies, we explored thermochromic properties of poly(PCDA)/Zn^{2+}/ZnO nanocomposite dispersed in aqueous suspension and polymeric matrices [41,42]. The poly(PCDA)/Zn^{2+}/ZnO nanocomposite exhibited a two-step color transition upon increasing temperature, involving reversible blue-to-purple and then irreversible purple-to-red. The color-transition temperature of these two processes can be tuned by varying photopolymerization time [41]. In this contribution, we take a step forward to investigate molecular origins of this thermochromic behavior.

Fig. 2 illustrates the absorption spectra of poly(PCDA)/Zn^{2+}/ZnO films measured upon increasing photopolymerization time from 5 to 120 min. At photopolymerization time of 5 min, the absorption spectrum constitutes of a peak at 640 nm and a vibronic shoulder at 590 nm, corresponding to the presence of blue phase. The increase of photopolymerization time results in the growth of a broad shoulder at relatively high wavelength region. At 90 min, two peaks at about 670 and 690 nm are detected. The observation of these new red-shift peaks reflects the formation of new electronic species with relatively long conjugation length. We believe that the increase of photopolymerization time affects the backbone length of poly(PCDA) and hence its electronic properties. The further increase of photopolymerization time to 120 min causes the growth of a peak at 610 nm. Detailed analysis of the absorption spectra is available in our previous study [41]. It is worthwhile to note that our samples remain blue during this photopolymerization process. The absorption spectra do not show the growth of a peak at 540 nm, which is a signature of the red phase.

Fig. 3 presents the color-transition behaviors of poly(PCDA)/Zn^{2+}/ZnO films prepared by photopolymerizing for 5 and 30 min. The variation of absorption spectra indicates the color transition at different temperature regions. At room temperature, the samples are in blue phase with an absorption peak at 640 nm. Upon increasing temperature, the nanocomposite films change color at different temperatures, depending on the photopolymerization time. For poly(PCDA)/Zn^{2+}/ZnO5m polymerized for 5 min, the reversible blue-to-purple color transition is detected at about 90 °C where the λ_{max} of absorption spectrum shifts to 585 nm (Fig. 3c). Increasing temperature to 110 °C causes the shift of λ_{max} to about 535 nm corresponding to the purple-to-red color transition.

The increase of photopolymerization time to 30 min significantly affects the thermochromic properties of the nanocomposite film. The blue-to-purple color-transition temperature of poly(PCDA)/Zn^{2+}/ZnO30m drops to about 70 °C where the λ_{max} of absorption spectrum shifts to 590 nm. In contrast, the purple-to-red color transition temperature is detected at about 150 °C, which is higher than that of the poly(PCDA)/Zn^{2+}/ZnO5m (Fig. 3c). Therefore, the increase of photopolymerization time causes the decrease of blue-to-purple color-transition temperature while the purple-to-red one shows an opposite trend. The two-step color transition is similar to the thermochromic properties of poly(PCDA)-Na and poly(PCDA)-Zn complexes [19,36,48]. However, the variation of color-transition temperature upon increasing the photopolymerization time has never been reported in these systems.

3.2. Interfacial interaction, backbone conformation and molecular packing

In general, the color-transition temperature of pure PDAs can be controlled by varying side chain structure, which in turn affects the strength of interactions within the assemblies. For example, the decrease of alkyl side chain length of PDAs results in systematic decrease of color-transition temperature [26,39]. What are the molecular origins that cause the variation of color-transition temperature in the system of poly(PCDA)/Zn^{2+}/ZnO nanocomposite? To answer this question, we use infrared spectroscopy to characterize the conformational change of alkyl side chains and the interfacial interactions between poly(PCDA) head groups and ZnO nanoparticle. Raman spectroscopy is utilized to investigate conformational change of poly(PCDA) conjugated backbone upon increasing photopolymerization time.

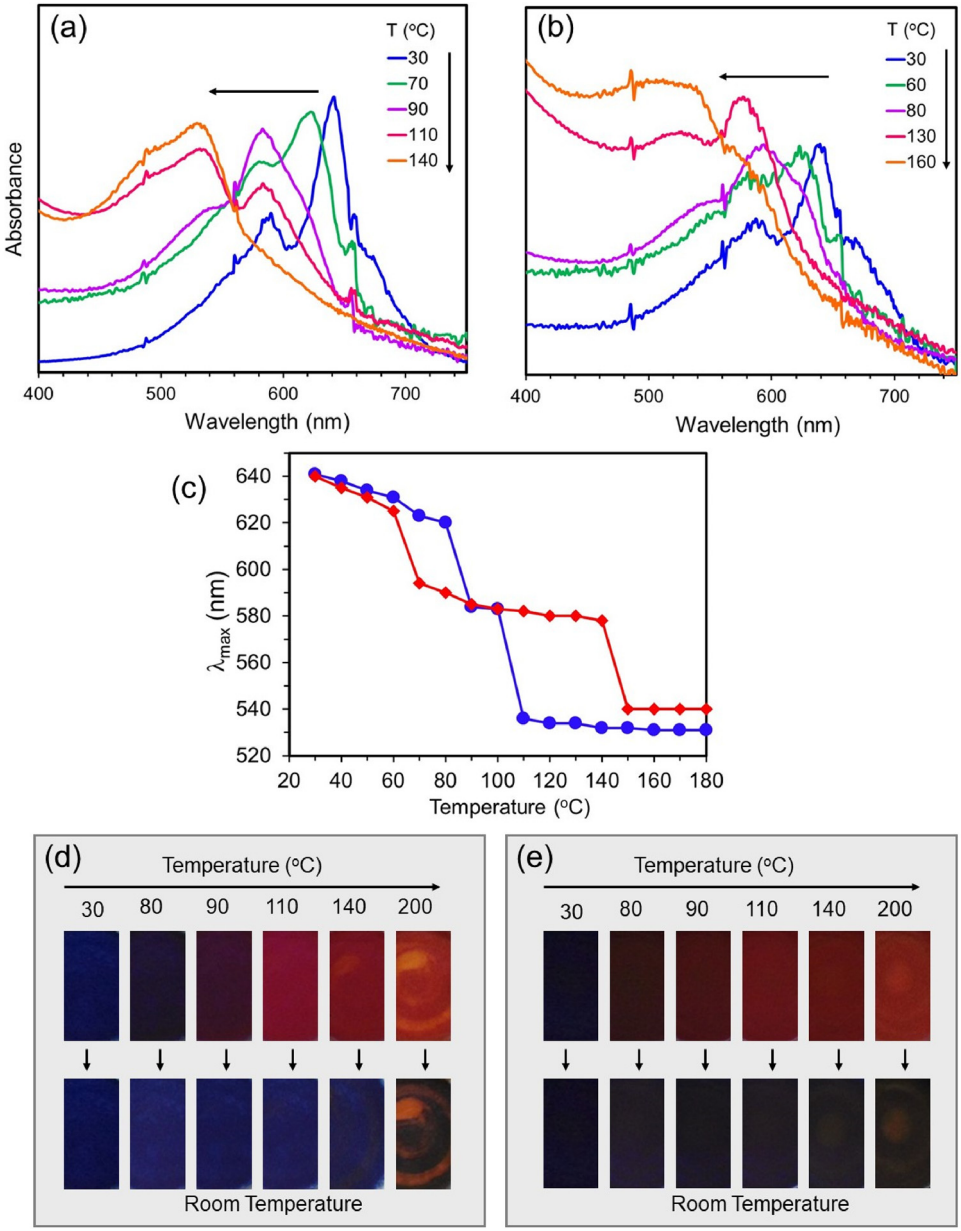

Fig. 3. Absorption spectra and photographs of poly(PCDA)/Zn^{2+}/ZnO nanocomposite films obtained at different temperatures, (a,d) poly(PCDA)/Zn^{2+}/ZnO5m and (b,e) poly(PCDA)/Zn^{2+}/ZnO30m. (c) Plots of λ_{max} versus temperature of (●, blue) poly(PCDA)/Zn^{2+}/ZnO5m and (♦, red) poly(PCDA)/Zn^{2+}/ZnO30m. (For interpretation of the references to color in this figure legend, the reader is referred to the web version of this article).

Fig. 4a illustrates FT-IR spectra of the poly(PCDA)/Zn^{2+}/ZnO30 m measured at room temperature after being annealed at different temperatures. The vibrational bands at 2849 and 2918 cm^{-1} of blue-phase nanocomposite are assigned to the $\nu_s(CH_2)$ and $\nu_{as}(CH_2)$ stretching vibrations of alkyl side chains, respectively. These bands indicate all-trans conformation of the alkyl side chains [48–51]. The band at 1460 cm^{-1} is assigned to the methylene scissoring, $\delta(CH_2)$. The strong ionic interaction between head group of poly(PCDA) and Zn^{2+}/ZnO nanoparticles is indicated by the peaks at 1540 and 1398 cm^{-1} corresponding to $\nu_{as}(COO^-)$ and $\nu_s(COO^-)$ stretching vibrations of carboxylate anion, respectively (Fig. 4c) [44,48]. We note that a small peak at 1725 cm^{-1} indicates the presence of some carboxylic head groups.

The annealing of nanocomposite at 100 °C for 5 min induces the blue-to-purple color transition, which is a reversible process. The FT-IR pattern measured upon cooling to room temperature remains unchanged indicating that the molecular arrangement of alkyl side chains and head group can be restored to the original state. The increase of annealing temperature to 200 °C causes the purple-to-red color transition. The color transition is partially irreversible at this state. We observe a line broadening of the peak at 1540 cm^{-1}. The increase of annealing time at 200 °C–30 min causes a complete irreversible transition to the red phase. A growth of broad shoulder at about 1600 cm^{-1} is clearly detected. This observation indicates that the local environment of carbonyl group at the interfacial region has changed. This is attributed to the rearrangement of carboxylate head group, causing the variation of its vibrational spring constant. It is worthwhile to note that the vibrational bands at 2849 and 2918 cm^{-1} remain at the same position corresponding to all-trans conformation of alkyl side chains in the red phase. The increase of photopolymerization time from 5 to 120 min hardly affects the FT-IR pattern as shown in Fig. 4b. This observation indicates that the molecular arrangement of alkyl side chains and carboxylate head group does not change with the increasing of photopolymerization time.

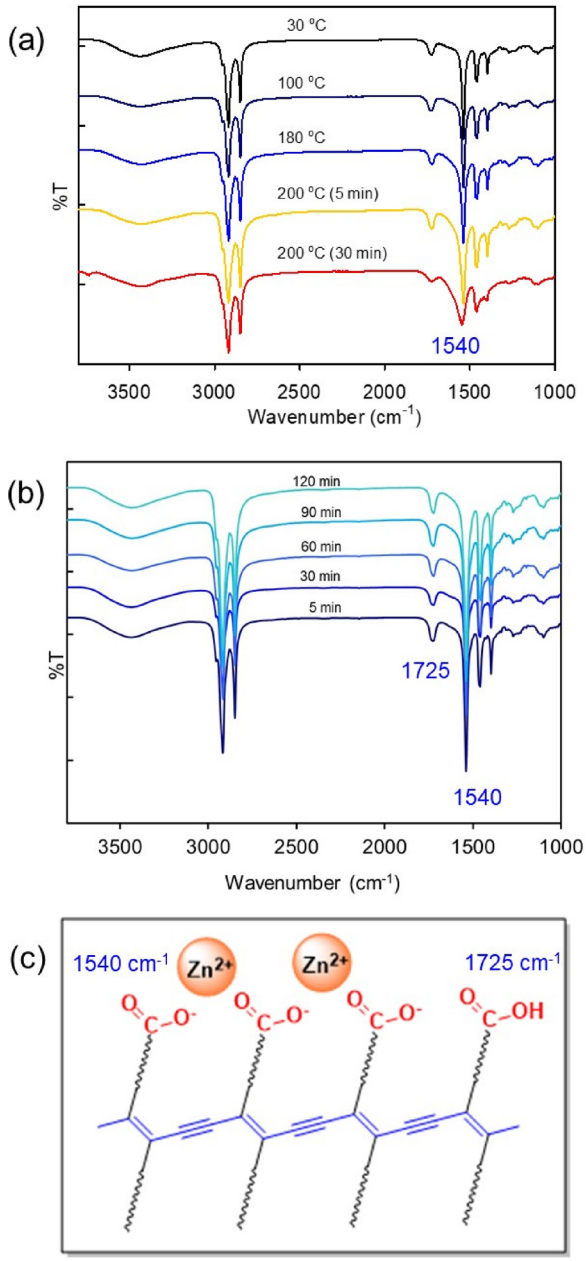

Fig. 4. (a) FT-IR spectra measured at room temperature of poly(PCDA)/Zn^{2+}/ZnO30m nanocomposite after being annealed at different temperatures. (b) FT-IR spectra measured at room temperature of poly(PCDA)/Zn^{2+}/ZnO nanocomposite prepared by varying photopolymerization time. (c) Interaction between carboxylate head group and Zn^{2+} ion within the nanocomposite.

Interestingly, we detect a systematic variation of molecular arrangement of PDA conjugated backbone. The Raman spectrum of pure poly(PCDA) in blue phase are known to exhibit two major peaks at 2080 and 1451 cm^{-1} which can be assigned to the C≡C and C═C stretching modes of the PDA conjugated backbone, respectively [14,36,46]. These peaks shift to 2116 and 1511 cm^{-1} in the red phase attributed to the relaxation of poly(PCDA) backbone into new local environment. This is consistent with previous studies that observe the shrinkage of unit cell during the blue-to-red color transition of poly (PCDA) [20,21]. The Raman spectra of poly(PCDA)/Zn^{2+}/ZnO nanocomposite are shown in Fig. 5a. The poly(PCDA)/Zn^{2+}/ZnO5m polymerized for 5 min exhibits C≡C and C═C stretching modes at 2076 and 1450 cm^{-1}, respectively. When the photopolymerization time is increased to 30 min, the C≡C and C═C stretching bands split into two peaks. New bands are detected at 2094 and 1474 cm^{-1}. These new bands shift to 2097 and 1483 cm^{-1}, respectively, upon increasing the photopolymerization time to 120 min (Table 1s in supporting information). The intensity ratios at 1475/1450 cm^{-1} and 2097/2075 cm^{-1} systematically increase with the photopolymerization time (Fig.1s in Supporting information). Our observation indicates that the rearrangement of poly(PCDA) conjugated backbone into new local environment takes place upon increasing the photopolymerization time (Fig. 5b).

The presence of two distinct peaks for the C≡C and C═C bonds indicates the co-existence of two species. The change of intensity ratio corresponds to the variation of mole fraction of these species. Since the nanocomposites in this study exhibit rather broad size distribution as shown in Fig. 1b, we believe that the poly(PCDA) conjugated backbone relaxes to new local environment at different states of photopolymerization depending on the size of assemblies. It is important to note that the Raman signal of C≡C bond in the PCDA monomer locates at 2101 cm^{-1} [52]. However, previous studies have shown that the intensity of this peak is extremely weak [52,53]. Therefore, the presence of some residual PCDA monomer in this system has a minor effect on the pattern of Raman spectra in this study.

Previous studies of poly(PCDA)/ZnO nanocomposite [46] and poly (PCDA)-Na [36] observed the shift of C≡C and C═C stretching bands to higher wavenumbers upon increasing the temperature to 100 °C. The blue shift indicates a relaxation of poly(PCDA) conjugated backbone, resulting in the formation of purple phase. In this study, however, all samples still exhibit a blue color at room temperature. The measurements of UV/Vis absorption spectra detect the growth of a broad peak at 690 nm, reflecting the formation of new electronic species with relatively long conjugation length (Fig. 2). We suggest that the increase of poly(PCDA) backbone length upon increasing photopolymerization time reduces the chain rigidity, which in turn allows partial relaxation into new local environment (Fig.5b). Previous studies have shown that the increase of photopolymerization time of pure PDAs causes the shrinkage of unit cell and the rearrangement of alkyl side chains [20,21]. Similar structural transition possibly takes place in our system. We believe that the relaxation of poly(PCDA) backbone is a major factor that leads to the systematic variation of color-transition temperature.

It is worthwhile to note that previous studies of pure PDA films normally observe the blue-to-red color transition upon increasing photopolymerization time [52–55]. In our system, however, strong ionic interactions between the carboxylate head group and Zn^{2+}/ZnO resist the blue-to-red color transition. The nanocomposites remain in the blue phase when the photopolymerization time is increased to 120 min as indicated by the UV/Vis absorption and Raman spectra in Figs. 2 and 5, respectively. Our result is parallel to the previous study of PDA/Zn^{2+} system [54].

We also utilize X-ray diffraction (XRD) to explore the molecular packing of poly(PCDA)/Zn^{2+}/ZnO nanocomposite. Fig. 6a illustrates XRD patterns of the nanocomposite prepared with different photopolymerization times. The pattern is consistent with those of the poly (PCDA)-Zn and poly(PCDA)-Na complexes observed in previous studies, corresponding to lamellar structure [1,2,19]. The value of interlamellar d-spacing calculated from these diffraction peaks is about 5.4 nm (Fig. 6b). Since the d-spacing of pure poly(PCDA) is about 4.5 nm, the increase of d-spacing value in this system indicates the intercalation of Zn^{2+} ions into the bilayer structure [1,2]. Detailed investigation of the poly(PCDA)/Zn^{2+}/ZnO nanocomposite structure is given in our previous report [44]. Although Raman spectroscopy detects the relaxation of poly(PCDA) conjugated backbone upon increasing

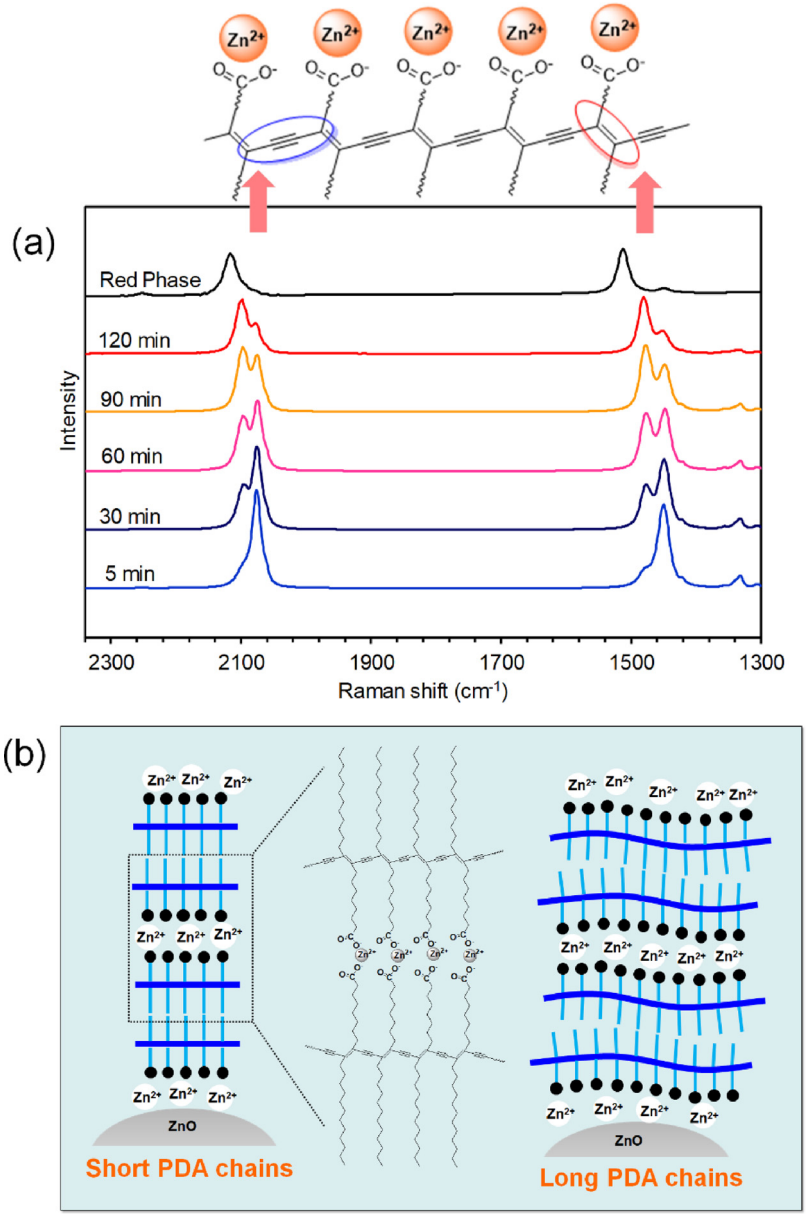

Fig. 5. (a) Raman spectra of poly(PCDA)/Zn^{2+}/ZnO nanocomposite obtained from different photopolymerization times. Spectrum of red-phase poly(PCDA) is included for comparison. (b) Proposed model for the molecular arrangement of short and long PDA chains within the nanocomposites. (For interpretation of the references to color in this figure legend, the reader is referred to the web version of this article).

photopolymerization time, the lamellar structure of nanocomposite is hardly affected. Fig. 6a shows that the nanocomposite prepared by increasing photopolymerization time from 5 to 120 min provide XRD peaks at approximately the same position. This observation indicates that the relaxation of poly(PCDA) backbone probably occurs in the length scale that cannot be detected by our XRD measurements. Our result is parallel with the previous study of poly(PCDA)-Na system, in which, the relaxation of backbone causing the blue-to-purple color transition, hardly affects the d-spacing of lamellar structure [19].

3.3. Thermal analysis of PDA/Zn^{2+}/ZnO nanocomposites

In this section, we utilize DSC to investigate the nature of phase transition relating to the color transition of PDA/Zn^{2+}/ZnO nanocomposites. The phase-transition temperatures obtained from two heating/cooling cycles of various pure PDAs and PDA/Zn^{2+}/ZnO nanocomposites are summarized in Table 1. For a comparison purpose, we first evaluate the results obtained from the systems of pure poly(PCDA), poly(TCDA) and poly(HDDA). The 1st heating cycle of pure poly(PCDA) detects a single endothermic peak at 60 °C. Since this melting transition is close to that of the PCDA monomer, it is assigned to the melting of alkyl side chains [51]. The phase transition of poly(PCDA) is closely related to its color-transition temperature. The cooling cycle reveals an exothermic peak at 43 °C, indicating the recrystallization of alkyl side chains. However, the poly(PCDA) remains in red phase. The X-ray scattering results from previous studies have shown that the blue and red phases are actually in different crystalline states at room temperature [19–21]. Our earlier study via XRD also observed lamellar

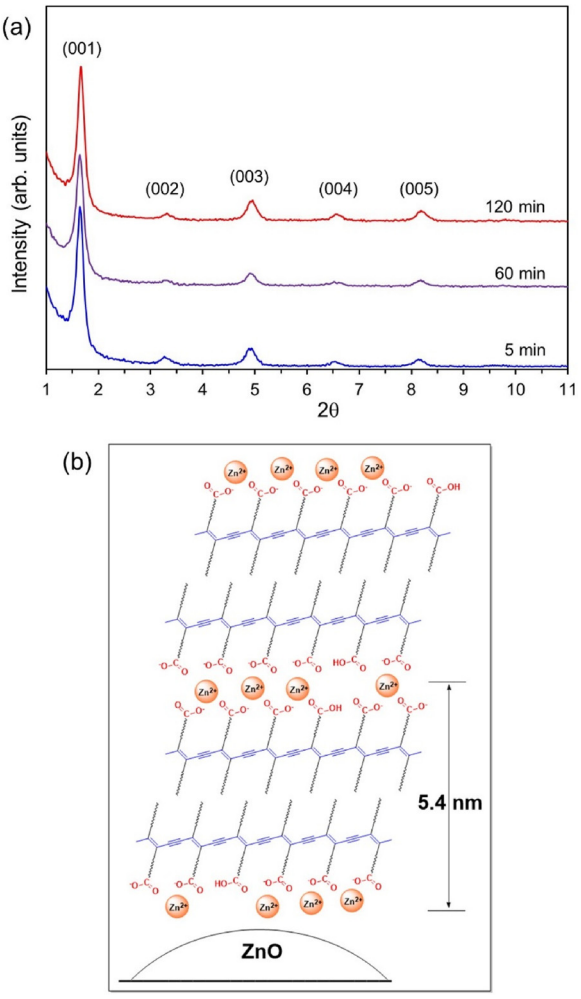

Fig. 6. (a) XRD patterns of poly(PCDA)/Zn^{2+}/ZnO nanocomposite obtained from different photopolymerization times. (b) Model for the molecular arrangement within the nanocomposites.

Table 1
Transition temperature of pure PDAs and PDA/Zn^{2+}/ZnO nanocomposites obtained from different photopolymerization times.

Samples	Peak transition temperature (°C)			
	1st heating	1st cooling	2nd heating	2nd cooling
Poly(HDDA)	45	25	42	–
Poly(TCDA)	52	37	50	35
Poly(PCDA)	60	43	58	44
Poly(PCDA)/Zn^{2+}/ZnO1m	86, 151	89	103	89
Poly(PCDA)/Zn^{2+}/ZnO5m	80, 162	84	100	83
Poly(PCDA)/Zn^{2+}/ZnO30m	62, 169	78	97	77
Poly(PCDA)/Zn^{2+}/ZnO60m	62, 177	76	96	75
Poly(PCDA)/Zn^{2+}/ZnO120m	54, 187	70	92	70
Poly(TCDA)/Zn^{2+}/ZnO30m	57, 113	99	110	97
Poly(HDDA)/Zn^{2+}/ZnO30m	39, 151	44	45	45

structure for both blue and red phases with slightly different values of interlamellar d-spacing [44]. The 2nd heating cycle of red phase shows a melting peak at 58 °C, which is quite close to that of the blue phase. The investigation of pure poly(TCDA) and poly(HDDA) provides consistent results. We note that the melting transition of poly(TCDA) and poly(HDDA) shifts to the lower temperature due to the shortening of alkyl side chains. Our results indicate that the melting and crystallization of pure PDAs mainly involve the alkyl side chains.

The system of PDA/Zn^{2+}/ZnO nanocomposites exhibits rather different phase transition behaviors. Fig. 7 illustrates the DSC thermogram of poly(PCDA)/Zn^{2+}/ZnO nanocomposite prepared with various photopolymerization times. Interestingly, the incorporation of ZnO nanoparticles into poly(PCDA) assembly results in two distinct melting points. The 1st heating cycle of poly(PCDA)/Zn^{2+}/ZnO5m reveals two melting peaks at 80 and 162 °C (Table 1). These phase transitions are consistent with the two-step color transition discussed in the first section. The 1st melting is related to the reversible blue-to-purple color transition. It is assigned to the melting of alkyl side chains. Higher melting temperature of the alkyl side chains for the nanocomposite compared to that of the pure poly(PCDA) is attributed to the presence of strong interfacial interactions. Additionally, the enhanced interactions provide reversible phase transition as revealed by DSC (Fig. 2s in Supporting information).

The further increase of temperature results in the 2nd melting transition that does not exist in the system of pure poly(PCDA). The investigation of poly(TCDA)/Zn^{2+}/ZnO and poly(HDDA)/Zn^{2+}/ZnO nanocomposites reveals consistent results as shown in Table 1. Our observation suggests that the presence of ZnO nanoparticles significantly promotes the organization of poly(PCDA) chains. A previous study on the system of poly(PCDA)-Na also detected two distinct phase transitions by DSC [19]. Their temperature-dependent XRD measurements indicated that the poly(PCDA)-Na maintained a lamellar structure above the 1st melting temperature. The lateral ordering of alkyl side chains, however, was reduced. The poly(PCDA)-Na became completely amorphous during the 2nd phase transition. According to this study, the 2nd phase transition of poly(PCDA)/Zn^{2+}/ZnO nanocomposite is attributed to the melting of rigid conjugated backbone. This melting process is related to the irreversible purple-to-red color transition. Our result is parallel to the previous study of comb-like polymers where two phase transitions are related to the melting of alkyl side chains and rigid backbone [56]. It is worthwhile to point out that DSC does not detect the melting of backbone in the system of pure poly (PCDA). This observation indicates that the ordering of poly(PCDA) backbone is drastically increased within the nanocomposites due to the presence of strong interfacial interactions.

The melting points of alkyl side chains and rigid backbone of poly (PCDA)/Zn^{2+}/ZnO nanocomposite are strongly influenced by the photopolymerization time. The 1st melting point shifts to 62 and 54 °C when the photopolymerizatime is increased to 30 and 120 min, respectively. The 2nd melting point, on the other hand, shows the opposite trend. It increases to 169 and 187 °C. The increase of photopolymerization time is expected to cause the increase of backbone length, which in turn induces partial relaxation as revealed by Raman spectroscopy (Fig. 5). We propose that the magnitude of segmental relaxation is a major factor dictating the melting point of alkyl side chains. The higher magnitude of segmental relaxation leads to the lower melting point, which relates to the decrease in reversible blue-to-purple color-transition temperature of the nanocomposite. The 2nd melting point is related to the length of poly (PCDA) backbone. When the backbone of poly(PCDA) becomes longer upon increasing photopolymerization time, it requires higher temperature to melt its crystalline structure. This behavior has been observed in the system of comb-like polymers constituting rigid backbone and flexible side chains [56].

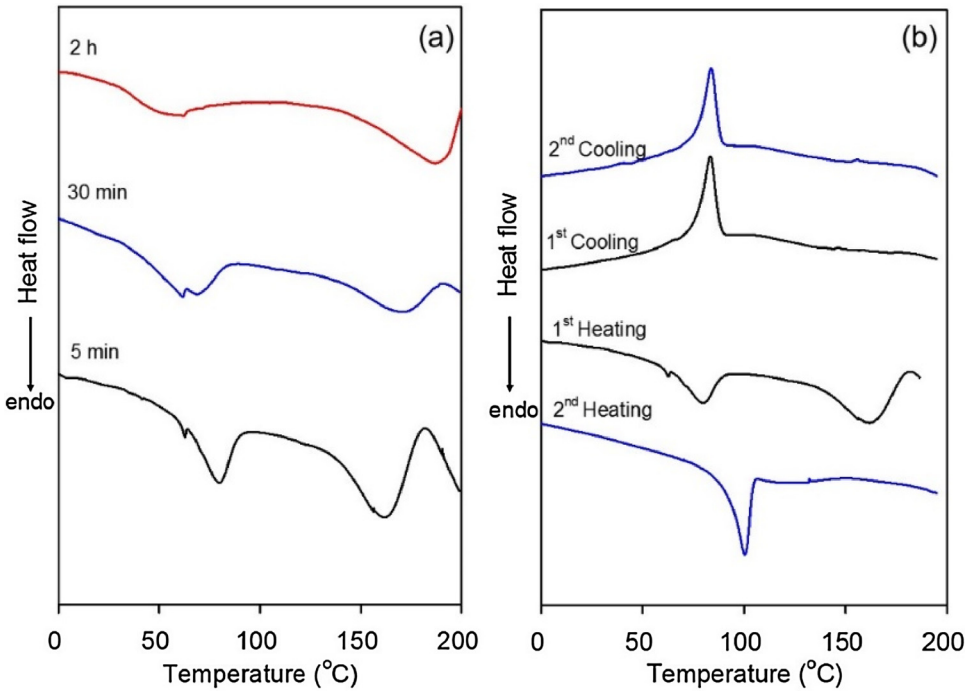

Fig. 7. (a) DSC curves of poly(PCDA)/Zn^{2+}/ZnO nanocomposite recorded from the 1st heating. (bottom) poly(PCDA)/Zn^{2+}/ZnO5m, (middle) poly(PCDA)/Zn^{2+}/ZnO30m and (top) poly(PCDA)/Zn^{2+}/ZnO120m. A small peak detected at about 62 °C is assigned to residual PCDA monomer. (b) DSC curves of poly(PCDA)/Zn^{2+}/ZnO5m obtained from two heating/cooling cycles.

The 1st cooling cycle of poly(PCDA)/Zn^{2+}/ZnO5m presents a single recrystallization peak at 84 °C, which is slightly higher than the melting temperature of alkyl side chains (Fig. 7b). We do not detect any recrystallization process at high temperature region. This observation indicates that the original packing structure of poly(PCDA) backbone is not restored upon cooling to room temperature. This is consistent with the color of poly(PCDA)/Zn^{2+}/ZnO nanocomposite, which remains in the red phase. The alkyl side chains, on the other hand, recrystallize into the organized structure. Our XRD results in the previous study showed that the red phase of poly(PCDA)/Zn^{2+}/ZnO nanocomposite exhibited lamellar structure with interlamellar d-spacing greater than that of the original blue phase [44]. The 2nd heating cycle of poly(PCDA)/Zn^{2+}/ZnO5m exhibits a single melting peak at 100 °C. This transition temperature is much higher than the melting temperature of alkyl side chains observed in the 1st heating cycle. We believe that the poly(PCDA) backbone and alkyl side chains in the nanocomposite organize into densely packed structure in the red phase. Therefore, it requires higher temperature to melt the crystalline structure of the red phase. The 2nd cooling cycle presents recrystallization process similar to that of the 1st cooling cycle. Our hypothesis is parallel to the result of previous study, which detects the shrinkage of unit cell during the blue-to-red color transition of poly(PCDA) [20].

We also investigate the effects of molecular structure on thermal stability of pure PDAs and PDA/Zn^{2+}/ZnO nanocomposites (Fig. 3s in Supporting information). The pure PDAs tend to loose significant weight at relatively low temperature range, attributed to the presence of residual monomer. The peak degradation temperature is detected around 438–448 °C. The variation of alkyl side chain length slightly affects the degradation temperature. In the system of PDA/Zn^{2+}/ZnO nanocomposites, the temperature at 5% weight loss significantly increases. It is clearly observed in the system containing 20 wt% of ZnO nanoparticles. This result suggests that the presence of strong interfacial interaction facilitates the conversion of monomers into PDA chains. Our UV/Vis absorption measurement shows consistent results, demonstrating much higher amount of blue phase PDAs within the nanocomposites compared to the system of pure PDAs. The increase of PDA chain length obtained via the increase of photopolymerization time hardly affects the degradation temperature.

Our major finding of this study is summarized in Fig. 8. The molecular interactions within pure PDA assemblies involve hydrogen bonds between carboxylic head groups, π-π interaction of backbone and dispersion interaction of the alkyl side chains. When thermal energy overcomes the overall interactions, the melting of lamellar structure takes place. This process causes the rearrangement of conjugated backbone, resulting in the irreversible blue-to-red color transition (Fig. 8a). Although the alkyl side chains recrystallize upon cooling to room temperature, the original state of PDA conjugated backbone cannot be restored. The addition of ZnO nanoparticles introduces strong ionic interaction between carboxylate head groups of PDA and Zn^{2+}/ZnO surface, which in turn promotes the molecular ordering of conjugated backbone. This allows the melting of alkyl side chains and conjugated backbone to take place at different temperature ranges. The melting of alkyl side chains induces slight relaxation of conjugated backbone, relating to the reversible blue-to-purple color transition. The further increase of temperature results in the melting of conjugated backbone and hence induces the irreversible purple-to-red color transition. The backbone length of PDA increases with increasing photopolymerization time. In this system, partial relaxation of the molecular segments occurs within the nanocomposites. Therefore, it requires relatively low temperature to melt the alkyl side chains. The melting of conjugated backbone, on the other hand, shifts to higher temperature due to the increase of chain length.

4. Conclusion

This study demonstrates that the color/phase transition behaviors of PDA/Zn^{2+}/ZnO nanocomposites can be systematically controlled by utilizing molecular engineering approach. The increase of PDA backbone length via photopolymerization process induces partial segmental relaxation within the nanocomposites. Raman spectroscopy detects the formation of new state of PDA conjugated backbone. The magnitude of backbone relaxation, depending on photopolymerization time, dictates the reversible blue-to-purple color transition temperature. The increase of backbone length also affects the irreversible purple-to-red color transition detected at relatively high temperature. The DSC measurements reveal that these color transitions are closely related to the melting transition of alkyl side chains and PDA backbone. Our approach for controlling the color/phase transition behaviors of PDA-based

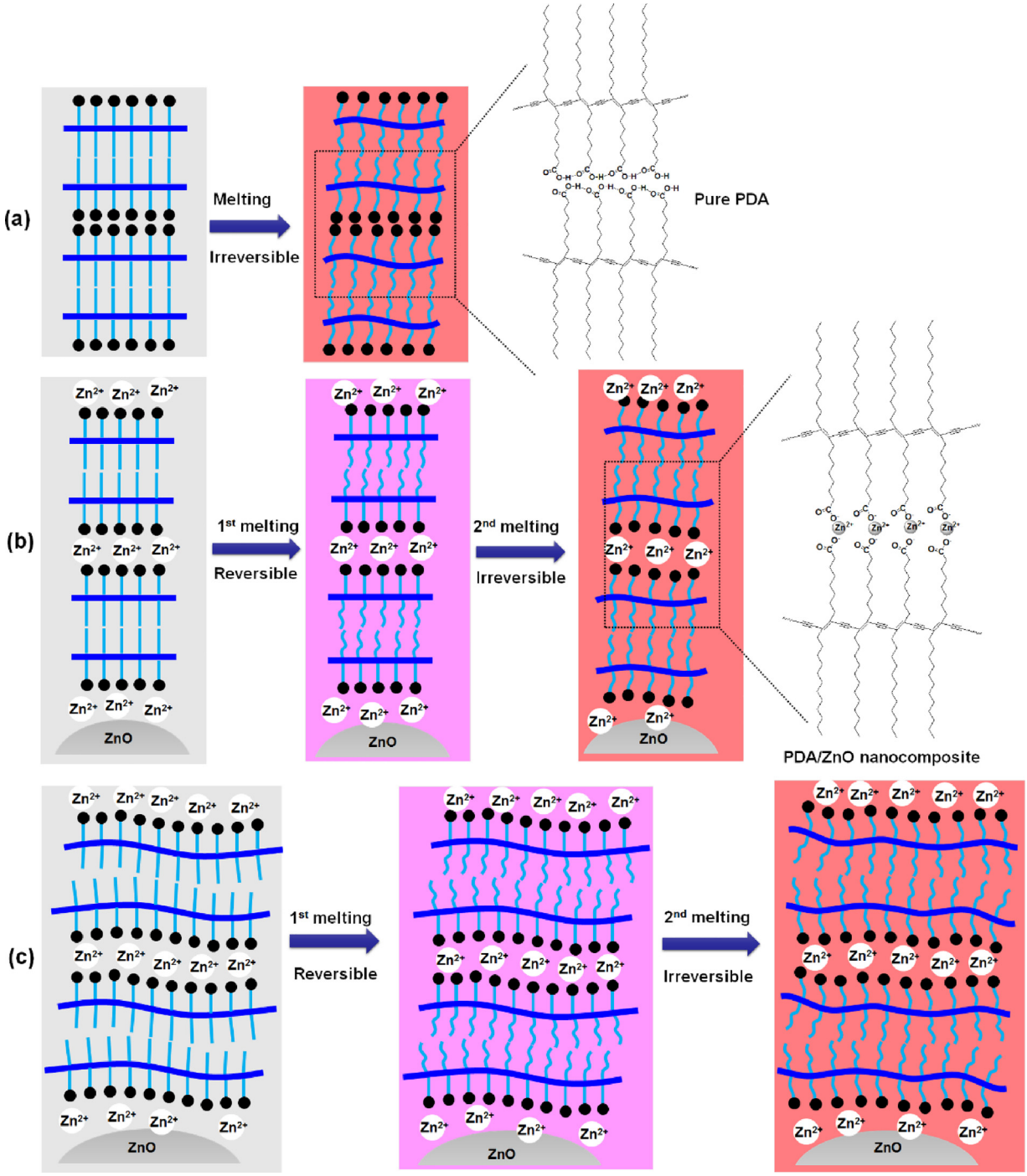

Fig. 8. Proposed models for phase/color transition behaviors upon increasing temperature of (a) pure PDAs (b, c) PDA/Zn^{2+}/ZnO nanocomposites prepared by short and long polymerization times, respectively.

materials is quite unique and never been observed in any other systems. Compared to the structural approach [27–33], our method is much simpler and allows systematic control over their color-transition properties. This approach could be utilized for improving the sensitivity of PDAs upon exposure to other stimuli such as solvents, acid/base and biomolecules. The topic is currently under investigation in our laboratories. Our study can provide a library of materials with controllable color-transition properties, extending their utilization in various applications.

Acknowledgements

This research has been supported by the Thailand Research Fund [RSA 5980020]. This work has been partially supported by the Nanotechnology Center (NANOTEC), Ministry of Science and Technology, Thailand, through its program of Center of Excellence Network.

Appendix A. Supplementary data

Supplementary material related to this article can be found, in the online version, at doi:https://doi.org/10.1016/j.colsurfa.2018.06.058.

References

[1] M. Takeuchi, H. Imai, Y. Oaki, Effects of the intercalation rate on the layered crystal structures and stimuli-responsive color-change properties of polydiacetylene, J. Mater. Chem. C 5 (2017) 8250–8255.

[2] M. Takeuchi, H. Imai, Y. Oaki, Real-time imaging of 2D and 3D temperature distribution: coating of metal-ion-intercalated organic layered composites with tunable stimuli-responsive properties, ACS Appl. Mater. Interfaces 9 (2017) 16546–16552.

[3] T. Wang, Y. Guo, P. Wan, X. Sun, H. Zhang, Z. Yua, X. Chen, A flexible transparent colorimetric wrist strap sensor, Nanoscale 9 (2017) 869–874.

[4] S. Dolai, S.K. Bhunia, S.S. Beglaryan, S. Kolusheva, L. Zeiri, R. Jelinek, Colorimetric polydiacetylene–aerogel detector for volatile organic compounds (VOCs), ACS Appl. Mater. Interfaces 9 (2017) 2891–2898.

[5] M.J. Shin, J.-D. Kim, Chromatic reversibility of multilayered polydiacetylene cast film, J. Ind. Eng. Chem. 35 (2016) 211–216.

[6] M.J. Shin, D.H. Byun, J.-D. Kim, Sensitivity limitation of the sensor fabricated with polydiacetylene, J. Ind. Eng. Chem. 23 (2015) 279–284.

[7] J.P. Rezende, G.M.D. Ferreira, G.M.D. Ferreira, L.H.M. Silva, H.S.M. Carmo, M.S. Pinto, A.C.S. Pires, Polydiacetylene/triblock copolymer nanosensor for the detection of native and free bovine serum albumin, Mater. Sci. Eng. C 70 (2017) 535–543.

[8] X. Sun, T. Chen, S. Huang, F. Cai, X. Chen, Z. Yang, L. Li, H. Cao, Y. Lu, H. Peng, UV-induced chromatism of polydiacetylenic assemblies, J. Phys. Chem. B 114 (2010) 2379–2382.

[9] X. You, X. Chen, G. Zou, W. Su, Q. Zhang, P. He, Colorimetric response of azobenzene-terminated polydiacetylene vesicles under thermal and photic stimuli, Chem. Phys. Lett. 482 (2009) 129–133.

[10] A. Kamphan, C. Gong, K. Maiti, S. Sur, R. Traiphol, D.P. Arya, Utilization of chromic polydiacetylene assemblies as a platform to probe specific binding between drug and RNA, RSC Adv. 7 (2017) 41435–41443.

[11] H. Peng, X. Sun, F. Cai, X. Chen, Y. Zhu, G. Liao, D. Chen, Q. Li, Y. Lu, Y. Zhu, Q. Jia, Electrochromatic carbon nanotube/polydiacetylene nanocomposite fibres, Nat. Nanotechnol. 4 (2009) 738–741.

[12] R. Varghese Hansen, L. Zhong, K.A. Khor, L. Zheng, J. Yang, Tuneable electrochromism in weavable carbon nanotube/polydiacetylene yarns, Carbon 106 (2016) 110–117.

[13] H. Wang, S. Han, Y. Hu, Z. Qi, C. Hu, Polydiacetylene-based periodic mesoporous organosilicas with colorimetric reversibility under multiple stimuli, Colloid Surf. A-Physicochem. Eng. Asp. 517 (2017) 84–95.

[14] A. Kamphan, N. Traiphol, R. Traiphol, Versatile route to prepare reversible thermochromic polydiacetylene nanocomposite using low molecular weight poly (vinylpyrrolidone), Colloid Surf. A-Physicochem. Eng. Asp. 497 (2016) 370–377.

[15] S. Lu, C. Jia, X. Duan, X. Zhang, F. Luo, Y. Han, H. Huang, Polydiacetylene vesicles for hydrogen peroxide detection, Colloid Surf. A-Physicochem. Eng. Asp. 443 (2014) 488–491.

[16] T. Pattanatornchai, N. Charoenthai, R. Traiphol, Influences of structural mismatch on morphology, phase transition temperature, segmental dynamics and color-transition behaviors of polydiacetylene vesicles, J. Colloid Interface Sci. 432 (2014) 176–181.

[17] C. Khanantong, N. Charoenthai, S. Wacharasindhu, M. Sukwattanasinitt, N. Traiphol, R. Traiphol, Influences of solvent media on chain organization and thermochromic behaviors of polydiacetylene assemblies prepared from monomer with symmetric alkyl tails, J. Ind. Eng. Chem. 58 (2018) 258–265.

[18] J. Olmsted III, M. Strand, Fluorescence of polymerized diacetylene bilayer films, J. Phys. Chem. 87 (1983) 4790–4792.

[19] J. Pang, L. Yang, B.F. McCaughey, H. Peng, H.S. Ashbaugh, C.J. Brinker, Y. Lu, Thermochromatism and structural evolution of metastable polydiacetylenic crystals, J. Phys. Chem. B 110 (2006) 7221–7225.

[20] Y. Lifshitz, Y. Golan, O. Konovalov, A. Berman, Structural transitions in polydiacetylene Langmuir films, Langmuir 25 (2009) 4469–4477.

[21] A. Fujimori, M. Ishitsuka, H. Nakahara, E. Ito, M. Hara, K. Kanai, Y. Ouchi, K. Seki, Formation of the newly greenish organized molecular film of long-chain diynoic acid derivatives by photopolymerization and its structural study using near-edge X-ray absorption fine structure (NEXAFS) spectroscopy, J. Phys. Chem. B 108 (2004) 13153–13162.

[22] R.R. Chance, G.N. Patel, J.D. Witt, Thermal effects on the optical properties of single crystals and solution-cast films of urethane substituted polydiacetylenes, J. Chem. Phys. 71 (1979) 206–211.

[23] R.R. Chance, Chromism in polydiacetylene solutions and crystals, Macromolecules 13 (1980) 396–398.

[24] M. Wenzel, G.H. Atkinson, Chromatic properties of polydiacetylene films, J. Am. Chem. Soc. 111 (1989) 6123–6127.

[25] A. Kamphan, N. Charoenthai, R. Traiphol, Fine tuning the colorimetric response to thermal and chemical stimuli of polydiacetylene vesicles by using various alcohols as additives, Colloid Surf. A-Physicochem. Eng. Asp. 489 (2016) 103–112.

[26] A. Kamphan, C. Khanantong, N. Traiphol, R. Traiphol, Structural-thermochromic relationship of polydiacetylene (PDA)/polyvinylpyrrolidone (PVP) nanocomposites: effects of PDA side chain length and PVP molecular weight, J. Ind. Eng. Chem. 46 (2017) 130–138.

[27] D.J. Ahn, S. Lee, J.M. Kim, Rational design of conjugated polymer supramolecules with tunable colorimetric responses, Adv. Funct. Mater. 19 (2009) 1483–1496.

[28] U. Jonas, K. Shah, S. Norvez, D.H. Charych, Reversible color switching and unusual solution polymerization of hydrazide-modified diacetylene lipids, J. Am. Chem. Soc. 121 (1999) 4580–4588.

[29] Q. Ye, X. You, G. Zou, X. Yu, Q. Zhang, Morphology, structure and chromatic properties of azobenzene-substituted polydiacetylene supramolelular assemblies, J. Mater. Chem. 18 (2008) 2775–2780.

[30] J.-M. Kim, J.-S. Lee, H. Choi, D. Sohn, D.J. Ahn, Rational design and in-situ FTIR analyses of colorimetrically reversibe polydiacetylene supramolecules, Macromolecules 38 (2005) 9366–9367.

[31] S. Wacharasindhu, S. Montha, J. Boonyiseng, A. Potisatityuenyion, C. Phollookin, G. Tumcharern, M. Sukwattanasinitt, Tuning of thermochromic properties of polydiacetylene toward universal temperature sensing materials through amido hydrogen bonding, Macromolecules 43 (2010) 716–724.

[32] S. Ampornpun, S. Montha, G. Tumcharern, V. Vchirawongkwin, M. Sukwattanasinitt, S. Wacharasindhu, Odd–even and hydrophobicity effects of diacetylene alkyl chains on thermochromic reversibility of symmetrical and unsymmetrical diyndiamide polydiacetylenes, Macromolecules 45 (2012) 9038–9045.

[33] S. Lee, J. Lee, M. Lee, Y.K. Cho, J. Baek, J. Kim, S. Park, M.H. Kim, R. Chang, J. Yoon, Construction and molecular understanding of an unprecedented, reversibly thermochromic bis-polydiacetylene, Adv. Funct. Mater. 24 (2014) 3699–3705.

[34] J. Lee, M. Pyo, S.-H. Lee, J. Kim, M. Ra, W.-Y. Kim, B.J. Park, C.W. Lee, J.-M. Kim, Hydrochromic conjugated polymers for human sweat pore mapping, Nat. Commun. 5 (2014) 3736.

[35] S. Balakrishnan, S. Lee, J.-M. Kim, Thermochromic reversibility of conjugated polymers derived from a diacetylenic lipid containing lithium salt, J. Mater. Chem. 20 (2010) 2302–2304.

[36] L. Yu, S.L. Hsu, A spectroscopic analysis of the role of side chains in controlling thermochromic transitions in polydiacetylenes, Macromolecules 45 (2012) 420–429.

[37] K.-Y. Fu, D.-Y. Chen, Nanocomposites of polydiacetylene and rare earth ions with reversible thermochromism, Chin. J. Chem. Phys. 27 (2014) 465–470.

[38] N. Traiphol, N. Rungruangviriya, R. Potai, R. Traiphol, Stable polydiacetylene/ZnO nanocomposites with two-steps reversible and irreversible thermochromism: the influence of strong surface anchoring, J. Colloid Interface Sci. 356 (2011) 481–489.

[39] A. Chanakul, N. Traiphol, R. Traiphol, Controlling the reversible thermochromism of polydiacetylene/zinc oxide nanocomposites by varying alkyl chain length, J. Colloid Interface Sci. 389 (2013) 106–114.

[40] A. Chanakul, N. Traiphol, K. Faisadcha, R. Traiphol, Dual colorimetric response of polydiacetylene/Zinc oxide nanocomposites to low and high pH, J. Colloid Interface Sci. 418 (2014) 43–51.

[41] N. Traiphol, K. Faisadcha, R. Potai, R. Traiphol, Fine tuning the color-transition temperature of thermoreversible polydiacetylene/zinc oxide nanocomposites: the effect of photopolymerization time, J. Colloid Interface Sci. 439 (2015) 105–111.

[42] S. Toommee, R. Traiphol, N. Traiphol, High color stability and reversible thermochromism of polydiacetylene/zinc oxide nanocomposite in various organic solvents and polymer matrices, Colloids Surf. A: Physicochem. Eng. Asp. 468 (2015) 252–261.

[43] A. Chanakul, R. Traiphol, N. Traiphol, Colorimetric sensing of various organic acids by using polydiacetylene/zinc oxide nanocomposites: effects of polydiacetylene and acid structures, Colloids Surf. A: Physicochem. Eng. Asp. 489 (2016) 9–18.

[44] N. Traiphol, A. Chanakul, A. Kamphan, R. Traiphol, Role of Zn^{2+} ion on the formation of reversible thermochromic polydiacetylene/zinc oxide nanocomposites, Thin Solid Films 622 (2017) 122–129.

[45] A. Chanakul, R. Traiphol, N. Traiphol, Utilization of polydiacetylene/zinc oxide nanocomposites to detect and differentiate organic bases in various media, J. Ind. Eng. Chem. 45 (2017) 215–222.

[46] A. Patlolla, J. Zunino, A.I. Frenkel, Z. Iqbal, Thermochromism in polydiacetylene-metal oxide nanocomposites, J. Mater. Chem. 22 (2012) 7028–7035.

[47] H. Peng, J. Tang, L. Yang, J. Pang, H.S. Ashbaugh, C.J. Brinker, Z. Yang, Y. Lu, Responsive periodic mesoporous polydiacetylene/silica nanocomposites, J. Am. Chem. Soc. 128 (2006) 5304–5305.

[48] X. Huang, S. Jiang, M. Liu, Metal ion modulated organization and function of the Langmuir – Blodgett films of amphiphilic diacetylene: photopolymerization, thermochromism, and supramolecular chirality, J. Phys. Chem. B 109 (2005) 114–119.

[49] H.L. Casal, H.H. Mantsch, D.G. Cameron, Interchain vibrational coupling in phase II (hexagonal) n-alkanes, J. Chem. Phys. 77 (1982) 2825–2830.

[50] S.J. Kew, E.A. Hall, pH response of carboxy-terminated colorimetric polydiacetylene vesicles, Anal. Chem. 78 (2006) 2231–2238.

[51] N. Mino, H. Tamura, K. Ogawa, Analysis of color transitions and changes on Langmuir-Blodgett films of a polydiacetylene derivative, Langmuir 7 (1991) 2336–2341.

[52] Y. Lifshitz, A. Upcher, O. Shusterman, B. Horovitz, A. Berman, Y. Golan, Phase transition kinetics in Langmuir and spin-coated polydiacetylene films, Phys. Chem. Chem. Phys. 12 (2010) 713–722.

[53] E. Shirai, Y. Urai, K. Itoh, Surface-enhanced photopolymerization of a diacetylene derivative in Langmuir-Blodgett films on a silver island film, J. Phys. Chem. B 102 (1998) 3765–3772.

[54] Y. Lifshitz, A. Upcher, A. Kovalev, D. Wainstein, A. Rashkovsky, L. Zeiri, Y. Golan, A. Berman, Zinc modified polydiacetylene Langmuir films, Soft Matter 7 (2011) 9069–9077.

[55] C. Girard-Reydet, R.D. Ortuso, M. Tsemperouli, K. Sugihara, Combined electrical and optical characterization of polydiacetylene, J. Phys. Chem. B 120 (2016) 3511–3515.

[56] S. Chen, H.-B. Luo, H.-L. Xie, H.-L. Zhang, Synthesis of comb polyphenylenes by Suzuki coupling from AB macromonomers, J. Polym. Sci. A: Polym. Chem. 51 (2013) 924–935.

ACS APPLIED NANO MATERIALS
Cite This: ACS Appl. Nano Mater. XXXX, XXX, XXX−XXX
Article
www.acsanm.org

Low-Temperature Reversible Thermochromic Polydiacetylene/Zinc(II)/Zinc Oxide Nanocomposites for Colorimetric Sensing

Natthanon Phonchai,[†] Chanita Khanantong,[‡,∥] Filip Kielar,[§] Rakchart Traiphol,*[,∥,#] and Nisanart Traiphol*[,†,⊥,▽]

[†]Laboratory of Advanced Chromic Materials, Department of Materials Science, Faculty of Science, Chulalongkorn University, Bangkok 10300, Thailand

[‡]Faculty of Science and Technology, Nakhon Sawan Rajabhat University, Nakhon Sawan 60000, Thailand

[§]Department of Chemistry and Center of Excellence in Biomaterials, Faculty of Science, Naresuan University, Phitsanulok 65000, Thailand

[∥]Laboratory of Advanced Polymer and Nanomaterials, School of Materials Science and Innovation, Faculty of Science, Mahidol University at Salaya, Phuttamonthon 4 Road, Nakorn Pathom 73170, Thailand

[⊥]Center of Excellence on Petrochemical and Materials Technology, Chulalongkorn University, Bangkok 10330, Thailand

[#]NANOTEC-MU Center of Excellence on Nanomaterials and Intelligence Systems, Nanocomposite, Nanosensor and Nanoelectronics, Faculty of Science, Mahidol University, Rama 6 Road, Ratchathewi, Bangkok 10400, Thailand

[▽]NANOTEC−CU Center of Excellence on Food and Agriculture, Department of Chemistry, Faculty of Science, Chulalongkorn University, Bangkok 10330, Thailand

Supporting Information

ABSTRACT: A series of reversible thermochromic polydiacetylene/zinc(II) ion/zinc oxide (PDA/Zn^{2+}/ZnO) nanocomposites have been prepared using seven types of diacetylene monomer. The shortening of the PDA alkyl tail from 12 to 6 methylene units systematically decreases color-transition temperature (T_{CT}) from 90 to 30 °C. Increasing the photopolymerization time during the preparation process further reduces the T_{CT} down to 10 °C. The shortening of alkyl segment adjacent to PDA headgroup causes unpredictable changes of T_{CT}. X-ray diffraction reveals variation of the molecular tilting angle within the bilayer structure of PDA depending on the length of alkyl segment. Infrared and Raman spectroscopies also detect the change of local interactions and backbone conformation within the nanocomposites. Our study provides a guideline for preparing reversible thermochromic materials with T_{CT} ranging from 10 to 90 °C. These nanocomposite materials can be utilized in various applications such as colorimetric sensors, smart labels, and thermochromic inks/paints that change color in the hot, cold, or ambient conditions.

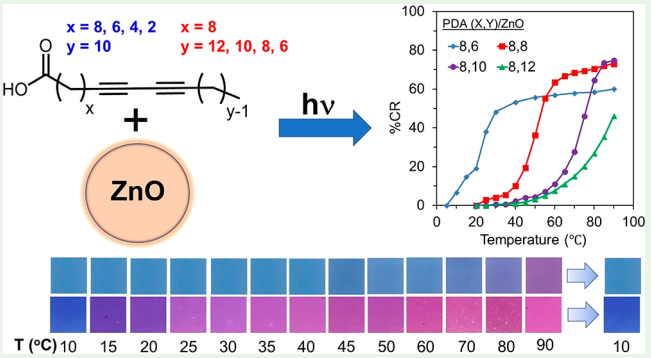

KEYWORDS: *Polydiacetylene, nanocomposites, reversible thermochromism, alkyl chain length, packing structure*

1. INTRODUCTION

Nowadays, colorimetric sensors have become popular tools to detect various classes of stimuli. Their unique advantages include simple detection, high sensitivity, and ease of sample preparation. Polydiacetylene (PDA) is a type of conjugated polymers that has been widely utilized for sensing applications.[1,2] This class of polymer is normally prepared via topotactic photopolymerization, providing a metastable state with blue color. It has been known that environmental perturbation of PDA assemblies by heat,[3−12] acid/base,[6,11,13−17] surfactants,[5,18−20] gases,[10,13,21] near-infrared light,[3] mechanical stress,[22] and biomolecules[2,23−26] results in color transition. Conformational changes of conjugated backbone and alkyl side chains have been suggested as main reasons for the color transition of PDA assemblies.[6,8,27−30]

Over the past few decades, development of reversible thermochromic PDA-based materials has received tremendous attention.[1,3−10,12,27,28,31−42] This mainly stems from their potential utilization in various technologies such as electrothermochromic displays,[43] counterfeiting materials,[44] smart textiles,[45] and inkjet printable thermal sensors.[1] Generally, reversible thermochromism can be obtained by increasing intra- and intermolecular interactions within the PDA

Received: May 9, 2019
Accepted: June 24, 2019
Published: June 24, 2019

DOI: 10.1021/acsanm.9b00876
ACS Appl. Nano Mater. XXXX, XXX, XXX−XXX

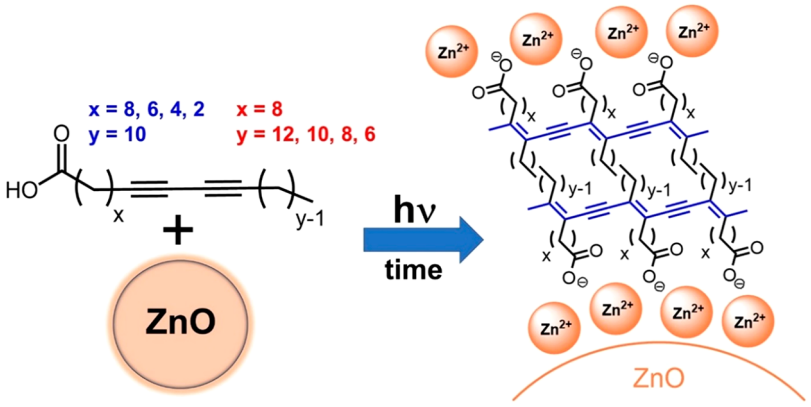

Figure 1. Schematic representation of the preparation of the PDA/Zn^{2+}/ZnO nanocomposites. The length of alkyl side chain and photopolymerization time are systematically varied.

assemblies. This can be achieved by two major approaches. The first one involves structural modification of PDA headgroup and alkyl side chain.[3−5,7,10,12,32−39] For example, while PDA prepared from 10,12-pentacosadiynoic acid (PCDA) exhibits irreversible color transition,[5,11] studies by Kim et al. demonstrated that modification of the poly(PCDA) headgroup with aromatic moieties resulted in reversible thermochromism at 90 °C.[39] Different headgroups were explored by other research works.[3,4,32,36,38] Wacharasindhu et al. connected the poly(PCDA) headgroup using various chemical linkers.[33−35] This class of bisdiynamide PDAs also exhibited reversible thermochromism at 90 °C.[12] An attempt to tune down the reversible color-transition temperature (T_{CT}) was performed by reducing alkyl chain length. The lowest T_{CT} of 45 °C was achieved. The second approach utilizes foreign materials to enhance interactions within the PDA assemblies. Several research groups reported that addition of various cations promoted strong ionic interactions with carboxylate headgroup of poly(PCDA).[27,28,31,40,46,47] The resulting poly(PCDA)/M^{n+} nanocomposites exhibited reversible thermochromism with T_{CT} of 90 °C. The noticeable advantage of this approach over the structural modification is the simpler preparation process.

Recent studies by our group demonstrated that a simple method of mixing poly(PCDA) with ZnO nanoparticle provides reversible thermochromism.[6,8,41,42,48,49] The Zn^{2+} ions released from ZnO nanoparticles intercalated with the carboxylate headgroup of poly(PCDA) via strong electronic interaction.[48] The poly(PCDA)/Zn^{2+}/ZnO nanocomposite exhibited reversible thermochromism at 90 °C. In an attempt to tune down $T_{CT,}$ 5,7-hexadecadiynoic acid (HDDA) was used in our previous study.[42] The shortening of alkyl segments reduced T_{CT} to 55 °C. We also introduced a new strategy for fine-tuning the T_{CT} by increasing photopolymerization time, which induced partial relaxation of PDA segments.[8,49] As a result, the poly(PCDA)/Zn^{2+}/ZnO nanocomposites with T_{CT} ranging from 45 to 90 °C were obtained.

Low-temperature thermochromic PDAs have been reported by several groups.[50−52] Studies by Kim et al. showed that the modification of headgroup using isocyanate or ester moieties reduced the strength of interactions within PDA assemblies, resulting in a drastic drop of T_{CT}.[50,51] The resultant PDAs exhibited irreversible blue-to-red color transition, ranging from 5 to 30 °C. Comprehensive work by Rougeau et al. also demonstrated that a systematic variation of headgroup structure and alkyl side chain length provided a series of PDAs with a wide range of T_{CT}. The irreversible T_{CT} as low as −50 °C was reported. These low-temperature thermochromic PDAs can be utilized as intelligent labels that determine the thermal history of products during the transportation or storage period. However, the PDA-based material that exhibits reversible thermochromism at a low-temperature region is quite rare. In fact, the reversible thermochromic PDA-based materials reported to date have a color-transition temperature above 40 °C.

In this study, we take a step toward demonstrating that the reversible thermochromic nanocomposite with T_{CT} below ambient condition can be achieved. We can obtain a reversible T_{CT} as low as 10 °C which has never been reported in any other PDA-based material. The reversible T_{CT} can be tuned between 10 to 90 °C. The nanocomposites with a wide range of reversible T_{CT} have a potential for being utilized as colorimetric sensors, thermochromic inks/paints, and smart labels that determine a real-time temperature of foods, beverages, and other products. Various types of diacetylene (DA) monomer were used to prepare PDA(x,y)/Zn^{2+}/ZnO nanocomposites, where x and y represent methylene units adjacent to the carboxylic headgroup and at the alkyl tail, respectively (Figure 1). The photopolymerization time was also varied to control the conformation of PDA backbone. The influences of PDA alkyl chain length on molecular packing, interfacial interactions, and backbone conformation are explored by various techniques.

2. EXPERIMENTAL SECTION

DA monomers, 4,6-heptadecadiynoic acid (DA(2,10)), 6,8-nonadecadiynoic acid (DA(4,10)), and 8,10-henicosadiynoic acid (DA(6,10)) were commercially available at Wako Chemical (Japan) whereas 10,12-tricosadiynoic acid (DA(8,10)) and 10,12-pentacosadiynoic acid (DA(8,12)) were purchased from Aldrich. The 10,12-nonadecadiynoic acid (DA(8,6)) and 10,12-henicosadiynoic acid (DA(8,8)) were synthesized as reported in the literature.[34] ZnO nanoparticles with particle size ranging from 20 to 160 nm were purchased from Nano Materials Technology (Thailand).[8] The PDA(x,y)/Zn^{2+}/ZnO nanocomposites were prepared as described in our previous reports.[41,42] The concentration of PDAs was 1 mM while the ZnO/PDA ratio was kept at 10 wt %. The blue phase of all nanocomposites was obtained by UV light irradiation (λ = 254 nm, 10 W) for 1 min.

Molecular packing structure of the nanocomposites was studied using X-ray diffractometer (XRD) (Bruker AXS Model D8 Discover, $\lambda(Cu-K_\alpha)$ = 1.54 Å). Dried samples were prepared by drop casting

DOI: 10.1021/acsanm.9b00876
ACS Appl. Nano Mater. XXXX, XXX, XXX−XXX

onto glass slides. Morphologies and particle size distribution of the nanocomposites were investigated by scanning electron microscopy (SEM, JEOL, JSM-6400) and dynamic light scattering (DLS, Brookhaven, ZetaPaLs). The infrared (IR) and Raman spectra were measured using Nicolet 6700 FT-IR spectrometer and FT-Raman spectrometer (PerkinElmer Spectrum GX) with a 1064 nm laser (Nd:YAG) as an excitation source. Thermochromic properties were investigated using UV−vis spectrophotometer equipped with a temperature-control unit (Analytik Jena Specord S100).

3. RESULTS AND DISCUSSION

3.1. Morphologies and Molecular Packing. Morphologies of PDA(x,y)/Zn^{2+}/ZnO nanocomposites are shown in Figure 2. The SEM image of PDA(8,12)/Zn^{2+}/ZnO nanocomposite reveals round-shape particles with diameter of ∼200 nm. A systematic increase of particle size is observed when the alkyl tail of PDA is shortened. The diameter of the PDA(8,6)/Zn^{2+}/ZnO nanocomposite is ∼1 μm. The morphology of the particle also changes to a sheetlike structure. The shortening of the alkyl segment adjacent to the carboxylate headgroup of PDA shows a similar trend. Micron-size particles are detected in the systems of PDA(4,10)/Zn^{2+}/ZnO and PDA(2,10)/Zn^{2+}/ZnO nanocomposites. The investigation of particle sizes in aqueous suspension by DLS also shows the increase in particle size with shortening of the length of PDA alky segment (Figure 3). As shown in our previous studies, this class of nanocomposite forms a core−shell structure (Figure 2h), in which, the ZnO nanoparticle acts as an anchoring substrate for the PDA carboxylate headgroup.[41,48] Because this study uses the same batch of ZnO nanoparticle, the increase of particle size indicates the growth of PDA/Zn^{2+} outer layer. Therefore, the shortening of PDA alkyl segment promotes the molecular assembly of PDA/Zn^{2+} layer within the nanocomposite. Theoretical study of surfactant systems has shown that the shortening of alkyl side chain strongly affects the packing parameter and aggregation number of the assemblies.[53] We believe that the change of packing parameter influences the growth mechanism of Zn^{2+}-intercalated bilayer structure within the nanocomposite. However, our nanocomposite system is quite complex due to the presence of strong Coulombic interaction between the carboxylate headgroup and Zn^{2+}/ZnO. More detailed study is required to understand the origins of this result. In comparison with our previous study on the system of pure PDAs,[11] the particle size of the nanocomposites is much larger. This observation also indicates that the presence of ZnO nanoparticle as an anchoring substrate facilitates the molecular organization within this system.

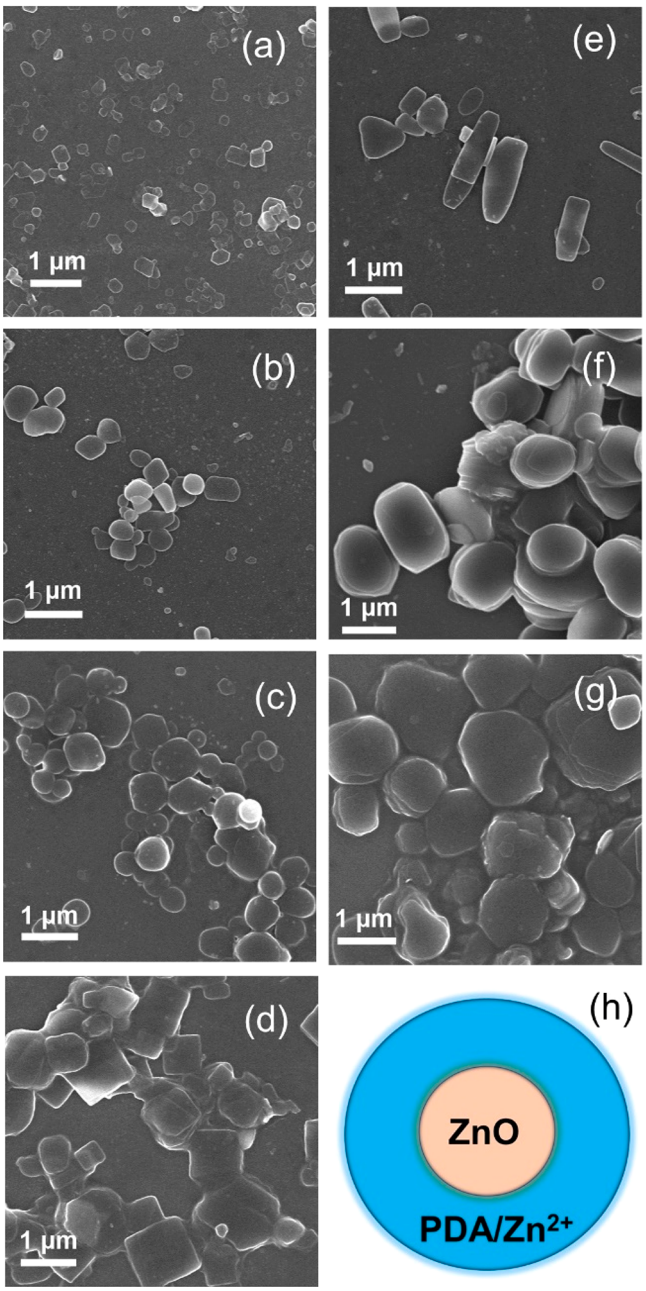

Figure 2. SEM images of PDA(x,y)/Zn^{2+}/ZnO nanocomposites where (x,y) are (a) (8,12), (b) (8,10), (c) (8,8), (d) (8,6), (e) (6,10), (f) (4,10), and (g) (2,10). (h) Schematic core−shell structure of the nanocomposites.

Molecular packing structure of the PDA(x,y)/Zn^{2+}/ZnO nanocomposites can be explored by XRD. It has been known that the PDAs form a bilayer lamellar structure where the interlamellar d-spacing can be determined from the length of the alkyl side chain.[5,11,28−31,41] In our previous study on this series of pure PDAs, a systematic decrease of d-spacing value with shortening of the alkyl side chain was observed.[11] For the bilayer structure of pure PDA(8,12), d-spacing value of 4.5 nm was reported. The XRD pattern of PDA(8,12)/Zn^{2+}/ZnO nanocomposite in Figure 4 corresponds to the bilayer structure. The average d-spacing value calculated from the diffraction peaks is 5.5 nm. The increase of d-spacing value indicates the intercalation of Zn^{2+} ions, released from ZnO nanoparticles, with PDA layers.[48] The XRD patterns of other nanocomposites also show larger d-spacing values compared to those of their pure PDA counterparts. The XRD patterns of DA(x,y)/Zn^{2+}/ZnO assemblies were also recorded (Figure S1, Supporting Information) to explore the change of molecular packing during topotactic photopolymerization process. Table 1 summarizes the average d-spacing values of all nanocomposites. Our XRD measurements show a slight decrease of d-spacing values when DA(x,y)/Zn^{2+}/ZnO assemblies are photopolymerized to form PDA(x,y)/Zn^{2+}/ZnO nanocomposites. The result is consistent with the previous studies, which reported the shrinkage of unit cell during the photopolymerization process.[29,30] However, a discrepancy was observed for the systems of DA(8,6)/Zn^{2+}/ZnO and DA(2,10)/Zn^{2+}/ZnO nanocomposite, where the d-spacing values did not decrease during the photopolymerization. Similar results were also reported in our previous study of pure

DOI: 10.1021/acsanm.9b00876
ACS Appl. Nano Mater. XXXX, XXX, XXX−XXX

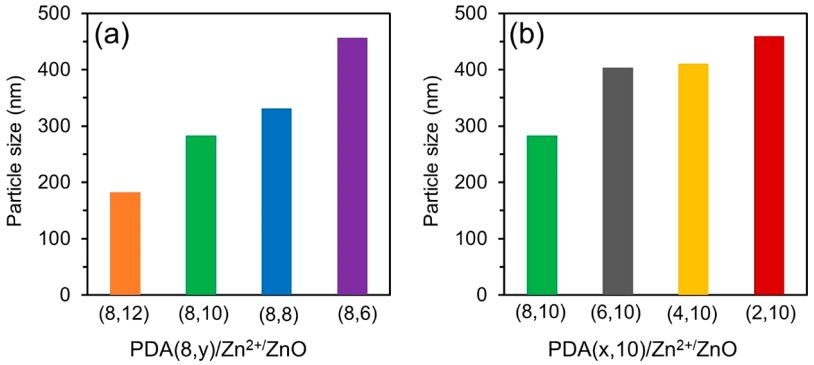

Figure 3. Median diameter of (a) PDA(8,y)/Zn^{2+}/ZnO and (b) PDA(x,10)/Zn^{2+}/ZnO nanocomposites obtained using DLS.

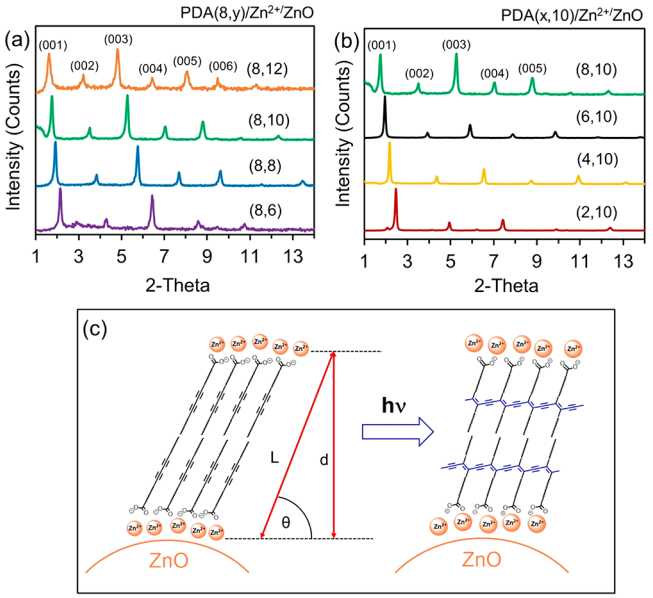

Figure 4. XRD patterns of (a) PDA(8,y)/Zn^{2+}/ZnO and (b) PDA(x,10)/ Zn^{2+}/ZnO nanocomposites. (c) An estimation of tilting angle (θ) in the bilayer structure of DAs. The L values are estimated from the extended length (L_0) of DA monomers and ionic diameter of Zn^{2+} ion. The d-values of the crystalline phase are calculated from the XRD data.

DA(8,6) and DA(2,10) monomers.[11] We believe that the shortening of the PDA alkyl segment could cause the increase of molecular confinement within the bilayer structure, affecting the mechanism of structural transition. More detailed study is required in order to reveal the origins of this behavior.

The d-spacing values of the bilayer structure were then used to estimate the molecular tilting angle (θ) with respect to lamellar plane as shown in Figure 4c. Here, we assume all-trans conformation of alkyl segment, head-to-head and tail-to-tail arrangement of the DA monomers. Because the DA molecules arrange into a highly organized lamellar structure, the assumption of an all-trans conformation of the alkyl segment is reasonable. We also measure FT-IR spectra of all samples to investigate the conformation of an alkyl segment (Figure S2, Supporting Information). The $\nu_s(CH_2)$ and $\nu_{as}(CH_2)$ of all samples are detected at 2848 and 2919 cm^{-1}, respectively, indicating the presence of an all-trans conformation.[15,47] The formation of gauche conformation would shift the vibrational bands to higher wavenumber. The L values are estimated from the extended length (L_0) of DA monomers and ionic diameter of Zn^{2+} ion (0.18 nm). The L_0 value of all DA monomers in Table 1 was reported in the previous studies.[11,40] The estimated θ value for the system of the pure DA(8,12) monomer is 48°.[11] The shortening of alkyl segment of DA(x,y) causes a slight variation of the θ value ranging from 47° to 48°. Interestingly, the θ value significantly increases to 55° in the bilayer structure of pure DA(2,10) monomer where the alkyl segment adjacent to the headgroup is relatively short. In the system of DA(8,12)/Zn^{2+}/ZnO nanocomposite, a drastic increase of θ value to 59° is detected. This result indicates that the Coulombic interaction between Zn^{2+} ion and carboxylate headgroup of DA(8,12) strongly influences the molecular arrangement within the bilayer structure. The shortening of DA alkyl tail also results in a systematic decrease of θ value. The bilayer structure of DA(8,6)/Zn^{2+}/ZnO nanocomposite exhibits θ value of 54°. A similar trend is observed when the alkyl segment adjacent to the carboxylate headgroup is shortened (Table 1). The θ value of DA(2,10)/Zn^{2+}/ZnO nanocomposite is 53°. It is worthwhile to note that the DA(2,10)/Zn^{2+}/ZnO nanocomposite exhibits a smaller θ value compared to that of the pure DA(2,10) monomer. This observation is opposite to the other DA(x,y) systems investigated in this study. Our results further emphasize the

Table 1. Bilayer d-Spacing Values of DA(x,y)/Zn^{2+}/ZnO and Resultant PDA(x,y)/Zn^{2+}/ZnO Nanocomposites[a]

DA(x,y)/Zn^{2+}/ZnO	molecular length (L_0, nm)	bilayer d-spacing (d, nm)	tilting angle (θ, °)	PDA(x,y)/Zn^{2+}/ZnO	bilayer d-spacing (d, nm)
DA(8,12)	3.18	5.6	59	PDA(8,12)	5.5
DA(8,10)	2.93	5.1	58	PDA(8,10)	5.0
DA(8,8)	2.68	4.7	58	PDA(8,8)	4.6
DA(8,6)	2.43	4.1	54	PDA(8,6)	4.1
DA(6,10)	2.68	4.5	54	PDA(6,10)	4.5
DA(4,10)	2.43	4.1	54	PDA(4,10)	4.0
DA(2,10)	2.18	3.6	53	PDA(2,10)	3.6

[a]Tilting angle (θ) values in the bilayer structure are estimated by using L= 2L_0 + Zn^{2+} diameter, where L_0 is a molecular length of extended DAs.

DOI: 10.1021/acsanm.9b00876
ACS Appl. Nano Mater. XXXX, XXX, XXX−XXX

important role of the length of the alkyl chain adjacent to the PDA headgroup on the molecular packing structure within the assemblies. A previous study of 2D monolayer structure also observed a significant change of packing structure when the length of the alkyl chain adjacent to the headgroup became relatively short.[54]

3.2. Tunable Reversible Thermochromism. In this section, the reversible thermochromic behavior of PDA(x,y)/Zn^{2+}/ZnO nanocomposites is adjusted by varying the alkyl chain and the UV light irradiation time. The shortening of the alkyl chain length reduces dispersion interactions within the system whereas the increase in UV light irradiation time affects the conformation of the conjugated backbone.[8,11] Absorption spectra of the initial blue phase of all nanocomposites are shown in Figure 5. The spectra of PDA(8,12)/Zn^{2+}/ZnO, PDA(8,10)/Zn^{2+}/ZnO, and PDA(8,8)/Zn^{2+}/ZnO nanocomposites exhibit the same λ_{max} value at 640 nm. The λ_{max} shifts to 670 nm in the nanocomposite system of PDA(8,6)/Zn^{2+}/ZnO (Figure 5a). The redshift of the λ_{max} value indicates the increase of conjugation length within PDA backbone when the alkyl tail becomes relatively short. We believe that the shortening of alkyl tail results in the increase of backbone rigidity and planarity, which, in turn, promotes the delocalization of π-electrons within the PDA(8,6)/Zn^{2+}/ZnO nanocomposite. The shortening of the alkyl segment adjacent to the carboxylate headgroup shows a similar trend. The spectra of PDA(6,10)/Zn^{2+}/ZnO and PDA(4,10)/Zn^{2+}/ZnO nanocomposites exhibit the shift of the λ_{max} value to 660 nm (Figure 5b). However, the nanocomposite prepared from PDA(2,10) has a shorter conjugation length with the λ_{max} value of 645 nm.

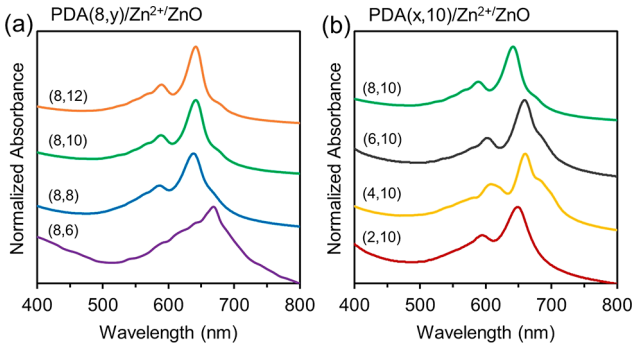

Figure 5. Absorption spectra of the initial blue phase of (a) PDA(8,y)/Zn^{2+}/ZnO and (b) PDA(x,10)/Zn^{2+}/ZnO nanocomposites. All spectra were measured at 20 °C except for PDA(8,6)/Zn^{2+}/ZnO, which was measured at 10 °C due to its color change at room temperature.

All PDA(x,y)/Zn^{2+}/ZnO nanocomposites prepared in this study exhibit reversible thermochromism. The effect of alkyl tail length on color-transition temperature (T_{CT}) is illustrated in Figure 6. Temperature-dependent absorption spectra of PDA(8,6)/Zn^{2+}/ZnO nanocomposite are shown in Figure 6a. An isosbestic point is clearly observed indicating the transition of two district electronic species. A drastic drop of λ_{max} value from 670 to 620 nm is detected at ~20 °C. However, the color of aqueous suspension remains blue at this temperature. A gradual transition to purple is detected at ~30 °C (Figure 6c). The increase of alkyl tail length in the nanocomposite system of PDA(8,8)/Zn^{2+}/ZnO results in the increase of T_{CT} to 50 °C where λ_{max} descends to 590 nm (Figure 6b). Color

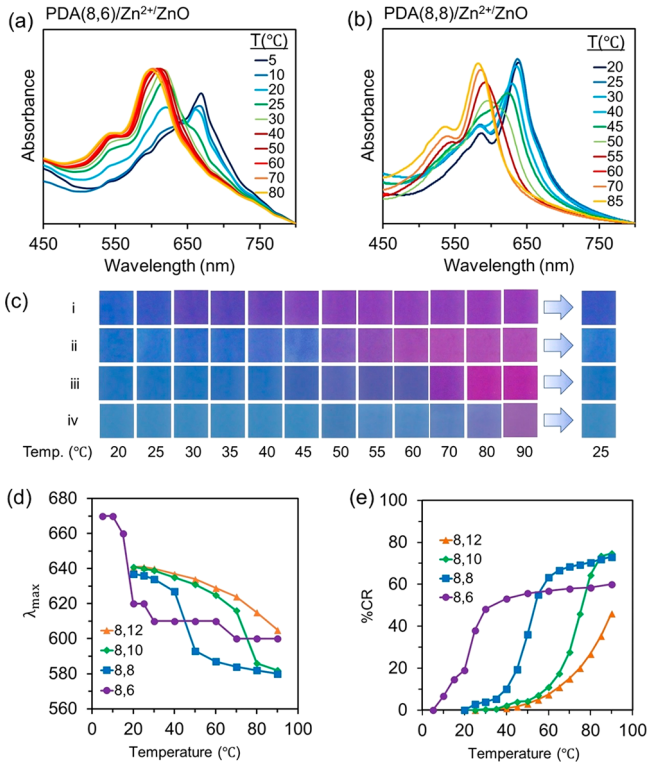

Figure 6. Absorption spectra of (a) PDA(8,6)/Zn^{2+}/ZnO and (b) PDA(8,8)/Zn^{2+}/ZnO nanocomposites measured upon increasing temperature. (c) Color photographs of PDA(8,y)/Zn^{2+}/ZnO nanocomposites taken upon heating/cooling ((i) y = 6, (ii) y = 8, (iii) y = 10, and (iv) y = 12). Plots of (d) λ_{max} and (e) %CR as a function of temperature.

photographs taken upon a heating/cooling cycle of PDA(8,y)/Zn^{2+}/ZnO nanocomposites are shown in Figure 6c. From naked-eye observation, the blue-to-purple color transition of PDA(8,6)/Zn^{2+}/ZnO, PDA(8,8)/Zn^{2+}/ZnO, PDA(8,10)/Zn^{2+}/ZnO, and PDA(8,12)/Zn^{2+}/ZnO nanocomposites occurs at 30, 50, 70, and 90 °C, respectively. Therefore, the increase of two methylene units within the alkyl tail causes the increase of T_{CT} by ~20 °C. A complete color reversibility is observed upon cooling to room temperature. The color reversibility persists up to 10 times of the heating/cooling cycles between 25 and 90 °C (Figure S4, Supporting Information). A study by differential scanning calorimetry (DSC) in our previous report showed that the reversible color transition related to the melting of the alkyl side chain.[8] Plots of colorimetric response (%CR) and λ_{max} versus temperature are shown in Figure 6d,e. The result demonstrates the systematic increase of the T_{CT} with the longer alkyl tail length, which is parallel to the pure PDA systems.[11] However, the pure PDAs of this series exhibit irreversible thermochromism with T_{CT} ranging from ~40 to ~60 °C. It is worthwhile to note that the PDA(8,6)/Zn^{2+}/ZnO nanocomposite exhibits color transition near ambient temperature. The T_{CT} of 30 °C is lower than those of other reversible thermochromic PDA-based materials previously reported in literature.

The variation of methylene unit adjacent to PDA headgroup leads to rather different results. Absorption spectra of PDA(2,10)/Zn^{2+}/ZnO and PDA(6,10)/Zn^{2+}/ZnO nanocomposites measured upon increasing temperature are shown in Figure 7(a,b). The PDA(2,10)/Zn^{2+}/ZnO nanocomposite exhibits a sharp transition at ~55 °C where the λ_{max} drops

DOI: 10.1021/acsanm.9b00876
ACS Appl. Nano Mater. XXXX, XXX, XXX−XXX

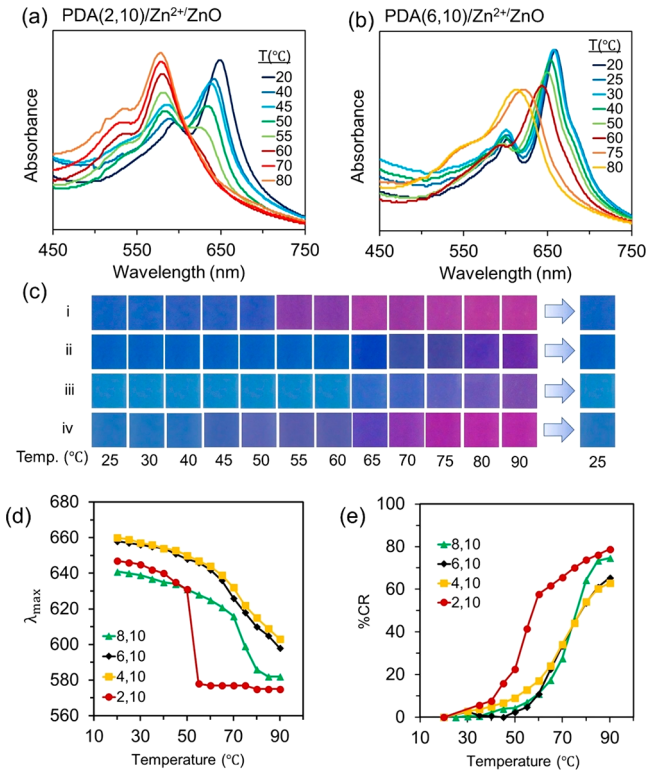

Figure 7. Absorption spectra of (a) PDA(2,10)/Zn^{2+}/ZnO and (b) PDA(6,10)/Zn^{2+}/ZnO nanocomposites measured upon increasing temperature. (c) Color photographs of PDA(x,10)/Zn^{2+}/ZnO nanocomposites taken upon heating/cooling ((i) x = 2, (ii) x = 4, (iii) x = 6, and (iv) x = 8). Plots of (d) λ_{max} and (e) %CR as a function of temperature.

from 640 to 580 nm. The color photographs in Figure 7c show a clear blue-to-purple color transition in this system. The increase of two methylene units in PDA(4,10)/Zn^{2+}/ZnO nanocomposite causes a significant increase of T_{CT} to 80 °C. However, color transition gradually occurs in this system, in which, λ_{max} gradually decreases to ~600 nm at 90 °C (Figure 7d). The two additional methylene units in the PDA(6,10)/Zn^{2+}/ZnO nanocomposite, however, scarcely increase the T_{CT} or alter the color-transition behavior (Figure 7d,e). Further increase of two methylene units results in the PDA(8,10)/Zn^{2+}/ZnO nanocomposite with the longest methylene segment in this series, which shows a sharp blue-to-purple color transition at ~70 °C. Our results indicate that the change of the length of the methylene segment adjacent to the PDA headgroup provides an unpredictable trend of T_{CT}. The investigation of pure PDAs of this series showed rather interesting thermochromic behaviors.[11] The shortening of alkyl segment in pure PDA(2,10) caused drastic increase of T_{CT}, which is related to the increase in local interactions between the headgroups. Studies by other research groups also detected the change of local interactions and molecular packing when the alkyl segment adjacent to the headgroup became relatively short.[54,55] The nature of local interactions of PDA(x,y)/Zn^{2+}/ZnO nanocomposites is explored in the following section utilizing FT-IR spectroscopy. It is worthwhile to note that these nanocomposites exhibit dual colorimetric response to both acid and base.[16,17,56] However, the color transition is not reversible due to the corrosion of ZnO core at low and high pH region. The colorimetric response of PDA(2,10)/Zn^{2+}/ZnO nanocomposite to acid and base is shown as an example (Figure S5, Supporting Information). Our previous study also shows that the PDA(8,12)/Zn^{2+}/ZnO nanocomposite can be dispersed in various organic solvents without changing the color.[57] We investigate the colorimetric response of PDA(2,10)/Zn^{2+}/ZnO nanocomposite to organic solvents in this study. This nanocomposite exhibits a colorimetric response to THF and propanol (Figure S6, Supporting Information). When the solvents are removed, the color does not reverse back to the original state. However, the colorimetric response to organic solvents allows their utilization as chemical sensors. This topic is currently being under investigation in our group.

Our previous studies demonstrated that the increase of UV photopolymerization time caused a systematic decrease of T_{CT} of the PDA(8,12)/Zn^{2+}/ZnO nanocomposite.[8,49] Here, we explore the nanocomposite systems of PDA(8,6)/Zn^{2+}/ZnO and PDA(2,10)/Zn^{2+}/ZnO with the shortest alkyl segment at the tail and headgroup position, respectively. Figure 8

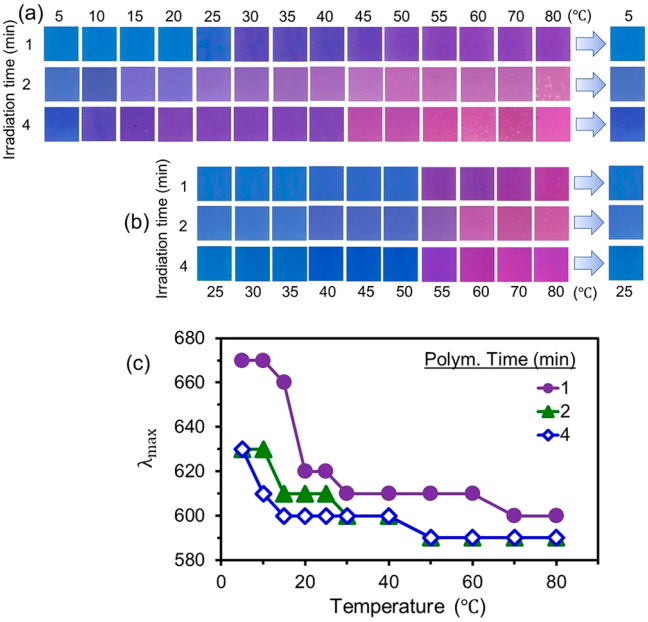

Figure 8. Color photographs of (a) PDA(8,6)/Zn^{2+}/ZnO and (b) PDA(2,10)/Zn^{2+}/ZnO nanocomposites taken upon heating/cooling. The nanocomposites were prepared using UV light irradiation time of 1, 2, and 4 min. (c) Plot of λ_{max} as a function of temperature of the PDA(8,6)/Zn^{2+}/ZnO nanocomposites.

illustrates thermochromic behavior of the nanocomposites prepared using photopolymerization time of 1, 2, and 4 min. It is clear that the increase of photopolymerization time exhibits a rather strong effect on the T_{CT} of PDA(8,6)/Zn^{2+}/ZnO nanocomposite. The color transition takes place at 30, 15, and 10 °C when the photopolymerization times are 1, 2, and 4 min, respectively. The plot of λ_{max} value versus temperature in Figure 8c shows an abrupt change at the transition region. These nanocomposites still exhibit complete reversible thermochromism upon cooling to 5 °C. The decrease of T_{CT} is attributed to partial relaxation of conjugated PDA backbone upon increasing photopolymerization time. Detailed discussion of this topic is available in our previous report.[8] It is important to point out that this nanocomposite is the first example of reversible thermochromic PDA-based material with T_{CT} lower than the ambient temperature. This property allows cold-

DOI: 10.1021/acsanm.9b00876
ACS Appl. Nano Mater. XXXX, XXX, XXX−XXX

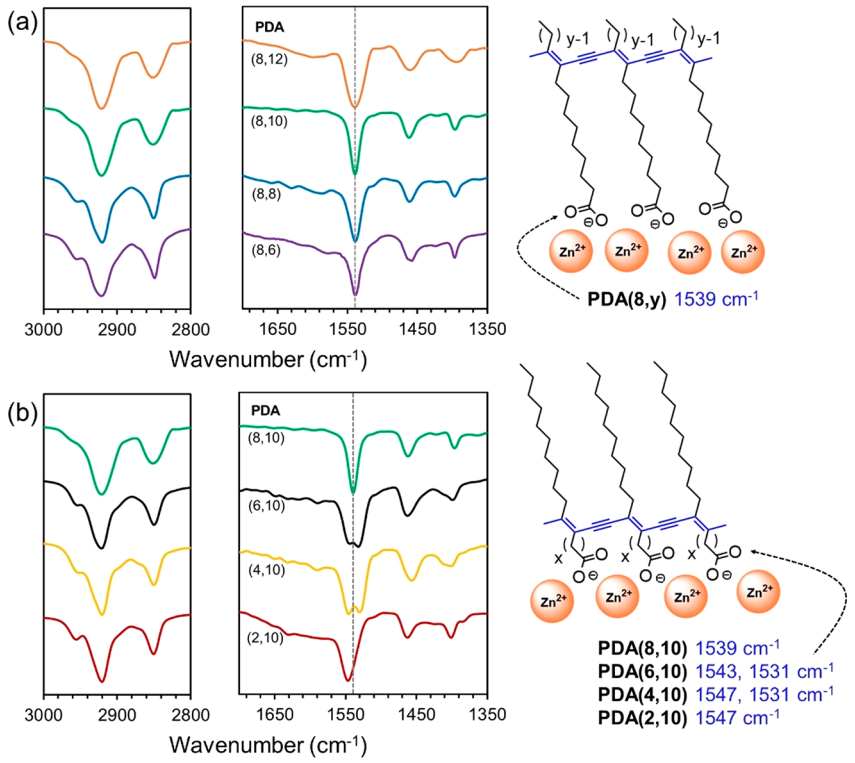

Figure 9. FT-IR spectra measured at room temperature and schematic representation of the interaction between Zn^{2+} ions and COO^{-} at PDAs headgroup of (a) PDA(8,*y*)/Zn^{2+}/ZnO and (b) PDA(*x*,10)/Zn^{2+}/ZnO nanocomposites. The stretching vibrational wavenumbers of Zn^{2+}-coordinated COO^{-} group reflect the strength of local interactions in each system.

activated color transition, which can extend their utilization in various technologies.

The investigation of the PDA(2,10)/Zn^{2+}/ZnO nanocomposite, however, shows different results. The increase of photopolymerization time from 1 to 4 min hardly affects the T_{CT} as shown in Figure 8b. Even after further increase of the photopolymerization time to 60 min, the T_{CT} remains roughly at ∼55 °C. Our observation suggests that it is more difficult to induce the relaxation of the PDA(2,10) conjugated backbone via the photopolymerization process. This is attributed to the relatively short alkyl segment adjacent to the PDA headgroup, which could cause the variation of local interactions and confinement of the backbone. Further study is required in order to understand the origin of this behavior.

Low-temperature thermochromic PDAs have been reported by several previous studies.[50−52] However, the color transition of those PDAs at low temperature is the irreversible one. Our nanocomposites exhibit reversible thermochromism at low temperature, which has never been reported. We also emphasize on the effect of the alkyl chain length at a different position. The shortening of the alkyl tail results in a systematic decrease of the T_{CT}. On the other hand, the shortening of the alkyl segment adjacent to the headgroup provides an unpredictable change of T_{CT}. The photopolymerization time is also a key factor for the T_{CT} in this study. The nanocomposites with a wide range of reversible T_{CT} have a potential for being utilized as colorimetric sensors, thermochromic inks/paints, and smart labels that determine a real-time temperature of foods, beverages, and other products.

3.3. Interfacial Interaction and Backbone Conformation. In this section, the FT-IR and FT-Raman spectroscopies are employed to explore the nature of local interactions and backbone conformation within the nanocomposites. The IR spectra of all PDA(*x*,*y*)/Zn^{2+}/ZnO nanocomposites are shown in Figure 9. In the system of PDA(8,*y*)/Zn^{2+}/ZnO nanocomposites, all spectra exhibit the same pattern. Peaks in the region of 2800−3000 cm^{-1} correspond to vibrational frequencies of alkyl segments.[5,6,15,47] Our previous studies showed that the IR spectra of pure PDAs constituted a broad peak near 1690 cm^{-1}, corresponding to hydrogen-bonded carbonyl stretching of −COOH headgroup.[6,8,11] This peak disappears from the IR spectra of nanocomposites. We detect a new peak at 1539 cm^{-1}, assigned to the ν_{as}COO stretching vibration of the carboxylate anion, which interacts strongly with the Zn^{2+} ion (Figure 9a). The increase of the overall interactions within this system results in the reversible thermochromism. Detailed analysis of the roles of ZnO nanoparticles and Zn^{2+} ion is available in our previous reports.[6,48] We observe that the shortening of PDA(8,*y*) alkyl tail hardly affects the position of peak at 1539 cm^{-1}. Therefore, the nature of local interactions between the carboxylate headgroup and the Zn^{2+} ion remains the same in this series. This observation suggests that the systematic decrease of color-transition temperature of the PDA(8,*y*)/Zn^{2+}/ZnO nanocomposites shown in Figure 6 mainly arises from the reduction of dispersion interactions due to the shortening of alkyl side chain.

The variation of alkyl segment adjacent to the carboxylate headgroup of PDA (*x*,10)/Zn^{2+}/ZnO nanocomposites shows rather interesting results (Figure 9b). In the nanocomposite system of PDA(6,10)/Zn^{2+}/ZnO, we observe the splitting of ν_{as}COO stretching vibration into 1543 and 1531 cm^{-1}. Previous studies reported that the ν_{as}COO peak of PDA shifted to different positions depending on the nature of local

DOI: 10.1021/acsanm.9b00876
ACS Appl. Nano Mater. XXXX, XXX, XXX−XXX

interactions with various cations.[27,47] Therefore, the detection of two vibrational peaks in this study indicates that the carboxylate headgroup of the PDA interacts with the Zn^{2+} ion in two different forms. A similar splitting pattern of ν_{as}COO stretching vibration is also observed in the nanocomposite system of PDA(4,10)/Zn^{2+}/ZnO. Our results shows that the shortening of alkyl segment adjacent to the PDA headgroup strongly influences the strength of local interactions between the carboxylate group and the Zn^{2+} ion. This behavior affects the color transition of the nanocomposites in an unpredictable manner as discussed in Figure 7. These two nanocomposites exhibit a gradual color transition with relatively high color-transition temperature. In the nanocomposite system of PDA(2,10)/Zn^{2+}/ZnO containing the shortest alkyl segment, a single peak of ν_{as}COO stretching vibration is detected. However, it is shifted from 1539 to 1547 cm^{-1}. This nanocomposite exhibits a sharp color transition with the lowest T_{CT} in this series.

The variation of alkyl chain length strongly affects the conformation of the PDA-conjugated backbone within the nanocomposites. Raman spectra of all samples are shown in Figure 10. It is known that a blue phase of pure PDA(8,12) exhibits distinct C≡C and C═C stretching frequencies at 2080 and 1451 cm^{-1}, respectively.[8,27,58] Thermal treatment of the metastable blue phase normally causes relaxation of PDA conjugated backbone into new local environment, resulting in color transition into red phase. The C≡C and C═C stretching frequencies shift to 2116 and 1511 cm^{-1}, respectively for red phase. Raman spectrum of PDA(8,12)/Zn^{2+}/ZnO nanocomposite shows two peaks at 2076 and 1448 cm^{-1}, corresponding to the backbone conformation in the blue phase. The shortening of the alkyl tail of PDA(8,10)/Zn^{2+}/ZnO and PDA(8,8)/Zn^{2+}/ZnO nanocomposites does not alter the position of the Raman peaks. In the nanocomposite system of PDA(8,6)/Zn^{2+}/ZnO, however, the peaks shift to 2105 and 1474 cm^{-1} indicating the relaxation of the PDA conjugated backbone. Because the positions of these peaks are different from those of the red phase, this type of relaxation is not due to the blue-to-red color transition. In fact, the absorption spectrum of PDA(8,6)/Zn^{2+}/ZnO nanocomposite measured at room temperature exhibits λ_{max} at 610 nm, and its color appears purple (Figure 6). We suggest that the shortening of alkyl tail causes the reduction of dispersion interaction within the nanocomposite, allowing partial relaxation of conjugated backbone. This type of backbone relaxation is similar to previous studies exploring the effects of temperature and photopolymerization time.[8,27]

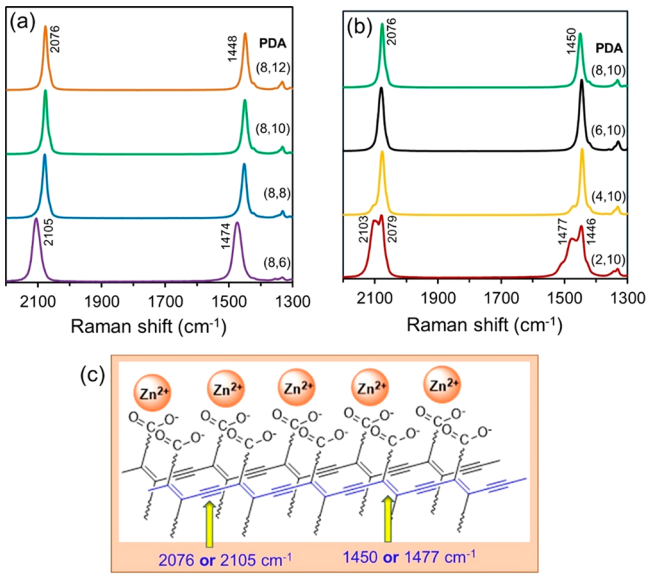

Figure 10. FT-Raman spectra of (a) PDA(8,*y*)/Zn^{2+}/ZnO and (b) PDA(*x*,10)/Zn^{2+}/ZnO nanocomposites measured at room temperature. (c) Vibrational wavenumbers of the triple bond and double bond within the conjugated backbone of PDA.

The shortening of alkyl segment adjacent to the PDA headgroup also leads to partial relaxation of the conjugated backbone within the nanocomposite. The Raman spectrum of PDA(2,10)/Zn^{2+}/ZnO nanocomposite shows splitting peaks in both vibrational regions. The peaks of C≡C and C═C stretching modes are observed at 2103/2079 and 1477/1446 cm^{-1}, respectively (Figure 10b). The growth of new peaks at 2103 and 1477 cm^{-1} indicates the relaxation of some PDA backbones into the purple phase. Absorption spectra in Figure 7a also show the growth of the peak at 585 nm. However, a large fraction of the PDA remains in the blue phase. Therefore, the sample appears blue at ambient conditions. Figure 10c illustrates the stacking of PDA conjugated backbone within its bilayer structure. We suggest that the structural relaxation relates to the decrease of stacking distance between the conjugated backbone of PDA. Our hypothesis is parallel to previous studies by X-ray scattering techniques reporting the shrinkage of the unit cell during the color transition process of PDA.[29,30]

4. CONCLUSION

Our study introduces a new approach for preparing reversible thermochromic PDA-based materials with color-transition temperature ranging from 10 to 90 °C. The reversible thermochromism below ambient condition is achieved via the combined molecular engineering at side chain moieties and PDA-conjugated backbone. The shortening of the side chain length at the tail position of the PDA provides a predictable reduction of the color-transition temperature, attributed to the decrease of dispersion interactions within the nanocomposite. On the other hand, it is rather difficult to predict the thermochromic behavior when the alkyl segment adjacent to the PDA headgroup is varied. This is mainly due to the variation in nature of local interactions between PDA headgroup and Zn^{2+} ion within the nanocomposite. The XRD and Raman spectroscopy also detect systematic changes of molecular tilting angle and backbone conformation within the bilayer structure when the side chain length is varied. Our major finding in this study provides a guideline for fabricating reversible thermochromic PDA-based materials with a wide range of color-transition temperature. This can extend their utilization in various applications such as colorimetric sensors, thermochromic inks/paints, and smart labels.

■ ASSOCIATED CONTENT

Supporting Information

The Supporting Information is available free of charge on the ACS Publications website at DOI: 10.1021/acsanm.9b00876.

Figure S1: XRD patterns of (a) DA(*x*,10)/Zn^{2+}/ZnO and (b) DA(8,*y*)/Zn^{2+}/ZnO nanocomposites. Figure S2: FT-IR spectra of (a) DA(8,*y*)/Zn^{2+}/ZnO and (b) DA(*x*,10)/Zn^{2+}/ZnO nanocomposites. The vibrational

DOI: 10.1021/acsanm.9b00876
ACS Appl. Nano Mater. XXXX, XXX, XXX−XXX

bands of $\nu_s(CH_2)$ and $\nu_{as}(CH_2)$ of all samples are detected at 2848 cm^{-1} and 2919 cm^{-1}, respectively, indicating the presence of all-trans conformation.[15,47] Figure S3: Absorption spectra upon heating of (a) PDA(8,10), (b) PDA(8,12), and (c) PDA(4,10)/Zn2^{+}/ZnO nanocomposites. Colorimetric response (CR) calculation. Figure S4: Change of %CR during 10 heating/cooling cycles between 25 °C and 90 °C of PDA(x,y)/Zn^{2+}/ZnO nanocomposites. Figure S5: Color transition of PDA(2,10)/Zn^{2+}/ZnO nanocomposite upon increasing or decreasing pH. The color transition is irreversible upon changing pH back to original pH 7. Figure S6: Color transition of PDA(2,10)/Zn^{2+}/ZnO nanocomposite upon addition of (top) propanol or (bottom) THF. When the solvents are removed by vacuum evaporation, the color does not reverse back to the original color. The corresponding absorption spectra are shown on the left. Figure S7: Absorption spectra upon heating of PDA(8,6)/Zn^{2+}/ZnO nanocomposite polymerized at (a) 2 and (b) 4 min. Figure S8: Absorption spectra upon heating of PDA(2,10)/Zn^{2+}/ZnO nanocomposite polymerized at (a) 2 and (b) 4 min. Figure S9: Color photographs taken upon heating and cooling the aqueous suspensions of varied polymerization time of PDA(2,10)/Zn^{2+}/ZnO nanocomposite (PDF)

AUTHOR INFORMATION

Corresponding Authors

*E-mail: Nisanart.T@chula.ac.th (N.T.).

*E-mail: Rakchart.tra@mahidol.ac.th (R.T.).

ORCID

Nisanart Traiphol: 0000-0002-1813-9284

Notes

The authors declare no competing financial interest.

ACKNOWLEDGMENTS

This research has been supported by the Thailand Research Fund [RSA 5980020]. This work has been partially supported by the National Nanotechnology Center (NANOTEC), NSTDA, Ministry of Science and Technology, Thailand, through its program of Research Network NANOTEC (RNN).

REFERENCES

(1) Qian, X.; Städler, B. Recent Developments in Polydiacetylene-Based Sensors. *Chem. Mater.* **2019**, *31*, 1196−1222.

(2) Wen, J. T.; Roper, J. M.; Tsutsui, H. Polydiacetylene Supramolecules: Synthesis, Characterization, and Emerging Applications. *Ind. Eng. Chem. Res.* **2018**, *57*, 9037−9053.

(3) Hu, B.; Sun, S.; Wu, B.; Wu, P. Colloidally Stable Monolayer Nanosheets with Colorimetric Responses. *Small* **2019**, *15*, 1804975.

(4) Mergu, N.; Kim, H.; Heo, G.; Son, Y.-A. Development of Naphthalimide-Functionalized Thermochromic Conjugated Polydiacetylenes and their Reversible Green-to-Red Chromatic Transition in the Solid State. *Dyes Pigm.* **2019**, *164*, 355−362.

(5) Khanantong, C.; Charoenthai, N.; Kielar, F.; Traiphol, N.; Traiphol, R. Influences of Bulky Aromatic Head Group on Morphology, Structure and Color-Transition Behaviors of Polydiacetylene Assemblies upon Exposure to Thermal and Chemical Stimuli. *Colloids Surf., A* **2019**, *561*, 226−235.

(6) Seetha, S.; Saymung, R.; Traiphol, R.; Traiphol, N. Controlling Self-Assembling and Color-Transition of Polydiacetylene/Zinc(II) ion/Zinc Oxide Nanocomposites by Varying pH: Effects of Surface Charge and Head Group Dissociation. *J. Ind. Eng. Chem.* **2019**, *72*, 423−431.

(7) Kim, M. J.; Angupillai, S.; Min, K.; Ramalingam, M.; Son, Y.-A. Tuning of the Topochemical Polymerization of Diacetylenes Based on an Odd/Even Effect of the Peripheral Alkyl Chain: Thermochromic Reversibility in a Thin Film and a Single-Component Ink for a Fountain Pen. *ACS Appl. Mater. Interfaces* **2018**, *10*, 24767−24775.

(8) Potai, R.; Faisadcha, K.; Traiphol, R.; Traiphol, N. Controllable Thermochromic and Phase Transition Behaviors of Polydiacetylene/Zinc(II) Ion/Zinc Oxide Nanocomposites via Photopolymerization: An Insight into the Molecular Level. *Colloids Surf., A* **2018**, *555*, 27−36.

(9) Oaki, Y.; Ishijima, Y.; Imai, H. Emergence of Temperature-Dependent and Reversible Colorchanging Properties by the Stabilization of Layered Polydiacetylene through Intercalation. *Polym. J.* **2018**, *50*, 319−326.

(10) Jeong, W.; Khazi, M. I.; Lee, D. G.; Kim, J.-M. Intrinsically Porous Dual-Responsive Polydiacetylenes Based on Tetrahedral Diacetylenes. *Macromolecules* **2018**, *51*, 10312−10322.

(11) Khanantong, C.; Charoenthai, N.; Phuangkaew, T.; Kielar, F.; Traiphol, N.; Traiphol, R. Phase Transition, Structure and Color-Transition Behaviors of Monocarboxylic Diacetylene and Polydiacetylene Assemblies: The Opposite Effects of Alkyl Chain Length. *Colloids Surf., A* **2018**, *553*, 337−348.

(12) Khanantong, C.; Charoenthai, N.; Wacharasindhu, S.; Sukwattanasinitt, M.; Traiphol, N.; Traiphol, R. Influences of Solvent Media on Chain Organization and Thermochromic Behaviors of Polydiacetylene Assemblies Prepared from Monomer with Symmetric Alkyl Tails. *J. Ind. Eng. Chem.* **2018**, *58*, 258−265.

(13) Nguyen, L. H.; Naficy, S.; McConchie, R.; Dehghani, F.; Chandrawati, R. Polydiacetylene-Based Sensors to Detect Food Spoilage at Low Temperatures. *J. Mater. Chem. C* **2019**, *7*, 1919−1926.

(14) Song, S.; Cho, H.-B.; Lee, H. W.; Kim, H. T. Onsite Paper-Type Colorimetric Detector with Enhanced Sensitivity for Alkali Ion via Polydiacetylene-Nanoporous Rice Husk Silica Composites. *Mater. Sci. Eng., C* **2019**, *99*, 900−904.

(15) Kew, S. J.; Hall, E. A. H. pH Response of Carboxy-Terminated Colorimetric Polydiacetylene Vesicles. *Anal. Chem.* **2006**, *78*, 2231−2238.

(16) Chanakul, A.; Traiphol, R.; Traiphol, N. Utilization of Polydiacetylene/Zinc Oxide Nanocomposites to Detect and Differentiate Organic Bases in Various Media. *J. Ind. Eng. Chem.* **2017**, *45*, 215−222.

(17) Chanakul, A.; Traiphol, R.; Traiphol, N. Colorimetric Sensing of Various Organic Acids by Using Polydiacetylene/Zinc Oxide Nanocomposites: Effects of Polydiacetylene and Acid Structures. *Colloids Surf., A* **2016**, *489*, 9−18.

(18) Chen, X.; Kang, S.; Kim, M. J.; Kim, J.; Kim, Y. S.; Kim, H.; Chi, B.; Kim, S. J.; Lee, J. Y.; Yoon, J. Thin-Film Formation of Imidazolium-Based Conjugated Polydiacetylenes and Their Application for Sensing Anionic Surfactants. *Angew. Chem., Int. Ed.* **2010**, *49*, 1422−1425.

(19) Lee, S.; Lee, K. M.; Lee, M.; Yoon, J. Polydiacetylenes Bearing Boronic Acid Groups as Colorimetric and Fluorescence Sensors for Cationic Surfactants. *ACS Appl. Mater. Interfaces* **2013**, *5*, 4521−4526.

(20) Shin, Y. J.; Shin, M. J.; Shin, J. S. Permeation-Induced Chromatic Change of a Polydiacetylene Vesicle with Nonionic Surfactant. *Colloids Surf., A* **2017**, *520*, 459−466.

(21) Rao, V. K.; Teradal, N. L.; Jelinek, R. Polydiacetylene Capacitive Artificial Nose. *ACS Appl. Mater. Interfaces* **2019**, *11*, 4470−4479.

(22) Terada, H.; Imai, H.; Oaki, Y. Visualization and Quantitative Detection of Friction Force by Self-Organized Organic Layered Composites. *Adv. Mater.* **2018**, *30*, 1801121.

(23) Wang, M.; Yu, Y.; Liu, F.; Ren, L.; Zhang, Q.; Zou, G. Single Polydiacetylene Microtube Waveguide Platform for Discriminating

DOI: 10.1021/acsanm.9b00876
ACS Appl. Nano Mater. XXXX, XXX, XXX−XXX

MicroRNA-215 Expression Levels in Clinical Gastric Cancerous, Paracancerous and Normal Tissues. *Talanta* **2018**, *188*, 27−34.
(24) Kamphan, A.; Gong, C.; Maiti, K.; Sur, S.; Traiphol, R.; Arya, D. P. Utilization of Chromic Polydiacetylene Assemblies as a Platform to Probe Specific Binding between Drug and RNA. *RSC Adv.* **2017**, *7*, 41435−41443.
(25) He, C.; Wang, M.; Sun, X.; Zhu, Y.; Zhou, X.; Xiao, S.; Zhang, Q.; Liu, F.; Yu, Y.; Liang, H.; Zou, G. Integrating PDA Microtube Waveguide System with Heterogeneous CHA Amplification Strategy towards Superior Sensitive Detection of miRNA. *Biosens. Bioelectron.* **2019**, *129*, 50−57.
(26) Jung, Y. K.; Park, H. G. Colorimetric Polydiacetylene (PDA) Liposome-Based Assay for Rapid and Simple Detection of GST-fusion Protein. *Sens. Actuators, B* **2019**, *278*, 190−195.
(27) Yu, L.; Hsu, S. L. A Spectroscopic Analysis of the Role of Side Chains in Controlling Thermochromic Transitions in Polydiacetylenes. *Macromolecules* **2012**, *45*, 420−429.
(28) Pang, J.; Yang, L.; McCaughey, B. F.; Peng, H.; Ashbaugh, H. S.; Brinker, C. J.; Lu, Y. Thermochromatism and Structural Evolution of Metastable Polydiacetylenic Crystals. *J. Phys. Chem. B* **2006**, *110*, 7221−7225.
(29) Lifshitz, Y.; Golan, Y.; Konovalov, O.; Berman, A. Structural Transitions in Polydiacetylene Langmuir Films. *Langmuir* **2009**, *25*, 4469−4477.
(30) Fujimori, A.; Ishitsuka, M.; Nakahara, H.; Ito, E.; Hara, M.; Kanai, K.; Ouchi, Y.; Seki, K. Formation of the Newly Greenish Organized Molecular Film of Long-Chain Diynoic Acid Derivatives by Photopolymerization and Its Structural Study Using Near-Edge X-ray Absorption Fine Structure (NEXAFS) Spectroscopy. *J. Phys. Chem. B* **2004**, *108*, 13153−13162.
(31) Takeuchi, M.; Gnanasekaran, K.; Friedrich, H.; Imai, H.; Sommerdijk, N. A. J. M.; Oaki, Y. Tunable Stimuli-Responsive Color-Change Properties of Layered Organic Composites. *Adv. Funct. Mater.* **2018**, *28*, 1804906.
(32) Mapazi, O.; Matabola, K. P.; Moutloali, R. M.; Ngila, C. J. High Temperature Thermochromic Polydiacetylene Supported on Polyacrylonitrile Nanofibers. *Polymer* **2018**, *149*, 106−116.
(33) Wacharasindhu, S.; Montha, S.; Boonyiseng, J.; Potisatityuenyion, A.; Phollookin, C.; Tumcharern, G.; Sukwattanasinitt, M. Tuning of Thermochromic Properties of Polydiacetylene toward Universal Temperature Sensing Materials through Amido Hydrogen Bonding. *Macromolecules* **2010**, *43*, 716−724.
(34) Phollookin, C.; Wacharasindhu, S.; Ajavakom, A.; Tumcharern, G.; Ampornpun, S.; Eaidkong, T.; Sukwattanasinitt, M. Tuning Down of Color Transition Temperature of Thermochromically Reversible Bisdiynamide Polydiacetylenes. *Macromolecules* **2010**, *43*, 7540−7548.
(35) Ampornpun, S.; Montha, S.; Tumcharern, G.; Vchirawongkwin, V.; Sukwattanasinitt, M.; Wacharasindhu, S. Odd−Even and Hydrophobicity Effects of Diacetylene Alkyl Chains on Thermochromic Reversibility of Symmetrical and Unsymmetrical Diyndiamide Polydiacetylenes. *Macromolecules* **2012**, *45*, 9038−9045.
(36) Lee, S.; Lee, J.; Lee, M.; Cho, Y. K.; Baek, J.; Kim, J.; Park, S.; Kim, M. H.; Chang, R.; Yoon, J. Construction and Molecular Understanding of an Unprecedented, Reversibly Thermochromic Bis-Polydiacetylene. *Adv. Funct. Mater.* **2014**, *24*, 3699−3705.
(37) Ahn, D. J.; Lee, S.; Kim, J. M. Rational Design of Conjugated Polymer Supramolecules with Tunable Colorimetric Responses. *Adv. Funct. Mater.* **2009**, *19*, 1483−1496.
(38) Ye, Q.; You, X.; Zou, G.; Yu, X.; Zhang, Q. Morphology, Structure and Chromatic Properties of Azobenzene-Substituted Polydiacetylene Supramolelular Assemblies. *J. Mater. Chem.* **2008**, *18*, 2775−2780.
(39) Kim, J.-M.; Lee, J.-S.; Choi, H.; Sohn, D.; Ahn, D. J. Rational Design and in-Situ FTIR Analyses of Colorimetrically Reversibe Polydiacetylene Supramolecules. *Macromolecules* **2005**, *38*, 9366−9376.
(40) Takeuchi, M.; Imai, H.; Oaki, Y. Effects of the Intercalation Rate on the Layered Crystal Structures and Stimuli-Responsive Color-Change Properties of Polydiacetylene. *J. Mater. Chem. C* **2017**, *5*, 8250−8255.
(41) Traiphol, N.; Rungruangviriya, N.; Potai, R.; Traiphol, R. Stable Polydiacetylene/ZnO Nanocomposites with Two-Steps Reversible and Irreversible Thermochromism: The Influence of Strong Surface Anchoring. *J. Colloid Interface Sci.* **2011**, *356*, 481−489.
(42) Chanakul, A.; Traiphol, N.; Traiphol, R. Controlling the Reversible Thermochromism of Polydiacetylene/Zinc Oxide Nanocomposites by Varying Alkyl Chain Length. *J. Colloid Interface Sci.* **2013**, *389*, 106−114.
(43) Shin, H.; Yoon, B.; Park, I. S.; Kim, J.-M. An Electrothermochromic Paper Display Based on Colorimetrically Reversible Polydiacetylenes. *Nanotechnology* **2014**, *25*, No. 094011.
(44) Yoon, B.; Lee, J.; Park, I. S.; Jeon, S.; Lee, J.; Kim, J.-M. Recent Functional Material Based Approaches to Prevent and Detect Counterfeiting. *J. Mater. Chem. C* **2013**, *1*, 2388−2403.
(45) Varghese Hansen, R.; Zhong, L.; Khor, K. A.; Zheng, L.; Yang, J. Tuneable Electrochromism in Weavable Carbon Nanotube/Polydiacetylene Yarns. *Carbon* **2016**, *106*, 110−117.
(46) Takeuchi, M.; Imai, H.; Oaki, Y. Real-Time Imaging of 2D and 3D Temperature Distribution: Coating of Metal-Ion-Intercalated Organic Layered Composites with Tunable Stimuli-Responsive Properties. *ACS Appl. Mater. Interfaces* **2017**, *9*, 16546−16552.
(47) Huang, X.; Jiang, S.; Liu, M. Metal Ion Modulated Organization and Function of the Langmuir-Blodgett Films of Amphiphilic Diacetylene: Photopolymerization, Thermochromism, and Supramolecular Chirality. *J. Phys. Chem. B* **2005**, *109*, 114−119.
(48) Traiphol, N.; Chanakul, A.; Kamphan, A.; Traiphol, R. Role of Zn^{2+} Ion on the Formation of Reversible Thermochromic Polydiacetylene/Zinc Oxide Nanocomposites. *Thin Solid Films* **2017**, *622*, 122−129.
(49) Traiphol, N.; Faisadcha, K.; Potai, R.; Traiphol, R. Fine Tuning the Color-Transition Temperature of Thermoreversible Polydiacetylene/Zinc Oxide Nanocomposites: The Effect of Photopolymerization Time. *J. Colloid Interface Sci.* **2015**, *439*, 105−111.
(50) Park, I. S.; Park, H. J.; Kim, J.-M A Soluble, Low-Temperature Thermochromic and Chemically Reactive Polydiacetylene. *ACS Appl. Mater. Interfaces* **2013**, *5*, 8805−8812.
(51) Park, I. S.; Park, H. J.; Jeong, W.; Nam, J.; Kang, Y.; Shin, K.; Chung, H.; Kim, J.-M. Low Temperature Thermochromic Polydiacetylenes: Design, Colorimetric Properties, and Nanofiber Formation. *Macromolecules* **2016**, *49*, 1270−1278.
(52) Rougeau, L.; Picq, D.; Rastello, M.; Frantz, Y. New Irreversible Thermochromic Polydiacetylenes. *Tetrahedron* **2008**, *64*, 9430−9436.
(53) Nagarajan, R. Molecular Packing Parameter and Surfactant Self-Assembly: The Neglected Role of the Surfactant Tail. *Langmuir* **2002**, *18*, 31−38.
(54) Guo, C.; Xue, J. D.; Cheng, L. X.; Liu, R. C.; Kang, S. Z.; Zeng, Q. D.; Li, M. Two Dimensional Self-Assembly of Diacetylenic Acid Derivatives and their Light-Induced Polymerization on HOPG Surfaces. *Phys. Chem. Chem. Phys.* **2017**, *19*, 16213−16218.
(55) Villarreal, T. A.; Russell, S. R.; Bang, J. J.; Patterson, J. K.; Claridge, S. A. Modulating Wettability of Layered Materials by Controlling Ligand Polar Headgroup Dynamics. *J. Am. Chem. Soc.* **2017**, *139*, 11973−11979.
(56) Chanakul, A.; Traiphol, N.; Faisadcha, K.; Traiphol, R. Dual Colorimetric Response of Polydiacetylene/ZnO Nanocomposites to Low and High pH. *J. Colloid Interface Sci.* **2014**, *418*, 43−51.
(57) Toommee, S.; Traiphol, R.; Traiphol, N. High Color Stability and Reversible Thermochromism of Polydiacetylene/Zinc Oxide Nanocomposite in Various Organic Solvents and Polymer Matrices. *Colloids Surf., A* **2015**, *468*, 252−261.
(58) Kamphan, A.; Traiphol, N.; Traiphol, R. Versatile Route to Prepare Reversible Thermochromic Polydiacetylene Nanocomposite Using Low Molecular Weight Poly(vinylpyrrolidone). *Colloids Surf., A* **2016**, *497*, 370−377.

DOI: 10.1021/acsanm.9b00876
ACS Appl. Nano Mater. XXXX, XXX, XXX−XXX

Journal of Industrial and Engineering Chemistry 72 (2019) 423–431

Contents lists available at ScienceDirect

Journal of Industrial and Engineering Chemistry

journal homepage: www.elsevier.com/locate/jiec

Controlling self-assembling and color-transition of polydiacetylene/zinc(II) ion/zinc oxide nanocomposites by varying pH: Effects of surface charge and head group dissociation

Supakorn Seetha[a], Rungarune Saymung[b,d], Rakchart Traiphol[b,d], Nisanart Traiphol[a,c,e,*]

[a] Laboratory of Advanced Chromic Materials, Department of Materials Science, Faculty of Science, Chulalongkorn University, Bangkok 10330, Thailand
[b] Laboratory of Advanced Polymers and Nanomaterials, School of Materials Science and Innovation, Faculty of Science, Mahidol University at Salaya, Phuttamonthon 4 Road, Nakhon Pathom 73170, Thailand
[c] Center of Excellence on Petrochemical and Materials Technology, Chulalongkorn University, Bangkok 10330, Thailand
[d] NANOTEC-MU Center of Excellence on Food and Agriculture, Faculty of Science, Mahidol University, Rama 6 Road, Ratchathewi, Bangkok 10400, Thailand
[e] NANOTEC-CU Center of Excellence on Food and Agriculture, Department of Chemistry, Faculty of Science, Chulalongkorn University, Bangkok 10330, Thailand

ARTICLE INFO

Article history:
Received 16 October 2018
Received in revised form 3 November 2018
Accepted 27 December 2018
Available online 30 December 2018

Keywords:
Polydiacetylene
Color transition
Sensor
Self-assembling
Surface charge
Dissociation

ABSTRACT

Polydiacetylene/zinc(II) ion/zinc oxide (PDA/Zn^{2+}/ZnO) nanocomposite exhibits reversible thermochromism and dual colorimetric response to acid/base. This contribution presents our ongoing development of the PDA/Zn^{2+}/ZnO nanocomposite for sensing applications by controlling ZnO surface charge and dissociation of PDA headgroup via pH adjustment. At pH >10, negative ZnO surface charge and PDA carboxylate headgroup significantly enhance molecular organization during the self-assembling process. An increase of the nanocomposite amount after photopolymerization is observed. Oppositely, pH <6 results in irreversible-thermochromic nanocomposites. Additionally, the nanocomposites prepared at different pH change color at different concentrations of chemical stimuli. Molecular packing, local interactions and PDA conformation are investigated.

Introduction

Stimuli-responsive polydiacetylenes (PDA) have shown a potential for being utilized in various applications such as thermal, chemical, biological and friction force sensors [1–16], sweat pore mapping [17], electro-thermochromic displays [18], counterfeiting materials [19], photodetectors [20] and smart textiles [21]. The preparation of PDA-based materials generally involves the self-assembling of diacetylene (DA) monomer into organized structures, following by topotactic polymerization via UV light irradiation [1,11,12]. The process yields a metastable state of PDA exhibiting a deep blue color. Upon subjected to external stimuli such as heat [4,11–13], solvents [5,7,14,15], acids/bases [11,22–25] and mechanical stress [8], the PDA side chain and/or conjugated backbone relax to a stable state. Segmental rearrangement during the relaxation process affects the conjugation length within the system, which causes the color transition, normally, from blue to red [26–28].

In order to control the color-transition behaviors of PDAs, chemical modification of the DA headgroup and/or side chain has been widely studied [1,3,4,6,7,9,11,13,16,29–35]. The method provides PDA-based materials with controllable color-transition temperature and reversible thermochromism in some cases [3,9,11,13,29–35]. This approach also allows molecular engineering to achieve specific interactions between PDAs and targeted chemical stimuli and biomolecules [1,4,6,16]. However, complicate, multi-step and time-consuming processes along with expensive chemicals and/or catalysts are usually required. Our research group has introduced a simple and cost-effective method to control color-transition behaviors of PDA by incorporating zinc oxide (ZnO) nanoparticles into the PDA assemblies [12,23–25,36–40]. The recent work by our group reveals that, in aqueous suspension, Zn^{2+} ions released from ZnO nanoparticles intercalate into the PDA bilayers [12,40]. This process yields strong interfacial interactions between PDA headgroups and ZnO nanoparticles.

The resulting PDA/Zn^{2+}/ZnO nanocomposite exhibits higher color-transition temperature comparing to pure PDA prepared from the same DA monomer [36,37]. The relatively strong overall

* Corresponding author at: Laboratory of Advanced Chromic Materials, Department of Materials Science, Faculty of Science, Chulalongkorn University, Bangkok 10330, Thailand.
E-mail address: Nisanart.T@chula.ac.th (N. Traiphol).

https://doi.org/10.1016/j.jiec.2018.12.045
1226-086X/

interactions within this system also provide reversible thermochromism. We further demonstrate that color-transition temperature of the nanocomposite can be tuned by varying alkyl side chain and backbone length of PDA [12,37,38]. In addition, the presence of ZnO nanoparticles allows dual colorimetric response of the nanocomposite to both acid and base [25]. This unprecedented behavior extends their utilization as colorimetric sensors for detecting various organic acids or bases dissolved in different media such as water, toluene and milk [23,24].

In this continuing study, we explore the roles of PDA headgroup dissociation and ZnO surface charge on the formation of nanocomposite and its properties. Upon increasing pH, carboxylic headgroup of the DA monomer, 10,12-tricosadiynoic acid (TCDA), can be converted to negatively charged carboxylate ones (Fig. 1) [22]. Surface charge of ZnO nanoparticles is also affected by pH variations (Fig. 1s, Supporting information). At pH 7, the ZnO surface charge is positive, then the value decreases and reaches isoelectric point at pH 8. In the higher pH region, the ZnO surface charge becomes negative. We hypothesize that the variations of pH during the preparation process could affect the strength of local interfacial interactions within the nanocomposite, and, hence, its color-transition behaviors. In this work, we prepare the PDA/Zn^{2+}/ZnO nanocomposites at pH ranging from 4 to 13. We have found that color-transition behaviors of the obtained nanocomposites upon exposure to heat, acid or base can be controlled by adjusting the pH during preparation. Origins of this behavior are elucidated by utilizing various techniques including X-ray diffraction, infrared and Raman spectroscopy.

Experimental

The TCDA monomer and ZnO nanoparticles were purchased from Fluka and Nano Materials Technology (Thailand), respectively. The ZnO diameter ranges from about 20 to 200 nm with the averaged value of about 65 nm [12]. Zeta potential of the ZnO nanoparticles in an aqueous suspension was measured at various pH using Brookhaven, ZetaPaLs. The preparation of poly(TCDA)/Zn^{2+}/ZnO nanocomposite was slightly modified from the procedure described in our previous works [36,37]. The concentration of TCDA was 1.0 mM and the ratio of ZnO to TCDA was 10 wt.% in all experiments. The mixtures were co-dispersed in aqueous medium by ultrasonication. HCl and NaOH solutions were used to adjust the pH of suspension during the mixing process. After incubation at 4 °C overnight, topotactic polymerization of the organized TCDA was performed by UV light irradiation (λ = 254 nm, 10 watts) for 4 min to obtain blue-phase poly(TCDA)/Zn^{2+}/ZnO nanocomposite. For comparison purpose, the pure poly(TCDA) was prepared employing the same procedure excepting the addition of ZnO nanoparticles.

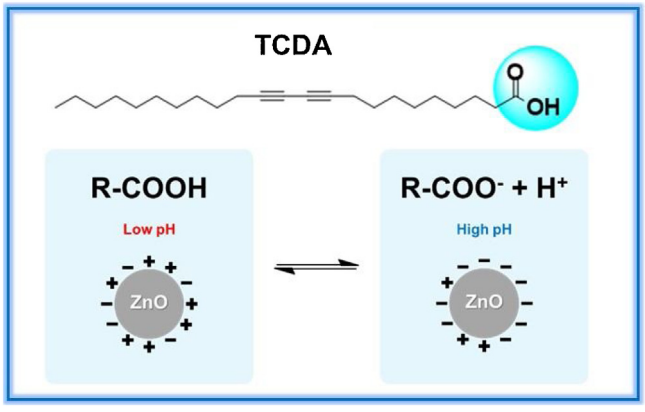

Fig. 1. Chemical structure of 10,12-tricosadiynoic acid (TCDA), its dissociation and surface charge of ZnO nanoparticles at low and high pH regions.

Particle size distribution of the pure poly(TCDA) and poly(TCDA)/Zn^{2+}/ZnO nanocomposite was obtained using dynamic light scattering technique (Brookhaven, ZetaPaLs). Absorption spectra were measured using a UV–vis spectrophotometer equipped with a temperature-control unit (Analytik Jena Specord S100). For determination of relative concentration of the nanocomposite, the absorbance (λ = 640 nm) obtained at pH 7 was used to normalize the absorbance obtained from the other conditions. FT-IR spectra were measured using Nicolet 6700 FT-IR spectrometer in a transmittance mode. Raman spectra were obtained using FT-Raman spectrometer (PerkinElmer Spectrum GX) with a 1064 nm laser (Nd: YAG) as an excitation source. Structure of the nanocomposite was studied using X-ray diffractometer (XRD) (Bruker AXS Model D8 Discover, $\lambda(Cu–K_\alpha)$ = 1.54 Å). Dried samples for these measurements were obtained by drop casting onto glass slides.

Results and discussion

Effects of pH on self-assembling behaviors

It is known that the aqueous suspension of ZnO nanoparticles at equilibrium state contains $Zn^{2+}{}_{(aq)}$, $Zn(OH)^{+}{}_{(aq)}$, $Zn(OH)_{2(aq)}$, $Zn(OH)_3{}^{-}{}_{(aq)}$, and $Zn(OH)_4{}^{2-}{}_{(aq)}$ species [41]. Concentration of these species absorbed onto the surface of ZnO nanoparticle gives rise to its surface charge, which strongly depends on pH of the suspension (Fig. 1s, Supporting information). ZnO surface charge is highly positive when pH is at 7, then, it converts to negative when pH is above 8. When mixing the pH-adjusted ZnO suspension with the TCDA monomer, the dissociation of carboxylic headgroup (—COOH) of the TCDA also involves. Previous study by Kew and Hall showed that the pKa of TCDA monomer ranged from 9.5 to 9.9 [22]. Based on this pKa value, the concentration of carboxylate ion, [—COO^-], in the suspension can be evaluated at specified pH (Fig. 2s, Supporting information). The —COOH group begins to dissociate around pH 8, then, [—COO^-] sharply increases with increasing pH from 8 to 11 and reaches 99% at pH 12.

The variation of pH strongly affects the self-assembling of TCDA monomer onto the ZnO nanoparticles. Fig. 2(a) illustrates the absorption spectra of poly(TCDA)/Zn^{2+}/ZnO nanocomposites prepared at different pH. A normal preparing condition (pH 7) provides an intense blue color suspension. When adjusting pH to 11, a large fraction of the —COOH headgroup is converted to the —COO^-, meanwhile, the surface charge of ZnO nanoparticles becomes highly negative. The suspension with more intense blue color is obtained. It is known that the topotactic photopolymerization of PDA materials requires specific arrangement of the diacetylene moieties within the assemblies [9,42]. Therefore, our observation indicates that increasing pH promotes the molecular ordering of TCDA monomer resulting in the increase of percent conversion to poly(TCDA) with blue color. The absorption spectrum of the suspension prepared at pH 11 is similar to that of pH 7. However, further increase of pH to 13, a suspension with intense red color is obtained with the λ_{max} shifted to 550 nm. The formation of a red-phase material at the high pH condition indicates the change of molecular arrangement within poly(TCDA) assemblies as described in a literature [26]. The dissolution of ZnO nanoparticles occurred at pH 13 as reported in our previous study [25] could be responsible for the formation of red-phase material. To investigate this hypothesis, samples are prepared at pH 6 and 4, in which the dissolution of ZnO nanoparticles also occurs. However, intense blue color suspensions are obtained at these conditions with small fraction of red phase indicated by a small peak at 550 nm in the absorption spectra. This result suggests that

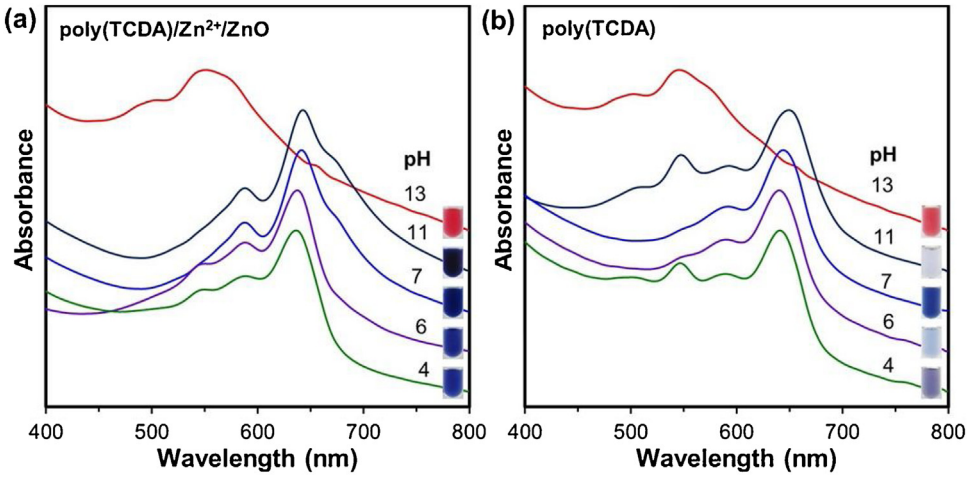

Fig. 2. Normalized absorption spectra of (a) poly(TCDA)/Zn^{2+}/ZnO nanocomposites and (b) pure poly(TCDA) assemblies prepared at various pH. (inset) Color photographs of as-prepared samples in aqueous suspensions.

the dissolution of ZnO nanoparticles exhibits a minor effect on this phenomenon.

The preparation of pure poly(TCDA) at the normal condition (pH 7) provides a blue suspension with less intense color compared to that of the nanocomposite. When the preparation process takes place at pH 11, 6 and 4, the blue color of pure poly (TCDA) drastically fades as shown in Fig. 2(b). It indicates that only a small fraction of TCDA monomer is converted to poly (TCDA). Comparing between poly(TCDA) and poly(TCDA)/Zn^{2+}/ZnO, our results illustrates that the presence of ZnO nanoparticles promotes the molecular organization of TCDA monomer. This attributes to strong interactions between —COOH and/or —COO^- headgroups of TCDA monomer and Zn^{2+}/ZnO surface. The increase of pH to 11 results in the increase of —COO^- fraction, which, in turn, increases the strength of local interactions with Zn^{2+}/ZnO surface. Our result also shows that the incorporation of ZnO nanoparticles allows the preparation of PDA-based materials at relatively high and low pH conditions, which could extend their utilization in many applications. It is worthwhile to note that the preparation of pure poly(PCDA) at pH 13 provides an intense red color suspension similar to the system of the nanocomposite. Therefore, the formation of red phase is likely to arise from the complete dissociation of the —COOH headgroup. A previous study by Pang et al. also provided a red phase PDA when adding a large amount of NaOH to the system during the preparation process [26]. The authors observed the intercalation of Na^+ ions with bilayer of PDA, which altered the molecular packing within the assemblies.

We further investigate the relative concentration of the nanocomposite prepared at various pH. Absorbance of the blue phase at 640 nm, proportional to concentration of the nanocomposite, is determined for each preparing condition. The result is normalized by absorbance value obtained at pH 7. The plot between relative concentration of the nanocomposite and preparing pH is illustrated in Fig. 3. The increase of pH from 7 to 9 hardly affects concentration of the nanocomposite. When the pH is further increased to 10, concentration of the nanocomposite abruptly increases. At pH 11, it increases up to twice the value of the one prepared at pH 7. The increase of nanocomposite concentration at this pH range is parallel to the increase of —COO^- group concentration. This observation signifies the role of —COO^- group on the self-assembling behavior within the nanocomposites. It is worthwhile to note that the decrease of pH to 6 results in a significant decrease of the nanocomposite

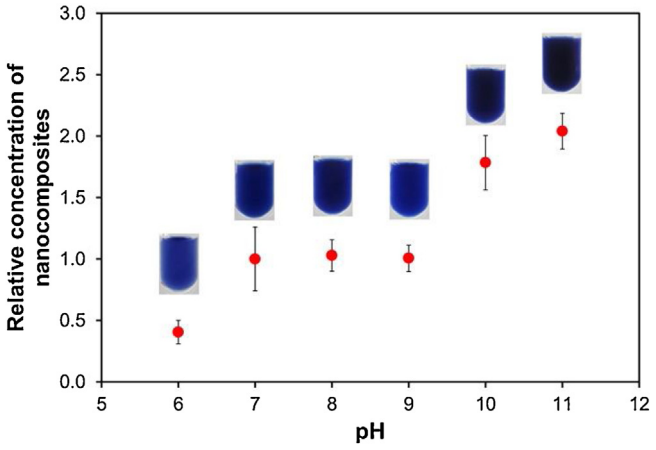

Fig. 3. Relative concentration and color photographs of poly(TCDA)/Zn^{2+}/ZnO nanocomposites prepared at various pHs. Average values and error bars were obtained from 5 batches.

concentration. This is due to partial dissolution of ZnO nanoparticles in acidic condition [25]. The variation of preparing pH slightly affects the particle size of assemblies (Fig. 3s, Supporting information).

Packing structure, interfacial interaction and molecular conformation

In this section, the molecular organization within assemblies is probed using various techniques. Dried films of all samples were prepared by drop casting on glass slides. Fig. 4(a) illustrates XRD patterns of the pure poly(TCDA) assembly comparing to the poly (TCDA)/Zn^{2+}/ZnO nanocomposites prepared at various pH. It has been reported in literatures that this class of material exhibits a bilayer lamellar structure [26,28,43,44]. The XRD pattern of pure poly(TCDA) exhibits three peaks corresponding to diffraction planes of the lamellar structure. An interlayer lamellar d-spacing of poly(TCDA) is 4.16 nm (Fig. 4s, Supporting information). The XRD pattern of nanocomposite prepared at pH 7 exhibits five peaks. The detection of additional two diffraction peaks indicates the increase of molecular ordering within the nanocomposite. In addition, the interlayer d-spacing increases to 5.03 nm, indicating the intercalation of Zn^{2+} ions within the bilayer of poly(TCDA) as shown in Fig. 4(b). Since the ionic diameter of Zn^{2+} ion is rather small

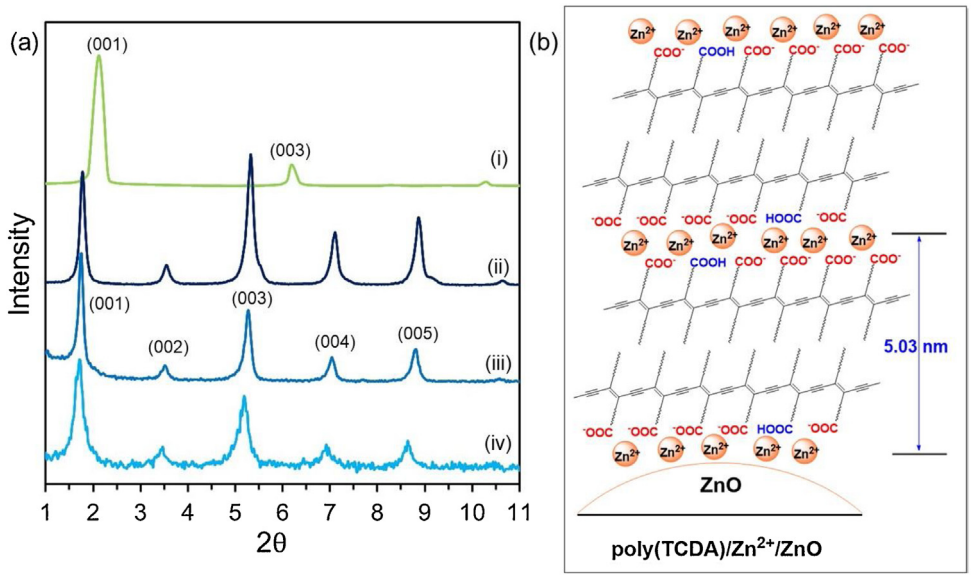

Fig. 4. (a) XRD pattern of (i) pure poly(TCDA) and poly(TCDA)/Zn^{2+}/ZnO nanocomposites prepared at (ii) pH 11, (iii) pH 7 and (iv) pH 4. (b) Molecular packing models of poly (TCDA)/Zn^{2+}/ZnO nanocomposite.

(~0.18 nm), the intercalation is not a sole contribution to the increase of interlayer d-spacing. Tilting angle of the poly(TCDA) alkyl side chain with respect to the plane of lamellar layer might also increase as described in previous studies [43,44]. We note that the Zn^{2+} ions in our system release from the ZnO nanoparticle during the preparation process [40]. The intercalated structure with comparable interlamellar d-spacing value is also observed for the nanocomposite prepared at pH 11. It is important to point out that the ZnO nanoparticle mostly dissolves at pH 4 [25]. However, the packing structure similar to the other conditions is still attained.

Fig. 5(a) shows FT-IR spectra of pure poly(TCDA) comparing to those of poly(TCDA)/Zn^{2+}/ZnO nanocomposites prepared at various pH. The spectrum of pure poly(TCDA) exhibits a broad band near 1693 cm^{-1} assigned to hydrogen-bonded carbonyl stretching of the —COOH headgroup [22]. The peaks around 1470–1420 cm^{-1} are due to the methylene scissoring vibration of alkyl side chain. For the nanocomposite prepared at pH 7, new peaks at 1540 and 1398 cm^{-1} are clearly observed corresponding to the asymmetric and symmetric stretching vibrations, respectively, of the carboxylate anion coordinated with Zn^{2+} cation as illustrated in Fig. 5(b) [40,46]. The nanocomposite prepared at pH 11 exhibits a similar FT-IR pattern. Additionally, a new peak at 1560 cm^{-1} is detected corresponding to the presence of strong interaction between the carboxylate anion and Na^{+} cation [45]. This observation suggests that the pH modification using NaOH also incorporates Na^{+} ion into the bilayer structure (Fig. 5(b)). Partial dissolution of ZnO nanoparticles occurs at pH 6, 5 and 4. At these conditions, the growth of broad band at 1618 cm^{-1} is detected. It is known that the vibrational frequency of carboxylate anion varies with the strength of local interaction with cation [46]. Since our system does not contain any other cations, this peak is assigned to a new type of the Zn^{2+}-coordinated carboxylate group (Fig. 5(b)) with different strength of local interaction from the one detected at 1540 cm^{-1}. We note that the peak of hydrogen bonded —COOH group at 1693 cm^{-1} reappears at pH 4, attributed to the protonation of HCl acid. Our FT-IR results indicate that the variation of preparing pH strongly affects the strength of local interactions within the nanocomposites.

Conformational change of conjugated backbone and alkyl side chain of the poly(TCDA)/Zn^{2+}/ZnO nanocomposites is explored by Raman spectroscopy. It is known that the C≡C and C=C stretching modes of PDA conjugated backbone in a blue phase occur at ~2080 and ~1450 cm^{-1}, respectively [12,45,47–50]. Perturbation of PDA assemblies by thermal treatment usually induces the relaxation of conjugated backbone and side chain, causing the color transition to red phase. The C≡C and C=C stretching modes in the new local environments shift to ~2116 and ~1511 cm^{-1}, respectively [12,45]. The Raman bands in the region of 1150–1000 cm^{-1} also provide useful information about the conformation of alkyl side chain [51,52]. Previous study by Park et al. showed that the Raman spectrum of crystalline DA monomer exhibited several sharp peaks in this region, corresponding to *all-trans* conformation of the long alkyl side chain [51]. The DA monomer in melted state, on the other hand, showed a rather broad peak, indicating the presence of some *gauche* conformation.

Raman spectra of the nanocomposites prepared at pH 7 and 11 show strong peaks at 2076 and 1450 cm^{-1} indicating a backbone conformation in blue phase (Fig. 6(a)). The detection of sharp peaks at 1123, 1101, 1082, 1065 and 1050 cm^{-1} also suggests the presence of *all-trans* conformation of the alkyl side chain. For the system of nanocomposite prepared at pH 6, a growth of new peaks at 2097 and 1478 cm^{-1} is detected, corresponding to the stretching vibration of the C≡C and C=C bonds, respectively. The result indicates that a large fraction of PDA conjugated backbone relaxes into a new local environment. The new PDA conformation is an intermediate state between the commonly known blue and red phases. This observation is consistent with the results obtained from FT-IR study, in which, two types of Zn^{2+}-coordinated carboxylate group are detected at this preparing condition. We believe that the partial dissolution of ZnO nanoparticles at pH 6 reduces the strength of interfacial interactions within the nanocomposite, allowing partial relaxation of conjugated backbone. The intermediate phase of PDA backbone was also observed in our previous study, in which, the nanocomposites were prepared by increasing photopolymerization time [12]. The presence of this intermediate phase significantly affects their color-transition behaviors.

The preparation of nanocomposites at pH 5 and 4 induces further relaxation of conjugated backbone. An additional peak at 1500 cm^{-1} is detected at preparing condition of pH 5. Decreasing pH to 4 causes a growth of two peaks at 2114 and 1512 cm^{-1},

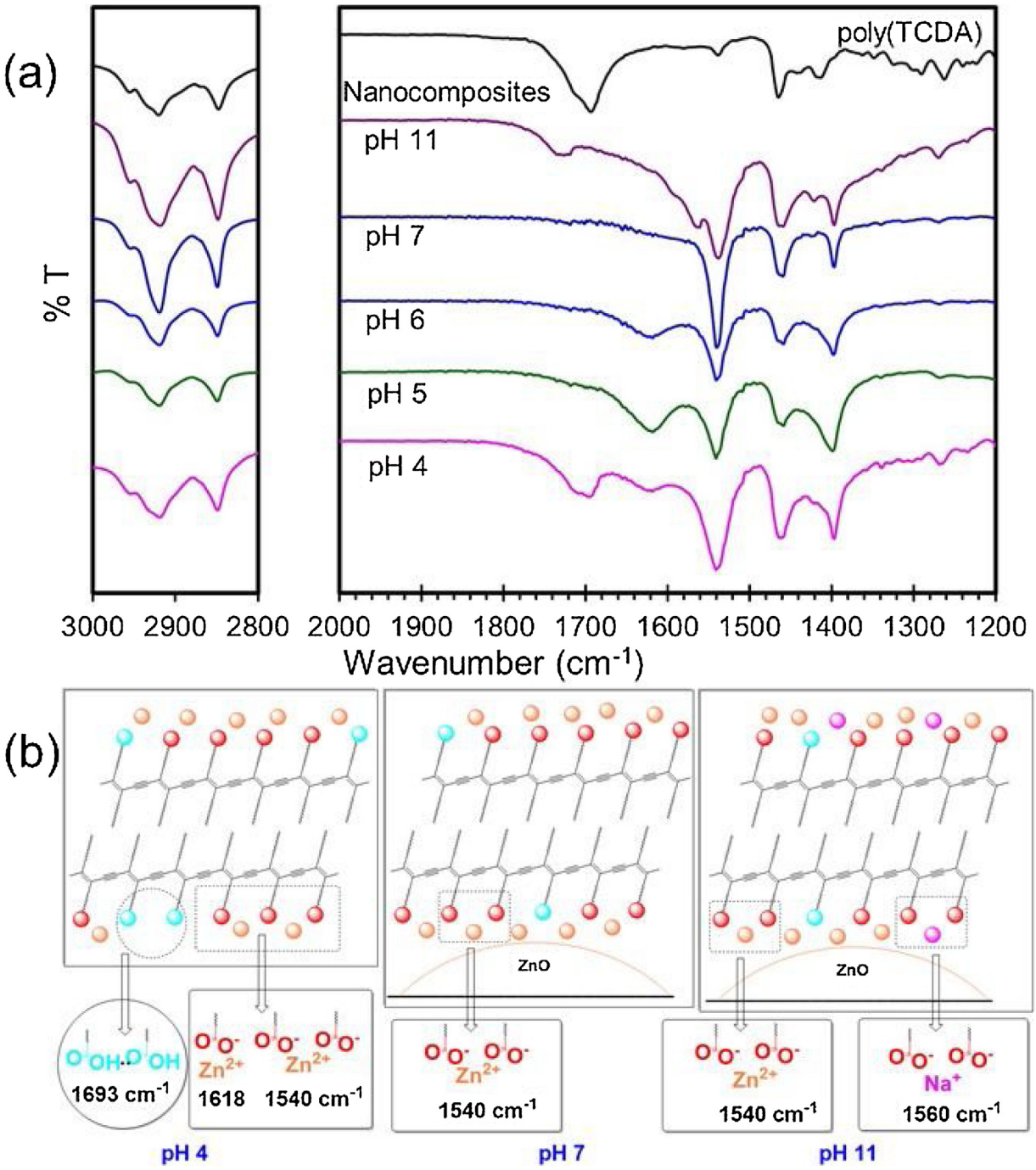

Fig. 5. (a) FT-IR spectra of pure poly(TCDA) and poly(TCDA)/Zn^{2+}/ZnO nanocomposites prepared at pH 11, pH 7, pH 6, pH 5 and pH 4. (b) Models for local molecular interactions within the nanocomposites prepared at pH 4, pH 7 and pH 11.

indicating partial relaxation of some conjugated backbone into the red phase. Previous studies by X-ray scattering detected the shrinkage of unit cell during the blue-to-red color transition, where the stacking distance between conjugated backbones was reduced (Fig. 6(a), bottom) [27,28]. The conformational change of alkyl side chain is also detected. The sharp peaks in the region of 1150–1000 cm^{-1} merge together, becoming a broad peak at 1065 cm^{-1}. The observation of broad peak in this region indicates the presence of some *gauche* conformation within the alkyl side chain as illustrated in Fig. 6(a, b). We suggest that the strength of interfacial interactions is further reduced at preparing condition of pH 4. This allows the relaxation of some conjugated backbone into the red phase and causes the conformational change of alkyl side chain. It is worthwhile to note that the XRD results in Fig. 4 do not detect any change of the interlamellar d-spacing. The change of molecular packing structure is likely to take place at different length scale.

Colorimetric response to temperature, acid and base

The variation of preparing pH significantly affects the strength of inter-/intramolecular interactions and molecular conformation within the nanocomposites, causing a drastic change of their thermochromic behaviors. Fig. 7(a, b) show temperature-

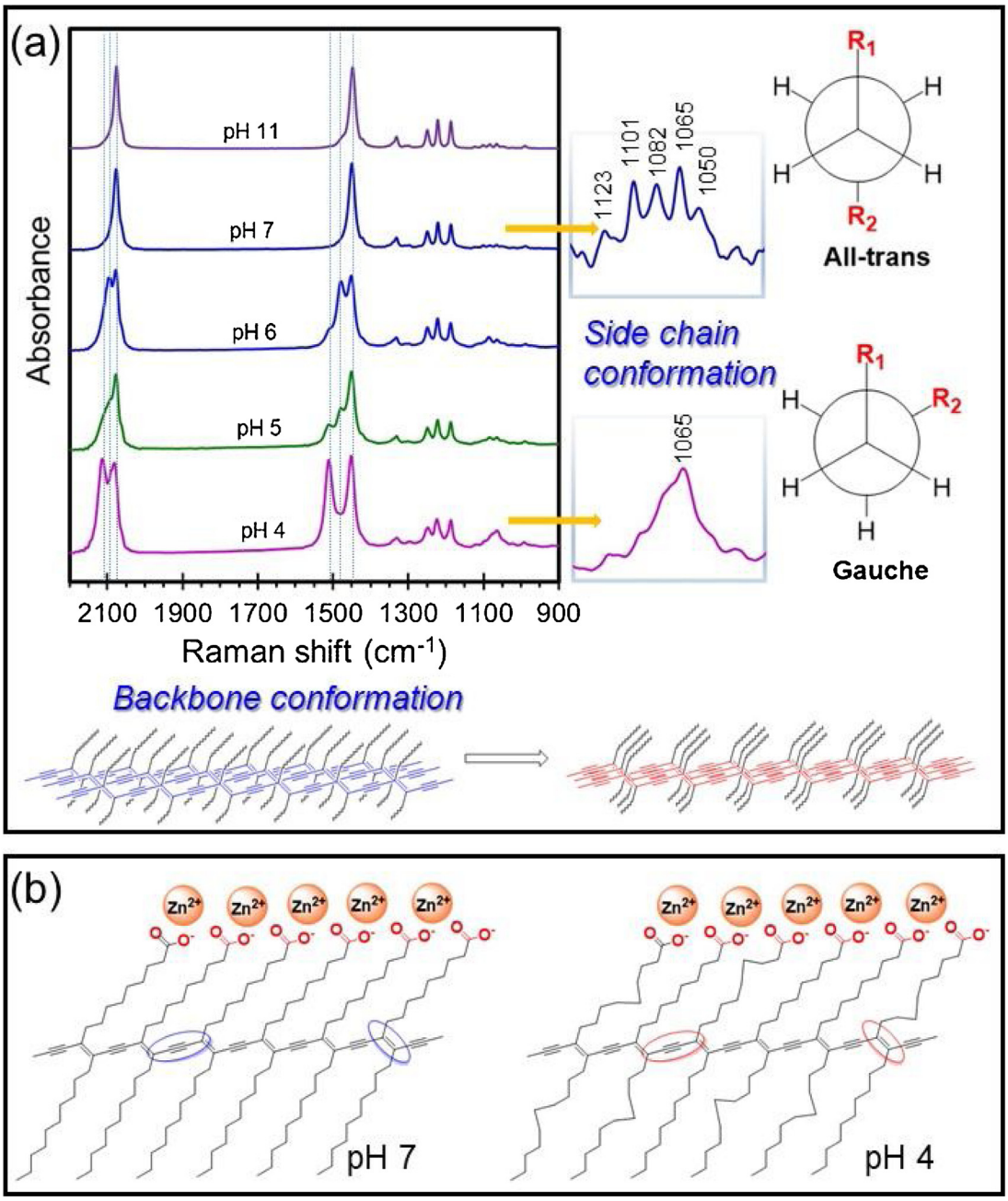

Fig. 6. (a) Raman spectra of poly(TCDA)/Zn^{2+}/ZnO nanocomposites prepared at pH 11, pH 7, pH 6, pH 5 and pH 4. Dotted lines mark peaks at three different positions corresponding to three conformations of backbone. (right) Expanded 1150–1000 cm^{-1} region of Raman spectra shows *all-trans* or *gauche* conformation of alkyl side chain. (bottom) Proposed models of molecular rearrangement causing the shift of vibrational bands of double and triple bonds within the conjugated backbone. (b) Change of side chain conformation at pH 7 and pH 4.

dependent absorption spectra of the nanocomposites prepared at pH 11 and pH 4. At room temperature, all nanocomposites in aqueous suspensions are in the blue phase (Fig. 7(c)). Increasing temperature induces segmental rearrangement of the PDA chains, which, in turn, causes the blue shift of absorption spectra. For the nanocomposite prepared at pH 11, an abrupt change of absorption spectrum is detected at the transition temperature of 65 °C. At this state, the suspension appears purple and the λ_{max} shifts to 597 nm. The plots of colorimetric response (%CR) and λ_{max} values show a sharp increase of %CR and the drop of λ_{max} value at color-transition region (Fig. 5s, Supporting information). The nanocomposite prepared at pH 7 also exhibits the blue-to-purple color transition at 65 °C. The absorption spectra of these nanocomposites fully reverse back to the original pattern upon cooling to room temperature. Their complete thermochromic reversibility persists for at least 10 heating/cooling cycles (Fig. 6s, Supporting information).

The preparation of nanocomposites at pH 6 and 4 provides rather different thermochromic behaviors. The color photographs in Fig. 7(c) show that color transition takes place at 50 °C and 40 °C for the nanocomposites prepared at pH 6 and pH 4, respectively. The decrease of color-transition temperature corresponds to the weakening of inter- and intramolecular interactions within the nanocomposites as revealed by the FT-IR and Raman studies in the previous section. The nanocomposite prepared at pH 6 exhibits a partial reversible thermochromism. This result is consistence with

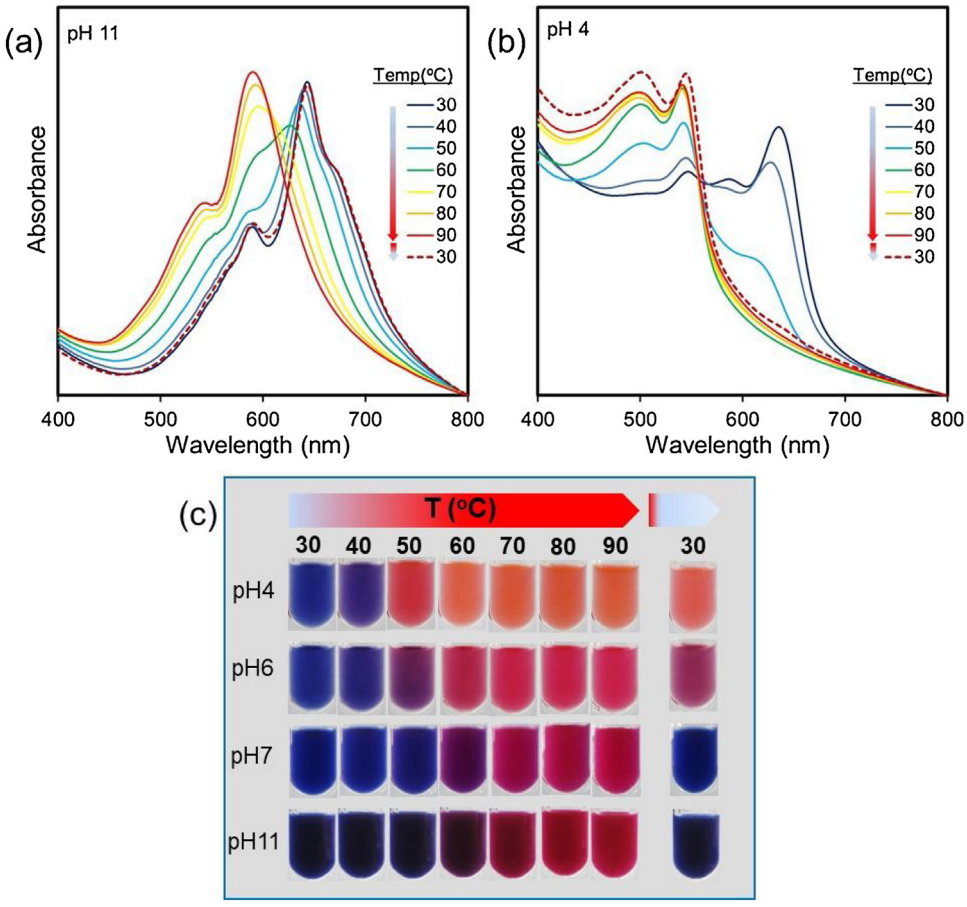

Fig. 7. Temperature-dependent absorption spectra of the poly(TCDA)/Zn^{2+}/ZnO nanocomposites prepared at (a) pH 11 and (b) pH 4. (c) Color photographs of the nanocomposite suspensions prepared at different pH taken upon heating to 90 °C, followed by cooling to 30 °C.

the Raman study, in which, two types of backbone conformation are detected at this condition. We believe that the partial dissolution of ZnO nanoparticle plays a major role on the thermochromic reversibility of the nanocomposite. When the preparing pH is decreased to 4, most of the ZnO nanoparticles are dissolved [25]. The nanocomposite prepared at this condition shows a complete irreversible thermochromism. It is worthwhile to point out that the XRD result in the previous section observes a Zn^{2+}-intercalated structure within the nanocomposite prepared at pH 4. This observation suggests that the presence of ZnO nanoparticle is essential to achieve a complete reversible thermochromism.

Thin films of the nanocomposite prepared at pH 4 exhibit irreversible thermochromism at about 60 °C (Fig. 7s, Supporting information). On the other hand, films of the nanocomposites prepared at pH 7 and 11 exhibit reversible blue-to-purple color transition at about 90 °C. Their thermochromic reversibility persists up to about 160 °C. The further increase of temperature to 200 °C causes irreversible color transition to the red phase. Raman spectrum of the red phase shows the stretching vibration of the C≡C and C=C bonds at 2115 and 1512 cm^{-1}, respectively, corresponding to the relaxation of poly(TCDA) backbone (Fig. 8s, Supporting information). A broad peak at 1065 cm^{-1} is also detected, indicating the presence of some *gauche* conformation of alkyl side chain. However, our previous study via XRD did not observe any significant change of the interlamellar d-spacing of the bilayer structure of nanocomposite in red phase [40].

In the last section, colorimetric response of the nanocomposites to acid and base is investigated. For the nanocomposite prepared at

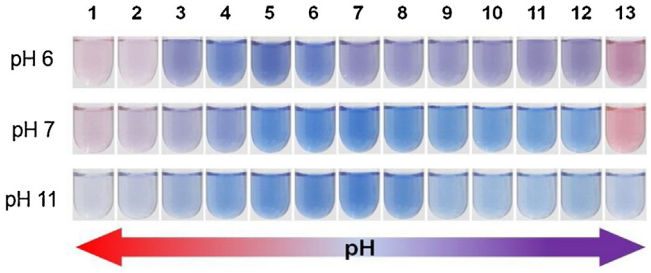

Fig. 8. Color photographs of the nanocomposites taken upon varying pH.

pH 7, the blue-to-red color transition takes place at pH 13 as shown in Fig. 8. The λ_{max} of absorption spectrum shifts to about 545 nm (Fig. 9s, Supporting information). Decreasing pH to 1 also induces color transition of the nanocomposite. The mechanism responsible for this dual color-transition behavior was described in our previous studies [23–25]. The dissolution of ZnO nanoparticle in the core region plays a major role for inducing the color-transition. For the nanocomposite prepared at pH 6, the ZnO core is partially dissolved, resulting in the increase of sensitivity. The suspension changes to purple at pH 8. For the acidic region, the color transition is observed at pH 2. The nanocomposite prepared at pH 11 exhibits rather different behavior. The color of nanocomposite suspension remains blue at pH 1 and 13. It indicates that the blue phase of this nanocomposite is rather stable under extremely low and high pH conditions. This finding can extend fabrication and utilization of the nanocomposite as sensing materials in applications with

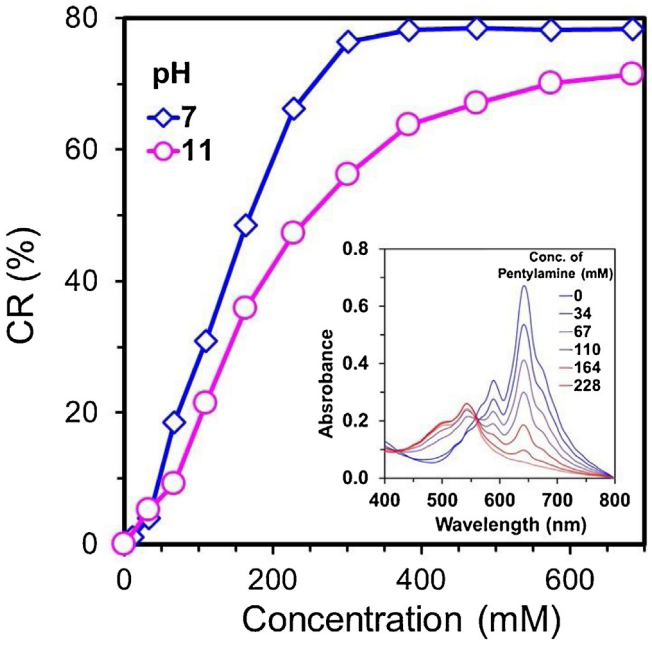

Fig. 9. Colorimetric response (%CR) of poly(TCDA)/Zn^{2+}/ZnO nanocomposite upon increasing concentration of pentylamine. The nanocomposites were prepared at pH 7 and pH 11. (inset) The variation of absorption spectra upon increasing concentration of pentylamine.

extreme pH conditions. To understand the origins of high color stability of the nanocomposite, we investigate its structure described in the previous section. The FT-IR study reveals that Zn^{2+} and Na^{+} ions incorporate into bilayer structure of the nanocomposite prepared at pH 11. As discussed in our previous report, the color transition of nanocomposite requires the penetration of H^{+} or OH^{-} ions through the PDA shell to react with the ZnO core [25]. Therefore, it could be more difficult to penetrate the PDA shell in the system of nanocomposite prepared at pH 11 due to the presence of additional intercalated Na^{+} ion.

We further investigate the color-transition behavior of nanocomposites using pentylamine as a stimulus. This long chain base provides greater extent of penetration into the PDA shell comparing to the OH^{-} ion [23]. Both nanocomposites prepared at pH 11 and 7 exhibit blue-to-red color transition as shown in Fig. 9, however, at different concentrations of pentylamine. For the nanocomposite prepared at pH 7, it requires ~165 mM of pentylamine to induce the color transition (CR of 50%). The concentration increases to ~230 mM for the nanocomposite prepared at pH 11. We note that the pH of nanocomposite suspension is adjusted to 7 prior to this experiment. The results confirm that color-transition behavior of the nanocomposite can be controlled by manipulating the molecular organization during the self-assembling process.

Conclusion

This research demonstrates that the molecular assembling and color-transition behavior of the poly(TCDA)/Zn^{2+}/ZnO nanocomposites can be systematically controlled by varying pH of the suspensions during preparation process. The variation of pH affects the surface charge of ZnO nanoparticle and the dissociation of —COOH headgroup. At the normal preparing condition of pH 7, TCDA headgroups are mostly —COOH while the ZnO surface charge is positive. The obtained nanocomposite exhibits reversible thermochromism and dual colorimetric response to both acid and base. When the preparing pH is increased to 11, the —COOH headgroup is mostly converted to the —COO^{-} one, meanwhile, the ZnO surface charge becomes highly negative. The molecular ordering of TCDA monomer is promoted at this condition, resulting in the increase of percent conversion during photopolymerization process. The obtained nanocomposite exhibits reversible thermochromism similar to that of the normal condition. Interestingly, blue phase of the nanocomposite obtained at pH 11 is rather stable at extremely high and low pH conditions. The decrease of preparing pH to 4 causes partial dissolution of ZnO nanoparticles, resulting in the decrease of inter-/intramolecular interactions within the nanocomposites. Partial relaxation of conjugated backbone and alkyl side chain of the poly(TCDA) occurs in this system. The nanocomposite exhibits irreversible thermochromism and increasing of sensitivity upon exposure to acid or base. The results in this study provide a new approach to prepare PDA-based materials at a wide range of pH, which is impracticable for the system of pure PDA. The ability to control color-transition behaviors can extend their utilization in various applications.

Acknowledgments

This research has been supported by the Thailand Research Fund [RSA 5980020]. This work has been partially supported by the National Nanotechnology Center (NANOTEC), NSTDA, Ministry of Science and Technology, Thailand, through its program of Research Network NANOTEC (RNN).

Appendix A. Supplementary data

Supplementary data associated with this article can be found, in the online version, at https://doi.org/10.1016/j.jiec.2018.12.045.

References

[1] J.T. Wen, J.M. Roper, H. Tsutsui, Ind. Eng. Chem. Res. 57 (2018) 9037.
[2] G.M.D. Ferreira, G.M.D. Ferreira, M.C. Hespanhol, J.P. Rezende, A.C.S. Pires, P.F.R. Ortega, L.H.M. Silva, Food Chem. 241 (2018) 358.
[3] O. Mapazi, K.P. Matabola, R.M. Moutloali, C.J. Ngila, Polymer 149 (2018) 106.
[4] Y. Zhang, L. Bromberg, Z. Lin, P. Brown, T.V. Voorhis, T.A. Hatton, J. Colloid Interface Sci. 528 (2018) 27.
[5] B. Gao, G. Yuan, L. Ren, J. Mater. Sci. 53 (2018) 6698.
[6] M. Wanga, Y. Yub, F. Liu, L. Ren, Q. Zhang, G. Zou, Talanta 188 (2018) 27.
[7] D.-H. Park, J.-M. Heo, W. Jeong, Y.H. Yoo, B.J. Park, J.-M. Kim, ACS Appl. Mater. Interfaces 10 (2018) 5014.
[8] H. Terada, H. Imai, Y. Oaki, Adv. Mater. 30 (2018) 1801121.
[9] M.J. Kim, S. Angupillai, K. Min, M. Ramalingam, Y.-A. Son, ACS Appl. Mater. Interfaces 10 (2018) 24767.
[10] M. Kim, Y.J. Shin, S.W. Hwang, M.J. Shin, J.S. Shin, J. Appl. Polym. Sci. 135 (2018) 46394, doi:http://dx.doi.org/10.1002/APP.46394.
[11] C. Khanantong, N. Charoenthai, T. Phuangkaew, F. Kielar, N. Traiphol, R. Traiphol, Colloids Surf. A 553 (2018) 337.
[12] R. Potai, K. Faisadcha, R. Traiphol, N. Traiphol, Colloids Surf. A 555 (2018) 27.
[13] C. Khanantong, N. Charoenthai, S. Wacharasindhu, M. Sukwattanasinitt, N. Traiphol, R. Traiphol, J. Ind. Eng. Chem. 58 (2018) 258.
[14] M.-C. Tu, J.A. Cheema, U.H. Yildiz, A. Palaniappan, B. Liedberg, J. Mater. Chem. C 5 (2017) 1803.
[15] S. Dolai, S.K. Bhunia, S.S. Beglaryan, S. Kolusheva, L. Zeiri, R. Jelinek, ACS Appl. Mater. Interfaces 9 (2017) 2891.
[16] A. Kamphan, C. Gong, K. Maiti, S. Sur, R. Traiphol, D.P. Arya, RSC Adv. 7 (2017) 41435.
[17] D.-H. Park, B.J. Park, J.-M. Kim, Acc. Chem. Res. 49 (2016) 1211.
[18] H. Shin, B. Yoon, I.S. Park, J.-M. Kim, Nanotechnology 25 (2014) 094011.
[19] B. Yoon, J. Lee, I.S. Park, S. Jeon, J. Lee, J.-M. Kim, J. Mater. Chem. C 1 (2013) 2388.
[20] Q.-M. Wang, Z.-Y. Yang, Carbon 138 (2018) 90.
[21] R. Varghese Hansen, L. Zhong, K.A. Khor, L. Zheng, J. Yang, Carbon 106 (2016) 110.
[22] S.J. Kew, E.A.H. Hall, Anal. Chem. 78 (2006) 2231.
[23] A. Chanakul, R. Traiphol, N. Traiphol, J. Ind. Eng. Chem. 45 (2017) 215.
[24] A. Chanakul, R. Traiphol, N. Traiphol, Colloids Surf. A 489 (2016) 9.
[25] A. Chanakul, N. Traiphol, K. Faisadcha, R. Traiphol, J. Colloid Interface Sci. 418 (2014) 43.
[26] J. Pang, L. Yang, B.F. McCaughey, H. Peng, H.S. Ashbaugh, C.J. Brinker, Y. Lu, J. Phys. Chem. B 110 (2006) 7221.
[27] Y. Lifshitz, Y. Golan, O. Konovalov, A. Berman, Langmuir 25 (2009) 4469.

[28] A. Fujimori, M. Ishitsuka, H. Nakahara, E. Ito, M. Hara, K. Kanai, Y. Ouchi, K. Seki, J. Phys. Chem. B 108 (2004) 13153.
[29] N. Charoenthai, T. Pattanatornchai, S. Wacharasindhu, M. Sukwattanasinitt, R. Traiphol, J. Colloid Interface Sci. 360 (2011) 565.
[30] T. Pattanatornchai, N. Charoenthai, S. Wacharasindhu, M. Sukwattanasinitt, R. Traiphol, J. Colloid Interface Sci. 391 (2013) 45.
[31] T. Pattanatornchai, N. Charoenthai, R. Traiphol, J. Colloid Interface Sci. 432 (2014) 176.
[32] S. Wacharasindhu, S. Montha, J. Boonyiseng, A. Potisatityuenyion, C. Phollookin, G. Tumcharern, M. Sukwattanasinitt, Macromolecules 43 (2010) 716.
[33] C. Phollookin, S. Wacharasindhu, A. Ajavakom, G. Tumcharern, S. Ampornpun, T. Eaidkong, M. Sukwattanasinitt, Macromolecules 43 (2010) 7540.
[34] S. Ampornpun, S. Montha, G. Tumcharern, V. Vchirawongkwin, M. Sukwattanasinitt, S. Wacharasindhu, Macromolecules 45 (2012) 9038.
[35] L. Rougeau, D. Picq, M. Rastello, Y. Frantz, Tetrahedron 64 (2008) 9430.
[36] N. Traiphol, N. Rungruangviriya, R. Potai, R. Traiphol, J. Colloid Interface Sci. 356 (2011) 481.
[37] A. Chanakul, N. Traiphol, R. Traiphol, J. Colloid Interface Sci. 389 (2013) 106.
[38] N. Traiphol, K. Faisadcha, R. Potai, R. Traiphol, J. Colloid Interface Sci. 439 (2015) 105.
[39] S. Toommee, R. Traiphol, N. Traiphol, Colloids Surf. A: Physicochem. Eng. Asp. 468 (2015) 252.
[40] N. Traiphol, A. Chanakul, A. Kamphan, R. Traiphol, Thin Solid Films 622 (2017) 122.
[41] A. Degen, M. Kosec, J. Eur. Ceram. Soc. 20 (2000) 667.
[42] P. Tanphibal, K. Tashiro, S. Chirachanchai, Macromol. Rapid Commun. 37 (2016) 685.
[43] M. Takeuchi, H. Imai, Y. Oaki, J. Mater. Chem. C 5 (2017) 8250.
[44] M. Takeuchi, H. Imai, Y. Oaki, ACS Appl. Mater. Interfaces 9 (2017) 16546.
[45] L. Yu, S.L. Hsu, Macromolecules 45 (2012) 420.
[46] X. Huang, S. Jiang, M. Liu, J. Phys. Chem. B 109 (2005) 114.
[47] A. Kamphan, N. Traiphol, R. Traiphol, Colloid Surf. A 497 (2016) 370.
[48] Y. Lifshitz, A. Upcher, O. Shusterman, B. Horovitz, A. Berman, Y. Golan, Phys. Chem. Chem. Phys. 12 (2010) 713.
[49] E. Shirai, Y. Urai, K. Itoh, J. Phys. Chem. B 102 (1998) 3765.
[50] Y. Lifshitz, A. Upcher, A. Kovalev, D. Wainstein, A. Rashkovsky, L. Zeiri, Y. Golan, A. Berman, Soft Matter 7 (2011) 9069.
[51] I.S. Park, H.J. Park, W. Jeong, J. Nam, Y. Kang, K. Shin, H. Chung, J.-M. Kim, Macromolecules 49 (2016) 1270.
[52] J.L. Lippert, W.L. Peticolas, Proc. Natl. Acad. Sci. U.S.A. 68 (1971) 1572.